Functional Studies on the Rotavirus Non-Structural Proteins NSP5 and NSP6

by

Edward Rainsford

A thesis submitted for the degree of Doctor of Philosophy

Department Biological Sciences

University of Warwick

Coventry

United Kingdom

September 2005

Table of Contents

Materials and Methods

Discussion

List of Figures

List of Tables

Acknowledgement

I would like to thank my supervisor Professor Malcolm McCrae for his advice and support during my PhD and special thanks to Gill Scott the Rota/Adeno lab technician for all the help and technical assistance. I would not have made it this far without the support of my family so thanks mum, dad and Tom for everything. Thank you to all of my friends and colleagues at Warwick University who were always there to help me out with advice when I needed it. Most of all I would like to thank all the past and present members and the Rota/Adeno lab it's been great fun in the lab as well as hard work. I am sure I would have gone insane without the many distractions and nights out with everyone from Virology and Micro I, I couldn't have asked to make better friends and thanks to the guys back home for always making life more entertaining.

Declaration

All the results presented in this thesis were obtained by the author unless otherwise stated and no part has been previously presented in application for a degree. All the sources of information and materials are indicated in the text.

Abbreviations

A	Adenine
Å	Angstrom
aa	Amino acids
ADRV	Adult Diarrhoeal rotavirus
Amp	Ampicillin
APS	Ammonium persulfate
ATP	Adenosine triphosphate
ATTC®	American Type and Tissue Culture
BAP	Bacterial alkaline phosphatase
β-gal	β-galactosidase
Bis-Tris	Bis-(2-hydroxyethy1)-imino-tris-(hydroxymethyl) methane
bp	Base pair
BSA	Bovine serum albumin
BTV	Bluetongue virus
C	Cytosine
CaMV	Cauliflower mosaic virus
CAT	Chloramphenicol acetyltransferase
cDNA	Complementary DNA
cpe	Cytopathic effect
CMV	Cytomegalovirus
CsCl	Caesium chloride
dG	Free energy at 37°C
DHBV	Duck hepatitis B virus

DMEM	Dulbecco's modification of Eagle's minimal essential medium
DMSO	Dimethylsulphoxide
DNA	Deoxyribonuclei acid
DNTP	Deoxynucleotide triphosphate
ds	Double stranded
DTT	Dithioreitol
E.coli	*Escherichia coli*
EDTA	Ethylenediaminetetraacetic acid
EGTA	Ethyleneglycolbis(aminoethylether)tetra-acetic acid
eIF2	Eukaryotic initiation factor 2
eIF3	Eukaryotic initiation factor 3
eIF4B	Eukaryotic initiation factor 4 B
eIF4E	Eukaryotic initiation factor 4 E
eIF-4GI	Eukaryotic initiation factor 4GI
ELISA	Enzyme linked immunosorbent assay
EM	Electron microscopy
EMCV	Encephlomyocarditis virus
ER	Endoplasmic reticulum
FCS	Foetal calf serum
FMDV	Foot and mouth disease virus
g	Gram
g	Centrifugal force
G	Guanine
GDP	Guanosine diphosphate
GFP	Green fluorescence protein

GMEM	Glasgow modified Eagle's minimal essential medium
GP	Glycoprotein
GSH	Reduced gluathion
GST	Glutathione S transferase
GTP	Guanosine triphosphate
HCl	Hydrochloric acid
His	Histidine
HIV	human immunodeficiency virus
hr	Hour
HRP	Horseradish peroxidase
IAA	Isoamyl alchol
Ig	Immumoglobulin
IPTG	Isopropyl β-D-1-thiogalactopyraniside
IRES	Internal ribosome entry site
Kan	Kanamycin
kb	Kilobase pair
Kd	Dissociation constants
kDa	KiloDalton
kg	Kilogram
L	Litre
LB	Luria-Bertani
m	Metre
M	Molar
mM	Milimolar
μ	Micro

MAb	Monoclonal antibody
MCS	Multiple cloning site
MES	2-Morpholinoethanesulfonic acid
Met	Methionine
min	Minute
moi	Multiplicity of infection
MOPS	3-Morpholinopropanesulfonic acid
mRNA	Messenger RNA
ND	Not determined
Ni-NTA	Nickel-nitrilotriacetic acid
NLS	Nuclear localisation signal
NSP	Non structural protein
NTP	Nucleotide triphosphates
OD	Optical density
O/N	Over night
ORF	Open reading frame
PABP	Poly (A) binding protein
PAGE	Polyacrylamide gel electrophoresis
PBS	Phosphate buffered saline
PCR	Polyerase chain reaction
PEG	Polyethylene glycol
pfu	Plaque forming units
pH	$-\log_{10}[H^+]$
pi	Post-infection
psi	Pounds per square inch

PTB	Polypyrimidine tract binding protein
RER	Rough endoplasmic reticulum
Ris	Replication intermediates
RNA	Ribonucleic acid
rpm	Revolutions per minute
RSV	Respiratory syncytial virus
S	Svedbergs
s	Second
ss	Single Stranded
Sarkosyl	*N*-dodecanoylsarcosinate
SDS	Sodium dodecyl sulphate
SV40	Simian virus 40
T	Triangulation number
TAE	Tris-acetate EDTA
TBE	Tris-borate EDTA
TCA	Trichloroacetic acid
TE	Tris EDTA
TEMED	N, N, N, N-Tetramethyl-ethylenediamine
T_m	Melting temperature
tRNA	Transfer Ribonucleic acid
Tris	Tris[hydroxymethyl]aminomethane
TS	Temperature sensitive
U	Enzyme units
UAS	Upstream activating sequence
UKtc	United Kingdom tissue-culture adapted strain of bovine rotavirus

USA	United States of America
UTR	Untranslated region
UV	Ultraviolet
VLP	Virus-like particle
VP	Viral protein
VPg	Genome linked protein
v/v	Volume for volume
w/v	Weight for volume
WHO	World Health Organization

Summary

The rotavirus replication cycle has not been fully characterised, one vital stage of virus replication involves large cytoplasmic occlusion bodies termed viroplasms. These are the sites of synthesis and replication of dsRNA, packaging of viral RNA into newly synthesized cores and the formation of double-shelled pre-virions. The detailed mechanism by which these events occur is poorly understood but is thought to be mediated by the non-structural proteins localised to these structures.

Rotavirus gene segment 11 expresses two proteins NSP5 and NSP6 which are found in alternate open reading frames. NSP5 exists is several isoforms which differ on their level of phosphorylation. It has been shown to be essential for virus replication and localises to the viroplasms. The smaller NSP6 protein is the most uncharacterised of all of the rotavirus proteins. It has however been shown to interact with NSP5 and has been tentatively suggested to be localised to the viroplasms.

To further investigate these two proteins the pET expression system was utilised to obtain purified protein which was subsequently used to generate monospecific polyclonal antisera. Studies into the function and localisation of these proteins found that both localised to the viroplasms and their relative distributions within these structures were defined. NSP6 was found to be expressed at a low level throughout the course of a rotavirus infection and in contrast to other non-structural proteins, to have a high rate of turnover. The RNA binding ability of both NSP5 and NSP6 was investigated using quantitative filter binding assays and these showed both have sequence independent nucleic acid binding ability. Studies were also conducted into the mechanism of NSP6 expression from the second open reading frame of gene 11, the results obtained being consistent with a leaky scanning mechanism of expression.

Introduction

Chapter 1

Rotaviruses and their replication

1.1. Rotaviruses and diarrhoeal disease

Rotaviruses are the major contributing factor to severe diarrhoea in children and young animals worldwide (Kapikian *et al.*, 2001). The majority of children will have been infected with rotavirus by the age of 3 years old, both in the developed and developing world (Bern and Glass, 1994; Glass *et al.*, 1996). Previous to the discovery of rotaviruses 10% to 30% of child diarrhoeal causative agents could be accounted for by known bacterial, parasitic or viral pathogens. It was not until 1973 that rotaviruses were identified by electron microscopy (EM) as the cause of human childhood diarrhoea (Bishop *et al.*, 1973). Since then rotaviruses have been identified as an important pathogens accounting for large costs both in economic terms and in terms of human lives.

A study performed by Parashar and colleagues showed that rotaviruses cause approximately 2 million hospitalisations and between 352,000 and 592,000 deaths per year in children under the age of 5 years (Parashar *et al.*, 2003). The disparity in the severity of illness caused by these viruses between a developed and a developing country is striking, with the study finding that 82% of these deaths occurred in the poorest countries (Figure 1.1). There is a 1 in 205 chance of a child under the age of 5 dying from rotavirus induced diarrhoea in low income countries such as, India (a low World Bank Income Group is classified as spending <U.S. $756 of gross national product or GNP per capita), as compared to a 1 in 48,680 chance in a high income group country such as the United Kingdom (a high World Bank Income Group is classified as spending >U.S. $9,265 of GNP per capita). The availability of

re-hydration therapy, access to clean water and adequate hospital treatment are all key factors in determining the severity of disease (Parashar *et al.*, 2003).

Although mortality is far less in the developed world the financial burden of rotaviruses is still high, with an estimated 2.7 million rotavirus diarrhoeal episodes in the United States per year, which result in the hospitalisation of 50,000 children. The cost of direct medical care in the United States is an estimated at $274 million with a social cost of $1 billion (Tucker *et al.*, 1998).

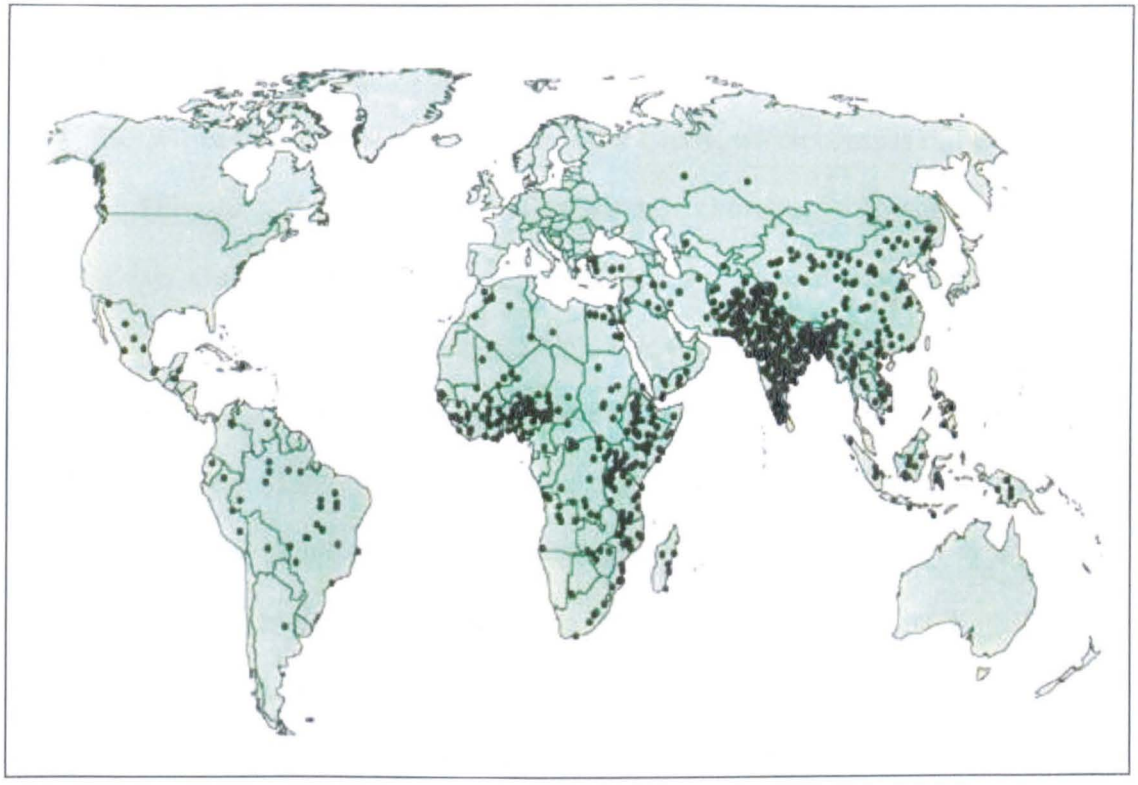

Figure 1.1 Global mortality attributed to rotavirus per annum
Global distribution of the number of annual death attributed to rotavirus infection, each dot represents 1000 childhood deaths per year.

Adapted from Glass et *al.*, 1997

1.2. Classification

1.2.1. Reoviridae

Rotaviruses are members of the Reoviridae family, which consists of twelve genera: Fijivirus, Aquareoviridae, Cypovirus, Orbivirus, Phytoreovirus, Oryzaviridae, Orthoreovirus, Rotavirus, Seadornavirus, Mycoreovirus, Coltivirus and Idnoreovirus (Mertens, 2004; Mayo, 2005). The viruses in this family have 10, 11 or 12 gene segments of dsRNA, encapsidated within a non-enveloped icosahedral virion of 60-100nm (Table 1.1). The Reoviridae family can be separated into two structurally distinct groups the turreted and the smooth-core viruses (Hill *et al.*, 1999). The core particles of the members of the Reoviridae have a T = 2 organisation (T is the triangulation number). The turreted group of viruses genera include the Orthoreovirus, Aquareoviridae, Cypovirus, Fijivirus and Oryzaviridea, they all share an incomplete T = 13 layer which is penetrated by a turret-like structures (Hill *et al.*, 1999). The other group includes Rotavirus, Orbivirus, Coltivirus and Phytoreovirus, these have a complete T = 13 forming channels with a five fold axis attached to subcores compose of 120 copies of a capsid protein (Grimes *et al.*, 1998; Merten, 2004).

Members of the Reoviridae family are important pathogens infecting a wide variety of different species including humans (rotavirus), animals (bluetongue virus and African horse sickness virus) and plants (rice dwarf virus) (Nibert and Schiff, 2001).

Reoviridae genus	No. of genome segments	Hosts
Turreted[a]		
Orthoreovirus	10	mammals, birds, reptiles
Aquareoviridae	11	fish, mollusks
Cypovirus	10	insects
Fijivirus	10	plants, insects[b]
Oryzaviridea	10	plants, insects[b]
Non turreted[a]		
Rotavirus	11	mammals, birds
Orbivirus	10	mammals, birds, arthropods[b]
Coltivirus	12	mammals, arthropods[b]
Phytoreovirus	12	plants, insects[b]
Newly assigned[c]		
Seadornavirus	12	mammals, insects
Mycoreovirus	11-12	fungi
Idnoreovirus	10	insects

Table 1.1 Feature of members of the Reoviridae family

[a] Proposed division of the Reoviridae based on the presence or absence of turret-like protein projecting around fivefold axes from innermost capsid layer.
[b] Served as vector for transmission to other hosts.
[c] Newly assigned genera in family Reoviridae.

Table reproduced and adapted from Nibert and Schiff, 2001 and Mertens, 2004.

1.2.2. Rotaviruses

Rotaviruses have a tripled shelled virion, which measures 100nm in diameter and contains the 11 dsRNA genome segments (Figure 1.2) (Kapikian *et al.*, 2001) which vary in size from 0.6 to 3.3 kilobases (Mattion *et al.*, 1994). The genome segments encode only one protein with the exception of the smallest gene segment 11 which is dicistronic (McCrae & McCorquodale, 1982; Mattion *et al.*, 1991). The name rotavirus comes from the virion's distinctive appearance when viewed under the EM, where the wheel-like structures evident lead to the name derived from *rota* the Latin for wheel (Flewett *et al.*, 1974). Rotaviruses share several universal characteristics including: an 11 dsRNA genome, the size of their virions, the three concentric shells of the infectious particle, the presence of 60 spikes that protrude from the outer shell, the presence of an RNA dependent RNA polymerase and the other enzymes needed for ssRNA message production in the virion, the capacity for genetic reassortment and a morphgenic pathway that involves immature particles budding into the endoplasmic reticulum (ER) (Estes, 2001).

Rotaviruses can be divided into groups; subgroups and serotypes, there are seven distinct groups of rotaviruses A to G, groups A to E were identified in the early 1980's on the basis of serology and RNA fingerprinting (Bridger *et al.*, 1982; Pedley *et al.*, 1983; Bridger, 1994), groups F and G have been tentatively proposed based largely on serological evidence (reviewed by Saif & Jiang, 1994). Groups A, B and C have been found in both humans and animals, with group A being the major cause of disease in humans. To date groups D to G have only been isolated from animals, with group F and G only detected in birds. Group A viruses can undergo

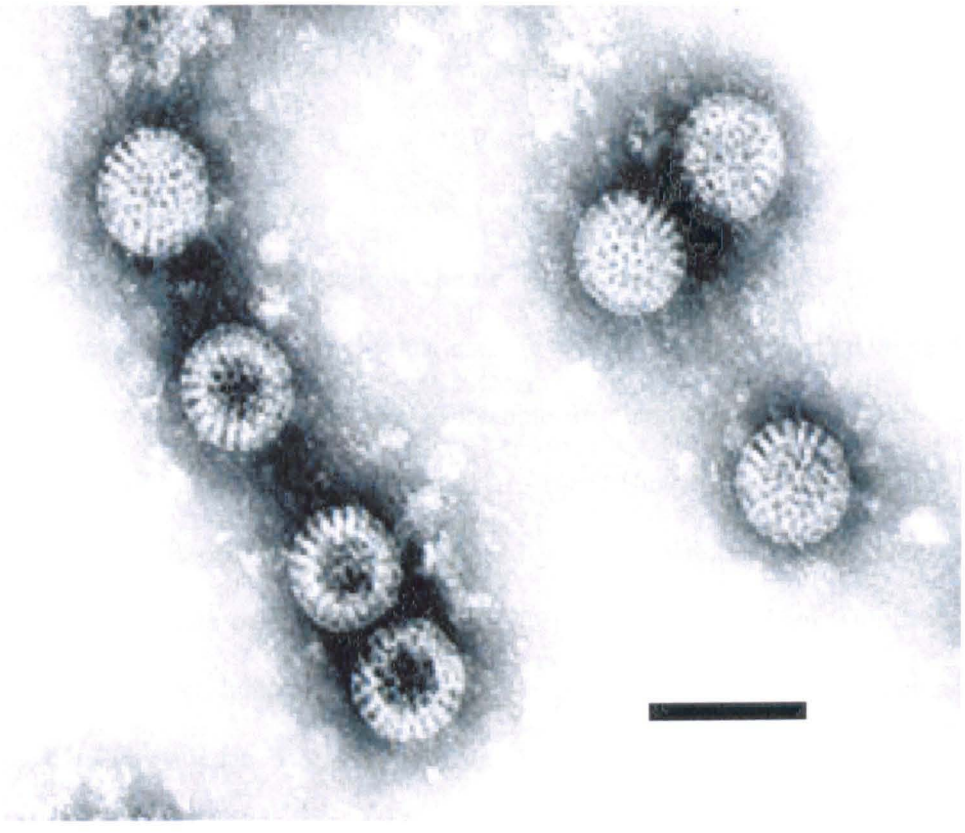

Figure 1.2 Morphology of the rotavirus particle
Negative stain transmission electron microscope image of rotavirus particles in cell culture, demonstrating the wheel-like nature of the virion (bar = 100 nanometer).

Source: F.P. Williams, U.S. Environmental Protection Agency

genetic reassortment with other group A viruses however, no reassortment of group A viruses has been detected with viruses from different groups (Yolken *et al.*, 1988). Group A viruses are the major cause of disease in children and young animals, whereas the group B viruses have been associated predominantly with adult diarrhoeal infections, the first outbreak being detected in 1983 in China (Su *et al.*, 1983; Hung *et al.*, 1983). The virus causing this outbreak was named adult diarrhoeal rotavirus (ADRV) and was responsible for outbreaks of severe diarrhoea in numerous rural areas of China (Chen *et al.*, 1985; Hung *et al.*, 1987). In these outbreaks 85% of those infected were over 15 years old with the highest number infected over 30 years of age (Hung *et al.*, 1987). Outbreaks of group B rotavirus have occurred in both India and Bangladesh; group B rotavirus has also been either serologically identified or isolated in Australia, Mexico, Japan, Thailand and the United Kingdom (Krishnan *et al.*, 1999; Sanekata *et al.*, 2001 and Mackow, 2002).

Group C viruses were first identified in piglets with servre diarrhoea in 1980 (Saif *et al.*, 1980) and were later identified as human pathogens after isolation from human faecal samples which were obtained from several countries (Bridger *et al.*, 1986). A more recent study in rural Colombia found that up to 25% of the diarrhoeal cases found to be negative for the presence of group A rotaviruses were positive for group C rotaviruses (Gutierrez *et al.*, 2003).

The pattern of the gene segments separation by polyacrylamide gel electrophoresis (PAGE) can be used to some degree as an indication to which group a particular virus belongs, in a procedure termed electropherotyping (Estes *et al.*, 1994; Holmes, 1996). This technique was used to determine to which group isolates

of rotavirus belonged. However, within the group A viruses the electropherotype pattern was found not to compare with the antigenic specificity defined by neutralisation. Two viruses of the same electropherotype may belong to different serotypes and viruses of the same serotype may possess different electropherotypes (Kapikian *et al.*, 2001). The gene segments can be put into size groups by which gene segments cluster together, for example in general the pattern for group A viruses is one of, four large segments, two medium size segments, three smaller segments and the two smallest segments (4-2-3-2). Several patterns have been observed in the group B rotaviruses including 4-2-1-1-1-1-1 for ADRV and 4-2-2-3 from two isolates of porcine and bovine origin (Pedley *et al.*, 1983).

Rotavirus groups have been further divided in the case of group A into subgroups based on the antigenic recognition of the VP6 protein that forms the middle shell of the virion. Epitopes on VP6 have been used to group virus isolates into one of four categories: subgroup I, subgroup II, subgroup I + II and non I, non II (Hoshino *et al.*, 1987; Svensson *et al.*, 1988). Monoclonal antibodies have subsequently been produced that specifically recognise sub group antigen I or II and the amino acids involved in these interactions have also been mapped (Greenberg *et al.*, 1983; Lopez *et al.*, 1994).

In group A rotaviruses, virus isolates have also been divided into serotypes based on plaque reduction neutralisation assays using sera generated against the outer capsid proteins (Estes, 2001). The VP7 glycoprotein (G) has been found to be the major contributing factor in defining serotype, 14 G serotypes have been identified to-date, with 10 isolated from humans (Hoshino & Kapikian, 1996). This

may in part be due to the larger amount VP7 proteins found in the virion. The VP4 protein (protease sensitive protein or P) also stimulates the production of neutralising antibodies has been used to classify viruses into serotypes. A system of VP4 classification using sequence analysis and hybridisation analysis has distinguished 21 separate genotypes. More recently a system involving neutralisation assays has been developed that has identified 13 VP4 serotypes. For the most part these serotypes are in agreement with the separation by genotype (Kapikian *et al.*, 2001; Hoshino & Kapikian, 1996). To identify a specific virus first the P (VP4) number as determined by serotyping, then followed by the designated genotype number in brackets, after which the G (VP7) number is given, for example, the human Wa isolate is designated P1A[8]G1 using this system (Santos & Hoshino, 2005).

1.3. Epidemiology

Rotaviruses are ubiquitous infections with greater than 90% of children by the age of 3 years testing positive for antibodies to rotavirus, the highest incidence of infection occurring between 6 and 24 months (Huilan *et al.*, 1991). Rotaviruses are thought to be spread via the faecal-oral route, with 34.5% of all child diarrhoeal patients in a Washington D.C. hospital testing positive for the presence of rotavirus in their faeces (Brandt *et al.*, 1983). The majority of rotavirus infections are asymptomatic and high titres of antibody to these viruses can be detected in adults suggesting continued subclinical infection through out life. The factors involved in the change from a susceptible age (<5 years) for virus induced disease to a non-susceptible age

(>5 years) are unknown. However disease in the elderly has also been documented (Bern & Glass, 1994).

In temperate climates like the United Kingdom rotavirus displays a seasonal pattern with peaks in the cooler months, the reasons for this cycling are unknown as this pattern of infection is reminiscent of an airborne virus but no evidence exists of a respiratory route of infection (Crowley *et al.*, 1997).

A large study of the distribution of G and P serotypes/genotypes of 45,571 strains of rotavirus showed that 88.5% of rotavirus cases worldwide were caused by G1, G2, G3 and G4 in conjunction with P[8] or P[4]. When the distribution of serotypes was divided by geographical location the four serotypes P[8]G1, P[4]G2, P[8]G3 and P[8]G4 were found to cause up to 90% of rotavirus infections in North America, Europe and Australia. However, these serotypes only account for 68% of infections in South America and 50% in Africa. This is indicative of a dramatic change in G and P types across the globe. A clear example of which is the P[8]G1 serotype which represents 70% of all rotavirus infections in North America, Europe and Australia but only 30% of infections in South America and 23% in Africa. Overall a much wider variety of serotypes cause disease in South America, Asia and Africa with no clear serotype dominating on these continents (Santos & Hoshino, 2005).

1.4. Structure of the rotavirus particle and genome

1.4.1. Structure of the rotavirus virion

The rotavirus virion is composed of three concentric shells, these are the core composed of VP1, VP2 and VP3 which encloses the dsRNA genome, the middle shell composed entirely of VP6 and the outer shell composed of VP7 which forms the smooth surface of the virus and VP4 which protrudes from the outer shell as a spike of roughly 10nm (Figure 1.3) (Prasad *et al.*, 1988; Prasad *et al.*, 1994; Yeager *et al.*, 1994). These particles are often referred to as being single layered, double layered or triple layered. The double layered and triple layered virions have a T = 13 icosahedral structure. There are 132 channels in the virion which run from the outer shell to the inner core. There are three types of channel which are classified by their position and size; there are twelve type I channels which are 40Å wide opening at the outer surface of the virion, and running down the icosahedral five fold axes. Sixty type II channels are found at the six-coordinated positions surrounding the five fold axes. There are sixty, type III channels which are 55 Å wide, 140 Å deep and are found on the six-coordinated positions around the three fold axes. The type I channels have been postulated as being involved in the export of the messenger RNA formed within the core of the particle. The channels allow entry of nucleoside-triphosphastes substrates for the RNA dependent RNA polymerase (RdRP) (Patton & Spencer, 2000).

The single layered particle is composed of 120 copies of VP2 arranged into 60 dimers on a T = 1 icosahedral lattice, and the major structural element of the core.

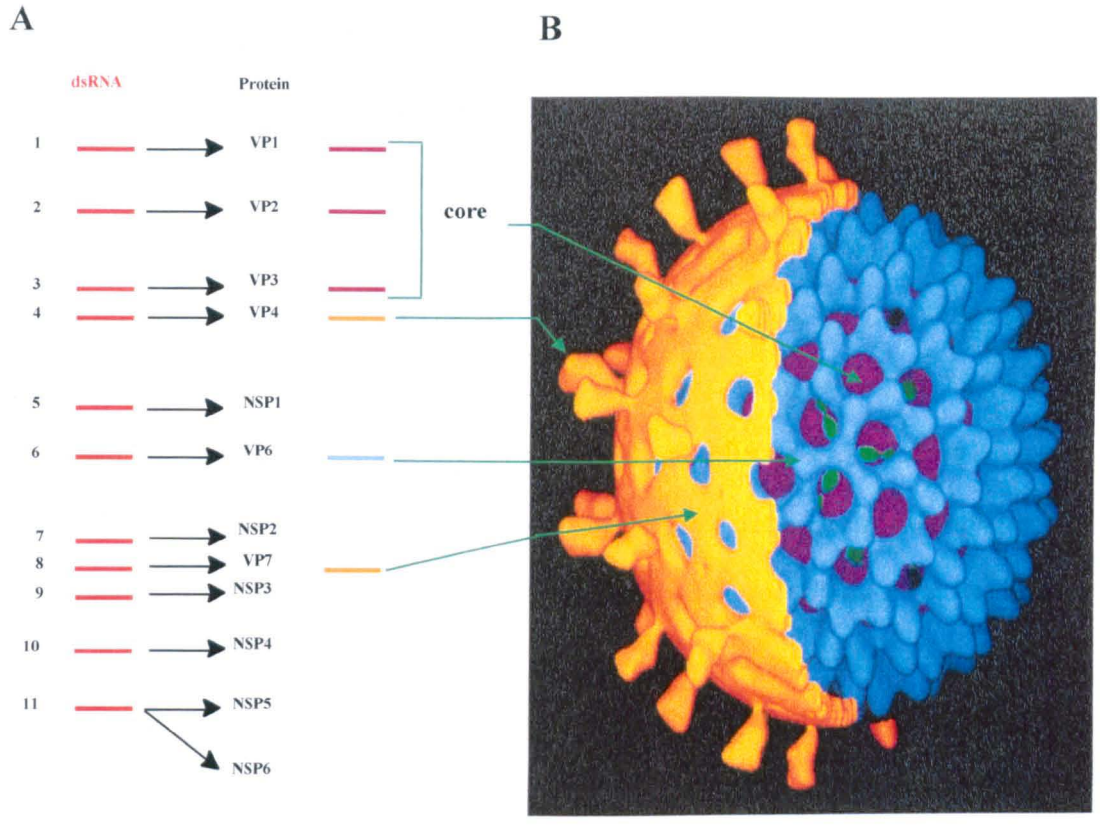

Figure 1.3 Structure of the rotavirus virion
Panel A shows a graphical representation of the electropherotype of a group A rotavirus strain, indicating the protein coding assignments for each of the 11 genome segments. The position of each of the structural proteins in the virion is indicated on

Panel B which shows a cryo EM reconstruction of a rotavirus particle with the three concentric layers composing the virion.

Adapted by the rotavirus group University of Warwick from Prasad *et al.*, 1988

The two protein monomers arranged in the asymmetric units, are called T = 2 icosahedral structures and have one monomer pointing towards the five fold axes and the other slightly offset from this. The N-terminus of the VP2 protein has been shown to have RNA binding capability (Labbe *et al.*, 1994) and it is the N-terminal region of the protein that points towards the viral genome where it is thought to interact with the dsRNA genome (Prasad *et al.*, 1996; Jayaram *et al.*, 2004). Within the shell formed by the VP2 protein there is the dsRNA genome, which is thought to exist in a coil around one of the 12 copies of VP1 and VP3 RNA dependent RNA polymerase (RdRP)-capping complex found at the five fold axes. The possibility that the icosahedral core T = 1 symmetry may restrict the number of copies of the RdRP-capping complex to 12 has been proposed to be the reason why no members of the Reoviridae have more than 12 genome segments (Gouet *et al.*, 1999; Patton & Spencer, 2000).

The VP6 protein forms the middle shell of the whole particle surrounding the core; there are 780 molecules of VP6 arranged into trimers. The VP6 protein appears to be necessary for the transcriptional ability of the core structure (Prasad *et al.*, 1988). The addition of the VP6 layer increases structural integrity of the particle and the resulting double layered particle can survive in the environment for an extended period of time (Zeng *et al.*, 1996).

The outer layer is formed by VP4 and VP7, the VP4 protein forms spikes that protrude from the virion and VP7 which is a glycoprotein forms the surface of the particle. VP7 interacts with the VP6 layer and forms the outer surface on the virion, there are 780 copies of the protein which forms 260 trimers that give the T =

13 icosahedral shape of this shell (Estes, 2001). The VP4 protein which forms 60 spikes extending from the outer surface has been implicated in cell attachment, cell penetration, haemaglutination, neutralisation and virulence (Estes, 2001). The spike is asymmetric and interacts with two VP7 molecules; at its base there is a large globular domain that interacts with the six VP6 molecules that surround the type II channel (Estes, 2001). VP4 is sensitive to proteolitic cleavage, splitting the VP4 (88kDa) protein into VP5* (60kDa) and VP8* (28kDa) (Fiore *et al.*, 1991). This has been shown to have a dramatic effect on infectivity; trypsinised virus has been shown to enter cells at much greater efficiency (Kaljot *et al.*, 1988; Keljo *et al.*, 1988).

1.4.2. Physiochemical properties of the virion

The stability of the virus particle is dependent on the presence of calcium, which appears to stabilise the VP7 glycoprotein. In the presence of calcium chelating agents, such as EDTA and EGTA, the outer layer is stripped off leaving double layered particles. The outer layer formed by VP4 and VP7 has been shown to be essential for normal virus infectivity (Gajardo *et al.*, 1997; Ruiz *et al.*, 1996). Calcium has been detected within triple layered particles but not found in double layered particles (Shahrabadi & Lee, 1986).

The middle shell can be removed to leave single layered particle by using chaotrophic agents such as sodium thiocynate or high concentrations of calcium chloride (Almeida *et al.*, 1979; Cohen *et al.*, 1979). Triple and double layered particles can be separated by caesium chloride (CsCl) or sucrose gradient

centrifugation. Triple layered particles separate at a density of 1.36 g/cm^{3}in CsCl and sediment at 520S to 530S in sucrose. The double layered particles have a density of 1.38 g/cm^{3}and sediment at 380S to 400S and the single layered particles have a density of 1.44 g/cm^{3}and sediment at 280S (Tam *et al.*, 1976; Bican *et al.*, 1982).

The virus particle is very stable in the environment and can remain infectious at room temperature for months, however repeated freeze thawing has been shown to reduce virus titres (Narang *et al.*, 1983). It has also been shown to be resistant to fluorocarbons, ether, chloroform and non-ionic detergents; which may result from the lack of a lipid membrane surrounding the virus (Estes *et al.*, 1979). Treatment with SDS has been shown to destroy infectivity. Other disinfectants that have been shown to effect rotavirus infectivity are 95% ethanol, phenol, chlorine and formalin (Narang *et al.*, 1983).

1.4.3. The Rotavirus genome

The rotavirus gene segments are all monocistronic with the exception of the smallest gene segment 11, which has been found to encode for two proteins (Estes & Cohan, 1989; Mattion *et al.*, 1991). The genome segments range from 667bp to 3302bp for the simian SA11 virus strain (Estes, 2001). The viral mRNA is highly (58% to 67%) A +U rich and contains a 5'-terminal cap structure ($m^7GpppG^{(m)}GPy$) but lacks a poly(A) tail (Imai *et al.*, 1983; McCrae & McCorquodale, 1983). The viral mRNAs have untranslated regions (UTRs) flanking the open reading frames, whose sequences vary widely between individual genes except for short 5' and 3' consensus sequences. These short consensus sequences at the 5' and 3' termini are

5'-GGC-poly(A/U)-3' and 5'-AUGUGACC-3' respectively (Desselberger & McCrae, 1994). The positive strand mRNA's of members of the Reoviridae serve two functions within the infected cell: they are used for the translation of viral proteins and also serve as a template for the synthesis of minus strand in the production of dsRNA (Nonoyama *et al.*, 1974). *Cis*-acting regulatory elements have been found within the 3' conserved sequence on all 11 gene segments, these have been shown to be required for the replication of transcripts in a cell free system (Patton *et al.*, 1996; Wentz *et al.*, 1996). The signals concerned are thought to involve secondary/tertiary structures rather than primary sequences (Chen *et al.*, 2001). Viral transcripts that lack the 3' consensus sequence cannot serve as templates for the synthesis of dsRNA, however if the 3' consensus sequence is fused to an mRNA of non-viral origin this can then be replicated by the viral RdRP complex but at a lower level than wild type viral mRNA (Patton & Spencer, 2000).

1.4.4. Genomic rearrangements

Rearrangements of the rotavirus genome have been detected these are usually in the form of head to tail duplications (Estes, 2001). Rearrangement is often found in virus that has been passaged in tissue culture at a high multiplicity of infection (m.o.i.) however, rearrangement has been detected in a wide variety of both human and animal primary isolates (Desselberger, 1996). Rotavirus strains which contain extra gene segments or larger than normal gene segments by gene concatemerisation have also been identified (Pedly *et al.*, 1984; Scott *et al.*, 1989; Ballard *et al.*, 1992). Several studies have shown numerous deletion and mutations in gene segment 5

which encodes NSP1, these studies showed that this protein is not required for growth in tissue culture (Tian *et al.*, 1993; Hau & Patton, 1994). Several gene segment 11 reassortants have been characterised. These are classified as long, short or super-short due to the electropherotype pattern produced. Rotaviruses usually have a long electropherotype pattern however duplications in the gene 11 sequence cause a shift to a shorter pattern and a switch between gene 10 and gene 11 due to the increase in size of the gene 11 sequence (Matsui *et al.*, 1990). The short and super-short gene 11 sequences are caused by partial or full duplications Kojima *et al* (1996b) characterised a gene 11 reassortant in which the 664bp gene from the parent strain had been duplicated in a head to tail fashion creating a 1182bp gene and a super-short electrophoretic pattern. From determination of key nucleotide positions it was determined that the duplication must have occurred during plus strand synthesis rather, than minus strand synthesis (Kojima *et al.*, 1996b). A region located between nucleotides 328 to 618 were found to in several strains was found to be duplicated extending the 3' UTR (Matsui et al., 1990). A gene 11 rearrangment containing a complete duplication of the NSP5 coding region in a head to tail arrangement was characterised by Chnaiderman *et al.*, (1998). The strain carrying this rearrangement was found to create larger plaques than the parental strain. The gene 11 segment by the use of reassortment was transferred from the parental porcine strain to an SA-11 background for further analysis. The SA-11 strain carrying the duplicated gene 11 also had an increased plaque size when compared SA-11 indicating that the gene 11 strain introduced carried with it an increase in pathogenicity (Chnaiderman *et al.*, 1998). This however was proposed to be due to

several point mutations within the NSP5 coding region rather than from the duplicated sequence (Chnaiderman *et al.*, 1998; Chnaiderman *et al.*, 2002). Further characterisation revealed that the point mutations removed several serine residues and was less hyperphosphorylated than normal NSP5. Also viral protein synthesis and the concentration mRNA in the strain carrying the rearranged gene 11 occurred at earlier time points that in SA11. Less dsRNA production was also noted leading to the hypothesis that NSP5 phosphorylation regulates the fate of mRNA to either protein synthesis or dsRNA production (Chnaiderman *et al.*, 2002).

1.5. Protein coding assignments of the rotavirus proteins

Rotavirus produces six structural and six non-structural genes, the coding assignments were originally elucidated for the UKtc virus by *in vitro* translation analysis using mRNA transcripts or denatured dsRNA (Figure 1.3) (McCrae & McCorquodale, 1982). The smallest gene segment, of the 11 dsRNA genome segments, encodes two proteins; all of the other genes are monocistronic. Gene segments are ordered by their migration by electrophoreses.

The order of the gene segments varies among rotavirus strains and identification of the proteins coded has relied on techniques such as gene-specific probes, reassortant analysis, and sequence homology or on biochemical and immunological analysis in a cell free *in vitro* translation system (Dyall-Smith *et al.*, 1983; Gombold *et al.*, 1985; Green *et al.*, 1987; McCrae & McCorquodale, 1982). An overview of rotavirus protein coding assignments can be seen in (Table 1.2).

Genome Segment	Protein product	Molecular Mass kDa	Mature Protein Modified	Location	Number of Molecules per virion
1	VP1	125		Core	ND
2	VP2	94	Cleaved	Core	120
3	VP3	88		Core	ND
4	VP4 VP5* +VP8*	88	Cleaved	Outer Shell	120
5	NSP1	53		Nonstructural	
6	VP6	41			780
7	NSP3	34		Nonstructural	
8	NSP2	35		Nonstructural	
9	VP7	38	Cleaved Glycosylated	Outer Shell	780
10	NSP4	28	Glycosylated	Nonstructural	
11	NSP5	26	O-Glycosylated	Nonstructural	
	NSP6	12		Nonstructural	

Table 1.2 Coding assignments and features of rotavirus proteins
Table showing the 11 genome segments and the proteins encoded from them, together with their molecular size, modification, function and number found per virion. The apparent molecular weights are for SA11 rotavirus polypeptides analysed by SDS-PAGE. ND = not yet determined.

Adapted from Kapikian, Hoshino & Chanock, 2001

1.5.1. Rotavirus structural proteins

1.5.1.1. VP1

The largest of the rotavirus genes, gene segment 1 encodes VP1, which is a minor component of the viral core and has been proposed to be the RNA dependent RNA polymerase (RdRP) (Cohen *et al.*, 1989; Mattion *et al.*, 1994). A number of studies have provided evidence for VP1 being the viral RdRP. Using a recombinant baculovirus expression system to create rotavirus core-like particles the proteins necessary for RNA synthesis were assayed (Zeng *et al.*, 1996). A core-like particle containing VP1, VP2 and VP3 was able to transcribe RNA, as was a core-like particle containing VP1 and VP2. However, VP2 alone and a core-like particle containing VP2 and VP3 were not able to transcribe RNA. This indicates that VP1 is essential for RNA production (Zeng *et al.*, 1996). The VP1 protein has the four sequence motifs that are shared between other proteins proposed to be RdRP (Cohen *et al.*, 1989; Fukuhara *et al.*, 1989; Mitchell *et al.*, 1990). A further consistent observation is the fact that temperature sensitive mutants mapped to VP1 cannot produce RNA at non-permissive temperatures (Chen *et al*,. 1990). VP1 has nucleotide binding ability, experiments performed using cross linking between VP1 and the photosensitive nucleotide analog [α-^{32}P] azido-adenosine triphosphate resulted in active VP6 particles losing their ability to transcribe RNA in the presence of light (Valenzuela *et al.*, 1991). VP1 is a component of the baculovirus-expression particles and replication intermediates that have replicase activity (Gelegos & Patton, 1989; Zeng *et al.*, 1996). VP1 specifically recognises the 3' end of viral

RNA containing the *cis*-acting replication signals (Patton *et al.*, 1996), in addition the RdRP activity of VP1 appears to be dependent on the presence of VP2 (Patton *et al.*, 1997).

1.5.1.2. VP2

VP2 is the major structural protein of the viral core, constituting 12% of the total virion protein, it encapsidates the dsRNA genome and the minor core proteins VP1 and VP2 (Kumar *et al.*, 1989). In a baculovirus expression system VP2 was shown to bind ssRNA and dsRNA in a sequence independent manner however, ssRNA binds with a much greater affinity, it was also shown to bind genomic RNA in purified single-shelled particles. The nucleic acid binding domain of the protein has been located between amino acids 1 and 132 (Labbe *et al.*, 1994). Studies have shown that removal of the first 25 amino acids was sufficient to remove the RNA binding ability of VP2 (Boyle & Holmes, 1986; Labbe *et al.*, 1994; Prasad *et al.*, 1996). Removal of the first 25 amino acids also abolished the ability of VP2 to encapsidate VP1 and VP3 into core-like particles in a baculovirus expression system (Zeng *et al.*, 1998). The importance of the N terminal region of VP2 can also be seen by studying the primary and secondary sequence of this region which contains several motifs that are common among RNA binding proteins. There is a predicted helix-turn-helix secondary structure between amino acids 65 to 121, a series of heptad repeats of lysine and glutamic acid residues between amino acids 53 to 81 and a RSKKEAKNA(AAKLA)VEIL motif which has been found in the RNA binding domain of several well characterized RNA binding proteins such as the

human RNA-dependent P1/eIF-2α protein kinase (Michell & Both, 1990, McCormack *et al.*, 1992; Labbe *et al.*, 1994). VP2 has been shown to be able to independently self assemble into core particles, and the N-terminus RNA binding domain does not appear to be essential for this property (Labbe *et al.*, 1994).

1.5.1.3. VP3

VP3 is found in the core of the virion associated to the viral dsRNA genome (McCrae & Faulker-Valle, 1981). A baculovirus expression system expressing core-like particles has shown that VP3 binds to the N-terminus of VP2, which in turn is the domain of VP2 which binds RNA (Labbe *et al.*, 1994; Zeng *et al.*, 1998). VP3 is also a sequence independent RNA binding protein with affinity for ssRNA (Patton & Chen, 1999). It has been identified as the guanylyltransferase capping protein, which places 5' caps onto viral mRNA molecules (Liu *et al.*, 1992; Pizzaro *et al.*, 1991). This activity has been demonstrated to be non specific with VP3 being able to cap any RNA initiating with both guanine and adenine residues. However, VP3 does preferentially bind uncapped RNA rather than capped RNA (Patton & Chen, 1999). Methyltransferase activity has also been detected showing the multifunctional properties of VP3 (Chen *et al.*, 1999).

Sequence analysis using RT-PCR of VP3 from multiple strains of rotavirus showed that there is a 94% sequence identity among human group A rotavirus VP3 proteins and a 79% homology between mammalian VP3 sequences (Cook & McCrae, 2004). There appears to be a species specific conservation of VP3 sequence with high homology found within viruses from one species but a high level of

sequence divergence between viruses of different species. Investigation into the sequences involved in the putative enzymatic site showed that the motifs KXTAMDXEXP at amino acid 385 and KXXGNNH at amino acid 545 were conserved in both group A and C rotaviruses (Cook & McCrae, 2004).

1.5.1.4. VP4

VP4 is part of the outer layer of the virion and forms the spikes that protrude from the virion surface (Pasad *et al.*, 1990). It is an 88kDa protease sensitive protein that is the P type neutralising antigen used for classification of rotavirus strains into serotypes (Offit & Blavat, 1986; Fiore *et al.*, 1991). VP4 is the haemagglutinin and has been purported to be the cell attachment protein (Kalica *et al.*, 1983; Crawford *et al.*, 1994; Ruggeri and Greenberg, 1991). It also interacts with the VP6 protein in the inner shell of the virion (Shaw *et al.*, 1993).

Treatment of virus with trypsin has been shown have greater infectivity (Kaljot *et al.*, 1988; Keljo *et al.*, 1988) and this has been linked to the cleavage of VP4 to produce VP5* (60kDa) and VP8* (28kDa) (Fiore *et al.*, 1991). The VP4 spike was initially thought to be a dimer of VP4 subunits however recent work has shown it to be a trimer, where two VP4 molecules form the rigid spike and a third molecule is left flexible. However it has been proposed that during entry the three cleaved VP5* molecules form a trimer of the membrane interaction domains, resulting from the release of the VP8* cleavage product and exposing the hydrophobic apex of the VP5* antigen domain (Dormitzer *et al.*, 2005; Lopez *et al.*, 1991; Mattion *et al.*, 1994). It has been suggested that this hydrophobic domain may

then insert into the cell membrane causing it to fold back exposing the potential fusion domain which in turn leads to entry of the virus into the cell (Dormitzer *et al.*, 2005; Lopez *et al.*, 1991; Mattion *et al.*, 1994). In line with this hypothesis the VP5* cleavage product has been shown to be able to permeablise membranes (Denisova *et al.*, 1999)

VP4 and the VP8* cleavage product can both activate NF-kappaB through a TRAF2-NF-kappaB-inducing kinase signalling pathway (LaMonica *et al.*, 2001). VP4 and VP8* both contain three TNFR-associated factor (TRAF) binding motifs. When expressed *in vivo* VP4 and VP8* both caused a 5 to 7 fold increase in NF-kappaB activity and upregulated TRAF2-mediated NF-kappaB activation. This suggests that rotavirus actively changes cellular signalling and directly effect cellular transcriptional responses (LaMonica *et al.*, 2001).

1.5.1.5. VP6

The hydrophobic VP6 protein forms the middle shell of the rotavirus virion it is the major virion protein constituting 51% of the total protein in the particle (Mattion *et al.*, 1994; Smith *et al.*, 1989). It can spontaneously form trimers and this is its native form within virus particles (Estes *et al.*, 1987). These trimers can be dissociated and reformed by varying the pH (Tosser *et al.*, 1992). VP6 interacts with VP2, VP4 and VP7 and is highly antigenic and immunogenic (Estes *et al.*, 1987; Gorziglia *et al.*, 1985; Sabara *et al.*, 1987). Deletion mutagenesis has mapped a region essential for trimerisation to amino acids 246 to 314 (Affranchino & González, 1997). Proline 308 has also been shown to be important for the stability of

VP6 trimers (Shen *et al.*, 1994). The N-terminal region has been proposed to be an important domain of VP6, possibly involved in transporting viroplasmic occlusion bodies (Mansell *et al* 1994). VP6 has been shown to interact with B-cells via surface immunoglobulins (Parez *et al.*, 2004).

1.5.1.6. VP7

VP7 forms the smooth surface of the mature virion, it is a glycoprotein that contains N-linked high mannose oligosaccharides which are processed via trimming (Arias *et al.*, 1982; Ericson *et al.*, 1983 Kabcenell & Atkinson, 1985). $Man_8GlcNAc_2$ and $Man_6GlcNAc_2$ oligosaccharides are found on the VP7 protein during viral replication and Man_6GlcNA_2 and $Man_5GlcNAc_2$ are found on the mature virus particle (Kabcenell & Atkinson, 1985; Kabcenell *et al.*, 1988). The VP7 ORF is 326 amino acids in length however the first initiation codon has a suboptimal Kozak consensus sequence which directs the initiation of translation. There is a second initiation codon 90 base downstream of the first which is in a much better Kozak consensus sequence. The initiation codons are both preceded by hydrophobic domains at amino acids 6 to 23 and 33 to 44 respectively; it is these domains that have been implicated in the transport of the VP7 protein to the endoplasmic reticulum (ER). A potential third in frame initiation codon is present in some but not all virus strains. A single glycosylation site at amino acid 69 is used in the SA11 and UKtc rotavirus strains but, other strains have three potential glycosylation sites of which only two are thought to be used (Kouvelos *et al.*, 1984; Kelvelos *et al.*, 1984; Sato *et al.*, 1986; Estes & Cohen, 1989). The VP7 ER signal is located at the N-

terminus of the protein and is cleaved at amino acid 51, the amino terminal residue of VP7 found in purified virus is blocked by pyroglutamic acid (Stirzaker *et al.*, 1987).

VP7 is glycosylated as it is inserted into the membrane of the ER; this insertion is directed by the signal sequence (Both *et al.*, 1983; Ericson *et al.*, 1983; Kabcenell & Atkinson, 1985). Two regions between amino acids 51 to 61 and 61 to 111 have been implicated in retention of VP7 to the ER (Poruchynsky & Atkinson, 1988; Poruchynsky *et al.*, 1985; Stirzaker *et al.*, 1987; Whitfeld *et al.*, 1987). A number of amino acids found between these regions at amino acids 57 to 63, with the sequence LPITGS, has been demonstrated to be highly conserved among rotaviruses (Mattion *et al.*, 1994). The ITG has been shown via mutation analysis to be essential for ER retention (Maass & Atkinson, 1994). However, the exact process involved in VP7 ER retention is still not fully understood.

VP7 forms trimers and has been shown to interact with VP4 and NSP4 within infected cells (Maass & Atkinson, 1990), these interactions and the presence of calcium appear to be crucial elements in the formation of the outer layer and the correct placement of VP7 into the mature virus particle (Dormitzer & Greenberg, 1992; Poruchynsky & Atkinson, 1991; Poruchynsky *et al.*, 1991; Shahrabadi & Lee, 1986; Shahrabadi *et al.*, 1987). Silencing of VP7 by siRNA does not affect double layered particle production but, no triple-layered particles were seen to be produced and enveloped double-layered particles were observed to accumulate in the ER lumen (Lopez *et al.*, 2004).

1.5.2. Rotavirus non-structural proteins

1.5.2.1. NSP1

The NSP1 protein is encoded by gene segment 5 and is a 58kDa protein that is poorly conserved among rotavirus strains (Dunn *et al.*, 1994; Xu *et al.*, 1994; Kojima *et al.*, 1996). However, the region between amino acids 42 and 72 in the N-terminus of the protein has been found to be conserved over most rotavirus strains. This region is highly cystiene rich and has been predicted to form two zinc finger motifs (Hau *et al.*, 1994, Brottier *et al.*, 1992). NSP1 has been found to be non-essential for virus growth in tissue culture, by using several mutant strains containing deletion of regions including the cystiene rich N-terminus of gene 5 (Tian *et al.*, 1993; Hau & Patton, 1994; Okada *et al.*, 1999; Taniguchi *et al.*, 1996). NSP1 knock down, using siRNA specific for gene 5, has also shown it to be non-essential for virus replication in tissue culture (Silvestri *et al.*, 2004). Gene 5 reassortants have also been used to show that the N-terminus is the functional region of the protein (Tian *et al.*, 1993; Hau & Patton, 1994).

The NSP1 protein is localised to the cytoplasm within the infected cells and has been shown to localise with the cytoskeleton when analysed by sub-cellular centrifugation (Hau & Patton, 1994). NSP1 has specific affinity for the 5' end of viral mRNA which has been linked to the N-terminal cystiene rich region of the protein (Brottier *et al.*, 1992; Hua *et al.*, 1994).

The NSP1 protein has been shown to be an antagonist of the interferon (IFN) signalling pathway (Barro & Patton, 1993). NSP1 binds to IFN regulatory factor 3

(IRF3) which responds to infections by phosphorylation, dimerisation and nuclear translocation where it causes activation and release of IFN. NSP1 causes degradation of IRF3 via a proteasome-dependent pathway, this ability was mapped to the C terminus of NSP1 (Graff *et al.*, 2002; Barro & Patton, 2005). NSP1 has been found to undergo rapid mutation when rhesus rotavirus (RRV) was serially passaged at high multiplicity of infection (MOI) leading to defective NSP1 (Kearney *et al.*, 2004).

1.5.2.2. NSP2

NSP2 is a highly basic 35 kDa protein that is the most abundant viral protein found within the infected cell (Petrie *et al.*, 1984). It self-assembles into stable octomers (Schuck *et al.*, 2001) which is the functional form of the protein (Kattoura *et al.*, 1994; Taraporewala *et al.*, 2002). Crystal structure analysis of the NSP2 protein has shown that the NSP2 monomer is composed of two separate domains, separated by a 25 Å deep cleft (Jayaram *et al.*, 2002). The N-terminal domain is mostly formed from α-helices and contains a 24 residue basic loop which is the proposed ssRNA binding site. The C-terminal domain forms a histidine triad (HIT)-like fold which is common amongst nucleotidyl hydrolases, there is no primary sequence homology between NSP2 and other nucleotidyl hydrolases. The histidine triad, His 221, His 225 and His 110 located near the base of the cleft are thought to be the site of NTP binding and hydrolysis.

NSP2 has been localised to the viroplasms which are cytoplasmic occlusion bodies that form between 2-3 hours post infection. These have been shown to be

sites for the synthesis and replication of dsRNA, the packaging of viral dsRNA into newly synthesised cores and the steps of viral morphogenesis that result in the formation of double-shelled pre-virions (Petrie *et al.*, 1984; Altenburg *et al.*, 1980; Esparza *et al.*, 1980; Patton & Gallegos, 1990; Patton *et al.*, 1997; Wentz *et al.*, 1996). Early investigations using temperature sensitive mutants showed that NSP2 is essential for viroplasm formation and virus replication (Ramig & Petrie, 1984; Gombold *et al.*, 1985), later studies using siRNA knock down of NSP2 have shown that loss of NSP2 leads to inhibition of viroplasm formation, genome replication, virion assembly, and synthesis of the other viral proteins (Silvestri *et al.*, 2004). NSP2 has been shown to have sequence independent ssRNA binding ability, with octamers of protein binding RNA co-operatively to form higher ordered complexes (Kattoura *et al.*, 1992; Taraporewala *et al.*, 2002). NSP2 has also been shown to have helix-destabilising activity, this unlike other helicases is Mg^{2+} and ATP independent (Taraporewala and Patton, 2001). It also possesses NTPase activity that is Mg^{2+} dependent and can hydrolyse any NTP to NDP. Cross-linking assays have been used to show that NSP2 binds VP1 and NSP5 in the infected cell (Kattoura *et al.*, 1994; Afrikanova *et al.*, 1998)

1.5.2.3. NSP3

NSP3 is a 36 kDa protein that is found distributed throughout the cytoplasm of the infected cell and which has been shown to form homodimers (Mattion *et al.*, 1992; Piron *et al.*, 1999; Estes, 2001). NSP3 is composed of two separate domains, the N-terminal domain specifically binds the 3' consensus sequence of viral mRNA,

X-ray crystal structure analysis has shown that NSP3 forms a heart shaped dimer with the mRNA buried deep within the cleft of the two monomers (Deo *et al.*, 2002). The dimerisation domain has been localised to between amino acids 163 to 237 (Piron *et al.*, 1999).

NSP3 specifically binds to the 3' terminus of viral mRNA by the consensus sequence GACC (Poncet *et al.*, 1993; Poncet *et al.*, 1994). NSP3 is a functional homolog of poly A binding protein (PABP) (Both *et al.*, 1984) and binds the translation initiation factor eIF4G with a higher affinity than PABP (Groft & Burley, 2002; Piron *et al.*, 1998). The specific binding of NSP3 to viral mRNA and the subsequent displacement of PABP in the translation initiation complex has been proposed to cause circularisation of the viral mRNA transcript and preferential translation. This in turn leads to host cell shut off and the inability for capped and polyadenylated cellular mRNA to be translated (Padilla-Noriega *et al.*, 2002; Poncet *et al.*, 1994; Vende *et al.*, 2000).

A novel cellular protein has been shown to interact with NSP3; RoXaN (rotavirus X protein associated with NSP3) has been identified as a 110 kDa protein that maybe involved in protein-protein interactions and RNA binding. A leucine-aspartate repeat motif between amino acids 244 to 341 has been shown to interact with the dimerisation domain of NSP3; this interaction has been detected within virus infected cells (Vitour *et al.*, 2004).

1.5.2.4. NSP4

NSP4 is a 28kDa transmembrane glycoprotein localised to the ER with a vital role in virus morphogenesis (Ericson *et al.*, 1982; Kabcenell & Atkinson, 1985). The protein is composed of three hydrophobic domains (H1 – H3), two N-linked high mannose glycosylation sites are located within the first hydrophobic domain and a predicted amphipathic α-helix that overlaps a folded coiled-coil region. The H2 domain contains a predicted transmembrane domain that spans the ER membrane the C-terminus is hydrophilic and extended (Chan *et al.*, 1988). The polypeptide backbone of NSP4 also contains an uncleaved signal sequence (Both *et al.*, 1983; Baybutt & McCrae, 1984).

The C-terminus of NSP4 has been proposed to be an intracellular receptor for double layered particles and to mediate their transport into the ER (Au *et al.*, 1993; Taylor *et al.*, 1992; Taylor *et al.*, 1993). Evidence to support this comes from studies which show double-layered particles will only bud into ER containing NSP4 (Au *et al.*, 1993; Meyer *et al.*, 1989). The NSP4 protein has been predicted to form a homotetramer (Taylor *et al.*, 1996) and be involved in the removal of the transient membrane from budded double-layered particles (Tian *et al.*, 1996). Glycosylation is thought to be required for the removal of membranes by NSP4 (Suzuki *et al.*, 1984). NSP4 also contains a VP4 binding domain suggesting that it may possess some function in the construction of the virions outer layer (Au *et al.*, 1993; Tian *et al.*, 1996). Silencing of NSP4 expression using siRNA resulted in the incorrect distribution of a number of viral proteins and no production of double or triple layered particles (Lopez *et al.*, 2004).

NSP4 among group A viruses, has very highly conserved sequence with 98% homology between strains (Lin & Tian, 2003). This highly conserved sequence identity is only found within rotavirus groups but, not seen between groups, with less than 10% sequence identity between group A and group B NSP4 sequences, but within the group B viruses there is a 93% sequence sequence identity (Guzman & McCrae, 2005). Despite this lack of primary sequence identity there is a high level of secondary sequence similarity and possibly epitope configuration as sera generated against purified group B protein was able to detect group A NSP4 by immunofluorescence in both infected and transfected cells (Guzman & McCrae, 2005).

NSP4 was the first viral endotoxin documented, its effects were first observed when purified NSP4 protein was introduced intraperitoneally and caused age-dependent diarrhoea in mice (Ball *et al.*, 1996). NSP4 appears to stimulate the secretion of intra cellular calcium (Ca^{2+}) and chloride ions (Estes, 2001), there is some evidence that NSP4 may act as a viroporin creating a Ca^{2+} channel leading to export of Ca^{2+} from the cell (Ruiz *et al.*, 2005). The increased Ca^{2+} permeability of the plasma membrane leads to a progressive rise in cytosolic Ca^{2+} concentration (Michelangeli *et al.*, 1991; Perez *et al.*, 1999), Ca^{2+} stabilized the outer capsid of the virion and induces cell death. It has also been proposed that Ca^{2+} mediated secretory pathways of water and electrolytes maybe triggered by the increased Ca^{2+} concentration contributing to the onset of diarrhoea (Ruiz *et al.*, 2000).

1.5.2.5. NSP5

NSP5 is the larger of the two proteins expressed from the smallest segment of the rotavirus genome, gene segment 11 (Figure 1.4) (Dyall-Smith *et al.*, 1981; Mattion *et al.*, 1991). It is a dimeric, O-linked glycosylated protein that has been localised to the viroplasm in virus infected cells (Petrie *et al.*, 1984; Gonzalez & Burrone, 1991; Gonzalez *et al.*, 1998). The NSP5 protein has been shown to bind ssRNA and dsRNA with equal affinity in a sequence independent manner (Vende *et al.*, 2002), and to interact with the viral proteins VP1, VP2 and NSP2 (Afrikanova *et al.*, 1998; Berois *et al.*, 2003). NSP5 is a highly serine/threonine rich (24%) protein that exists in several isoforms which vary on their level of phosphorylation, the phosphorylation of the protein causes retardation when analysed by SDS-PAGE electrophoresis and has lead to the identification of three separate species of 26, 28 and 30-34 kDa (Welch *et al.*, 1989; Afrikanova *et al.*, 1996; Poncet *et al,*. 1997; Blackhall *et al.*, 1997). It has been suggested that NSP5 has putative autocatalytic kinase activity potentially leading to autophosporylation of the protein (Welch *et al.*, 1989; Poncet *et al.*, 1997; Torres-Vegas, 2000). NSP5 synthesis has been detected 2 hours post infection however the 28 and 30–34 kDa isoforms were not detected until 4 hours post infection (Blackhall *et al.*, 1997; Blackhall *et al.*, 1998). Current evidence suggests that NSP5 autocatalytic kinase activity probably only accounts for a small proportion of NSP5 phosphorylation. The generation of the hyperphosphorylsated form (30-34 kDa) has been shown to be up-regulated by the presence of NSP2 (Afrikanova *et al.*, 1998).

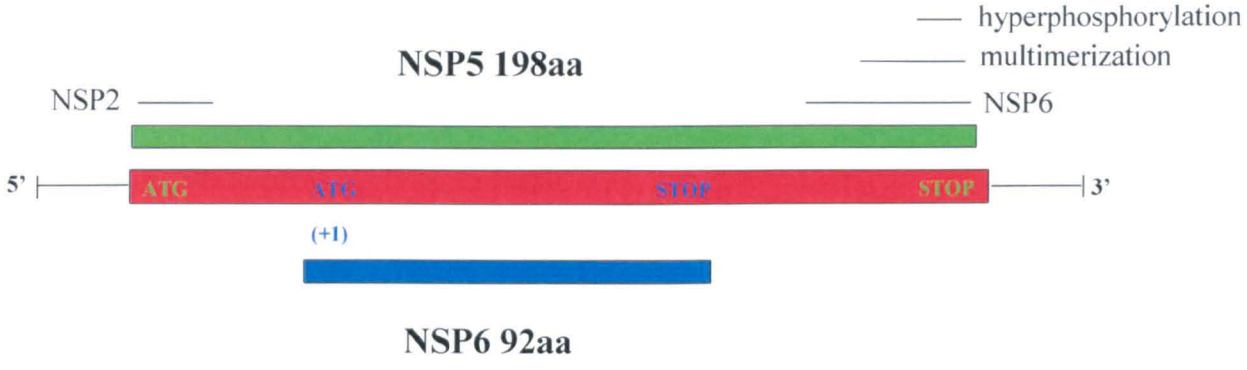

Figure 1.4 Functional domains of rotavirus gene segment 11
The gene 11 coding regions for NSP5 (green) and NSP6 (blue) are demonstrated on the diagram. The interaction domains of NSP5 proposed to bind NSP2 and NSP6, along with the regions required for multimerization and hyperphosphoryltion are also indicated.

Adapted from Torres-Vega *et al.*, 2000

It is however still unclear as to how NSP2 causes up-regulation of NSP5 and several theories have been proposed i) the binding of NSP2 triggers an increase in the autocatalytic kinase activity of NSP5, ii) the NTPase activity of NSP2 generates phosphates that are transferred from NSP2 to NSP5 (Taraporewala *et al.*, 1999; Vende *et al.*, 2002), iii) the binding of NSP2 leads to conformational changes in NSP5 allowing cellular kinases to phosphorylate previously blocked residues on the protein (Blackhall *et al.*, 1998; Eichwald *et al.*, 2002).

The NSP2 binding domain of NSP5 has been localised to the N-terminal region however a 33 amino acid N-terminal deletion mutant which could not bind NSP2 was still able to undergo hyperphosphorylation (Afrikanova *et al.*, 1998), whereas a C-terminal deletion mutant lost this ability, the removal of just the 10 C-terminal amino acids was enough to block hyperphosphorylation (Afrikanova *et al.*, 1998; Torres-Vega *et al.*, 2000). Dimerisation of NSP5 has been shown to be dependent upon the 28 C-terminal amino acids, which contains no serine or threonine residues and is therefore not a site for phosphorylation, this suggests that NSP5 multimerisation is essential for hyperphosphorylation (Torres-Vega *et al.*, 2000).

A number of phosphorylation sites have been detected within NSP5, four serine residues (Ser-153, Ser-155, Ser163, and Ser-165) contained in an acidic region have been found to have homology to casein kinase II (CK2) phosphorylation sites (Eichwald *et al.*, 2002). In later experiments performed by Eichwald *et al.*, (2004) using synthetic peptides, CK2 was not able to phosphorylate NSP5 substrates however, casein kinase I (CK1) was shown to cause the phosphorylation of the

synthetic peptides as well as bacterial expressed NSP5 mutants indicating that it was a strong candidate for the cellular kinase involved in NSP5 phosphorylation (Eichwald *et al.*, 2004).

A serine residue at position 67 was shown to be vital to hyperphosphorylation of NSP5 and a probable target for a cellular kinase. It appears to become accessible to hyperphosphorylation only in the presence of NSP2 or in mutants lacking the N-terminal 33 amino acids and/or a 50 amino acid region downstream of Ser-67 between amino acids 80 to 130. These regions may block Ser-67 phosphorylation until NSP2 binding causes a conformational shift exposing the region between them containing Ser-67. Evidence suggests that phosphorylation of Ser-67 is the first crucial step in hyperphosphorylation and only after this step further phosphorylation events can occur (Eichwald *et al.*, 2004). Mutants containing deletions of the N-terminal 33 amino acids and the 50 amino acid deletion from amino acids 80 to 130 were both able to undergo hyperphosphorylation when transfected alone. By contrast two other deletion mutants lacking either amino acids 33 to 80 or 130 to 180 were unable to be hyperphosphorylated when transfected alone, presumably due to the fact that the first deletion lacks Ser-67 and the latter one contains the regions thought to block Ser-67 phosphorylation. When either of the mutants that were able to undergo hyperphosphorylation was co-transfected with either of the mutants unable to show hyperphosphorylation then, hyperphosphorylation of both could be detected (Eichwald *et al.*, 2004). This is evidence that the phosphorylation of Ser-67 is a critical step, after which, subsequent phosphorylation events can occur leading to

hyperphosphorylation. The C-terminus was shown to be essential for all hyperphosphorylation events to occur, strongly linking it to NSP5 dimerisation (Eichwald *et al.*, 2004). One study has suggested that the level of NSP5 phosphorylation may be linked to positive sense ssRNA being directed from translation to dsRNA replication (Chnaiderman *et al.*, 2002).

Co-transfection of NSP2 and NSP5 expressing plasmids leads to the formation of viroplasm-like occlusion bodies, hyperphosphorylation and both N and C terminal domains of NSP5 have been shown to be necessary for the formation of these structures (Fabbretti *et al.*, 1999). The binding of NSP2 can be mimicked by the creation of N-terminal NSP5 fusion proteins, leading to the formation of viroplasm-like structures in the absence of NSP2. The formation of these viroplasm-like structures was dependent on leaving the C-terminus of NSP5 unmodified however, hyperphosphorylation was not found to be essential for viroplasm-like structure formation (Mohan *et al.*, 2003). One study has observed that the number of viroplasms in a virus infected cell decreases over time, whilst the size of the viroplasms increases and that the viroplasm was composed of NSP2 at its core with an outer ring of NSP5 protein (Eichwald *et al.*, 2004).

NSP5 expression, like NSP2, has been shown to be essential for virus replication, siRNA and intracellular antibodies have both been used to knockdown the expression of NSP5 in virus infected cells leading to loss of viroplasm formation and viral replication (Vascotto *et al.*, 2004; Lopez *et al.*, 2005).

1.5.2.6. NSP6

NSP6 is the least well characterized of all of the rotavirus proteins, it is encoded in a +1 alternate reading frame in gene segment 11 which lies entirely within the NSP5 ORF. NSP6 is a 92-98 amino acid protein depending on the strain and has been suggested to localise to viroplasms in virus infected cells (Mattion *et al.*, 1991). Yeast two hybrid and co-immunoprecipitation experiments from cells co-transfected with the NSP5 and NSP6 ORF's, have shown it to interact with NSP5. This interaction has been localised to the C-terminal region of NSP5 which has been shown to be involved in both NSP5 dimerisation and hyperphosphorylation (Torres-vega *et al.*, 2000). Sequence analysis of gene 11 from different virus isolates has revealed that not all of them appear to actually encode NSP6 protein. Two human virus isolates Mc323 (Kojima *et al.*, 1996) and 512-C (Wu *et al.*, 1998) do not possess the NSP6 start codon, while the Alabama strain of lapine virus (Gorziglia *et al.*, 1989) and the porcine OSU strain (Gonzalez & Burrone, 1989) both appear to have truncated open reading frames for NSP6. Also group B and group C gene segment 11 sequences do not contain the NSP6 ORF. The group B gene 11 sequence shows low sequence identity compared to the group A gene 11 sequences. However there is 71.9% nucleotide sequence similarity between group B gene 11 sequences (Petric *et al.*, 1991). The lack of conservation of NSP6 in some rotavirus strains and low level of expression found within virus infected cells, has led to the suggestion that NSP6 may play a non-essential regulatory role during the virus replication cycle (Mattion *et al.*, 1991; Torres-vega *et al.*, 2000; Lopez *et al.*, 2005).

1.6. The Rotavirus Replication cycle

1.6.1. Rotavirus replication

Rotaviruses replicate entirely within the cytoplasm and have a lytic lifecycle (Estes, 2001). The replication cycle when studied in monkey kidney cells produces the maximum virus yields in 10 – 12 hours (McCrae & Faulkner-Valle, 1981) however, in differentiated human intestinal cell lines replication appears to be much slower with maximum virus yield detected at 20 – 24 hours (Jourdan *et al.*, 1997). The virus particle contains all the enzymes necessary for the generation of mRNA and dsRNA. The positive sense RNA transcripts, generated by these enzymes can act as mRNA or templates for minus-strand synthesis (Estes, 2001). All viral RNA synthesis appears to occur in large electron dense cytoplasmic occlusion bodies termed viroplasms (Silvestri *et al.*, 2004). Double layered particles are formed within the viroplasms and an unusual feature of the rotavirus life cycle is the transient envelope stage gained by double-layered particles budding through the ER membrane after which the final outer layer of the virion is acquired. Progeny virions are released mainly, but not exclusively by cell lysis rather than through budding at the cell surface (Estes, 2001). The rotavirus replication cycle is summarised in figure 1.4.

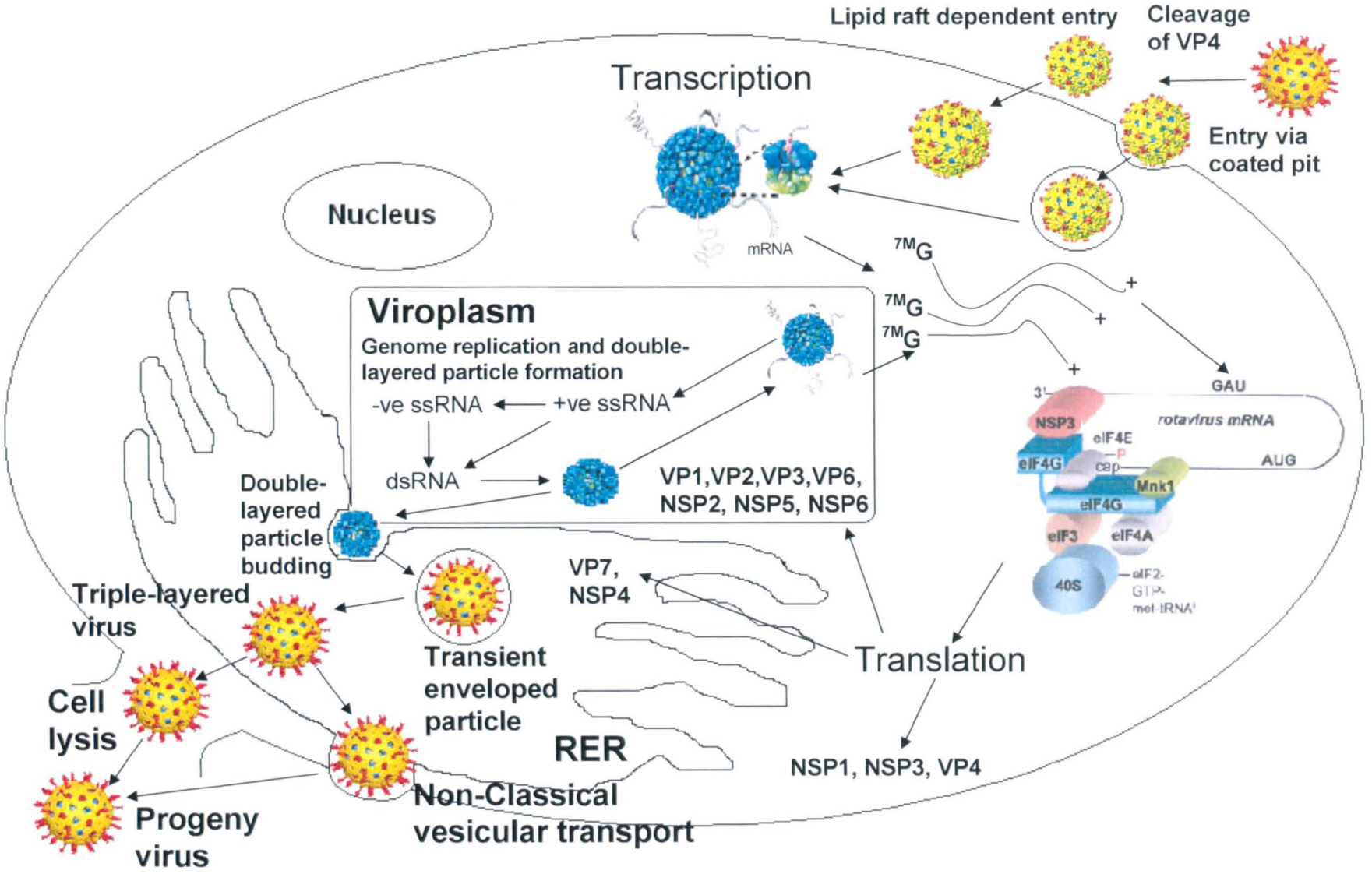
Lipid raft dependent entry
Cleavage of VP4
Transcription
Entry via coated pit
Nucleus
mRNA
7MG
Viroplasm
Genome replication and double-layered particle formation
-ve ssRNA
+ve ssRNA
dsRNA
VP1,VP2,VP3,VP6, NSP2, NSP5, NSP6
Double-layered particle budding
VP7, NSP4
Triple-layered virus
Transient enveloped particle
Cell lysis
RER
Translation
NSP1, NSP3, VP4
Non-Classical vesicular transport
Progeny virus
GAU
NSP3
rotavirus mRNA
eIF4E
eIF4G
cap
AUG
Mnk1
eIF3
eIF4A
40S

Figure 1.5 Rotavirus replication cycle
The virus particle attaches to the host cell mediated by the cleavage of VP4 to VP5* and VP8*. Entry has been shown to be lipid raft dependent but virus particles have been detected by electron microscopy to enter the cell by coated pits and found internally in intracellular vesicles. Once internalised, the virus quickly loses its outershell and transcription is activated within the double-layered particles. Translation of viral mRNA is enhanced by the NSP3 protein which specifically binds viral mRNA and replaces PABP in the initiation complex. The non-structural proteins NSP2, NSP5 and NSP6 form viroplasms within which VP1, VP2, VP3 and VP6 have been localised. Secondary transcription, replication of the dsRNA genome and the formation of new double layered particles occur within the viroplasm. The VP7 and NSP4 proteins localise to the ER and via the NSP4 protein which acts as an intracellular receptor the double-layered particles bud from the viroplasm into the ER. Transiently enveloped virus particles are formed and subsequently triple layered particles. The mature triple layered virus particles then exits the cell by host cell lysis or by non-classical vesicular transport.

Adapted from Estes, 2001, with cryoEM images taken from Schneider & Mohr, 2003; Jayaram *et al.*, 2004; Pesavento *et al.*, 2005.

1.6.2. Attachment

Rotavirus attachment and entry is a multistep process that involves the interactions of several molecules (Mendez *et al.*, 1999; Lopez & Arias, 2004). Only triple layered particles have been shown to be infectious (Crawford *et al.*, 1994; Jourdan *et al.*, 1998). Virus attachment has been proposed to be by VP4 (Crawford *et al.*, 1994; Ruggeri & Greenberg, 1991) or by its cleavage product VP5* (Zarate *et al.*, 2000), however the proteolytic cleavage of VP4 to VP5* and VP8* is not required for cell binding (Clark *et al.*, 1981; Fukuhara *et al.*, 1988). Rotaviruses have a specific cell tropism *in vivo* infecting the mature enterocytes of the villi of the small intestine however; spread of the infection through the intestine has been observed (Mossel & Ramig, 2003).

Some animal rotaviruses have been shown to require sialic acid for attachment, as demonstrated using neuraminidase (NA) treated cells which showed a great reduction in rotavirus infection levels (Bastardo & Holmes, 1980). The infectivity of the majority of human isolates was not however blocked by NA treatment, these isolates being termed NA-resistant (Yolken *et al.*, 1987; Fukudome *et al.*, 1989; Ciarlet & Estes, 1999). NA-resistant strains may still use sialic acid for attachment as SA moieties that are internal in the oligosaccharide but are not affected by NA however, these experiments were perform in tissue culture and not in the gut environment (Delorme *et al.*, 2001). The VP4 genotype appears to be the critical factor in conveying NA sensitivity (Ciarlet *et al.*, 2002). Several SA containing cellular receptors have been identified for different rotavirus strains, such as the ganglioside GM3 for porcine strain OSU (Rolsma *et al.*, 1998) and

ganglioside GM1 in the case of the human strain KUN and MO (Guo *et al.*, 1999). Recent work suggests that the binding of SA by VP4 causes a conformational change in the VP4 molecule leading to the trimeric VP5* form which may have further post attachment interactions with other cellular receptors (Pesavento *et al.*, 2005).

Rotavirus appears to interact sequentially with several proteins and recently a model of rotavirus entry has been proposed (Figure 1.5) (Lopez & Arias, 2004). This suggests that the VP8 subunit of VP4 protein interacts with the SA containing receptor (Fiore *et al.*, 1991; Fuentes-Panana *et al.*, 1995). The binding of VP8 to the SA receptor has been proposed to trigger a conformational change in VP4 to form the trimeric VP5* (Lopez & Arias, 2004). The binding of integrin α2β1 has been implicated in attachment of some strains and observed to be involved in post attachment interaction events in others (Ciarlet *et al.*, 2002; Graham *et al.*, 2003; Londrigan *et al.*, 2003). The interaction between α2β1 has been localised to the DGE motif on VP4 an area located within the VP5* subunit and is proposed to be the second interaction after SA binding (Zarate *et al.*, 2000; Lopez & Arias, 2004). Post attachment interactions appear to play a vital part in virus infection and after the initial interactions of VP5* and VP8* with SA and α2β1 three other host cell proteins appear to be involved in virus infection. These are hsc70 and the integrins αvβ2 and αxβ3. The interaction of hsc70 with the virus is mediated by VP5* in a domain between amino acids 642 to 658 (Zarate *et al.*, 2003; Guerrero *et al.*, 2002). The interaction with αvβ2 and αxβ3 appears to be mediated by VP7 (Guerrero *et al.*,

2000; Zarate *et al.*, 2000; Graham *et al.*, 2003). The order these latter interactions occurs in still remains unclear (Lopez & Arias, 2004).

Ganglioside GM1 subunits α2 and β3 as well as hsc70 have all been associated with lipid rafts and virus particles have also been found to localised to these cholesterol rich membrane lipid domains during infection (Isa *et al.*, 2004). Evidence for the involvement of lipid rafts in the attachment of rotavirus comes from experiments using inhibitors of N-glycosylation and glycolipid synthesis which dramatically reduce the levels of virus infection (Guerrero *et al.*, 2000).

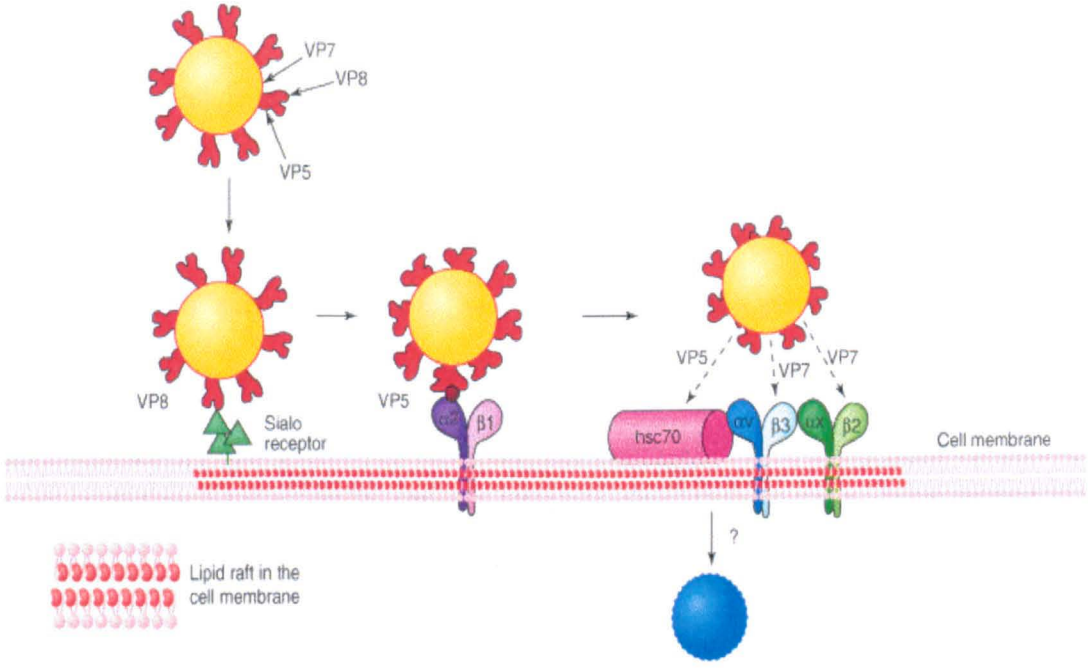

Figure 1.6 A model for rotavirus attachment to a host cell
The suggested initial contact of the virus with the cell surface is between a sialic acid (SA)-containing cell receptor and the VP8* domain of VP4 protein. This initial interaction of the virus with SA probably induces a conformational change on VP4, which allows the virus to subsequently interact with integrin α2β1, through the DGE domain on VP5*. Once these initial events have occurred three more interactions are thought to take place, these are between: (i) the KID domain of VP5 and the ligand-binding domain of hsc70, (ii) the CNP region of VP7 and integrin αvβ3, and (iii) the GRP domain of VP7 and integrin αxβ2. The exact order of these attachment events remains unclear but ultimately leads to entry, uncoating of the virus and activation of transcription of the double-layered particle seen here in blue.

Adapted from Lopez & Arias, 2004

1.6.3. Rotavirus entry and uncoating

Early electron microscopy studies suggested that rotavirus entry might be mediated by endocytosis, rotavirus particles were detected in coated pits and in a variety of vesicles (Perie *et al.*, 1981; Quan & Doane, 1983). However, electron microscopy has also been used to show that trypsin treated virus entered the cells by direct membrane penetration whereas non-trypsinated virus entered cells by endocytosis in a process which did not lead to productive infection (Suzuki *et al.*, 1985). Later experiments using drugs that block the acidification of endosomes and the transport of endocytic vesicles had no effect on infectivity suggesting that endocytosis is not involved in virus entry (Fukuhara *et al.*, 1987; Ludert *et al.*, 1987; Kaljot *et al.*, 1988; Bass *et al.*, 1995; Cuadras *et al.*, 1997). By contrast the drug bafilomycin A1 which inhibits the endosomal proton-ATPase pump did block rotavirus infection (Chemello *et al.*, 2002) In addition solublised VP4 and VP7 have been shown to permiablise membranes (Charpilienne *et al.*, 1997) as has the hydrophobic domains of the VP5* cleavage product (Denisova *et al.*, 1999; Dowling *et al.*, 2000). These observations have lead to the suggestion that an endosomal protein driven-ATPase pump may lead to a lowered Ca^{2+} concentration causing solublisastion of the outer capsid proteins and permeabilisation of the endosome and release of the double-layered particle into the cytoplasm (Chemello *et al.*, 2002). Set against this is other evidence suggesting that endocytosis is not involved in virus entry. Drugs and dominant negative mutants which impair clathrin and caveolae-mediated endocytosis were found to have no effect on the entry of rotaviruses. However, dominant negative cell mutants which do not express dynamin, a GTPase

known to be involved in membrane scission events could not be infected (Sanchez-San Martin *et al.*, 2004). These observations and the apparent dependence of lipids for viral entry may suggest that rotavirus may enter by a raft-dependent endocytosis pathway (Nabi & Le, 2003).

Virus uncoating appears to be dependent on Ca^{2+} concentration changes which lead to the loss of the outer coat protein and activation of the virion associated RNA dependent RNA polymerase. This can also be achieved *in vitro* by the use of chelating agents such as EDTA (Cohen *et al.*, 1979).

1.6.4. Transcription

Rotavirus transcription occurs within the double-layered particle after uncoating and requires ATP (Spencer & Arias, 1981). Under single step growth conditions with the SA11 strain of virus growing in monkey kidney cells the maximum levels of transcription can be detected at 9 to 12 hours post infection (Stacy-Phipps & Patton, 1987). The transcriptase complex formed by VP1 and VP2 has been localised to the five fold axes of the VP2 shell (Prasad *et al.*, 1996). It has been proposed that there are 12 VP1-VP3 heterodimers one at each five axes fold anchored by interactions with VP2 (Luongo *et al.*, 2000; Ramadevi *et al.*, 1998; Sandino *et al.*, 1994). The genome has been detected by cryo EM microscopy to be organised into ordered concentric layers within the core structure and it has been suggested that it winds around the replicase complex in a spiral (Gouet *et al.*, 1999; Prasad *et al.*, 1996; Reinisch *et al.*, 2000). Newly transcribed RNA exits the core via the type I channels in the VP2 layer (Lawton *et al.*, 1997). Each of the transcriptase

units appears to function independently each possibly only transcribing a single strand of the genome, this independent nature can be seen in the observations that mRNA of each genome segment is not produced in equimolar amounts, whereas the dsRNA genome is made in equimolar amounts during its replication (Johnson & McCrae, 1989; Patton, 1990). There is some evidence to suggest that the RdRP complex can reengage the 5'-end of the template RNA after finishing transcription at the 3'-end, as the two are thought to be in close proximity to each other (Banerjee & Shatkin, 1970; Cohen, 1977; Spencer & Arias, 1981; Yazaki *et al.*, 1986). The viral transcripts are all positive sense full length copies of the minus strand from the dsRNA template (McCrae & McCorquodale, 1983). There is also evidence that control of viral gene expression occurs at the transcriptional and translational level (Johnson & McCrae, 1989).

1.6.5. Translation

Rotavirus mRNA does not contain a polyadenylation signal and is not polyadenylated nevertheless, the final four bases of the rotavirus mRNA (GACC) have been shown to be a translational enhancer (Chizhikov & Patton, 2000). It has been suggested that the 5' and 3' termini of the mRNA's form stable pan handle structures during translation (Patton *et al.*, 1993; Patton *et al.*, 1996). The pan handles do not form perfect duplexes with the 3' termini and the importance of the single stranded nature of the 3' terminus has been shown in two ways. First, mutations of the 5' terminus create complementary base pairing with the 3' terminus which greatly reduces dsRNA synthesis. Alternatively the annealing of

complementary deoxyoligonucleotides to the 3' consensus sequence abolished dsRNA replication, whereas annealing of oligonucleotides to other parts of the mRNA had no effect on synthesis (Chen & Patton, 1998). The levels of viral mRNA's and proteins were measured in virus infected cells revealing that there was quantitative and temporal control of gene expression at both the transcriptional and translational levels (Johnson & McCrae, 1989). Evidence suggests that post-transcriptional control of rotavirus gene expression is mediated by translational efficiency of individual viral mRNAs (Mitzel *et al.*, 2003).

Rotaviruses cause host cell shut off by blocking translation of cellular mRNA which leads to preferential translation of viral mRNA. The rotavirus non-structural protein NSP3 has been found to be a functional homolog of PABP and binds with a higher affinity to eIF4G (Both *et al.*, 1984; Eiden, 1993; Quin *et al.*, 1991 and Grofts & Burley, 2002). The NSP3 protein specifically binds to the 3' terminus of viral mRNAs by the consensus sequence UGACC and because it competes more effectively with PABP for binding of the translation initiation complex, viral mRNA is preferentially translated. This leads diminished host cell protein synthesis as capped and polyadenylated cellular mRNA can no longer access the translational machinery (Poncet *et al.*, 1994).

1.6.6. Genome replication

Plus and minus strand synthesis can both be detected at 3 hours post infection (Stacy-Phipps & Patton, 1987; McCrae & Faulkner-Valle, 1981), the level of minus strand synthesis peaks at 6 to 9 hours post infection in monkey kidney cells which is somewhat earlier than the maximum of plus sense strand. The delay in the maximum amount of plus strand production has been postulated as being due to the accumulation of proteins required for the assembly of transcriptase particles (Stacy-Phipps & Patton, 1987). The synthesis of dsRNA is thought to occur within subviral particles after segment selection and packaging, meaning that genome assortment of viral mRNA must occur prior to RNA replication. During this process, each individual virion acquires a single copy of each individual genome segment. How this occurs and the mechanism and signals involved is unclear, however the consensus sequences found at the 5' and 3' termini are thought to be involved in directing packaging of mRNA molecules (McCrae & McCorquodale, 1983). The UTR regions of each gene segment are found to be highly conserved and are thought to be involved in directing genome segment specific encapsidation (Clarke & McCrae, 1983; Desselberger & McCrae, 1994).

Within the viroplasms three distinct species of replication intermediate (RI) have been detected, termed the pre-core RI, the core RI and the double-layered RI. The pre-core RI appears to be composed of viral RNA plus VP1 and VP3 and the non-structural proteins NSP1 and NSP3 (Gallegos & Patton, 1989). The fact that only NSP1 and NSP3 reproducibly co-purify with the precore RI suggests that these complexes maybe assembled on the cytoskeleton (Patton, 1995).

The core RI contains all of the structural proteins found within the rotavirus single shelled core particle (VP1, VP2 and VP3) as well as containing the non-structural proteins NSP2 and NSP5. The double-layered RI is identical to the core RI with the exception that it also contains the VP6 protein (Gallegos & Patton, 1989).

Recent evidence suggests that mRNA is primarily produced within the viroplasms and that no pathways exist for the importation of mRNA into the viroplasms, which if correct points to the presence of two separate species of positive sense RNA those that exit from the viroplasms which act as mRNA and those that are retained within the viroplasms that are utilised as templates for minus strand synthesis and the formation of dsRNA (Silvestri *et al.*, 2004).

Cis-acting signals involved in genome replication have been localised within the 26 3'-terminal non-coding region *in vitro* (Chen *et al.*, 1994). Deletion mutants were analysed to define the minimal promoter for minus strand synthesis which was found to be the seven 3' terminal nucleotides 5'UGUGACC-3' (Wentz *et al.*, 1996; Patton *et al.*, 1996). The 5' UTR and the initial part of the 3' UTR have been shown to contain sequences that stimulate RNA replication. They are thought to act by complementary binding to create a pan handle structure which promotes RNA replication (Chen & Patton, 1998). The single stranded nature of the 3'-terminus in this structure has been shown to be essential for minus strand synthesis (Chen *et al.*, 2001). Complementary oligonucleotides to non-conserved sequences present either at the 5' or 3' termini blocked replication of their specific target gene but not that of other viral genes, indicating that non-conserved sequences in the rotavirus segment

terminal regions contain gene specific information that promotes RNA replication (Barro *et al.*, 2001).

1.6.7. Virus assembly and release

Rotaviruses are thought to assemble sequentially with the VP2 layer being applied to the pre-core followed by the VP6 layer to form double-layered particles (Patton & Gallegos, 1990). Both these processes occur within the viroplasms (Richardson *et al.*, 1986).

The double-layered particles move from the viroplasms by budding into the ER, a process that leaves a transient membrane around the double-layered particle. Rotavirus maturation is dependent on the Ca^{2+} concentration (Shahrabadi & Lee, 1986) and double-layered particles will not bud into the ER in the absence of Ca^{2+} (Shahrabadi *et al.*, 1987).

VP7 and NSP4 are localised within the ER and are co-translationally glycosylated before insertion into the ER membrane (Ericson *et al.*, 1983; Kabcenell & Atkinson, 1985). The C-terminus of NSP4 has been proposed to be the intracellular receptor for double-layered particles and mediate their transport into the ER (Au *et al.*, 1993; Taylor *et al.*, 1992; Taylor *et al.*, 1993), NSP4 has also been implicated as being involved in the removal of the transient membrane from budded double-layered particles (Tian *et al.*, 1996) a process that involves NSP4 glycosylation (Suzuki *et al.*, 1984). It is within the ER that the outer layer of VP4 and VP7 is assembled to give mature virions in a process that is not fully understood (Estes, 2001).

Once mature virions have been assembled they are released by host cell lysis (Altenburg *et al.*, 1980; McNulty *et al.*, 1976). However, a large fraction of this viral yield remains associated with cell debris after lysis, suggesting a possible role for the cellular cytoskeleton in virus assembly and transport (Musalem & Espejo, 1985).

1.7. Effect on host cell

Rotaviruses infect mature enterocytes of the villi of the small intestine leading to shortening and atrophy of the villi, distended cisternae in their ER, mitochondrial swelling and sparse irregular microvilli (Moon, 1994). Malabsorption of damaged intestinal villus enterocytes has been thought to be the major contributing factor to rotavirus induced diarrhoea. However, studies on piglets and mice detected diarrhoea ahead of detectable damage to the villi (Ward *et al.*, 1996; Shaw *et al.*, 1995). This observation has led to the suggestion that the enteric nervous system (ENS), activated by intestinal inflammation is a major contributing factor in the onset of diarrhoea by triggering secretion of electrolytes and water from the small intestine (Lundgren *et al.*, 2000). The intestinal inflammation observed may be related to the toxic effects of the NSP4 protein which causes an increase in Ca^{2+} permeability of the membrane (Tian *et al.*, 1994).

Host cell shut off has been detected in infected cells by 4 hours post infection (McCrae & Faulker-Valle, 1981) and recently the NSP3 protein has been shown to be involved in the shut off of cellular translation (Padilla-Noriega *et al.*, 2002). The membranes of infected cells also display increased permeability to calcium, sodium and potassium at 4 hours post infection (Michealgeli *et al.*, 1991).

1.8. Vaccine development

The mortality and economic cost of rotavirus related disease has prompted efforts to develop an effective vaccine. Several problems have been encountered in the development of a vaccine, the complex nature of the protective immune response against infection, the great antigenic diversity of rotaviruses, the variety of animal reservoirs, and the short lived nature of the protective immunity (Offit, 1994; Conner *et al.*, 1994). Most efforts have concentrated on the generation of live attenuated strain vaccines in order to stimulate local intestinal immunity as evidence has suggested that protection is related to the generation of IgA antibodies (Offit, 1994; Kapikain *et al.*, 2001).

Initial vaccine efforts focused on a Jennerian approach using an attenuated antigenically related virus derived from a non-human host (Kapikian, 1994). The first three vaccines generated by this method had varying ranges of efficacy with between 0 and 76% protection against any rotavirus diarrhoea and 0 to 100% against severe disease (Parashar *et al.*, 1998). In order to improve the efficacy of the vaccine a modified Jennerian approach was developed, in this approach a human/animal recombinant virus was constructed expressing all of the four major serotype VP7 molecules (Parashar *et al.*, 1998).

The Rotashield^{TM} vaccine was launched in 1998 by Wyeth Lederle and was a rhesus-human reassortant tetravalent (RRV-TV) rotavirus vaccine. The vaccine was approved by the food and drug administration (FDA) in the USA and recommended by both the Advisory Committee on Immunization Practice (ACIP) and the American Academy of Paediatrics for vaccination to begin on children in the USA.

Over the following nine months 1.2 million doses were given to an estimated 600,000 children (Glass *et al.*, 2005). In July of 1999 the Center of Disease Control (CDC) reported that 15 cases of intussusception had been identified by the vaccine adverse events reporting system (VAERS) (CDC, 1999). Later that month the vaccine was suspended and by October had been withdrawn from the market by Wyeth Lederle (Glass *et al.*, 2005).

Since the withdrawal of the Rotashield® vaccine two new live attenuated vaccines are under development. Merck are developing RotaTeq® which is a pentavalent human-bovine reassortment and GlaxoSmithKline (GSK) are developing RotaRix® a monovalent attenuated human serotype G1 strain (Glass *et al.*, 2005).

1.9. Aims of Study

The aim of this thesis was to investigate the function(s) of the gene products of gene 11, the smallest of the rotavirus gene segments. Features of the NSP5 and NSP6 proteins were studied *in vitro* and *in vivo* in order to elucidate greater understanding of these two rotavirus non-structural proteins of unknown function.

Materials and Methods

Chapter 2

2.1. Suppliers

General chemicals were supplied by BDH Laboratory Suppliers, Fisher Scientific Equipment (Loughborough, Leicestershire), Merck Ltd., (Poole, Dorset) and Sigma-Aldrich Company Ltd, (Gillingham, Dorset), all were of an analytical and/or molecular biological grade. Double distilled water was always used throughout this study. Unless otherwise stated equipment and reagents were obtained from the following suppliers:

Applied Biosystems (Warrington, Yorkshire)

BigDye Terminator (v3.1) Ready Reaction Cycle Sequencing Kit.

Bio-Rad Laboratories (Hemel Hempstead, Hertfordshire)

Ammonium persulphate, N,N-methylene-bis-acrylamide, TEMED, sodium dodecyl sulphate (SDS).

Difco Laboratories (Basingstoke, Hampshire)

Bacto-agar, Bactor-tryptone, Yeast extract.

Fermentas UAB (Vilnius, Lithuania)

Prestained Protein Ladder 10-180 KDa. restriction and modification enzymes.

Fuji Photo Film Company Ltd (Tokyo, Japan)

Fuji medical X-ray film.

GE Healthcare, Amersham Biosciences (Amersham, Buckinghamshire)

Hybond^{TM} Nitrocellulose membranes, DAPI, Glutathione Sepharose 4B, RNAguard ^{TM} RNase inhibitor (porcine), [^{35}S] Methionine (37TBq/mmol), α-[^{32}P] UTP (30TBq/mmol), Amplify^{TM} fluorographic reagent.

Gibco-BRL Life Technolnologies Ltd. (Renfrewshire)

Restriction and modification enzymes, *Taq* DNA polymerase, 1 Kb DNA marker, T_4 RNA ligase.

Harlan Sera Labs (Bicester UK)

Monospecific anti-NSP5 sera.

Invitrogen Corporation, R & D Systems Ltd (Abingdon, Oxfordshire)

TA Cloning^{TM} System, restriction and modification enzymes, *Taq* DNA polymerase, 1 kb DNA ladder, Lipofectamine^{TM} 2000 Reagent, G418.

Immune Systems Ltd. (ISL), (UK)

Monospecific anti-NSP6 sera.

Molecular Probes Europe BV (Leiden, The Netherlands)

Alexafluor 466 and 594 secondary antibodies

Isoproply-β-D-thigalactopranoside (IPTG), Guanidine Hydrochloride.

New England Biolabs (UK) Ltd (Hitchin, Hertfordshire)

Restriction enzymes.

Novagen, Merck Biosciences Ltd., (Beeston, Nottinghamshire)

Restriction grade Factor Xa, Protease Inhibitor Cocktail II, PET 42b cloning kit, pET15 vector,

Promega (UK) Ltd, (Southampton)

Taq DNA polymerase, Reverse Transcriptase.

TNT® quick coupled Transcription/translation system.

Qiagen Ltd, (Crawley, West Sussex)

Gel extraction kit, DNA miniprep, QIA quick Gel extraction kit, QIAprep Spin Mini prep kit.

Roche Diagnostics Ltd, (Lewis, East Sussex)

Complete, Mini, EDTA-free protease inhibitor cocktail tablets.

Sigma-Aldrich Company Ltd (Gillingham, Dorset)

Butanol (molecular biology grade), trypsin, kanamycin, ampicillin, SigmaSpin™ Maxiprep kit, FITC conjugated goat anti-rabbit Immunoglobulin, High capacity Nickel Chelate Affinity Matrix (Ni-CAM) resin.

Stratagene (UK)

PhrGFP-C vector, phrGFP-N vector.

Whatman International Ltd (Maidstone, Kent)

Filter paper Grade 5 (70mm)

Department of Biological Sciences, University of Warwick – Media Preparation

LB broth, LB agar, MEM, G-MEM, DMEM, penicillin-streptomycin, Versene, trypsin, phosphate buffered saline (PBS), 10X TBE, 10X protein running buffer, 10X protein transfer buffer.

2.2. Materials

2.2.1. Standard buffers and solutions

5X SDS-PAGE loading buffer: 0.312M Tris-HCL (pH 6.8) 5% (w.v) SDS, 25% (v/v) β-mercaptoethanol, 25% (v/v) glycerol, 0.25% (v/v) bromophenol blue.

SDS-PAGE Staining solution: 0.1% Coomassie blue, R 50% Methanol, 10% glacial Acetic acid.

SDS-PAGE Destaining solution: 5% Methanol, 10% glacial Acetic acid.

4X Bis-Tris sample buffer: 4.0g Glycerol, 0.689g Trisma base, 0.666g Tris-HCl, 0.8 g SDS, 6mg EDTA in 10ml solution.

5 X Agarose gel loading buffer: 5X TAE/TBE, 50% (v/v) glycerol, 0.01% (w/v) bromophenol blue, 0.01% (w/v) xylene cyanol ff.

Chloroform/Isoamyl alcohol: 96% chloroform, 4% (v/v) iso-amyl alcohol.

Luria Broth (LB): 1% (w/v) bactotryptone, 0.5% (w/v) NaCl, 0.5% (w/v) yeast extract.

LB agar: LB containing 1.5% (w/v) bacto-agar

Phosphate buffer saline (PBS): 137mM NaCl, 2.7mM KCL, 4.3mM Na_2HPO_4, 1.4mM KH_2PO_4.

Phenol/chloroform/Isoamyl alcohol: 50% (v/v) Tris buffered phenol, 48% (v/v) chloroform, 2% (v/v) iso-amyl alcohol.

TAE (1X): 40mM Tris Acetate, 2mM EDTA pH 8.0.

TBE (1X): 89mM Tris. base, 89 mM boric acid, 2mM EDTA pH 8.0.

TE: 10mM Tris. HCL pH 8.0, 1mM EDTA.

Tissue Culture Media: Sterile PBS, Trypsin (0.25% in Tris-Saline), Versene (0.02% in PBS), L-glutamine (200mM), 5% $NaHCO_3$, penicillin and streptomycin sulphate (100,000,000U/100g in 200ml PBS), and tissue culture media including: Dulbecco's modification of Eagle's minimal essential medium (DMEM), Glasgow's modification of Eagle's minimal essential medium (GMEM) plus non-essential amino acids (NEAA; 0.89g L-alanine, 1.15g L-asparagine·H_2O, 1.33g L-aspartic acid, 0.75g glycine, 1.45g L-glutamic acid, 1.15g L-proline and 1.05g L-serine/litre) and 1X, 2X and GMEM minus methionine, valine, leucine and $NaHCO_3$. Preparation of the above was by the media preparation staff of the Department of Biological Sciences, University of Warwick. Foetal Calf Serum purchased from Gibco BRL.

2.2.2. Bacterial Strains.

The Bacterial strains *E.coli* INVαF' was obtained from the invitrogen TA Cloning™ System TA. The pET system host strain *E. coli* BLR (DE3) was obtained from Dr. D. Stott, University of Warwick.

2.2.3. Bacterial Growth Conditions.

The *E. coli* strains and BLR (DE3) were grown in LB media in the presence of absence of appropriate antibiotic. Liquid media was converted to solid media by the addition of agar (15g/L) prior to autoclaving.

2.2.4. Oligonucleotide Primers for PCR

Primer name	Sequence	Details
NSP6 ORF PCIneo 5'	5-GCGCTCGAGACCATGAATCATCTTCAACAGCGTCAAC-3'	5' primer to insert NSP6 ORF into the PCIneo vector
NSP6 ORF PCIneo 3'	5'-GCGTCTAGATCACTTTAATTCCTTTATTAAAG-3'	5' primer to insert NSP6 ORF into the PCIneo vector
NSP5 His tag 5'	5'-GCGCATATGCACCACCACCACCACCACATGTCTCTCAGTATTGACGTGAC-3	5' primer used for the addition of a 6 histidine tag for the NSP5 ORF
NSP5 His tag 3'	5'-CTGCAGGTGACCTCTCAGGTCAGACCTACA- 3'	3' primer used for the addition of a 6 histidine tag for the NSP5 ORF
NSP6 His tag 5'	5'-GCGCATATGCACCACCACCACCACCACATGAATCATCTTCAACAGCGTCA-3	5' primer used for the addition of a 6 histidine tag for the NSP6 ORF
NSP6 His tag 3'	5'-CTGCAGGATGAATCTAGGTTCGCATTCACT-3'	3' primer used for the addition of a 6 histidine tag for the NSP6 ORF
NSP6 ORF phrGFP-N1 5'	5'-GGAATTCCTCGAGGGCTTTAAAGCGTCTCAGTCG-3'	5' primer used to insert the NSP6 ORF into the phrGFP-N1 vector
NSP6 ORF phrGFP-N1 3'	5'-GCGTCTAGACTGCAGGTCACATAAGCGCTTTCTATTCTTG-3'	3' primer used to insert the NSP6 ORF into the phrGFP-N1 vector
Actin ORF PCIneo 5'	5'-GCAGGCTAGCATGGATGATGATATCGCCGCGCT-3'	5' primer used to insert the actin ORF into the PCIneo vector

Actin ORF PCIneo 3'	5'-GCGGCTCGAGCTAGAAG CATTTGCGGTGGA-3'	3' primer used to insert the actin ORF into the PCIneo vector
Gene11-CAT Step 1	5'-TCTTCTAGTATTTATAAA AATGGAGAAAAAAATCA CTGGATATAC-3'	First 5' primer used for the addition of the 5' of gene 11 to the 5' of the CAT ORF
Gene11-CAT Step 2	5'-GACGTGACGAGTCTTCC TTCTATTTCTTCTAGTAT TTATAAAAATGATGGA-3'	Second 5' primer used for the addition of the 5' of gene 11 to the 5' of the CAT ORF
Gene11-CAT Step 3	5'-GCGGCG CTC GAG ATG TCT CTC AGT ATT GAC GTG ACG AGT CTT CCT TCT ATTTC-3'	Third 5' primer used for the addition of the 5' of gene 11 to the 5' of the CAT ORF
Gene11-CAT Step 4	5'-GCGCTCGAGGGCTTTTA AAGCGCTAAAGTGATGT CTCTCAGTATTGACGTGA CGAGTC-3'	Forth 5' primer used for the addition of the 5' of gene 11 to the 5' of the CAT ORF and for insertion into the PCIneo vector
Gene11-CAT 3' primer	5'TATTCTAGATTACGCC CCGCCCTGC-3'	3' primer used for the amplification of the gene11-CAT fusion for cloning into the PCIneo vector
Gene11 PCIneo 5'	5'-GCGCTCGAGGGCTTTTA AAGCGCTACAGTG-3'	5' primer to insert gene11 sequence into the PCIneo vector
Gene11 PCIneo 3'	5'-GAATCTAGACTGCAGGT CACAAAACGGGTGTGGG G-3'	3' primer to insert gene11 sequence into the PCIneo vector
NSP5 ORF PCIneo 5'	5'-GCGCTCGAGTACAGTGA TGTCTCTCAGTAT-3'	5' primer to insert NSP5 ORF into the PCIneo vector
NSP5 ORF PCIneo 3'	5'-GCGTCTAGAACCTCTCA GGTCAGACCTACA-3'	3' primer to insert NSP5 ORF into the PCIneo vector

NSP5 phrGFP-N1 5'	5'-CGCGAGCTCATGTCTCTCAGTATTGACGTG-3'	5' primer used to insert the NSP5 ORF into the phrGFP-N1 vector
NSP5 phrGFP-N1 3'	5'-GCCAAGCTTCTACAAATCTTCGATCAATTGCAT-3'	3' primer used to insert the NSP5 ORF into the phrGFP-N1 vector
ORF1 5' *Cla* I	5'-CCTATCGATGTCTCTCAGTATTGACGTGACGAGTCT-3'	5' primer used to clone ORF1 into TA 2.1 before insertion into the pET-42b vector
ORF1 3'	5'-CTGCAGGTGACCTCTCAGGTCAGACCTACA-3'	3' primer used to clone ORF1 into TA 2.1 before insertion into the pET-42b vector
ORF2 5' *Cla* I	5'-CAGATCTGGCCATCGATGAATCATCTTCAA-3'	5' primer used to clone ORF2 into TA 2.1 before insertion into the pET-42b vector
ORF2 3'	5'-CTGCAGGATGAATCTAGGTTCGCATTCACT-3'	3' primer used to clone ORF2 into TA 2.1 before insertion into the pET-42b vector
Gene11 a22g 5'	5'-GCGCTACAGTGGTGTCTCTCAGTAT-3'	5' primer used for site directed mutagenesis of gene11 ATG start codon
Gene11 a22g 3'	5'-ATACTGAGAGACACCACTGTAGCGC-3'	3' primer used for site directed mutagenesis of gene11 ATG start codon
Gene11 t25g 5'	5'-GCTAGCCTCGAGATGGCTCTCAGTATTGAC-3'	5' primer used for site directed mutagenesis to improve kozak consensus sequence at ORF1 start codon
Gene11 t25g 3'	5'-GTCAATACTGAGAGCCATCTCGAGGCTAGC-3'	3' primer used for site directed mutagenesis to improve kozak consensus sequence at ORF1 start codon
Gene11-CAT-PCIneo g19a, a20c, g21c, t25g 5'	5'-GAGGGCTTTTAAAGCGCTACAACCATGGCTCTCAGTATTGACGTGACG-3'	5' primer used for site directed mutagenesis to improve kozak consensus sequence at ORF1 start codon

Gene11-CAT-PCIneo g19a, a20c, g21c, t25g 3'	5'-CGTCACGTCAATACTGAGAGCCATGGTTGTAGCGCTTTAAAAGCCCTC-3'	3' primer used for site directed mutagenesis to improve kozak consensus sequence at ORF1 start codon
Gene11 t23c 5'	5'-GCTAGCCTCGAGACGTCTCTCAGTATTGAC-3'	5' primer used for site directed mutagenesis of gene11 ATG start codon
Gene11 t23c 3'	5'GTCAATACTGAGAGACGTCTCGAGGCTAGC-3'	3' primer used for site directed mutagenesis of gene11 ATG start codon

2.3. Cell Culture

2.3.1. Cell lines.

The tissue culture cell line used in this study was BSC1 African Green Monkey Kidney epithelial ECACC No 85011422 (ECACC: European Collection of Cell Cultures) cells were grown in GMEM supplemented with 5% FCS growth medium and L-glutamine (2mM), penicillin (100U/ml) and streptomycin (100μg/ml).

2.3.2. Maintenance of tissue culture cells

Mammalian cell lines were maintained at 37°C in a 5% CO_2 incubator in a humidified atmosphere (150cm^2 flasks) using the appropriate media. When confluent, the cells were passaged as follows: cells were detached by rinsing the monolayer twice with versene followed by incubation with trypsin/versene (1:5) and disaggregation. Cells were re-seeded at a ratio of 1:4. All manipulations were

performed under sterile conditions in a Class II Laminar Flow Cabinet using standard aseptic techniques.

2.3.3. Freezing and recover of cell stocks

Cell stocks were prepared by suspending the cells from a 150cm^2 flask in 2ml of 8% (v/v) dimethylsulphoxide (DMSO) and 30% FCS in GMEM. Freezing vials were cooled slowly to –70% before immersion in liquid nitrogen for long term storage. Cell stocks were recovered by rapidly thawing at 37°C and adding the contents of one vial to a 150cm^2 flask containing pre-warmed medium. The medium was changed or the cells passaged the following day.

2.4. Antibody Production

2.4.1. Anti-NSP5

Monospecific anti-NSP5 serum was generated by Harlan Sera Labs (Bicester, UK). A single guinea pig was pre-bled and tested for rotavirus antibodies by indirect immunofluorescence. When the animal tested negative, it was injected i.m. with 200µl containing 25µg of purified His-NSP5 in PBS in the presence of Freud's complete adjuvant. The animal was sacrificed at day 30 and a final bleed taken.

2.4.2. Anti-NSP6

Monospecific anti-NSP6 was generated by ISL Ltd. A New Zealand White-Barrier rabbit was pre-bled and tested for rotavirus antibodies by indirect immunofluorescence. When the animal tested negative, it was injected intramuscularly (i.m.) with 500µl containing 200µg of purified NSP6 in PBS in the presence of Freud's complete adjuvant. The animal was boosted with the same dose 14 days later and five 5 ml bleeds were taken at 14 day intervals. The animal was sacrificed and a final bleed taken at day 70.

A second monospecific antisera was generated by Harlan Sera Labs (Bicester, UK). Two rats were pre-bled and tested for rotavirus antibodies by indirect immunofluorescence. When the animals tested negative, it was injected i.m. with purified His-NSP6 100 µl containing 20 µg of purified His-NSP6 in PBS in the presence of Freud's complete adjuvant. The animal was boosted with the same dose 7 days later and again 7 days after that followed a 200 µl test bleed taken 7 day after the final boost. The animals were sacrificed at day 35 and a final bleed taken.

2.5. Tissue Culture based assays and analysis

2.5.1. Virus Strains

The tissue culture adapted Compton UK (Uktc) strain of bovine rotavirus (G serotype 6) was provided by Prof. M.A. McCrae.

2.5.2. Transfection

For transient transfections BSC-1 cells were grown to 80% confluence in 12 well plates and transfected with 1.6μg DNA and 2μl Lipofectamine 2000 (Invitrogen). At 8 hours post transfection the DNA mix was removed and the cells overlaid with 2ml GMEM 1% FCS and incubated for a further 40 hours. For experiments requiring transfection of a plasmid followed by infection with UKtc rotavirus the cells were infected at an m.o.i. of 3 at 48 hours post transfection and then fixed 8 hours post infection.

2.5.3. Immunofluorescence microscopy and antibodies

Expression of green fluorescent protein (GFP) was monitored by confocal microscopy. Transfected cells were washed once with phosphate buffered saline (PBS) and then fixed in 100% methanol at -20°C for 20 minutes and then washed twice with PBS. Transfected cells that were subsequently infected were fixed using the same procedure at 8 hours post infection. The intracellular distribution of NSP5 was monitored by indirect immunofluorescence. For this, confluent BSC-1 cells grown in 6 well tissue culture dishes were infected with the UKtc strain of bovine rotavirus at an m.o.i. of 3 and incubated for 2, 4, 6, 10, 16, or 24 hours p.i. To stain for NSP5 coverslips were blocked in 1% bovine serum albumin (BSA) in PBS for 1 hour, washed 3 times in PBS and then incubated with guinea pig anti-NSP5 serum (1:100) in PBS 1% BSA for 1 hour. The coverslips were then washed 3 times with PBS and incubated with (1:100) Alexafluor 594 conjugated goat anti-guinea pig

serum (Molecular probes) and mounted for confocal microscopy using vector shield mounting media (Vector Laboratories).

2.5.4. Pulse-chase analysis

Confluent BSC-1 cells grown in 6 well tissue culture dishes were infected with the UKtc strain of bovine rotavirus at an m.o.i. of 3. To analyse the time course of NSP6 synthesis cells were incubated in methionine free medium until it was replaced with 200μCi of [^{35}S] methionine diluted in methionine free medium. Pulse labelling for 1 hour intervals was carried out starting at 1 hour post infection. For pulse-chase studies, cells were incubated for 3 hours after infection in methionine free GMEM and then radio-labelled for 5 hours in GMEM containing approximately 200μCi of ^{35}S methionine. Where appropriate a two hour chase was carried out by incubating radio-labelled cells in GMEM containing 50X the normal methionine concentration. Radio-labelled cells were harvested into 500μl of RIPA lysis buffer (50mM Tris-HCl buffer pH 7.4, 150mM NaCl, 1mM EDTA, 1% Triton X100, 1% Sodium deoxycholate, 0.1% SDS and 1 tablet per 10ml of Complete mini EDTA free protease inhibitor cocktail (Roche).

2.5.5. Immunoprecipitation

Immunoprecipitations were carried out by mixing 250μl of radio-labelled cell lysate with an equal volume of 2X IP-3 buffer (20mM Tris-HCl buffer pH 8.0, 100mM NaCl, 1mM EDTA, 1% NP-40, 1% sodium deoxycholate) and adding 20μl of hyper-immune guinea pig anti-NSP5 or rabbit anti-NSP6 serum. After 2 hours of

incubation at 4°C, 5mg/100µl of pre swollen protein A-sepharose CL-4B beads (Amersham) were added and incubation continued for a further 2 hours at 4°C. The beads were concentrated by centrifugation and resuspended in IP-2 buffer (20mM Tris-HCl buffer pH 8.0, 100mM NaCl, 1mM EDTA, 1% NP-40, 1% Na-deoxycholate, 20mg BSA). They were then washed sequentially in IP2 buffer containing 1M NaCl, IP-3 buffer (2X) and IP-1 buffer (20mM Tris-HCl buffer pH 8.0, 100mM NaCl, 1mM EDTA, 1% NP-40). Finally the beads were resuspended in 40µl of Tris-HCl pH 8.0 and 10µl cracking buffer (50mM Tris-HCl pH 8.0, 10% SDS, 2.5% β-mercaptoethanol, 50% glycerol and 0.01% bromophenol blue) added. Samples were then boiled for 5 minutes and proteins fractionated by PAGE on a 14% gel. After electrophoresis the gel was fixed for 30 minutes (30% methanol-10% acetic acid), soaked in Amplify (GE Healthcare) for 30 minutes, dried and fluorographed at -70°C.

2.6. Molecular Biology techniques

2.6.1. Quantification of DNA

DNA was quantified by spectrophotometry. Absorbance readings was taken at 260nm where an absorbance of 1.0 was taken as indicating a concentration of 50µg/ml for double stranded DNA or 20µg/ml for a single stranded DNA primer.

2.6.2. Agarose gel electrophoresis

DNA samples were analysed on agarose gels containing between 0.8% and 1.5% agarose and 1μg/ml ethidium bromide in 1X TAE/TBE. DNA samples and 1Kb ladder were prepared by the addition of 1/5 volume of 5 X TAE/TBE agarose gel loading buffer before being loaded into the preformed wells. Electrophoresis was performed at 70mA in 1X TAE/TBE running buffer for 60 – 90 minutes. Bands were visualized using Grab-IT (Ultraviolet Products Ltd., Cambridge), an annotating image capture system and printed on a digital graphic printer.

2.6.3. Phenol/Chloroform extraction

An equal volume of phenol/chloroform/isoamyl alcohol was added to the DNA solution and mixed by vortexing. The phenol/chloroform/isoamyl alcohol fraction was separated from the aqueous phase by centrifugation for 1minute in a microcentrifuge. The upper phase was removed and the lower phase discarded. The process was repeated and the resulting DNA solution was ethanol precipitated. An additional extraction using chloroform/isoamyl alcohol was performed before ethanol precipitation if additional purity was required.

2.6.4. Ethanol precipitation of nucleic acids

DNA was precipitated from solution by the addition of sodium acetate pH 5.2 to a final concentration of 0.3M and 2.5 volumes of ice-cold 100% ethanol. After precipitation for 30 minutes – 1 hour at -20°C, DNA was pelleted by centrifugation in a microcentrifuge for 20 minutes at 15,000 rpm. The pellet was washed with 70%

(v/v) ethanol, dried under vacuum and resuspended in 50mM Tris-HCl pH 8.0 or TE buffer. Otherwise, one volume of isopropanol was used in place of 2.5 volume of ethanol to precipitate DNA.

2.6.5. Dephosphorylation of vector DNA

The 5' phosphate groups were removed from DNA using bacterial alkaline phosphatase (BAP) under the conditions recommended by the manufacturer. BAP was inactivated and removed by phenol/chloroform extraction

2.6.6. Restriction enzyme digestion of DNA

Restriction enzyme digests were performed under the manufacturer's recommended conditions using the supplied 10X buffer solutions.

2.6.7. Blunt-ending of DNA

Protruding 5' extensions were removed using Mung Bean Nuclease under the conditions recommended by the manufacturer or filled using the Klenow fragment of *E. coli* DNA polymerase I (Sambrook *et al.*, 1989).

2.6.8. Recovery of DNA from agarose gel

DNA bands were excised from agarose gels under UV light using a sterile scalpel blade. The DNA was recovered using the QIAquick Gel Extraction Kit (Qiagen) according to the manufacturer's instructions.

2.6.9. Ligation of DNA fragments

DNA fragments were ligated into dephosphorylated DNA vector molecules. Ligation was allowed to precede at 15°C overnight and contained insert DNA, vector DNA, 1.5µl 10X ligation buffer (0.66M Tris-HCL pH 7.6, 50mM $MgCl_2$, 50mM DTT, 100mM ATP) and 1 unit T4 DNA ligase in a total volume of 15µl. The DNA ligation mixture was ethanol precipitated and the vacuum dried pellet resuspended in 50µl of distilled water.

TA cloning of PCR products into PCR2.1 (Invitrogen) was performed as per manufacturer's instructions using supplied reagents.

2.6.10. PCR amplification of viral genes

A standard PCR was performed in a final volume 25µl. This contained 200ng of template DNA, 0.5µM primer mixture, 1 X PCR mixture (2.8µl 10 X PCR buffer, 200µM dNTPs, 4.5mM $MgCl_2$, sterile water), and 2.5 units Taq polymerase. The solution was overlaid with 50µl liquid paraffin and subjected to 1 cycle of 94°C for 5 min and 53°C or 55°C for 1 min. 45 sec., 3 cycles of 72°C for 3 min., 95°C for 45 sec., and 53°C or 55°C for 1 min. 45 sec., 30 cycles of 72°C for 3 min., 95°C for 45 sec., and 53°C or 55°C for 45 sec, and 1 cycle 72°C for 10 min. 3µl of reaction mixture was then analysed by 0.8% agarose gel electrophoresis. In some cases, adjustments of the thermal cycling parameters were necessary to improve amplification specificity and target DNA yield.

2.6.11 RT-PCR reactions

RT-PCR reactions were performed using RMV reverse transcriptase. 600ng of viral dsRNA, 200ng of each primer and 0.5µl of RNA guard (Amersham) was made up to a final volume of 30µl. This dsRNA-primer mix was then incubated at 95°C for 2 minutes followed by 40°C for 4 minutes. A 2X reaction mixtures containing 5µl 10% Triton X, 50µl 25mM $MgCl_2$, 50µl 10X *Taq* polymerase PCR buffer, 16µl 1.5mM dNTP mix, 2µl RNA guard, 125µl dH_2O and 1.5µl AMV reverse transcriptase was prepared. 30µl of the 2X reaction mix was then dispensed into each RT-PCR reaction. The combined reaction mix and dsRNA-primer mix (final volume 60µl) was then incubated for 60 minutes at 42°C. At the end of the 60 minute incubation 0.5µl *Taq* DNA polymerase was added to each reaction. Following this the reactions were mixed and subjected to 40 cycles of 95°C for 1 min, 45°C for 1 min and 72°C for 3 minutes. Following this 1 cycle at 72°C for 10 min was performed.

2.6.12 CAT assays

The detection of CAT was performed using a Roche kit all procedures were carried out as per the manufacturer's instructions.

2.6.13 *In vitro* transcription and translation

The *In vitro* transcription and translation assays were performed using the TnT Quick couple *In vitro* transcription and translation system from Promega. All reactions were carried out as per the manufacturer's instructions

2.6.14. Preparation of competent cells for electroporation

Electro-competent *E.coli* cells were prepared by washing 200ml of mid log phase bacteria (OD_{590} = 0.4 – 0.5) twice with sterile ice-cold water. The bacteria were resuspended in 15ml of ice-cold water, washed again and resuspended in 0.5ml sterile ice-cold water.

2.6.15. Transformation of DNA into bacteria by electroporation

50µl of electro-competent bacteria were mixed with 10µl salt free ligated DNA or control DNA and pulsed in a BioRad Gene Pulse at 2.5kV with 25µF set as capacitance and 200Ω set on the pulse controller. Cells were immediately diluted into to 0.7ml LB and allowed to recover by shaking for 30 min at 37°C. The bacteria were then plated onto selective agar plates containing appropriate antibiotics and incubated overnight at 37°C. Recombinant clones were identified by restriction enzyme analysis of mini-prep DNA

2.6.16. Small scale preparation of plasmid DNA from bacteria (mini-prep)

Individual bacterial colonies were picked from agar plates into 10ml LB medium containing appropriate antibiotics and incubated overnight with continuous shaking at 37°C. For restriction enzyme analysis the plasmid DNA from 1.5ml of culture was prepared using an alkaline lysis technique (Sambrook *et al*, 1989) and the DNA pellets resuspended in 50µl 50mM Tris-HCl pH 8.0. For sequence analysis the plasmid DNA from 5ml of culture was isolated using the QIAprep Spin Miniprep Kit (Qiagen) according to manufacturer's instructions.

2.6.17. Large scale preparation for plasmid DNA from bacteria (maxi-prep)

10ml of LB containing appropriate antibiotics was inoculated with a single colony and incubated overnight with continuous shaking at 37°C. The overnight culture was subcultured into 1L of LB plus appropriate antibiotics and incubated O/N at 37°C with shaking. Maxipreps were carried out using a SigmaSpin™ Maxiprep kit (Sigma-Aldrich) as per manufacturer's instruction.

2.6.18. Vectors.

The pET expression vector pET42b was obtained from Novagen (Nottingham) and pET-15 was originally obtained by the rotavirus laboratory from Dr. D. Roper, University of Warwick. The pET-42b ™ vector was obtained from Novagen and pET4215b was created by Keun-Taik Chung (University of Warwick). The pET-His-NSP5 and pET-His-NSP6 plasmids were constructed by first cutting the pET42b vector (Novagen) with the restriction enzymes *Nde*I and *Pst*I to remove the GST tag region of the plasmid. The coding region of NSP5 and NSP6 were then amplified with specific primers containing an *Nde*I restriction site followed by 6 histidine residues at the 5' terminus and a *Pst*I restriction site at the 3' terminus of the ORF's. This PCR product was then cleaved with these restriction enzymes and ligated into the prepared pET42b vector.

The GFP-NSP6 and GFP-NSP5 plasmids were constructed by using PCR to generate a product of the NSP5 and NSP6 ORF's with *Sac*I at the 5' terminus and *Hind*III at the 3' terminus. The multicloning site of the vector phrGFP-N1

(Stratagene, La jolla, California, USA) and the PCR products cleaved with *Sac*I and *Hind*III and the two cDNA's ligated.

The cellular gene actin, Gene 11 of the UKtc strain of bovine rotavirus, NSP5 ORF, NSP6 ORF, Gene11-CAT construct and Gene 7 of the UKtc strain of bovine rotavirus were all amplified using PCR with primers that introduced an *Xho*I restriction site at the 5' terminus and an *Xba*I restriction site at the 3' terminus. These PCR products were then ligated into the multicloning site of the PCIneo (Promega) vector using these restriction enzyme sites. The PCIneo vector and the CAT-PCIneo vector were both obtained from Dr A.C. Marriott, University of Warwick. The vectors containing gene segment 4 and the 5'-terminal 100 nucleotides of gene segment 5 were constructed by K.T. Chung of Warwick University (unpublished data). The Luciferase T7 control DNA vector from the TNT® Quick coupled transcription/translation system (Promega) was used for the expression of Luciferase.

2.6.19. DNA Sequencing

DNA was sequenced by the Molecular Biology Service, University of Warwick using the dideoxy method (Sanger *et al.*, 1977) with BigDye Terminator (v3.1) Ready Reaction Cycle Sequencing Kit (Applied Biosystems (ABI), Warrington UK) and carried out on a GeneAmp PCR System 9700 (ABI). Raw sequence data was generated by capillary electrokinetic injection using an ABI prism Genetic Analyzer 3100 (ABI) and collected using ABI Prism 3100 Genetic Analyzer Data Collection Software version 1.1 (ABI) and edited using ABI Prism Sequencing Analysis Software version 3.7 (ABI). Sequences were then analysed

using Chromas (v1.45, Conor McCarthy, Griffith University Australia) and the DNAStar (DNAStar 5, DNASTAR Inc., Madison, WI) software packages.

2.6.20. Transformation of Bacterial Cells by Heat Shock

INVαF' cells (Invitrogen) were transformed with plasmid DNA by heat shock following the manufacturers instructions and plated on LB agar plates containing the appropriate antibiotics.

2.7. RNA Binding Assays

2.7.1. RNA Filter binding assay

2.5cm discs of Hybond ECL nitrocellulose (GE Healthcare) were boiled for 30 minutes in deionised water and then placed into a vacuum manifold. 500µl of filter binding buffer (FBB) (20mM HEPES buffer, 100mM NaCl, 5mM EDTA, 1mM DTT) was passed through them before addition of the 100µl samples. Purified NSP5 or NSP6 at varying concentrations was incubated at 30°C in duplicate in FBB with an excess (500nM) of ^{32}P UTP labelled ssRNA produced using a megascript RNA transcription kit (Ambion). After 30 minutes incubation samples were filtered through the nitrocellulose. Filters were washed twice with 500µl of FBB, air dried, and the amount of RNA bound measured using a scintillation counter (Tri-CARB 2900TR liquid scintillation analyzer Packard Bioscience Company). To investigate the effect of NaCl concentration on RNA binding the assay was performed using FBB supplemented with various concentrations of NaCl. RNA

competition assays were carried out using a fixed amount (500nM) of radio-labelled ssRNA and increasing amounts of cold competitor ssRNA, dsRNA or dsDNA. Cold competitor nucleic acid was added at 0%, 25%, 50%, 100%, 200% and 500% of the concentration of radio-labelled ssRNA (500nM = 100%).

2.7.2. Gel mobility shift assay

A transcription plasmid carrying the 5'-terminal 100 nucleotides of bovine rotavirus (UKtc) gene 5 was used to produce a radio-labelled ssRNA probe for gel mobility shift assays. 500nM of probe was incubated with varying amounts of NSP6 protein in gel mobility buffer (20mM HEPES buffer, 100mM NaCl, 5mM EDTA, 1mM DTT, 20% glycerol) at 30°C for 30 minutes. Samples were then analysed on a 1% TBE agarose gel run at 10 milliamps for 1 hour. The gel was dried and subject to autoradiography at -70°C using an intensifying screen.

2.8. Protein Analysis

2.8.1. Mass spectroscopy

Mass analysis of purified NSP5 and NSP6 was performed using MALDI-MS (matrix assisted laser desorption/ionization mass spectrometry) (Matilda, Micromass). As confirmation LC-ESI (liquid chromatography electrospray ionization) MS/MS (Micromass Q-Tof1, Waters) was used.

2.8.2. Determination of Protein Concentration

Protein concentrations were colourimetrically determined using the Lowry Protein Assay Method (Lowry *et al.*, 1951).

2.8.3. SDS-PAGE

Protein samples were resolved by SDS-polyacrylamide gel electrophoresis as described by Laemmli *et al* (1970).

2.8.4. Visualisation of Proteins

Proteins separated by PAGE were visualized with Coomassie blue G250 as described in Ausbel *et al* (1998).

2.8.5. Western Blotting

14% SDS-PAGE gels were used to separate proteins and then Western blotting was performed using an Amersham ECL advance kit and carried out using the manufacturers recommended conditions.

2.9. Protein Purification

2.9.1. Expression of recombinant proteins

Vectors containing the tagged coding regions of NSP5 and NSP6 were transformed into the BLR strain of *Escherichia coli*. An overnight (O/N) culture was diluted 1:100 in Luria-Bertani (LB) media and incubated with shaking at 37°C until

the optical density (OD_{590}) was between 0.5 and 1. Expression of the pET constructs was then induced by addition of 0.1mM IPTG and incubation with shaking continued for a further 4 hours at 37°C. Bacterial cells were recovered by centrifugation at 6,370*g* for 10 min using a JA10 rotor (Beckman).

2.9.2. Lysis of cells by French press

Recovered cells were suspended in 10ml of PBS and disrupted by being passed twice through a French press at 10,000 psi according to the manufacture's instructions (American Instrument Company, Silver Spring, Maryland, USA).

2.9.3. Recovery of soluble and insoluble fractions

Soluble and insoluble protein fractions were separated by centrifugation at 39200*g* (Beckman JA20 rotor) for 30 minutes. The insoluble fraction was recovered by washing the insoluble pellet twice in 20ml of 20mM Tris HCl pH7.5 before being resuspended in 6M guanidine hydrochloride and left to solubilise for at least 4 hours.

2.9.4. Glutathione-Agarose column

This soluble fraction of recombinant GST fusion protein was purified using glutathione agarose (GSH-agarose). The soluble GST-fusion was loaded onto a 5ml of column GSH-agarose equilibrated with PBS, pH 7.5 at a flow rate of 1ml/min and washed with same buffer. The binding proteins were then eluted with 10mM Tris-HCl, pH 8.0, 10mM reduced glutathione. The eluted proteins were monitored at

280nm using a Pharmacia LKB UV MII monitor and collected using a Pharmacia FRAC-100 fraction collector.

2.9.5. Metal Chelating column

Denatured His tagged proteins suspended in 6M guanidine hydrochloride was then purified using FPLC. 8M urea at pH8.0 was used to equilibrate a Ni^{++} chelating column. Solublised protein was then passed over the column which was washed first with 8M urea at pH 8.0 and then with 8M urea pH 6.0. The bound His tagged protein was then eluted from the column by dropping the pH by addition of concentrated HCl to pH 4 and finally to pH 3.5. The eluted proteins were monitored at 280 nm using a Pharmacia LKB UV MII monitor and collected using a Pharmacia FRAC-100 fraction collector.

2.9.6. Stepwise refolding of purified protein

Denatured protein was eluted from the Ni^{++} chelating column in 8M urea pH 3.5. The eluted protein was then refolded by stepwise dialysis against 20mM Tris-HCl buffer. The NSP5 protein was refolded from a solution of 8M urea pH 10, adjusted from the 8M urea pH 3.5 elution buffer by addition of 10M NaOH, and refolded in a stepwise gradient from 20mM Tris HCl pH 10 to 20mM Tris HCl pH 7.5. The NSP6 protein was refolded from the 8M urea pH 3.5 in a stepwise gradient from 20mM Tris HCl pH 4 to 20mM Tris HCl pH 7.

2.10. Computer Analysis

2.10.1. Sequence Alignments

DNA and protein sequence alignments were performed electronically in MegAlign, DNAStar Inc. (Technelysium, Queensland, Australia).

2.10.2. Plasmid Maps

Graphical representation of plasmids, including genes and restriction enzyme locations were generated using Clone Manager, SciED Central, v7.02.

2.10.3. Calculation of dissociation constants

Dissociation constants were calculated using the Prism 4 software (GraphPad Software). Graphs were produced plotting the amount of probe bound versus the concentration of protein in picomoles (pM) and then the dissociation constants extrapolated from the line of best fit.

Results

Chapter 3

Purification of the Rotavirus

NSP5 and NSP6 proteins

3.1. Aims

The aims of the work described in this chapter were: i) Construct expression vectors containing the ORF's of rotavirus gene 11, ii) Purify the expressed NSP5 and NSP6 proteins iii) Generate polyclonal monospecific sera to the purified proteins.

3.2. Introduction

3.2.1. Recombinant protein expression and purification

The development of recombinant protein expression and purification has led to great advances in the understanding of protein structure and function. It has enabled the development of *in vitro* assays of protein function, in order to determine properties, such as RNA binding and enzymatic activity, as well as enabling the determination of a protein's structure by X-ray crystallography and NMR spectroscopy. Following characterisation of a gene sequence it can be used to create purified protein via a number of methods. The range of techniques by which purified protein can be obtained has become very diverse, including many possible species for expression and the exploitation of many features of proteins to secure purification. The two most common systems for protein expression use *E. coli* and baculoviruses as hosts (Kingston & Brent, 2002).

The *E. coli* system uses a plasmid carrying the coding sequence of the protein of interest transformed into the bacteria, expression is generally controlled by a chemical inducer such as IPTG. When a bacterial culture has reached the

optimal optical density the inducer is added and expression of the protein begins, its concentration can reach up to 50% of the total cell protein following induction. The advantages of this system are that it is straight forward to use, can produce a large amount of protein in a short time and is very cost effective. There are however a number of disadvantages, including the lack of appropriate post translational modification and the formation of occlusion bodies; the latter are insoluble aggregates of mis-folded protein which occur due to the high levels of protein expression. The formation of occlusion bodies is not necessarily a draw back as they can be exploited for protein purification by solublising the protein using detergents and then removing the detergents via dialysis after the purification process to refold the protein (Amersham Biosciences, 2003a).

The baculovirus expression system uses homologous recombination between the baculovirus genome and a transfer or shuttle vector carrying the gene of interest to facilitate protein expression. The transfer vector which contains the gene of interest flanked by sections of a non-essential viral gene and a linear copy of the viral genome are co-tranfected into insect cells. This allows for homologous recombination to occur creating infectious virus that will express the inserted gene of interest when used to infect more insect cells. The recombinant viruses are plaque purified with a marker gene such as beta galactosidase to aid in their identification. After the recombinant virus has been isolated and grown to a sufficient titre, the virus can be used for protein expression. Expression in the baculovirus system is carried out in insect cells and is subsequently much more likely to be correctly post translationally modified, an advantage of this system. However, there are several

disadvantages of the baculovirus system including the higher costs than that of the *E. coli* system, the longer setup time and the post translational modifications are not always exactly as in mammalian cells, this being particularly relevant for glycosylation (Amersham Biosciences, 2003a).

After expression the next step is to purify the protein of interest from other proteins in the cells being used for expression. The protein can be separated using specific features of that particular protein, for example its size, charge, hydrophobicity or its affinity for a ligand. This separation is commonly achieved by liquid chromatography (Amersham Biosciences, 2003b).

To facilitate purification, fusion proteins are often made between the protein to be purified and a protein or protein fragment that has a known (reversible) affinity to a specific ligand. These fusions are referred to as tags and can range in length from very short such as, a 6 histidine (His) residues to large proteins such as, glutathione-S-transferase (GST). The tags are exploited by employing what is termed affinity chromatography (Kingston & Brent, 2002; Amersham Biosciences, 2003b).

3.2.2. pET vector system

The pET vector system provides a powerful approach for the expression of recombinant proteins in *E. coli*. It takes advantage of the highly selective nature of the bacteriophage T7 RNA polymerase and its associated promoter sequence, coupled with the high translational efficiency of the T7 gene 10 translation initiation signals, such that after only a few hours of induction, the induced target protein can

constitute the majority of the protein present in the bacterial cell. A further advantage of employing T7 transcription and translation signals is the tight regulation that it affords, allowing the target gene to remain transcriptionally silent in the uninduced state. The pET vectors also contain an affinity tag positioned in frame with the expressed ORF so that it can be used to purify the protein. The constructed plasmid is initially transformed into a strain of *E. coli* that does not carry the T7 RNA polymerase gene thereby removing possible problems of plasmid instability due to leaky expression of toxic proteins. Expression of the target fusion protein can then be achieved by using one of two methods (i) the non-expressing *E. coli* host can be infected with the bacteriophage λCE6 which carries the T7 RNA polymerase gene, (ii) the pET vector can be transformed into an *E. coli* strain carrying the T7 RNA polymerase gene in a chromosomal cassette under the control of lacUV5. Expression can then be induced via the addition of IPTG and further incubation of the bacterial culture. Following induction the bacterial cells can be lysed and the fusion protein purified by exploiting the affinity tag and appropriate affinity chromatography (Novagen, 2003).

3.2.3. Expression vector pET42b

The pET vector pET-42b was selected for expression of the rotavirus proteins. Following insertion into this vector the viral proteins expressed would carry both GST and His tags (Figure 3.1). Either of these tags could potentially be utilised to secure purification by affinity chromatography.

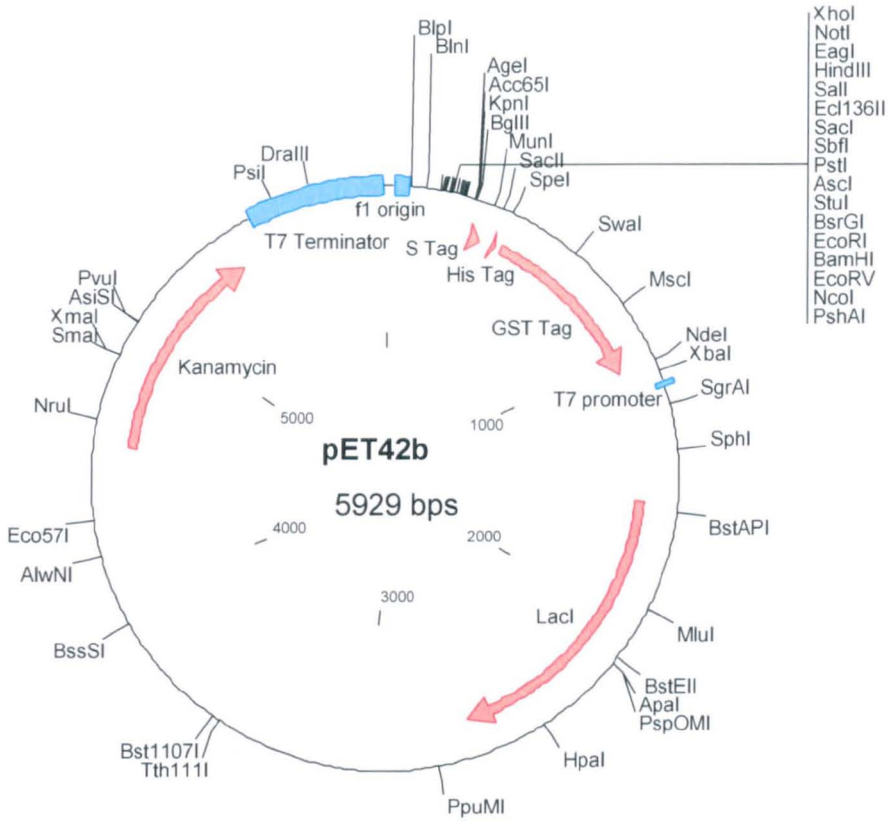

Figure 3.1 The pET42b(+) expression vector

Restriction map of the pET42b(+) cloning vector showing the 220aa GST•tag™ selected restriction enzyme sites and the T7 expression region. Also indicated is the multicloning region of the vector. A unique *Psh*AI restriction enzyme in the multicloning region when cleaved produces a blunt end cloning site allowing the insertion of the protein of interest directly after a Factor Xa protease site. The Factor Xa cleavage site can be used for the removal of the GST affinity tag after purification.

Proteins carrying a GST tag will bind strongly to glutathione immobilised on agarose and after the other proteins in the mixture have been washed away, the interaction can be reversed by the addition of buffer containing glutathione releasing the tagged protein of interest (Figure 3.2). An additional feature of pET42b is the presence of a unique *Psh*A1 restriction enzyme site within the multicloning region of the vector. Following cleavage with this enzyme a blunt end cloning site is produced and if the ATG start codon of the gene of interest can be inserted such that, it is in-frame with the vectors tags then it will follow directly after a Factor Xa protease cleavage site (Figure. 3.1) (Novagen, 2003). Following affinity purification the tags used in purifying the protein can be removed by cleavage with Factor Xa. This allows an authentic purified protein to be produced. The cleaved purification tags can then be removed from the protein of interest by rerunning the sample over the same affinity column as that used previously in purification. The affinity tags will again bind to the column whilst the protein of interest will pass straight through allowing its collection (Novagen, 2004).

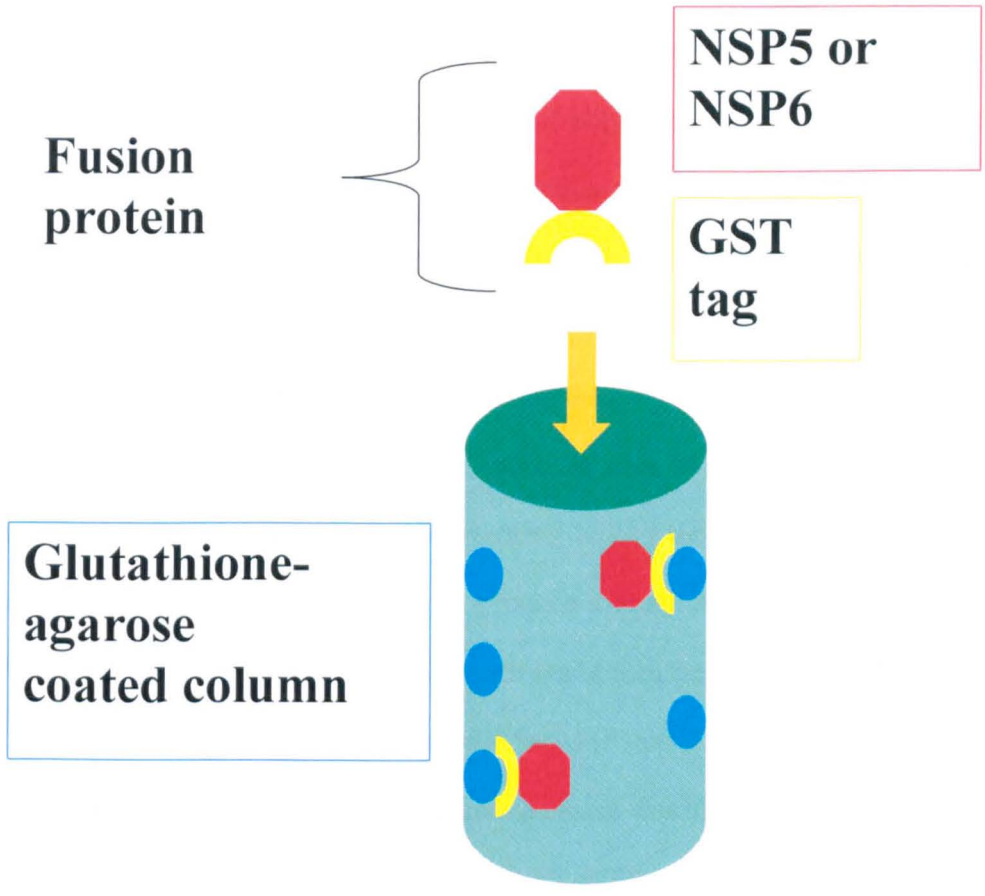

Figure 3.2 Affinity chromatography of a GST tagged protein
GST tagged protein was passed over the glutatione coated agarose and due to the affinity of GST for glutathione becomes bound whereas untagged proteins pass through the resin. The bound GST tagged protein can then be eluted using a washing buffer containing glutathione.

3.3. Results

3.3.1. Strategy for the amplification and insertion of the NSP5 and NSP6 coding sequences into pET42b

Access to purified viral proteins was essential to this project for use in both RNA binding assays and for the generation of polyclonal hyper immune sera to exploit in characterising the expression and function of the two proteins. To achieve this objective the Novagen pET vector expression system was employed. The cloning strategy for the insertion of the ORF's of NSP5 (ORF1) and of NSP6 (ORF2) into pET42b involved using PCR to introduce a *Cla*I restriction enzyme site immediately upstream of the ATG start codon of each of the ORF's. Following cleavage with the *Cla*I enzyme the 5' overhang left by the enzyme was removed using Mung Bean Nuclease digestion to produce a blunt ended copy of the ORF starting with the initiation ATG codon which could then be cloned on to the blunt end of the vector following its cleavage with *Psh*AI (Figure 3.3).

The first step in generating the required clones was to generate a copy of the rotavirus UKtc strain gene 11 sequence. The RT-PCR was performed using RMV reverse transcriptase and *Taq* DNA polymerase so that standard TA cloning could be performed using an Invitrogen one step TA cloning kit (Invitrogen, 2004). *Taq* DNA polymerase inserts single adenosine overhangs at the 5' and 3' termini of the PCR products (Invitrogen, 2004). Exploiting this feature a linearised cloning vector (pCR2.1) with single base thymidine overhangs could be used in a straight forward

A

5' ORF 1 Oligonucloetide

Cla I restriction site

↓

CAGATCTGGCCATCGATGTATCTCAGTATT

B

PCR Product cleaved with *Cla* I

CGATGTATCTCAGTATT
TACATAGAGTCATAA

C

PCR product after digestion with Mung Bean Nuclease.

ATGTATCTCAGTATT
TACATAGAGTCATAA

D

pET-42b cloning site

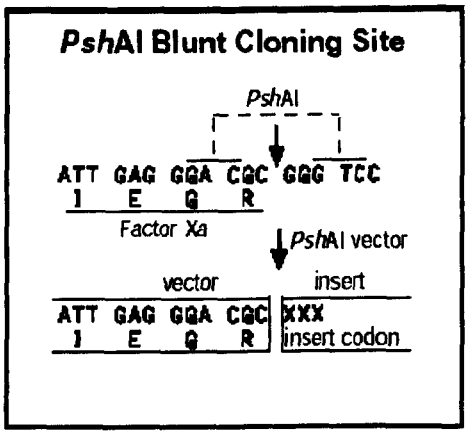

Figure 3.3 Strategy for cloning rotavirus ORF's into pET42b(+)
Flow-chart showing the insertion of the ORF1 PCR product into pET-42b vector. A) ORF1 PCR oligonucleotide showing *Cla* I restriction site. B) Cleaved PCR product with 5' overhang. C) Digestion of 5' overhang with Mung Bean Nuclease. D) Cleavage of pET-42b vector with *Psh*AI ready for insertion of blunt ended PCR products.

ligation between the amplified viral gene and the vector. This one step reaction removes the need for restriction enzymes digestion and amplicon purification. The pCR2.1 vector is a 3.9 kb plasmid supplied in linear form with single T overhangs ready for cloning. Recognition sites for the restriction enzyme *Eco*RI flank either side of the insertion site such that, this enzyme can be used to excise any insert as a single fragment provided no internal *Eco*RI sites were present within the insert. The dsRNA extracted from rotavirus UKtc strain virus particles were used as a template in the RT-PCR. Primers for gene segment 8 were used as a positive control for the gene 11 RT-PCR. Figure 3.4 shows a sample from each of these reactions in which the bands for gene 8 and gene 11 can be seen at 1.0 kb and 663 bp respectively (Figure 3.4). The gene 11 cDNA was then ligated into the pCR2.1 cloning vector which was transformed into the INVαF' strain of *E. coli*. Miniprep DNA from a selection of the clones was digested with *Eco*RI to release the cloned inserts, this showed that gene 11 had been successfully cloned (Figure 3.5). The clones were sequenced to select those that contained no *Taq* errors so that they could be used as a template for the NSP5 and NSP6 ORF PCR reactions.

PCR was performed with primers for the ORF's of NSP5 and NSP6 containing a *Cla*I restriction enzyme site (Figure 3.6a and 3.6b). The 3' primers for these PCR's contained a *Pst*I restriction enzyme site which was also found in the multicloning site of the pET-42b vector. Digestion of the amplified DNA with this restriction enzyme was used to ensure that the cDNA inserts would be ligated into the pET42b vector in the correct orientation. The PCR products were gel purified and cut with *Cla*I and Mung Bean Nuclease treated to form a blunt 5' end.

Following this treatment and gel purification *Pst*I was used to cleave the 3' end of the cDNA. A ligation was performed between this cDNA and the pET-42b vector which had been previously cleaved with *Psh*A1 and *Pst*I this ligation resulted in creation of the pET42b-ORF1 (Appendix 1.6) and pET42b-ORF2 (Appendix 1.7) plasmids which were then transformed into INVαF' *E. coli*. Respective plasmids from this transformation were miniprepped for sequencing to ensure the ORF were correctly inserted and that no mutational changes had been introduced during the sub-cloning. The plasmids were then transformed into the BLR strain of *E. coli* which contained the T7 RNA polymerase gene. BLR *E. coli* colonies from this transformation were grown up O/N and minipreps performed to identify those carrying plasmids containing the NSP5 and NSP6 ORF's (Figure 3.7a and 3.7b). These plasmids were again sequenced to verify that no mutational changes had been introduced.

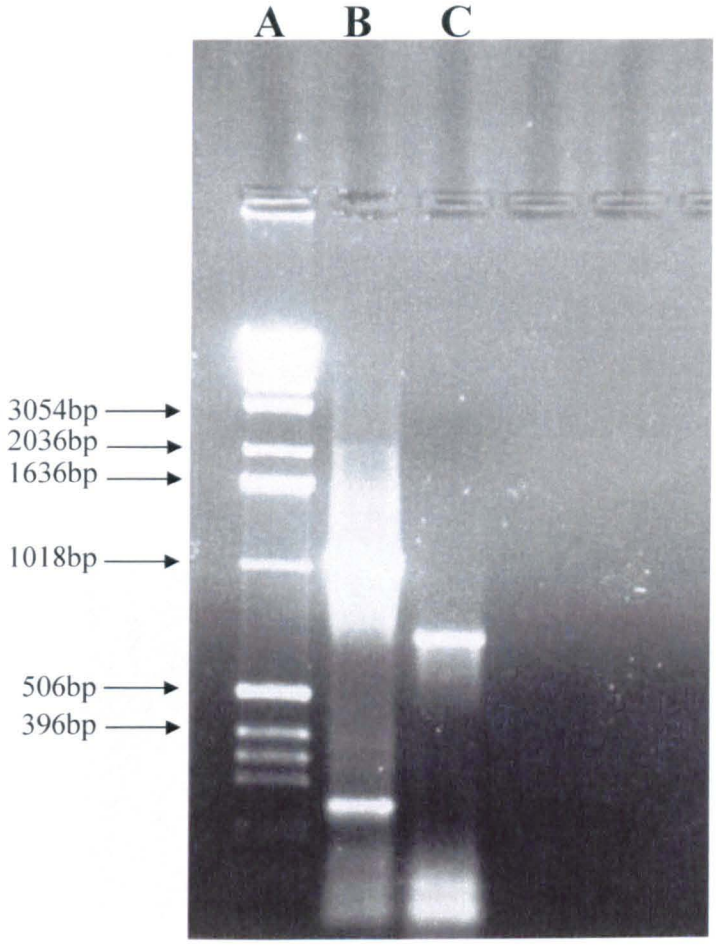

Figure 3.4 One step RT-PCR of rotavirus gene 11 from purified dsRNA of the UKtc strain of bovine rotavirus

An RT-PCR was carried out as described in the Materials and Methods. The products were fractionated on a 1% agarose gel stained with ethidium bromide and visualised using UV light. Track A) DNA marker size ladder, track B) Gene 8 positive control one step RT-PCR from rotavirus UKtc strain dsRNA and track C) Gene 11 one step RT-PCR from rotavirus UKtc strain dsRNA. Migration of the DNA size markers are indicated on the left hand side of the gel.

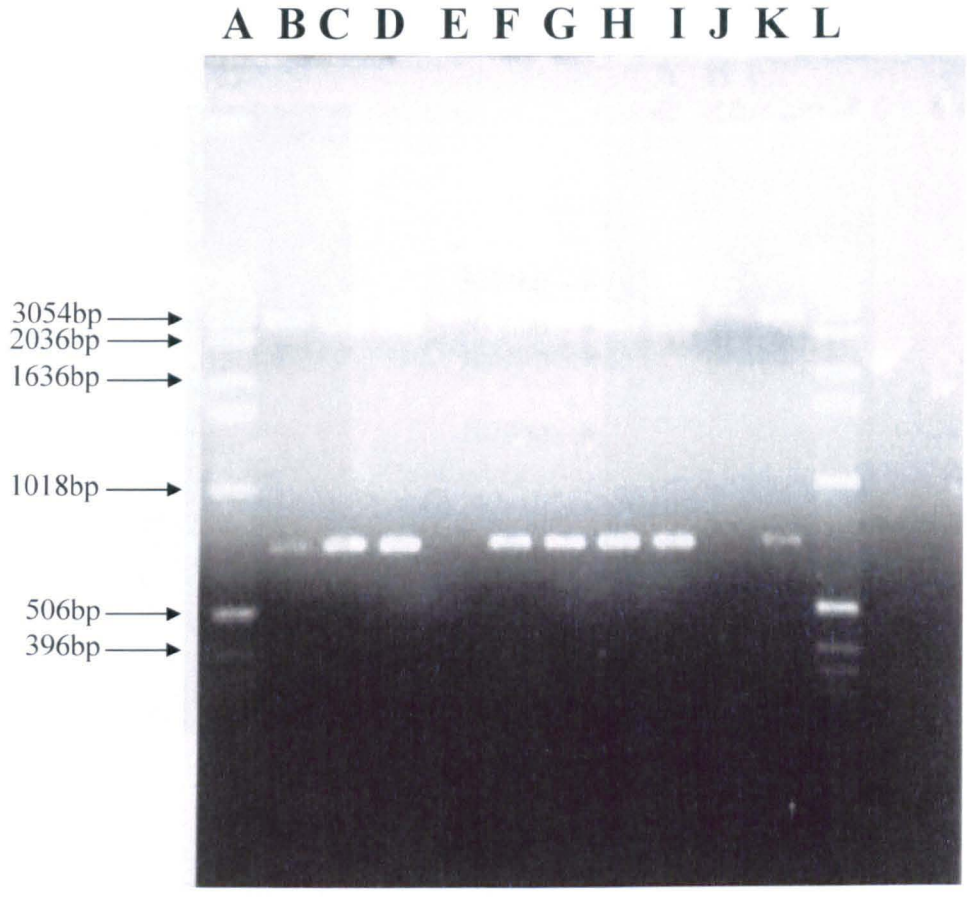

Figure 3.5 Restriction enzyme analysis of the putative gene 11 cDNA clones
A cDNA copy of gene 11 was generated using RT-PCR carried out as described in the Materials and Methods. This cDNA was cloned into the pCR2.1 vector using the Invitrogen TA cloning kit as described in the Materials and Methods. Single colonies were harvested and grown O/N at 37°C before being miniprepped as described in the Materials and Methods. The resulting plasmid DNA was cut with *Eco*RI to screen for potential inserts. The restriction digests were then fractionated on a 1% agarose gel stained with ethidium bromide and visualized using UV light. Track A) DNA size marker ladder, tracks B-K) Miniprepped colonies from the gene 11–pCR2.1 transformation cut with *Eco*RI, track L) DNA size marker ladder. Migration of the DNA size markers are indicated on the left hand side of the gel.

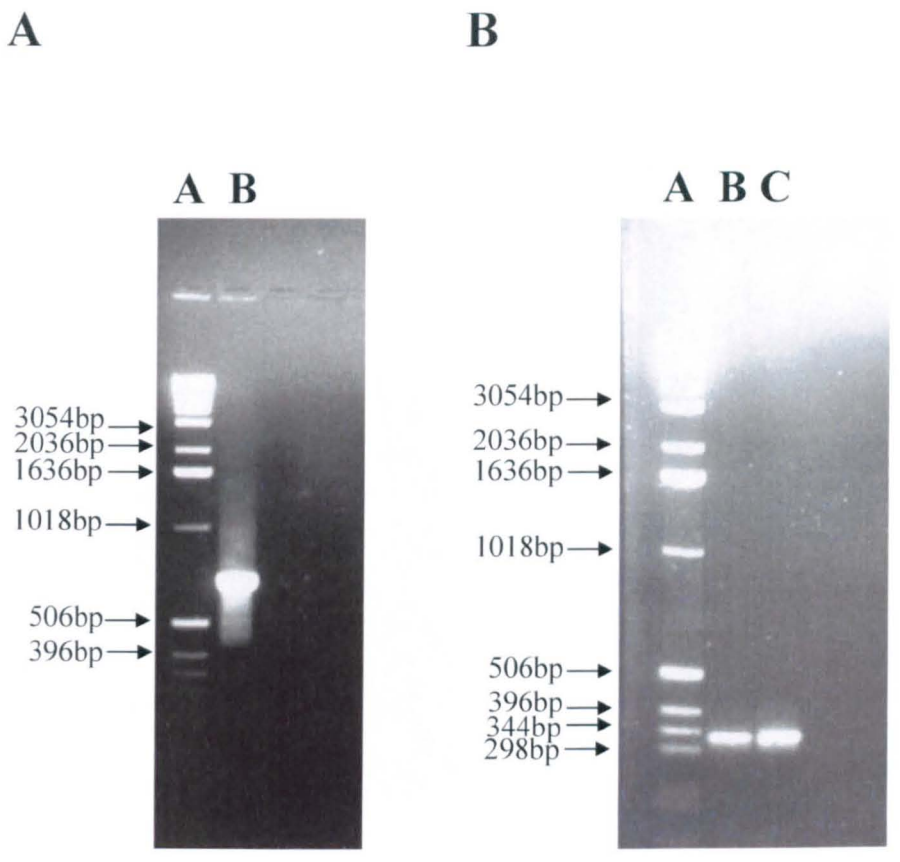

Figure 3.6 PCR amplification of ORF1 (Panel A) and ORF2 (Panel B) from rotavirus gene 11 UKtc strain

Panel A) PCR was carried out to generate a cDNA of ORF1 as described in the Materials and Methods. The products were fractionated on a 1% agarose gel stained with ethidium bromide and visualised using UV light. Track A) DNA size marker ladder, track B) PCR product of NSP5 ORF using primer containing a *Cla*I restriction enzyme sequence. Migration of the DNA size markers are indicated on the left hand side of the gel.

Panel B) PCR was carried out to generate a cDNA of ORF2 as described in the Materials and Methods. The products were fractionated on a 1% agarose gel stained with ethidium bromide and visualized using UV light. Track A) DNA size marker ladder) PCR product of NSP6 ORF using primer containing *Cla*I restriction site sequence at 2mM $MgCl_2$ and track C) PCR product of NSP6 ORF using primer containing *Cla*I restriction site sequence at 3mM $MgCl_2$. Migration of the DNA size markers are indicated on the left hand side of the gel.

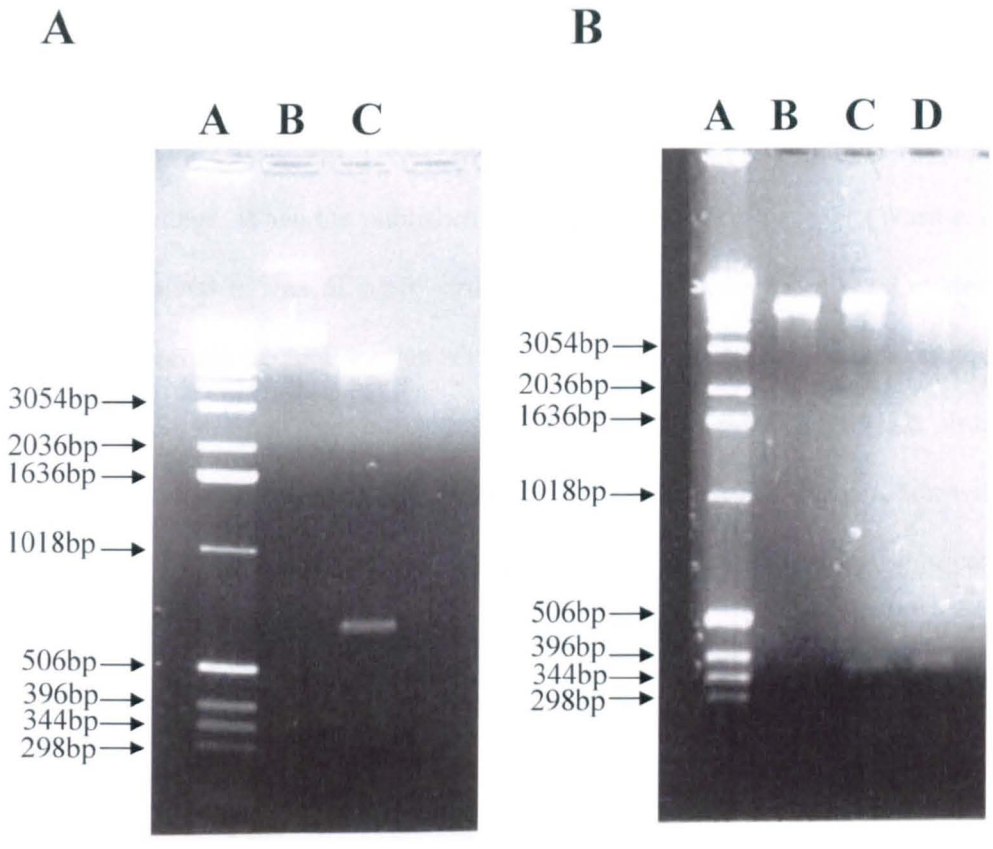

Figure 3.7 Restriction analysis of putative ORF1 (Panel A) and ORF2 (Panel B) clones in pET42b

Panel A) A cDNA copy of ORF1 was ligated into the pET42b vector as described in the Materials and Methods. Single colonies were harvested and grown O/N at 37°C before being miniprepped as described in the Materials and Methods. The resulting plasmid DNA cut with *Kpn*I and *Pst*I to screen for potential inserts. The restriction digest was then fractionated on a 1% agarose gel stained with ethidium bromide and visualized using UV light. Track A) DNA size marker ladder, track B) pET42b uncut and track C) pET42b cut with *Kpn*I and *Pst*I. Migration of the DNA size markers are indicated on the left hand side of the gel.

Panel B) A cDNA copy of ORF2 was ligated into the pET42b vector as described n the Materials and Methods. Single colonies were harvested and grown O/N at 37°C before being miniprepped as described in the Materials and Methods. The resulting plasmid DNA cut with *Kpn*I and *Pst*I to screen for potential inserts. The restriction digest was then fractionated on a 1% agarose gel stained with ethidium bromide and visualized using UV light. Track A) DNA size marker ladder, track B) pET42b uncut and track C) pET42b cut with *Kpn*I and *Pst*I. Track A) Invitrogen 1kb DNA ladder, tracks B-D) pET42b-ORF2 cut with *Kpn*I and *Pst*I. Migration of the DNA size markers are indicated on the left hand side of the gel.

3.3.2. Sequence analysis of rotavirus gene 11 UKtc strain

Sequencing of the gene 11 clones obtained following RT-PCR of genomic dsRNA extracted from the UKtc strain of bovine rotavirus produced some interesting findings. When the published sequence of the UKtc gene 11 (Ward *et al* 1985) is compared to that of other virus strains several differences were evident, differences at certain nucleotides that set the UKtc strain apart from the other strains. At nucleotide 17 in the 5' untranslated region there is an adenine in the UKtc strain while in all other rotavirus gene 11 sequences have a cytosine at this position with the exception of two human strains which have a thymine. The most significant difference however lies at the start of the coding region where in the UKtc sequence another adenine is found in place of a cytosine giving a TAT codon and a tyrosine amino acid. All other rotavirus gene 11 sequences have a TCT codon and a serine at this residue (Figure 3.8a).

The sequence of the UKtc gene 11 obtained in this study had cytosines in these positions and not adenines, as is found in the published sequence (Figure 3.8b). Sequence alignments generated using BLAST software showed that the sequences obtained in this study did show greater homology to that of the UKtc sequence indicating that it was not a gene 11 from another rotavirus strain that had been cloned. Figure 3.8 panel B shows the alignment of the first 30 nucleotides of nine sequences all from different clones and several different transformations against the published sequence of UKtc gene 11. This shows that the sequences from RT-PCR performed in this investigation have the same changes from the published sequence as seen in other

A

```
  G G C T T T T A A A G C G C T A C A G T G A T G T C T C T C  Majority

  ----------------+-----------------+-----------------+-
                  10                20                30
  ----------------+-----------------+-----------------+-
1 G G C T T T T A A A G C G C T A A A G T G A T G T A T C T C  gene11 UKtc
1 G G C T T T T A A A G C G C T A C A G T G A T G T C T C T C  human NSP5
1 G G C T T T - A A A G C G C T A C A G T G A T G T C T C T C  bovine gene 11
1 G G C T T T T A A A G C G C T A C A G T G A T G T C T C T C  human gene 11a
1 G G C T T T T A A A G C G C T A C A G T G A T G T C T C T C  human gene 11b
1 G G C T T T T A A A G C G C T A C A G T G A T G T C T C T C  human gene 11c
1 G G C T T T T A A A G C G C T A C A G T G A T G T C T C T C  simian gene 11
1 G G C T T T A A A A G C G C - A T A G T G A T G T C T C T C  human gene 11d
1 G G C T T T T A A A G C G C T A C A G T G A T G T C T C T C  porcine gene 11a
1 G G C T T T T A A A G C G C T A C A G T G A T G T C T C T C  porcine gene 11b
```

B

```
  G G C T T T T A A A G C G C T A C A G T G A T G T C T C T C Majority

  ----------------+-----------------+-----------------+-
                  10                20                30
  ----------------+-----------------+-----------------+-
1 G G C T T T T A A A G C G C T A A A G T G A T G T A T C T C  published UKtc
1 G G C T T T T A A A G C G C T A C A G T G A T G T C T C T C  RT-PCR colony 1
1 G G C T T T T A A A G C G C T A C A G T G A T G T C T C T C  RT-PCR colony 2
1 G G C T T T T A A A G C G C T A C A G T G A T G T C T C T C  RT-PCR colony 3
1 G G C T T T T A A A G C G C T A C A G T G A T G T C T C T C  RT-PCR colony 4
1 G G C T T T T A A A G C G C T A C A G T G A T G T C T C T C  RT-PCR colony 5
1 G G C T T T T A A A G C G C T A C A G T G A T G T C T C T C  RT-PCR colony 6
1 G G C T T T T A A A G C G C T A C A G T G A T G T C T C T C  RT-PCR colony 7
1 G G C T T T T A A A G C G C T A C A G T G A T G T C T C T C  RT-PCR colony 8
1 G G C T T T T A A A G C G C T A C A G T G A T G T C T C T C  RT-PCR colony 9
```

Figure 3.8 Comparative sequence analysis of the first 30 nucleotides of the published sequence for gene 11 of the UKtc strain and that obtained in this study

Panel A) Sequence alignments of the first 30 nucleotides of rotavirus gene 11 segments from the UKtc strain and several different strains of rotavirus. Differences between the published UKtc sequence and the other gene 11 sequences are marked in red.

Panel B) Sequence alignment of rotavirus UKtc strain gene segment 11 published sequence and the first 30bp of gene segment 11 RT-PCR products from RNA extracted from whole virus cloned into Invitrogen vector pCR2.1. Differences between the UKtc strain gene segment 11 and the cloned RT-PCR products sequences are marked in red.

rotavirus gene 11 sequences. This analysis clearly indicates that there were several nucleotide errors in the original sequencing of the UKtc strain gene 11. The sequence for this gene as determined in this study had a greater sequence identity to other rotavirus strains than was previously thought. The four nucleotide changes detected from the published sequence are both non-coding and coding occurring at nucleotides, a17c, a26c, c164t and t653a (Figure 3.9). These changes result in two amino acids changes in the NSP5 protein, the a26c causes a change at position 2 in the amino acid sequence from a tyrosine to a serine and the change c164t results in the amino acid sequence at position 48 changing from a serine to a phenylalanine (Figure 3.10a). Only one amino acid change was found in NSP6 and this was due to the nucleotide change c164t which results in a change at position 29 from a proline to a serine (Figure 3.10b). All of the above changes cause the gene segment 11 sequence of UKtc to become far similar to that found in other strains of rotavirus.

GGCTTTTAAAGCGCTACAGTGATGTCTCTCAGTATTGACGTGACGAGTCTTCCTTCT
GGCTTTTAAAGCGCTAAAGTGATGTATCTCAGTATTGACGTGACGAGTCTTCCTTCT

ATTTCTTCTAGTATTTATAAAAATGAATCATCTTCAACAGCGTCAACTCTTTCTGGA
ATTTCTTCTAGTATTTATAAAAATGAATCATCTTCAACAGCGTCAACTCTTTCTGGA

AAATCTATTGGTAGGAGTGAACAATATGTTTCACCAGATGCAGAAGCGTTCAGTAAA
AAATCTATTGGTAGGAGTGAACAATATGTTTCACCAGATGCAGAAGCGTCCAGTAAA

TACATGCTGTCGAAGTCTCCAGAAGATATTGGACCATCTGATTCTGCTTCAAACGAT
TACATGCTGTCGAAGTCTCCAGAAGATATTGGACCATCTGATTCTGCTTCAAACGAT

CCACTCACCAGCTTTTCGATTAGATCAAATGCAGTTAAGACAAATGCAGACGCTGGC
CCACTCACCAGCTTTTCGATTAGATCAAATGCAGTTAAGACAAATGCAGACGCTGGC

GTGTCTATGGATTCATCAGTACAATCACGACCATCAAGTAACGTTGGGTGCGATCAA
GTGTCTATGGATTCATCAGTACAATCACGACCATCAAGTAACGTTGGGTGCGATCAA

GTGGATTTCTCCTTTAATAAAGGAATTAAAGTGAATGCGAACCTAGATTCATCTATA
GTGGATTTCTCCTTTAATAAAGGAATTAAAGTGAATGCGAACCTAGATTCATCTATA

TCAGTGTCAACAAATTCAAGAAAGGAGAAGTCCAAAAATGACCATAAAAGTAGGAAA
TCAGTGTCAACAAATTCAAGAAAGGAGAAGTCCAAAAATGACCATAAAAGTAGGAAA

CACTACCCTAGAATTGAAGCAGAATCCGACTCAGATGATTACGTACTTGACGATTCA
CACTACCCTAGAATTGAAGCAGAATCCGACTCAGATGATTACGTACTTGACGATTCA

GACAGTGATGATGGCAAATGTAAAAACTGTAAATATAAAAGGAAGTATTTCGCACTG
GACAGTGATGATGGCAAATGTAAAAACTGTAAATATAAAAGGAAGTATTTCGCACTG

AGAATGAGAATGAAGCAAGTTGCCATGCAATTGATCGAAGATTTGTAGGTCTGACCT
AGAATGAGAATGAAGCAAGTTGCCATGCAATTGATCGAAGATTTGTAGGTCTGACCT

GAGAGGTCACTAGGGAGCTCCCCACACCCGTTTTGTGACC
GAGAGGTCACTAGGGAGCTCCCCACTCCCGTTTTGTGACC

Figure 3.9 Comparison between the published gene 11 nucleotide sequence and that determined in this study

Alignment of the UKtc strain gene 11 published sequence from Ward *et al.*, 1985 (red) and the RT-PCR product of UKtc strain gene 11 sequence generated in this study (blue). Four single nucleotide changes between these sequences are highlighted in green.

A

MYLSIDVTSLPSISSSIYKNESSSTASTLSGKSIGRSEQYVSPDAEASSKYMLSK

MSLSIDVTSLPSISSSIYKNESSSTASTLSGKSIGRSEQYVSPDAEAFSKYMLSK

SPEDIGPSDSASNDPLTSFSIRSNAVKTNADAGVSMDSSVQSRPSSNVGCDQV

SPEDIGPSDSASNDPLTSFSIRSNAVKTNADAGVSMDSSVQSRPSSNVGCDQV

DFSFNKGIKVNANLDSSISVSTNSRKEKSKNDHKSRKHYPRIEAESDSDDYVL

DFSFNKGIKVNANLDSSISVSTNSRKEKSKNDHKSRKHYPRIEAESDSDDYVL

DDSDSDDGKCKNCKYKRKYFALRMRMKQVAMQLIEDL

DDSDSDDGKCKNCKYKRKYFALRMRMKQVAMQLIEDL

Published UKtc strain NSP5 sequence

NSP5 sequence determined in this study

B

MNHLQQRQLFLENLLVGVNNMFHQMQKRPVNTCCRSLQKILDHLILLQTIHSPAFR

MNHLQQRQLFLENLLVGVNNMFHQMQKRSVNTCCRSLQKILDHLILLQTIHSPAFR

LDQMQLRQMQTLACLWIHQYNHDHQVTLGAIKWISPLIKELK

LDQMQLRQMQTLACLWIHQYNHDHQVTLGAIKWISPLIKELK

Published UKtc strain NSP6 sequence

NSP6 sequence determined in this study

Figure 3.10 Comparison of the published NSP5 and NSP6 amino acid sequences and those determined in this study

Panel A) shows the UKtc strain NSP5 amino acid sequence from both the published sequence from Ward *et al.*, 1985 (in black) and the RT-PCR sequence obtained from this study (in red).

Panel B) shows the UKtc strain NSP6 amino acid sequence from both the published sequence from Ward *et al.*, 1985 (in black) and the RT-PCR sequence obtained from this study (in blue).

3.3.3. Expression of GST-NSP5 and GST-NSP6

E. coli carrying the relevant plasmids was cultured on a large scale to allow an induction test to assay their ability to express the fusion proteins. Figure 3.11a shows that much of the GST-NSP5 fusion protein, with its expected size of approximately 60 kDa, was found in the soluble fraction of the induced *E. coli* lysate. By contrast figure 3.11b shows that the bulk of GST-NSP6 protein which had the expected size of 40 kDa was found to be in the insoluble fraction. Insoluble proteins cannot be directly purified, however a variety of methods are available to try and increase the solubility of such expressed proteins.

Protein insolubility can result from the rate at which it is synthesised following induction consequently lowering the growth temperature can increase the solubility. To investigate this possibility the induction of GST-NSP6 was performed for 4 hours at both 30°C and 37°C (Figure 3.12). Small amounts of GST-NSP6 were produced from the 30°C sample however the fusion protein was still insoluble. Several other protocols were investigated with the aim of solubilising the expressed protein including induction at room temperature, lowering of the concentration of IPTG added for induction and transforming the pET42b-ORF2 plasmid into alternative strains of *E. coli* containing the T7 RNA polymerase. However, none of these resulted in the production of soluble GST-NSP6.

A

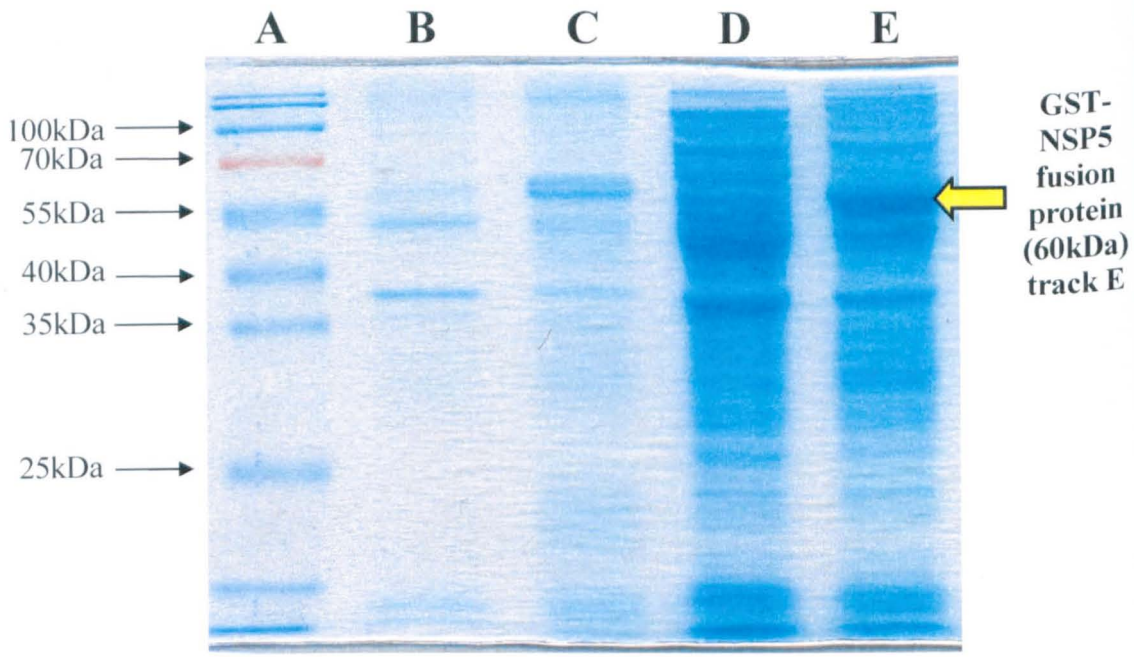
A
B
C
D
E
100kDa
70kDa
55kDa
40kDa
35kDa
25kDa
GST-NSP5 fusion protein (60kDa) track E

B

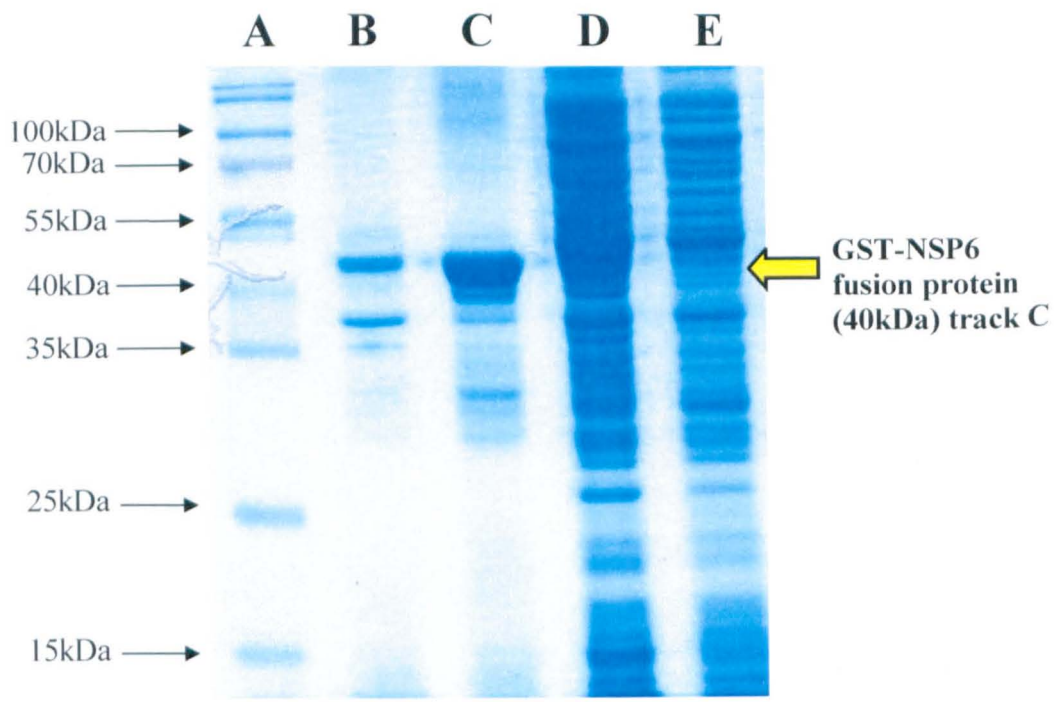
A
B
C
D
E
100kDa
70kDa
55kDa
40kDa
35kDa
25kDa
15kDa
GST-NSP6 fusion protein (40kDa) track C

Figure 3.11 Expression of GST tagged NSP5 and NSP6 from pET42b vectors
The BLR strain of *E. coli* containing either pET42b-ORF1 or pET42b-ORF2 was grown in 200ml LB at 37°C until the OD_{590} reached between 0.5 and 1. Each culture was then split into two and one half induced with a final concentration of 1mM IPTG. Both the uninduced and induced cultures were incubated for a further 4 hours at 37°C. The cells were recovered by centrifugation using a Beckman JA10 rotor at 6370*g* for 15 minutes at 4°C and lysed by use of a French press at 20,000 psi. The soluble and insoluble fractions were then separated by centrifugation in a Beckman JA20 rotor at 39200*g* for 30 minutes at 4°C. Insoluble proteins were solublised by incubation in 8M urea for 4 hours at room temperature. Samples of all fractions were fractionated on a 14% SDS-PAGE gel that was electrophoresed and stained with Coomassie blue as described in the Materials and Methods.

Panel A) Showing induction test for GST-NSP5. The yellow arrow indicates the position of the expressed GST-NSP5 fusion protein. Track A) Protein size markers 10-180 kDa, track B) Insoluble fraction from an uninduced culture, track C) Insoluble fraction from an induced culture, track D) Soluble fraction from an uninduced culture and track E) Soluble fraction from an induced culture. Migration of the protein size markers are indicated on the left hand side of the gel and the position of the GST-NSP5 protein is indicated by the yellow arrow.

Panel B) Showing induction test for GST-NSP6 the yellow arrow indicates the position of the expressed GST-NSP6 fusion protein. Track A) Protein size markers 10-180 kDa, track B) Insoluble fraction from an uninduced culture, track C) Insoluble fraction from an induced culture track D) Soluble fraction from an uninduced culture and track E) Soluble fraction from an induced culture. Migration of the protein size markers are indicated on the left hand side of the gel and the position of the GST-NSP6 is indicated by the yellow arrow.

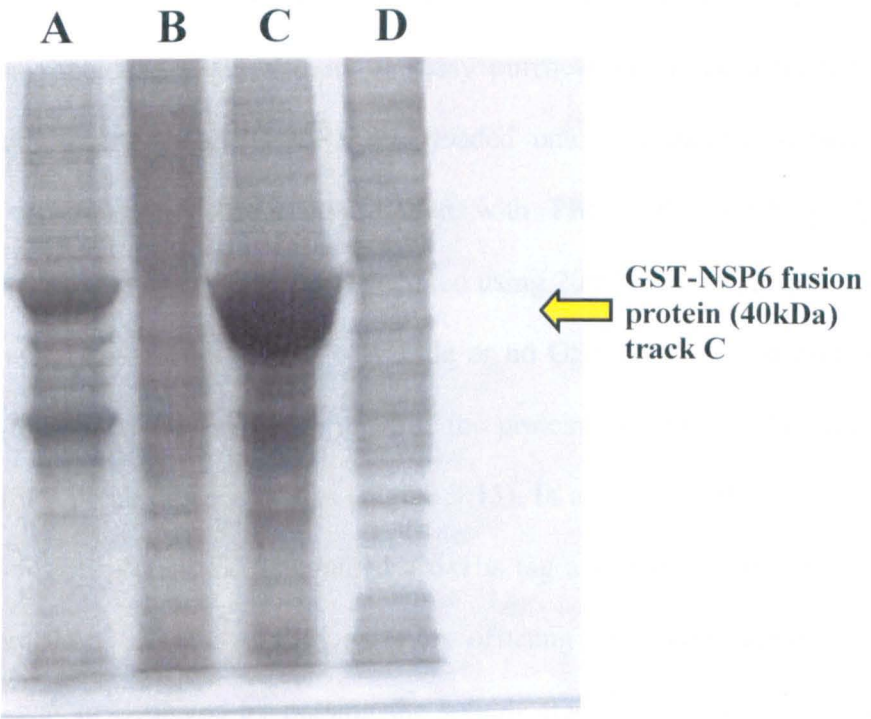

Figure 3.12 GST-NSP6 induction at 30°C and 37°C
A 200ml culture of *E. coli* carrying the pET42b-ORF2 plasmid was grown at 37°C until the OD_{590} was between 0.5 and 1. The culture was split into two equal halves and induced with a final concentration of 1mM IPTG. One half was incubated at 30°C for 4 hours and the other incubated at 37°C for 4 hours. The cells were recovered by centrifugation using a Beckman JA10 rotor at 6370*g* for 30 minutes at 4°C and lysed by use of a French press at 20,000 psi. The soluble and insoluble fractions were then separated by centrifugation using a Beckman JA20 rotor at 39200*g* for 30 minutes at 4°C and insoluble proteins solublised in 8M urea as described in the Materials and Methods. Samples were analysed by SDS-PAGE and stained with Coomassie blue as described in the Materials and Methods. Track A) Insoluble fraction of culture induced at 30°C, track B) Soluble fraction of culture induced at 30°C, track C) Insoluble fraction of culture induced at 37°C and track D) Soluble fraction of culture induced at 37°C. The position of the GST-NSP6 is indicated by the yellow arrow.

3.3.4. Purification of GST-NSP5

Expression of the GST-NSP5 fusion protein in the soluble fraction of bacterial lysates should have allowed for its easy purification. Induced bacterial lysates containing expressed GST-NSP5 was loaded onto a glutathione-agarose (GSH-agarose) purification column equilibrated with PBS. After washing the column with PBS the bound GST-NSP5 was eluted using 20mM Tris HCL, pH 8.0, containing 10mM glutathione. Unexpectedly little or no GST-NSP5 fusion protein was present in the eluted fractions with most of the protein appearing to be either GST or GST-NSP5 break down products (Figure 3.13). In addition to the GST tag, the GST-NSP5 fusion protein also contained a 6xHis tag and because of the poor yield eluted from the GSH-agarose the possibility of using this second protein tag for purification was investigated by passing the soluble fraction over a Ni^{++} metal chelating column. The column was equilibrated with PBS containing 10mM imidazole and the GST-NSP5 passed through it and allowed to bind. After washing to remove non-bound material the GST-NSP5 fusion protein was eluted with 500mM imidazole. The eluted protein contained only a small quantity of GST-NSP5 fusion protein and large amounts of non-specifically bound *E. coli* proteins (Figure 3.14). In an attempt to improve yields to a useful level a new GSH-agarose column elution buffer containing 75mM HEPES pH7.4, 150mM NaCl, 20mM reduced glutathione, 5mM DTT and 0.1%Triton X-100 was used giving better results and a usable amount of GST-NSP5 fusion protein being purified. There was still evidence of GST-NSP5 break down products in the eluted fractions but less than in previous attempts (Figure 3.15). This partially purified fusion protein was cut with Factor Xa,

the authentic cut NSP5 released by proteolytic cleavage and the GST tag are almost equivalent in size and it was not possible to separate the two by SDS-PAGE. The cleaved protein products were again passed over the GSH-agarose column, the NSP5 protein should have passed straight through the column whereas the cut GST tag should remain bound to the column. The flowthrough was collected and the column washed to remove all non-bound material, the bound GST tag was then eluted from the column as previously described. However little or no protein was found to flow through of the column indicating that the authentic NSP5 protein could not be isolated using this protocol (Figure 3.16).

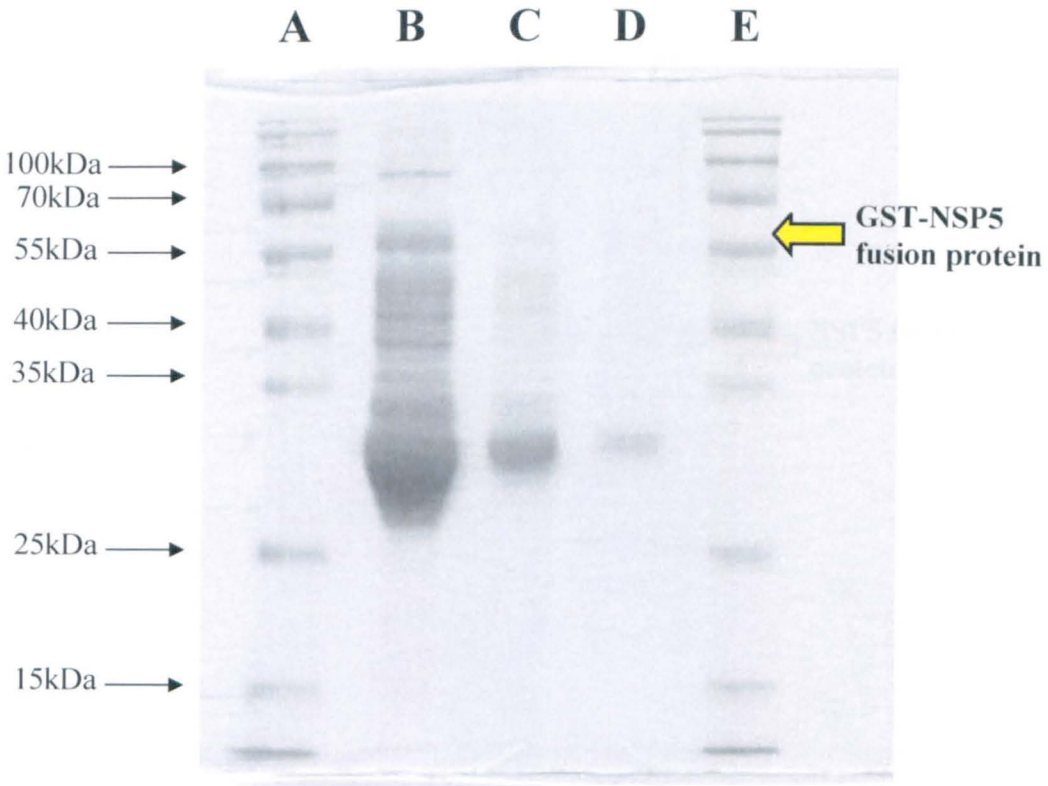

Figure 3.13 Purification of GST-NSP5 fusion protein using GSH-agarose affinity chromatography

Fractions eluted after GST-NSP5 fusion protein was passed through a glutathione-agarose (GSH-agarose) column were fractionated on a 10% SDS polyacrylamide gel that was stained with Coomassie blue as described in the Materials and Methods. Track A) Protein size markers 10-180 kDa, track B) first GST-NSP5 fraction eluted from GSH-agarose, C) second GST-NSP5 fraction eluted from GSH-agarose D) third GST-NSP5 fraction eluted from GSH-agarose and E) Protein size markers 10-180Kda. Migration of the protein size markers are indicated on the left hand side of the gel and the position of the GST-NSP6 is indicated by the yellow arrow.

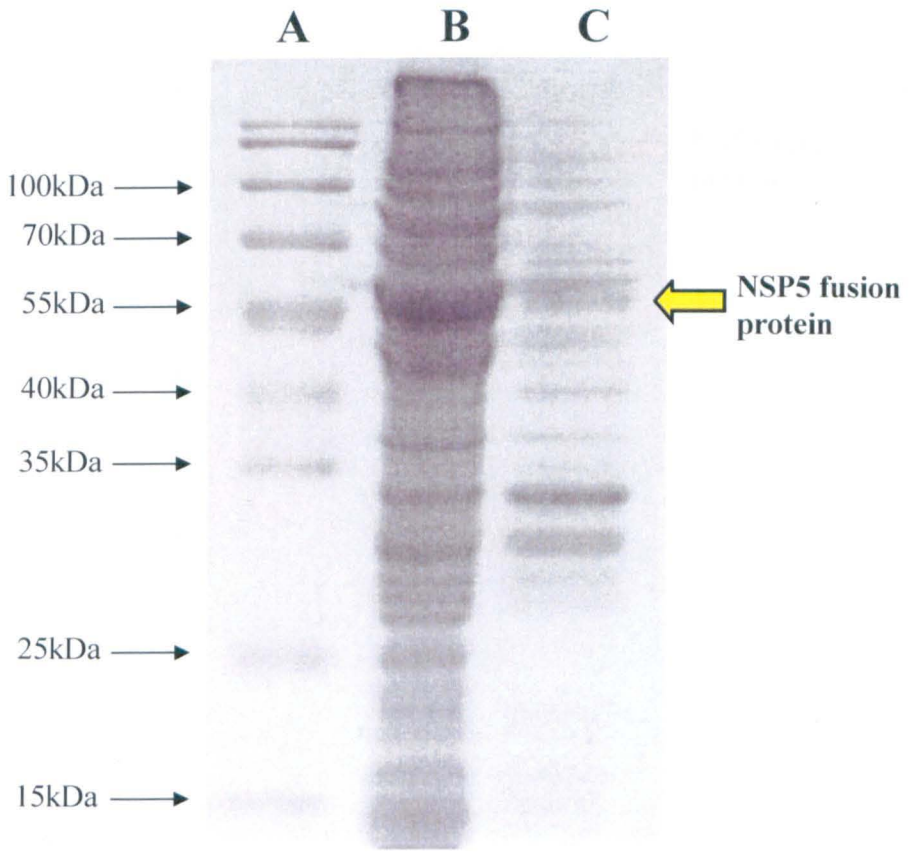

Figure 3.14 Purification of GST-NSP5 by Ni^{++} metal chelation chromatography
The soluble fraction of lysed bacteria induced to express NSP5 fusion protein from the pET42b-NSP5 vector was passed over a Ni^{++} metal chelating column equilibrated with PBS containing 10mM imidazole. Protein was eluted from the column using 500mM imidazole. The eluted protein was then fractionated on a 10% SDS-polyacrylamide gel which was stained with Coomassie blue as described in the Materials and Methods Track A) Protein size markers 10-180 kDa, track B) Soluble fraction before application to the column and track C) Eluted fraction from Ni^{++} metal chelating column. Migration of the protein size markers are indicated on the left hand side of the gel and the position of the NSP5 fusion is indicated by the yellow arrow.

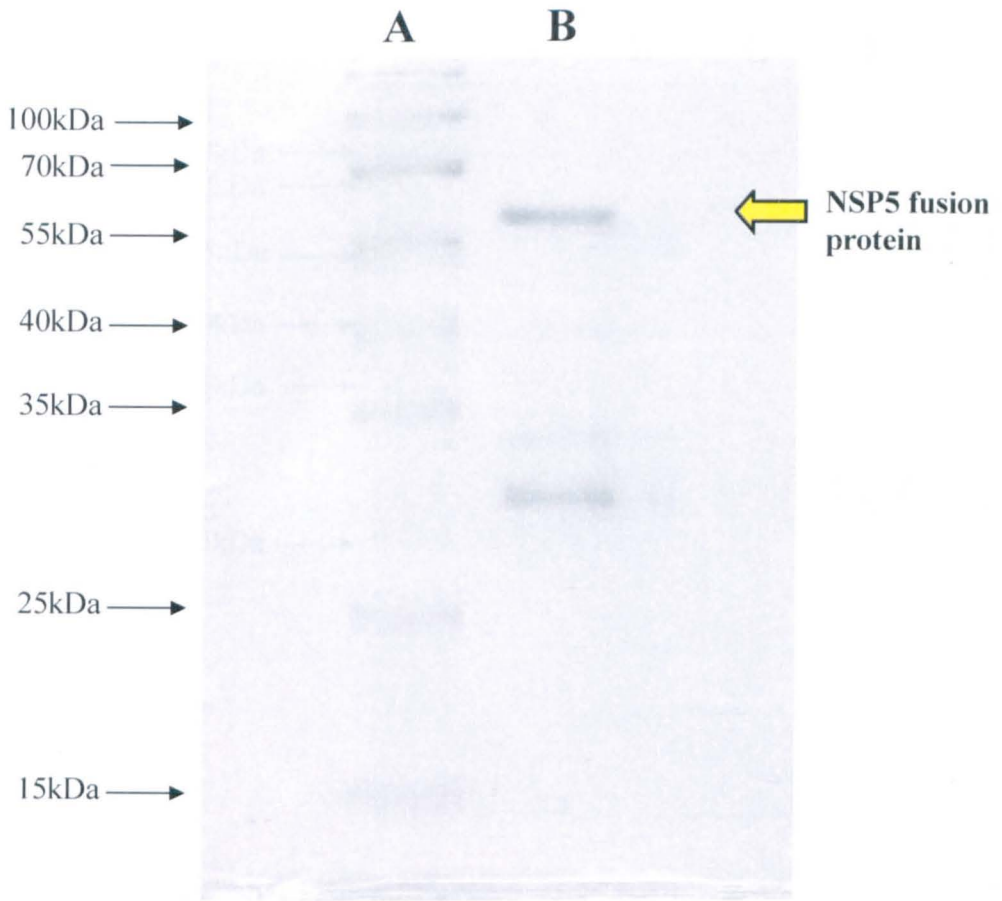

Figure 3.15 Chromatography of GST-NSP5 on GSH-agarose under stringent elution conditions

A GSH-agarose column was equilibrated with PBS. The soluble fraction of a lysed bacterial culture induced to express GST-NSP5 fusion protein was applied to the column which was subsequently washed with 3 column volumes of PBS. The bound protein was then eluted in 75mM HEPES pH7.4, 150mM NaCl, 20mM reduced glutathione, 5mM DTT and 0.1% Triton X-100. The eluted fractions were then fractionated on a 10% SDS polyacrylamide gel which was stained with Coomassie blue as described in the Materials and Methods. Track A) Protein size markers 10-180 kDa and track B) Eluted GST-NSP5. Migration of the protein size markers are indicated on the left hand side of the gel and the position of the NSP5 fusion is indicated by the yellow arrow.

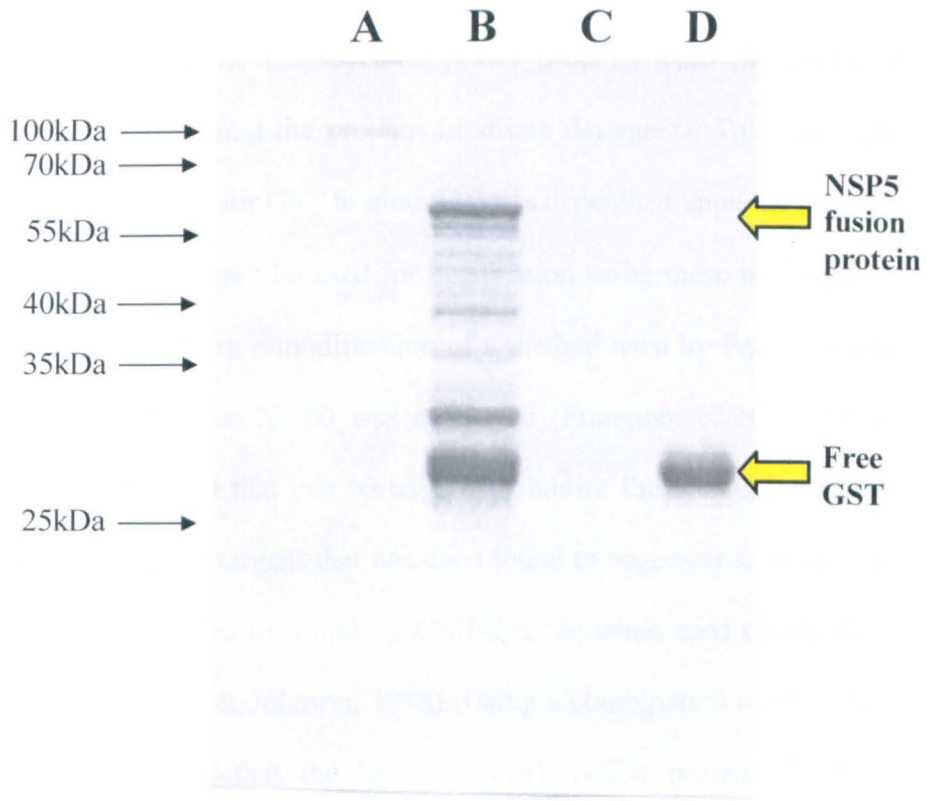

Figure 3.16 Factor Xa cleavage of GST-NSP5
The GST-NSP5 obtained by GSH-agarose chromatography was subjected to enzymatic cleavage by the Factor Xa. Factor Xa was added to a final concentration of 0.2U/µl as described in the Materials and Methods. This reaction mixture was incubated for 4 hours at 37°C. The cleaved protein was then passed through GSH-agarose following this bound GST was eluted in 75mM HEPES pH 7.4, 150mM NaCl, 20mM reduced glutathione, 5mM DTT and 0.1% Triton X-100. The protein flow through was subsequently fractionated on a 14% SDS polyacrylamide gel which was stained with Coomassie blue as described in the Materials and Methods. Track A) Protein size markers 10-180 kDa, track B) GST-NSP5 before cleavage with Factor Xa, track C) GSH-agarose column flow through containing authentic NSP5 protein and track D) Eluted fraction from the GSH-agarose column containing cleaved GST tag. Migration of the protein size markers are indicated on the left hand side of the gel and the position of the NSP5 fusion and free GST are indicated by the yellow arrow.

3.3.5. Purification of GST-NSP6

Several methods can be employed to purify proteins from the insoluble fraction which involve dissolving the proteins in strong detergents. This denatures the proteins and as the affinity for GST to glutathione is dependent upon the proteins conformation the GST tag cannot be used for purification using these methods. To try and circumvent this problem a modification of a method used by Frangioni and Neel using sarkosyl and Triton X-100 was employed (Frangioni & Neel, 1993). Sarkosyl is an ionic detergent that can be used to solublise the insoluble protein. Triton X-100 is a non-ionic detergent that has been found to sequester sarkosyl into its micelles and is known to be tolerated by GSH-agarose when used during GST fusion protein binding (Smith & Johnson, 1988). Using a combination of these two detergents it was discovered that the insoluble GST fusion protein could be solublised and rendered in such a state that it was now able to bind the GSH-agarose. A range of sarkosyl concentrations were used in order to find the concentration that gave the maximum protein solublisation but at the minimum concentration of sarkosyl. A solution with a 1% concentration of sarkosyl was found to be optimal (Figure 3.17a). A range of solutions were made by addition of Triton X-100 of 0%, 0.5%, 1% and 2% which were then applied to the GSH-agarose column to check for refolded protein binding. Only a small amount of GST-NSP6 protein was eluted from the column (Figure 3.17b), most of the protein washed through the column and did not bind.

A

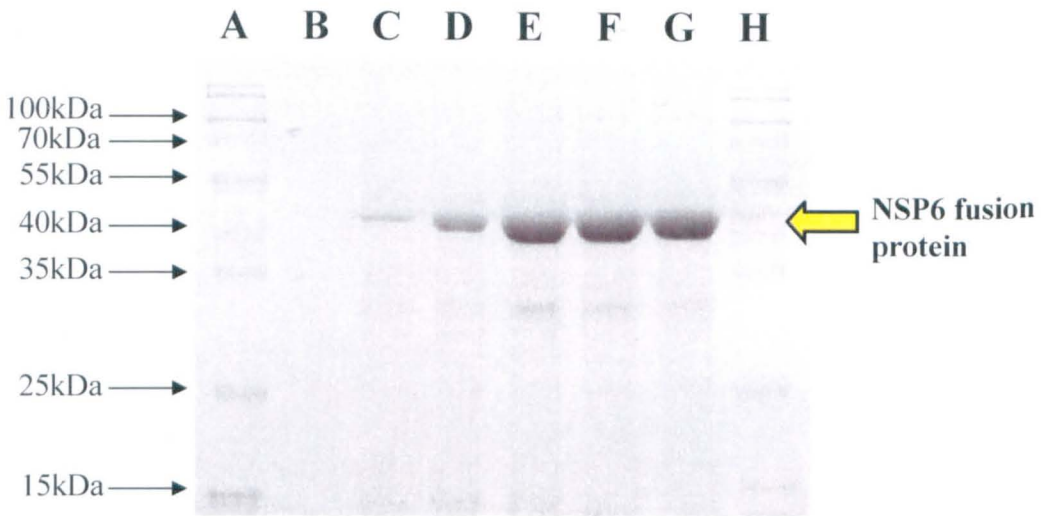
A B C D E F G H
100kDa
70kDa
55kDa
40kDa
35kDa
25kDa
15kDa
NSP6 fusion protein

B

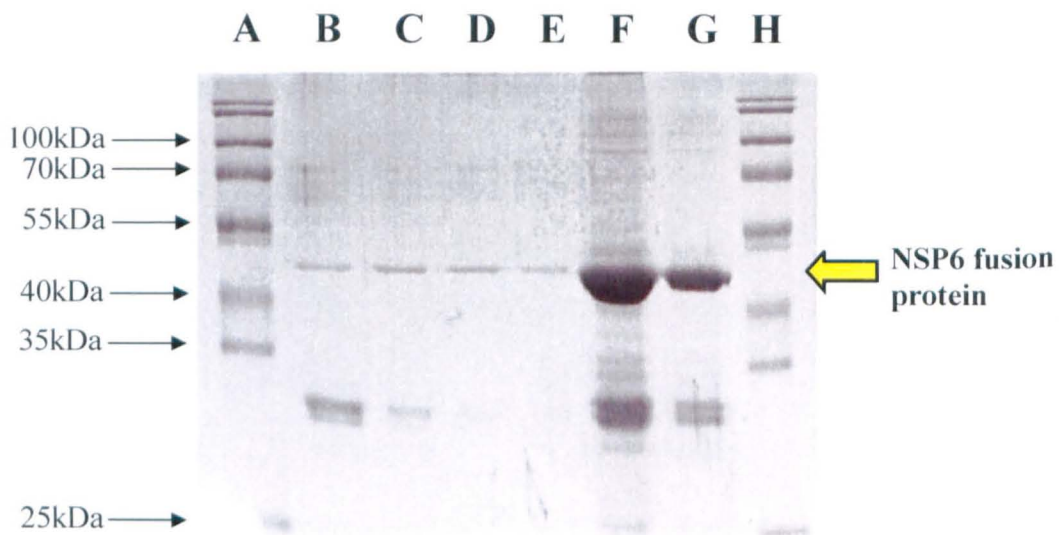
A B C D E F G H
100kDa
70kDa
55kDa
40kDa
35kDa
25kDa
NSP6 fusion protein

Figure 3.17 Purification of GST-NSP6 via sarkosyl solublisation and TritonX-100 treatment

Panel A) Shows a solublisation assay for insoluble GST-NSP6 with addition of differing amounts of sarkosyl. The insoluble fraction containing the GST-NSP6 fraction was isolated from a 500ml culture. This was resuspended in STE buffer (10mM Tris-HCl pH 8.0, 150mM NaCl 5mM DTT and 1mM EDTA). The fraction was split into six, where a different amount of sarkosyl was added to each to give a final concentration of 0%, 0.25%, 0.5%, 1%, 2% and 4%. This was done to determine the minimum concentration of sarkosyl needed in order to solublise the maximum amount of GST-NSP6 protein. Samples of each were resolved on a 10% SDS polyacrylamide gel which was stained with Coomassie blue as described in the Materials and Methods Track A) Protein size markers 10-180 kDa, track B) 0% sarkosyl added to GST-NSP6 insoluble protein, track C) 0.25% sarkosyl added to GST-NSP6 insoluble protein, track D) 0.5% Sarkosyl added to GST-NSP6 insoluble protein, track E) 1% sarkosyl added to GST-NSP6 insoluble protein, track F) 2% sarkosyl added to GST-NSP6 insoluble protein, track G) 4% sarkosyl added to GST-NSP6 insoluble protein and track H) Protein size markers 10-180 kDa. Migration of the protein size markers are indicated on the left hand side of the gel and the position of the NSP6 fusion is indicated by the yellow arrow.

Panel B) Shows the effect of addition of differing amount of Triton X-100 on purification of sarkosyl solublised GST-NSP6. The insoluble fraction of a 500ml culture was treated with STE buffer containing 1% sarkosyl. The solublised GST-NSP6 solution was then split into four and to each a different amount of triton X was added to give the final concentrations of 0%, 0.5%, 1% and 2%. These samples were then applied to a GSH-agarose column to look for refolded protein binding to the column which could then be eluted. The eluted fraction from these attempts at purification were resolved on a 10% SDS polyacrylamide which was stained with Coomassie blue as described in the Materials and Methods, along with the 1% and 2% Triton X-100 samples flow through from the column. Track A) Protein size markers 10-180 kDa, track B) 0% Triton X-100 GST-NSP6 eluted fraction, track C) 0.5 % Triton X-100 GST-NSP6 eluted fraction, track D) 1% Triton X-100 GST-NSP6 eluted fraction track E) 2% Triton X-100 GST-NSP6, track F) 1% Triton X-100 GST-NSP6 flow through of unbound protein from column, track G) 2% Triton X-100 GST-NSP6 flow through of unbound protein from column and track H) Protein size markers 10-180 kDa. Migration of the protein size markers are indicated on the left hand side of the gel and the position of the NSP6 fusion is indicated by the yellow arrow.

An alternative method of purification was attempted for NSP6 making use of the 6xHis tag which can be used for purification of denatured proteins on a Ni^{++} chelating column. The insoluble fraction containing the insoluble NSP6 fusion protein was dissolved in Guanidine hydrochloride (Gu-HCl) denaturing all of the insoluble protein. The Ni^{++} chelating column was equilibrated with 8M urea, pH 8.0 and subsequently used to bind and elute the GST-NSP6 under denatured conditions. The denatured GST-NSP6 was eluted in 8M urea pH 3.5 and then refolded by stepwise dialysis against 20mM Tris-HCl to a pH of 7 (Figure 3.18). Once the protein had been refolded it was treated with the Factor Xa protease in order to remove the tag region at the N-terminus of the NSP6 protein. However, as was found with the GST-NSP5 fusion protein all that was recovered using this method was degradation products and no authentic NSP6 could be isolated. This meant that this method could not be used for the purification of NSP6.

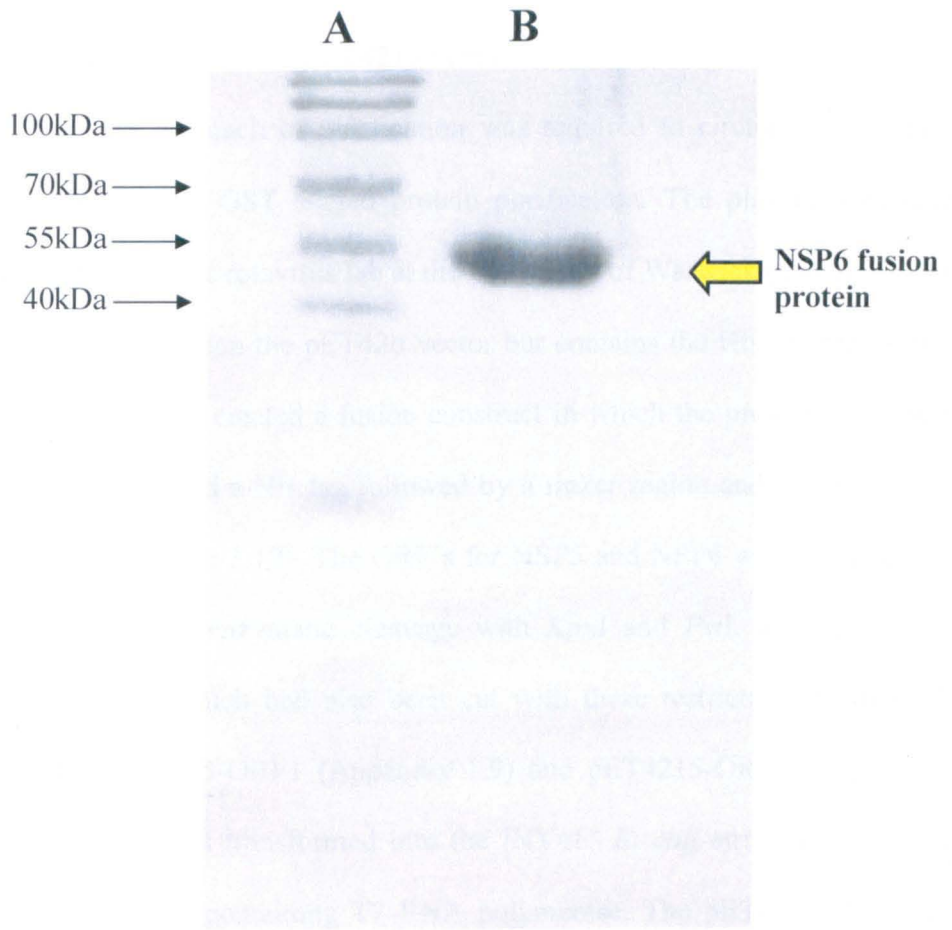

Figure 3.18 Purification of insoluble GST-NSP6 fusion protein from Ni^{++} chelating column

The insoluble fraction from a culture induced to express GST-NSP6 was denatured in 6M Gu-HCl and passed over a Ni^{++} chelating column equilibrated with 8M urea pH 8.0. The column was then washed with 8M urea pH 8.0 until all protein flow through was removed. The column was then washed with 3 column volumes of 8M urea pH 6.0 followed by 3 column volumes of 8M urea pH 4.0. Finally protein was eluted by washing with 3 column volumes of 8M urea pH 3.5 as described in the Materials and Methods. This protein was then refolded by stepwise dialysis against 20mM Tris to a pH of 7.0 as described in the Materials and Methods. The purified proteins were then fractionated on a 14% SDS polyacrylamide gel which was stained with Coomassie blue as described in the Materials and Methods. Track A) Protein size markers 10-180 kDa and track B) GST-NSP6 eluted from Ni^{++} chelating column under denatured conditions and refolded by stepwise dialysis against 20mM Tris to a pH of 7.0. Migration of the protein size markers are indicated on the left hand side of the gel and the position of the NSP6 fusion is indicated by the yellow arrow.

3.3.6. Expression and purification of pET4215-His-NSP5 and pET4215-His-NSP6 expressed from the pET4215 vector

A new approach of purification was required to circumvent the problems encountered during GST tagged protein purification. The plasmid pET4215 was developed within the rotavirus lab at the University of Warwick (Chung, 2004). This vector was based upon the pET42b vector but contains the His tag region from the pET15 vector. This created a fusion construct in which the protein expressed from this vector contained a His tag followed by a linker region ending in the factor Xa cleavage site (Figure 3.19). The ORF's for NSP5 and NSP6 were excised from the pET42b vector by enzymatic cleavage with *Kpn*I and *Pst*I, and ligated into the pET4215 vector which had also been cut with these restriction enzymes (Figure 3.20). The pET4215-ORF1 (Appendix 1.9) and pET4215-ORF2 (Appendix 1.10) constructs were first transformed into the INVαF' *E. coli* strain and then into the BLR *E. coli* strain containing T7 RNA polymerase. The pET4215-His-NSP5 and pET4215-His-NSP6 fusion proteins were both found to be in the insoluble fraction of the induced bacteria (Figure 3.21a and 3.21b). The purification of the two proteins from the insoluble fractions was undertaken using denatured purification and stepwise refolding. The pET4215-His-NSP5 protein and pET4215-His-NSP6 protein were eluted in 8M urea pH 3.5 and refolded by stepwise dialysis against 20mM Tris-HCl (Figure 3.22a and 3.22b). The pET4215-His-NSP5 protein was refolded from pH 10 to pH 7.5 and the pET4215-His-NSP6 protein was refolded from pH 4 to pH 7. The purified proteins were then subjected to Factor Xa digestion to remove the His tag and linker region. When the proteins were cleaved with Factor Xa a large

amount of protein degradation was observed preventing efforts to purify the cleaved protein.

Although this protein could not be used for functional assays the tagged purified pET4215-His-NSP5 and pET4215 His-NSP6 were successfully used to generate polyclonal sera to these proteins. The pET4215-His-NSP5 was used to generate guinea pig anti-NSP5 sera (Harlan sera labs, UK) as described in the Materials and Methods and the pET4215-His-NSP6 was used to generate rabbit anti-NSP6 sera (ISL Ltd, UK) as described in the Materials and Methods.

A

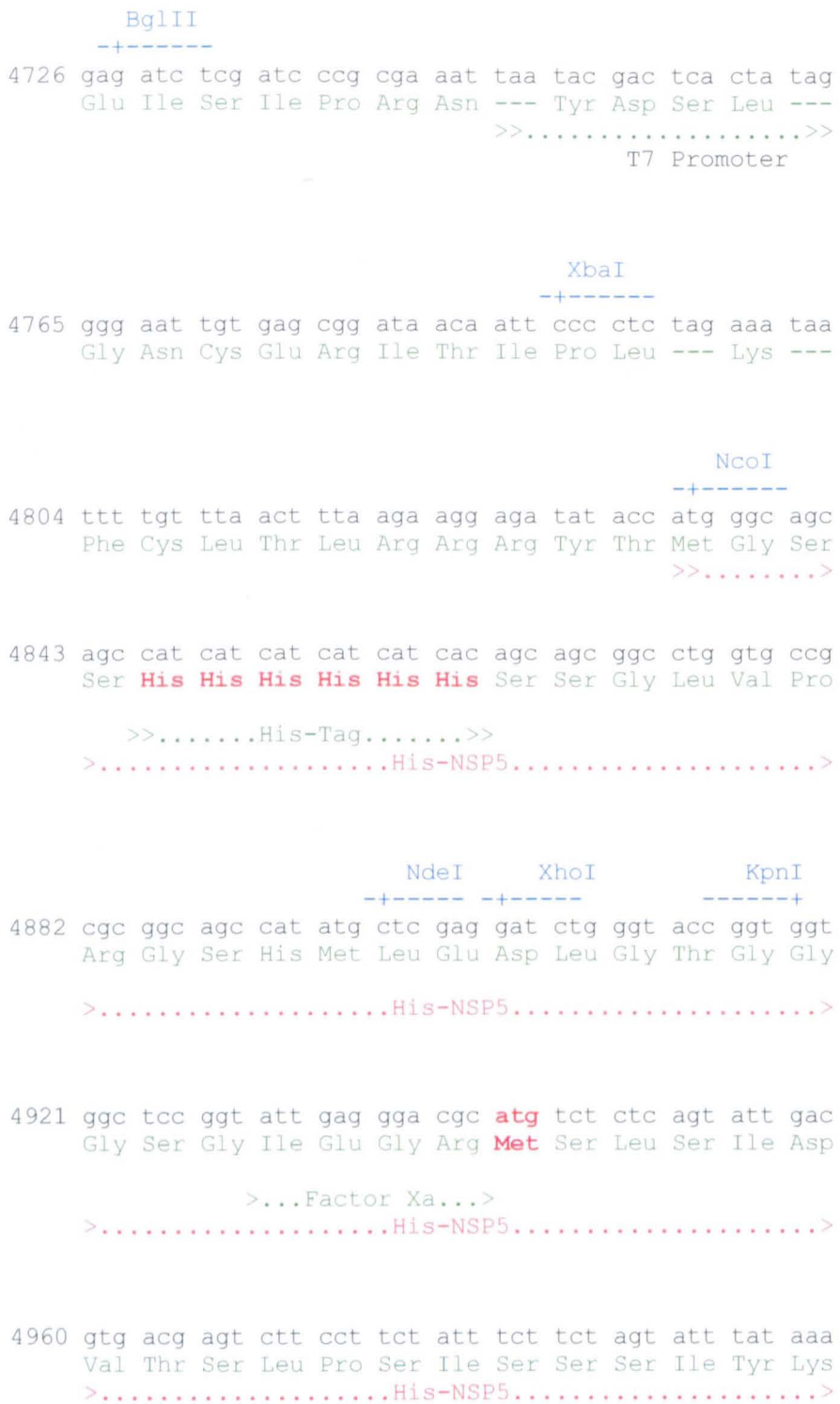
BglII
4726 gag atc tcg atc ccg cga aat taa tac gac tca cta tag
Glu Ile Ser Ile Pro Arg Asn --- Tyr Asp Ser Leu ---
T7 Promoter
XbaI
4765 ggg aat tgt gag cgg ata aca att ccc ctc tag aaa taa
Gly Asn Cys Glu Arg Ile Thr Ile Pro Leu --- Lys ---
NcoI
4804 ttt tgt tta act tta aga agg aga tat acc atg ggc agc
Phe Cys Leu Thr Leu Arg Arg Arg Tyr Thr Met Gly Ser
4843 agc cat cat cat cat cat cac agc agc ggc ctg gtg ccg
Ser His His His His His His Ser Ser Gly Leu Val Pro
His-Tag
His-NSP5
NdeI
XhoI
KpnI
4882 cgc ggc agc cat atg ctc gag gat ctg ggt acc ggt ggt
Arg Gly Ser His Met Leu Glu Asp Leu Gly Thr Gly Gly
His-NSP5
4921 ggc tcc ggt att gag gga cgc atg tct ctc agt att gac
Gly Ser Gly Ile Glu Gly Arg Met Ser Leu Ser Ile Asp
Factor Xa
His-NSP5
4960 gtg acg agt ctt cct tct att tct tct agt att tat aaa
Val Thr Ser Leu Pro Ser Ile Ser Ser Ser Ile Tyr Lys
His-NSP5

B

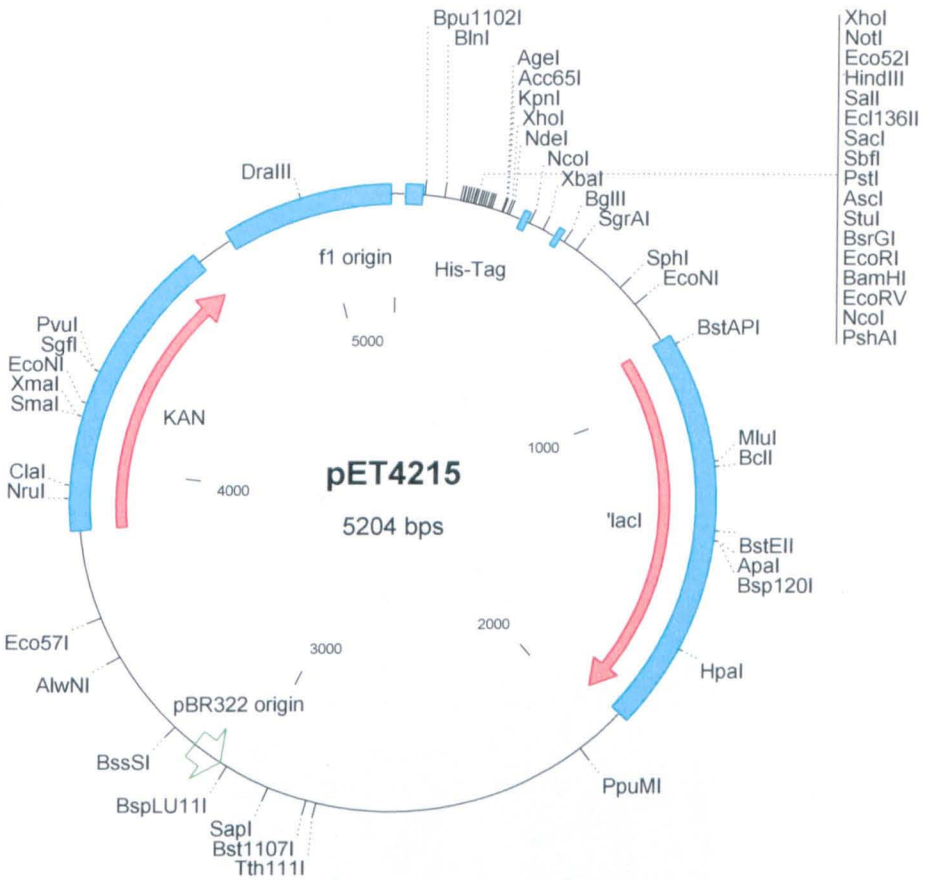

Figure 3.19 Restriction map of pET4215 and schematic of His linker region
Panel A) DNA sequence of the region of pET4215-ORF1 encoding the 6xHis tag and the linker region before the ORF of NSP5. Downstream of the 6xHis tag is a 22 amino acid linker region which is followed by a Factor Xa cleavage site. Restriction enzyme sites are indicated in blue and the amino acid sequence can be seen in green below the nucleotide triplets codons which encode them. The His tag and NSP5 start codon are both indicated in red.

Panel B) Representation of pET4215 constructed in the rotavirus laboratory (Chung, 2004). The vector was constructed by removing the GST tag from pET42b and replacing it with the His tag from the pET15 vector.

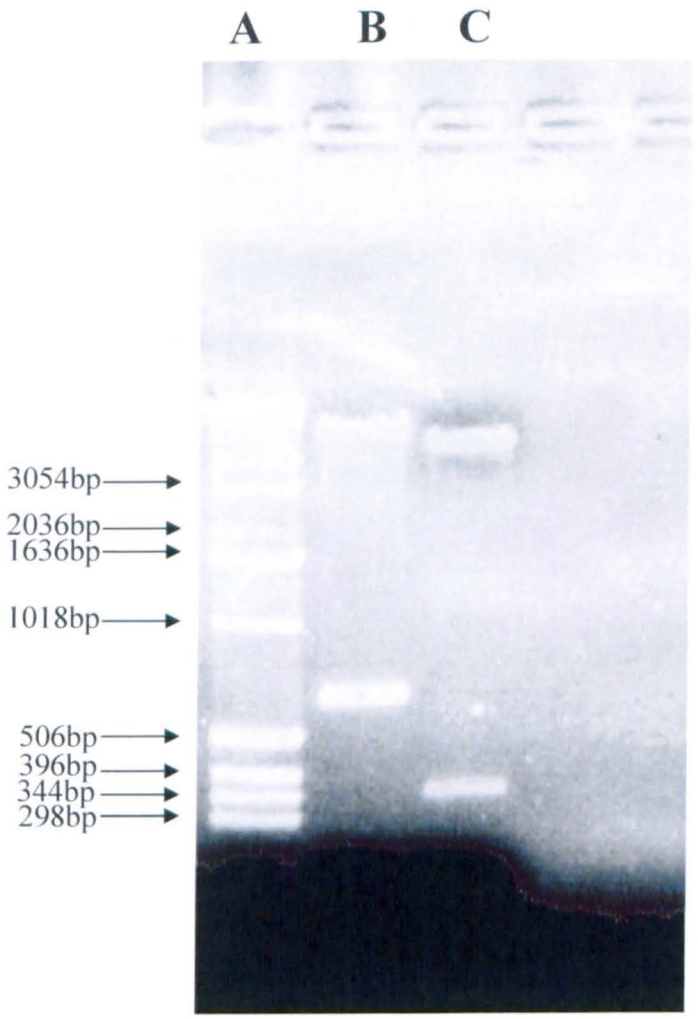

Figure 3.20 Restriction enzyme analysis of putative pET4215-ORF1 and pET4215-ORF2 clones

A cDNA copy of gene 11 ORF1 and ORF2 was generated using PCR carried out as described in the Materials and Methods. These cDNA were cloned into the pET4215 vector as described in the Materials and Methods. Single colonies were harvested and grown O/N at 37°C before being miniprepped as described in the Materials and Methods. The resulting plasmid DNA cut with *Kpn*I and *Pst*I to screen for potential inserts. The restriction digest was then fractionated on a 1% agarose gel stained with ethidium bromide and visualized using UV light as described in the Materials and Methods. Track A) DNA size marker ladder, track B) pET4215-ORF1 cut with *Kpn*I and *Pst*I and track C) pET4215-ORF2 cut with *Kpn*I and *Pst*I. Migration of the DNA size markers are indicated on the left hand side of the gel.

A

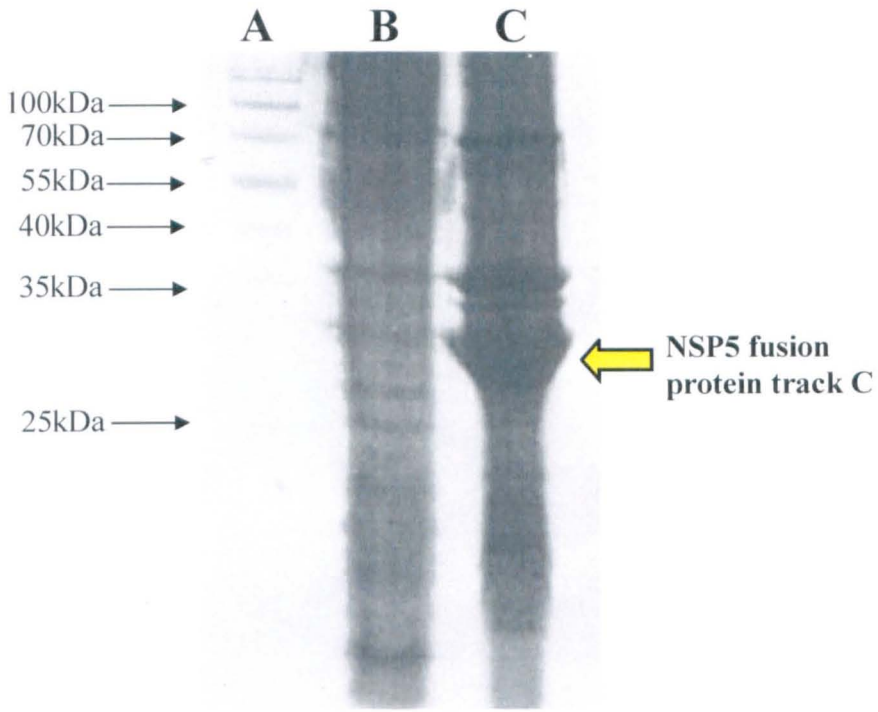
A
B
C
100kDa
70kDa
55kDa
40kDa
35kDa
25kDa
NSP5 fusion protein track C

B

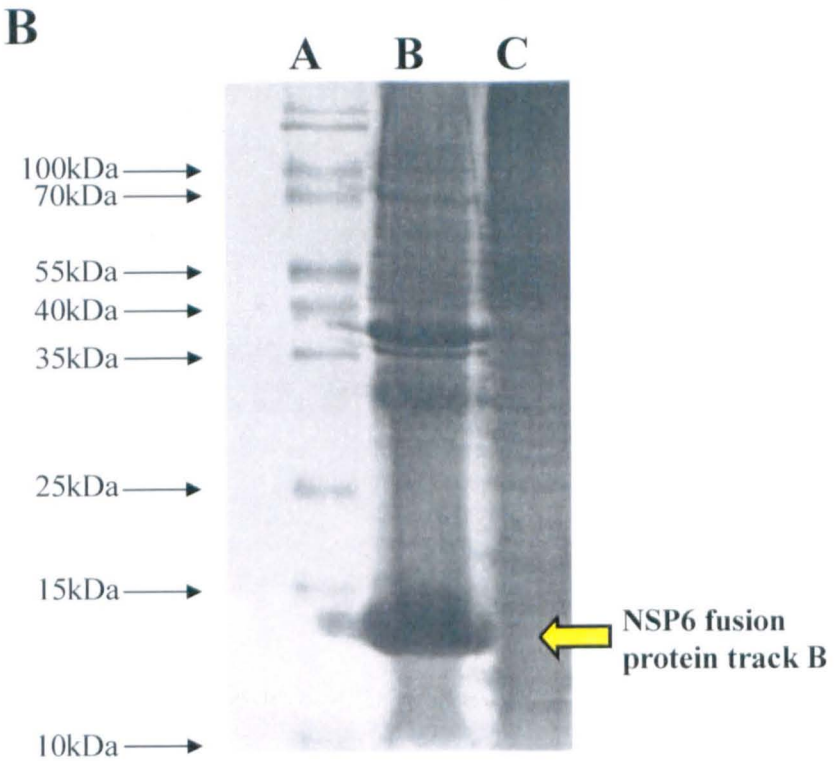
A
B
C
100kDa
70kDa
55kDa
40kDa
35kDa
25kDa
15kDa
10kDa
NSP6 fusion protein track B

Figure 3.21 Expression of His tagged NSP5 and NSP6 from pET4215-ORF1 and pET4215-ORF2

BLR *E. coli* containing either pET4215-ORF1 or pET4215-ORF2 were cultured in 500ml LB at 37°C until the OD reached between 0.5 and 1. IPTG was added to a final concentration of 1mM and cultures incubated for a further 4 hours. The cells were recovered by centrifugation and lysed by French press. The soluble and insoluble fractions were then separated by centrifugation and insoluble proteins solublised in 8M urea as described in the Materials and Methods. Both soluble and insoluble fractions from the induced cultures were then fractionated on a 14% SDS polyacrylamide gel which was stained with Coomassie blue as described in the Materials and Methods.

Panel A) Showing the induction test of His-NSP5 from pET4215-ORF1. Track A) Protein size markers 10-180 kDa, track B) Soluble fraction and track C) Insoluble fraction. Migration of the protein size markers are indicated on the left hand side of the gel and the position of the NSP5 fusion is indicated by the yellow arrow.

Panel B) Showing the induction test of His-NSP6 from pET4215-ORF2. Track A) Protein size markers 10-180 kDa, track B) Insoluble fraction and track C) Soluble fraction. Migration of the protein size markers are indicated on the left hand side of the gel and the position of the NSP6 fusion is indicated by the yellow arrow.

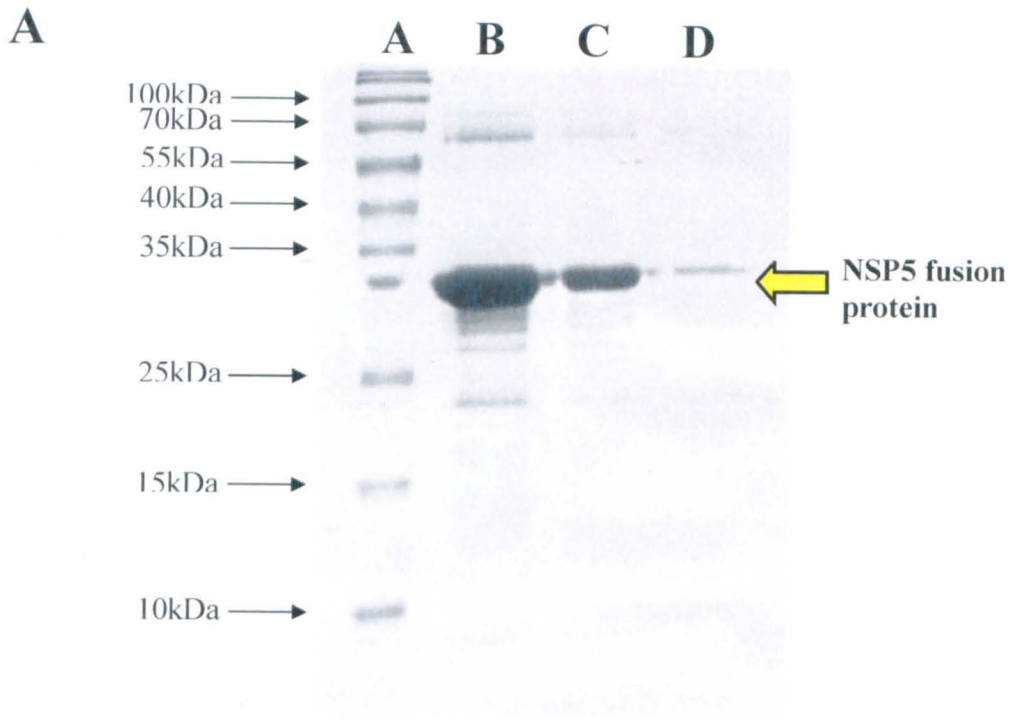
A
A
B
C
D
100kDa
70kDa
55kDa
40kDa
35kDa
25kDa
15kDa
10kDa
NSP5 fusion protein

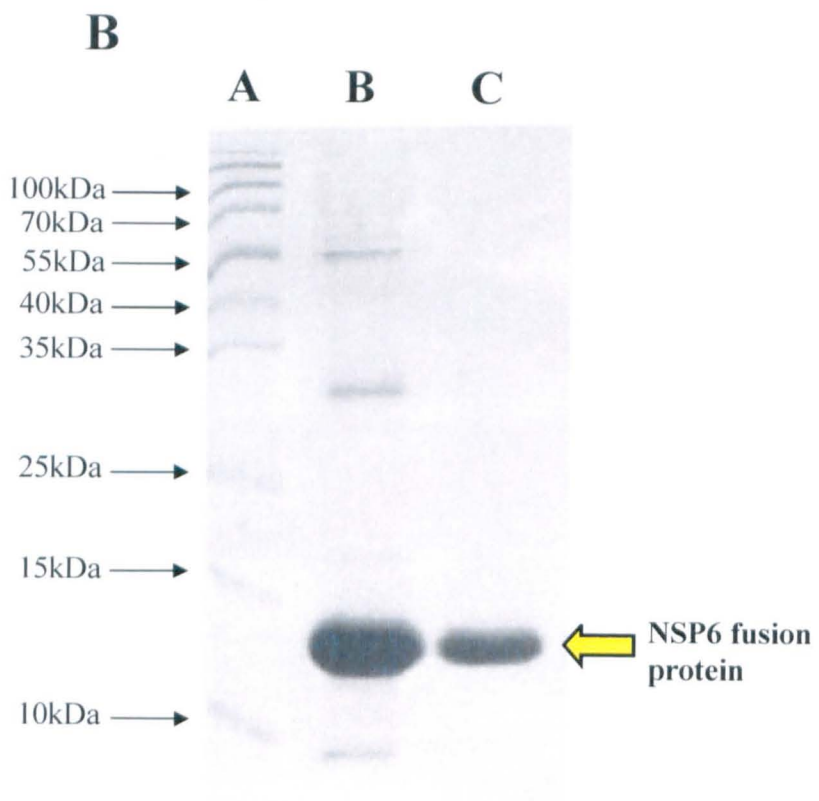
B
A
B
C
100kDa
70kDa
55kDa
40kDa
35kDa
25kDa
15kDa
10kDa
NSP6 fusion protein

Figure 3.22 Purification of His tagged NSP5 and NSP6 from pET4215-ORF1 and pET4215-ORF2

The insoluble fractions from cultures induced to express pET4215-His-NSP5 and pET4215-His-NSP6 were denatured in 6M Gu-HCl and passed over a Ni^{++} chelating column equilibrated with 8M urea pH 8.0. The column was then washed with 8M urea pH 8.0 until all protein flow through was removed. The column was then washed with 3 column volumes of 8M urea pH 6.0 followed by 3 column volumes of 8M urea pH 4.0. Finally protein was eluted by washing with 3 column volumes of 8M urea pH 3.5 as described in the Materials and Methods. The proteins were eluted from the column in 8M urea pH3.5 and refolded by stepwise dialysis against 20mM Tris-HCl. pET4215-His-NSP5 was refolded stepwise from 20mM Tris-Hcl pH 10 to pH 7.5 and pET4215-His-NSP6 was refolded by stepwise dialysis against 20mM Tris-HCl pH 4 to pH 7 as described in the Materials and Methods. The purified proteins were then fractionated on a 14% SDS polyacrylamide gel which was stained with Coomassie blue as described in the Materials and Methods.

Panel A) pET4215-His-NSP5 purified and refolded by stepwise dialysis against 20mM Tris-HCl 7.5. Track A) Protein size markers 10-180 kDa, tracks B-D) pET4215-His-NSP5 eluted fractions from Ni^{++} chelating column. Migration of the protein size markers are indicated on the left hand side of the gel and the position of the NSP5 fusion is indicated by the yellow arrow.

Panel B) pET4215-His-NSP6 purified and refolded by stepwise dialysis against 20mM Tris-HCl pH 7.5. Track A) Protein size markers 10-180 kDa, tracks B-C) pET4215-His-NSP6 eluted fractions from Ni^{++} chelating column. Migration of the protein size markers are indicated on the left hand side of the gel and the position of the NSP6 fusion is indicated by the yellow arrow.

3.3.7. Expression and purification of direct His tagged NSP5 and NSP6 proteins

The His tagged proteins expressed from the pET4215 vector had a large linker region between the His tag and the ORF's which could possibly interfere with the folding of the protein and increase instability leading to degradation during purification. To circumvent the problems encountered during purification of NSP5 and NSP6 with large tags and to remove the necessity for cleavage of these tags by Factor Xa, PCR was used to fuse a His tag directly to the 5' terminus of the two proteins. The 5' primer for these PCR's contained a unique restriction site of *Nde*I followed by the 6xhistidine residues and the start of the ORF. The 3' primer contained a *Pst*I restriction site. The pET42b vector was cut using these two restriction enzymes to completely remove the GST tagging domain. The gel extracted PCR products were cut with these restriction enzymes before being ligated into the open vector to create direct fusion His-NSP5 and His-NSP6 (Figure 3.23) Single colonies were then grown and minipreps performed in order to assess which contained the NSP5 and NSP6 ORF inserts (Figure 3.24a and 3.24b).

Induction tests showed that the protein expressed from these constructs were found in the insoluble fraction and both proteins were purified using a Ni^{++} chelating column as described above (Figure 3.25a and 3.25b). Following elution the His-NSP5 and His-NSP6 proteins were refolded by stepwise dialysis against 20mM Tris-HCl. His-NSP5 was refolded from 20mM Tris-HCl pH 10 to pH 7.5 and the His-NSP6 protein was refolded from 20mM Tris-HCl pH 4 to pH 7 (Figure 3.26a and 3.26b). This one step purification method created highly pure protein that required no further modification and could be used in functional assays. The purified NSP5

was found to exist as two discrete bands of 26 and 28 kDa when analysed by SDS-PAGE (Figure 3.26a). Mass spectrometry based N-terminal sequence analysis was used to establish that both of these bands were NSP5. Previous reports have indicated that different iso-forms of NSP5 can be generated by autophosphorylation of the protein (Afrikanova *et al.*, 1994; Blackhall *et al.*, 1998). The purification of NSP5 in two forms at 26 and 28 kDa might suggest that this has taken place in the bacterially expressed NSP5.

The purified NSP6 obtained with this protocol was also used to generate rat anti-NSP6 monospecific antisera (Harlan sera labs, UK) as described in the Materials and Methods.

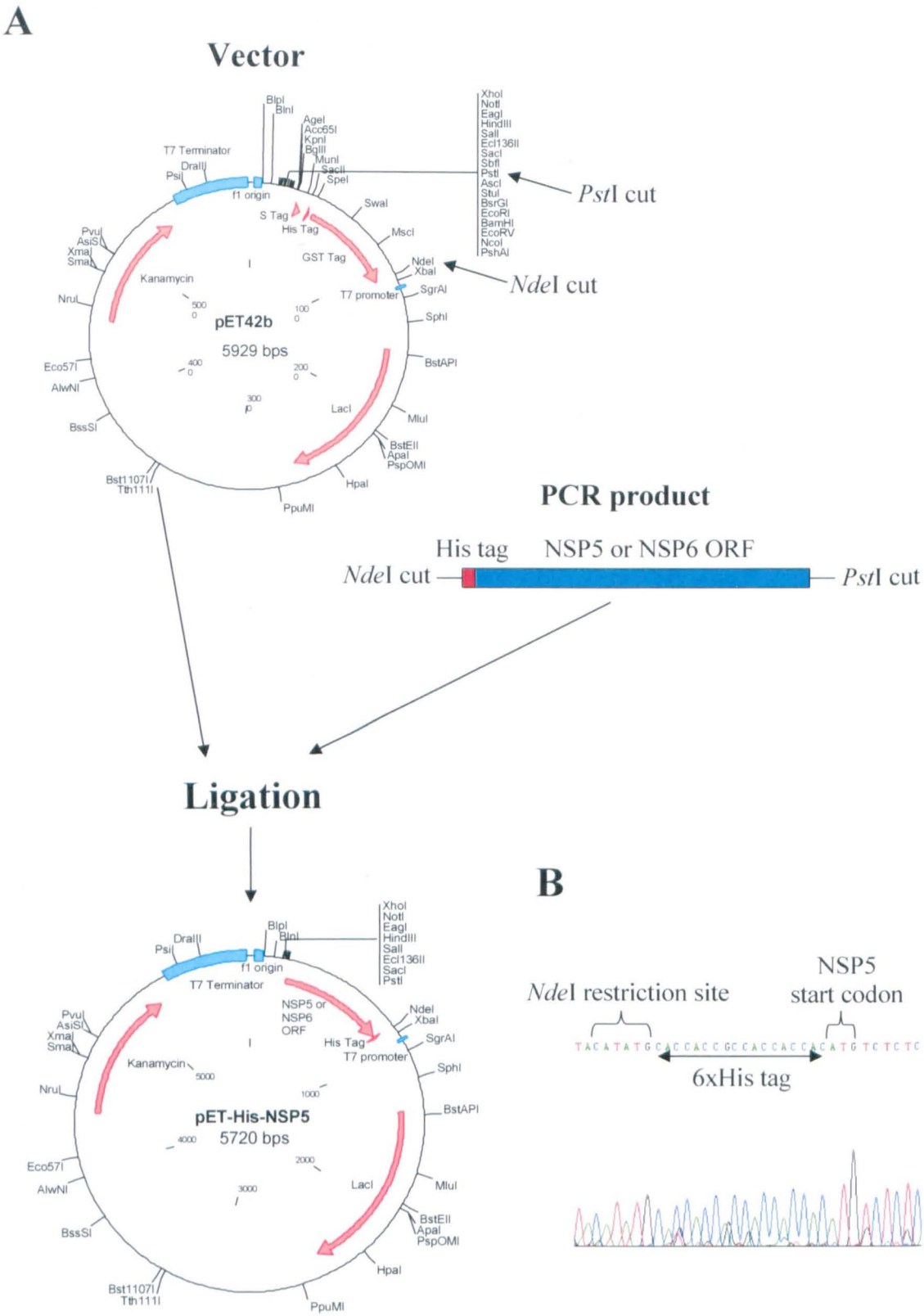
A
Vector
pET42b
5929 bps
T7 Terminator
f1 origin
S Tag
His Tag
GST Tag
T7 promoter
Kanamycin
LacI
PstI cut
NdeI cut
PCR product
His tag
NSP5 or NSP6 ORF
NdeI cut
PstI cut
Ligation
pET-His-NSP5
5720 bps
NSP5 or NSP6 ORF
B
NdeI restriction site
NSP5 start codon
6xHis tag

Figure 3.23 Strategy for cloning the NSP5 and NSP6 ORF's into a modified pET42b expression vector
Panel A) Schematic representation showing the insertion of PCR products of NSP5 and NSP6 ORF with a 6xHis tag at their 5' termini into a pET42b vector which lacked it's tagging region. The PCR products and the pET42b vector were cut with *Nde*I and *Pst*I restriction enzymes, gel purified and ligated as described in the Materials and Methods.

Panel B) DNA sequence chromatogram of pET-His-NSP5 construct showing the junction between the pET vector *Nde*I restriction site and the 6xHis tag ligated into the plasmid. The *Nde*I restriction site, 6xHis tag and the NSP5 start codon are identified at the top of the chromatogram.

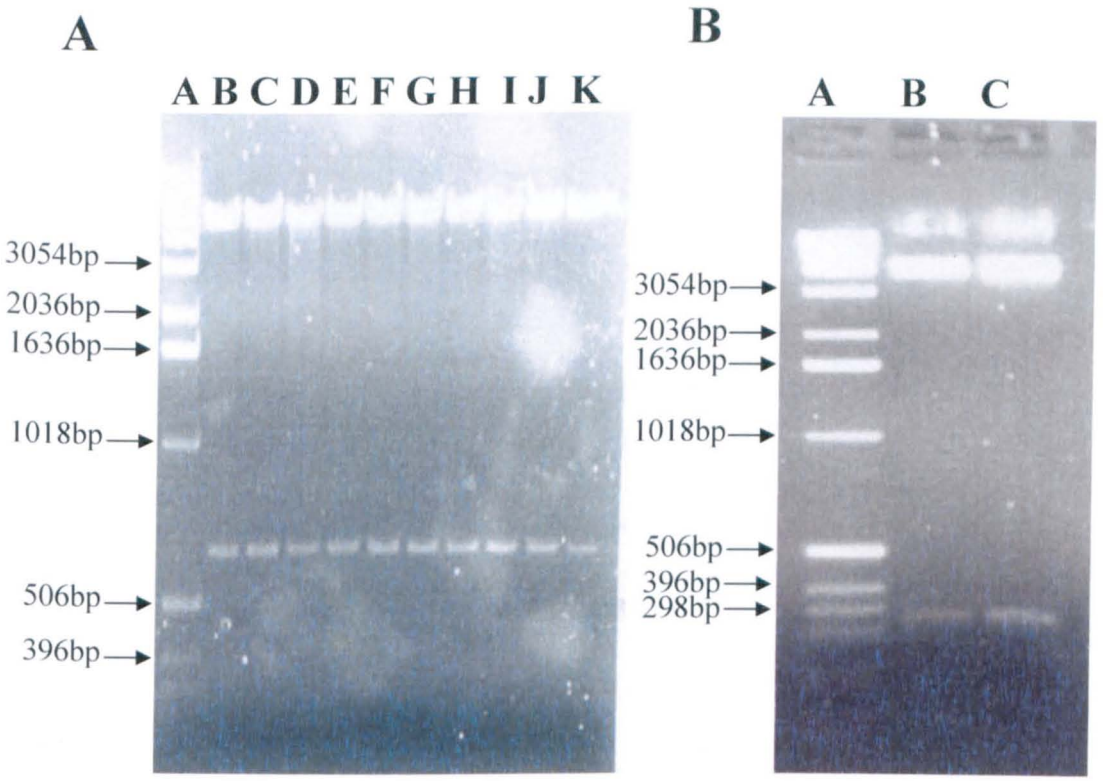

Figure 3.24 Restriction enzyme digestion analysis of the creation of pET42-HisORF1 and pET42-HisORF2

A cDNA copy of gene 11 ORF1 and ORF2 with direct 6xHis fusion tag was generated using PCR carried out as described in the Materials and Methods. This cDNA was cloned into a modified pET42b vector as described in the Materials and Methods. Single colonies were harvested and grown O/N at 37°C before being miniprepped as described in the Materials and Methods. The resulting plasmid DNA cut with *Nde*I and *Pst*I to screen for potential inserts. The restriction digest was then fractionated on a 1% agarose gel stained with ethidium bromide and visualized using UV light as described in the Materials and Methods.

Panel A) Tracks A-K pET42-HisORF1 colony screen using the *Nde*I and *Pst*I restriction enzymes to determine the presence of inserts. Track A) DNA size marker ladder, tracks B–K) Miniprepped colonies from the pET42-HisORF1 ligation cut with *Nde*I and *Pst*I. Migration of the DNA size markers are indicated on the left hand side of the gel.

Panel B) Tracks A-C pET42-HisORF2 colony screen using the *Nde*I and *Pst*I restriction enzymes to determine the presence of inserts. Track A) DNA size marker ladder, tracks B–C) Miniprepped colonies from the pET42-HisORF2 ligation cut with *Nde*I and *Pst*I. Migration of the DNA size markers are indicated on the left hand side of the gel.

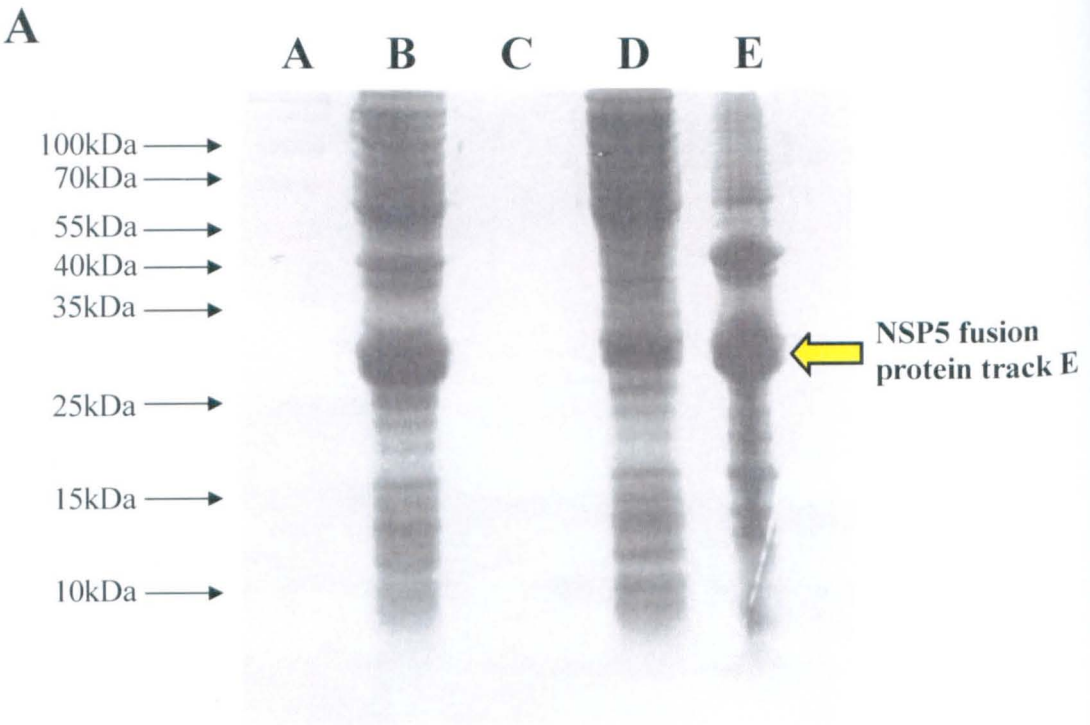
A
A B C D E
100kDa
70kDa
55kDa
40kDa
35kDa
25kDa
15kDa
10kDa
NSP5 fusion protein track E

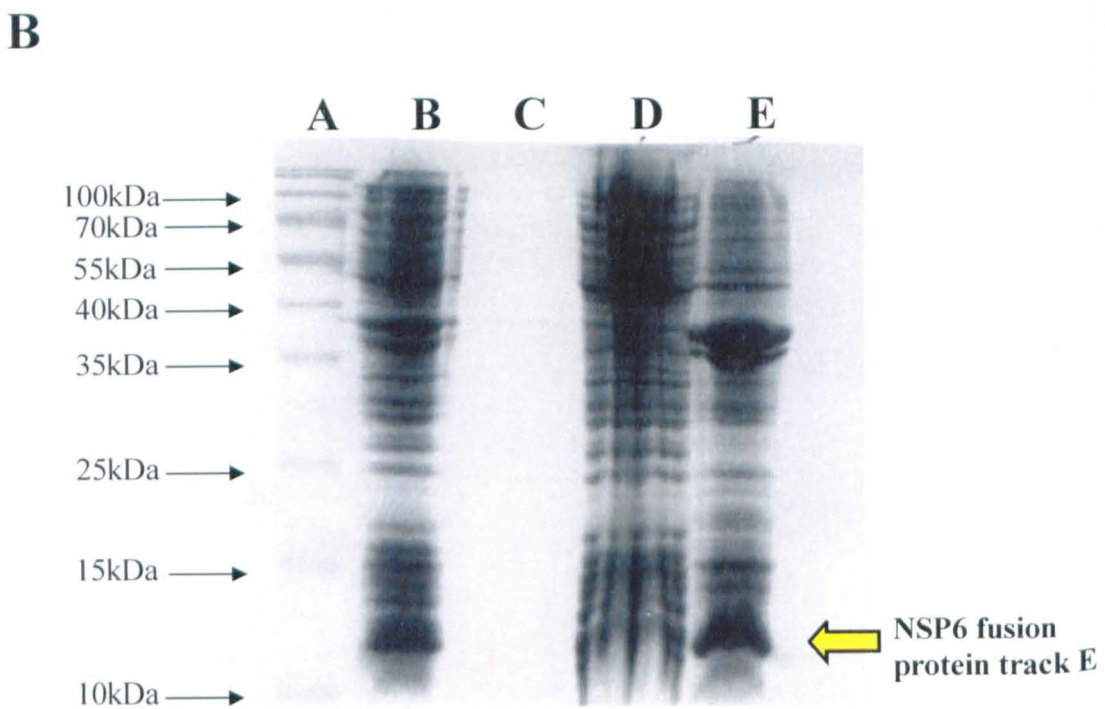
B
A B C D E
100kDa
70kDa
55kDa
40kDa
35kDa
25kDa
15kDa
10kDa
NSP6 fusion protein track E

Figure 3.25 Expression of His tagged NSP5 and NSP6
BLR *E. coli* cultures induced to express His-NSP5 or His-NSP6 in 500ml were incubated at 37°C until the OD reached between 0.5 and 1. IPTG was then added to a final concentration of 1mM and the cultures were incubated for a further 4 hours. Cells were recovered by centrifugation and lysed by French press. The soluble and insoluble fractions were then separated by centrifugation and insoluble proteins solublised in 8M urea as described in the Materials and Methods. Samples were fractionated on a 14% SDS-PAGE gel which was stained with Coomassie blue as described in the Materials and Methods.

Panel A) Expression of NSP5 with a His fusion tag. Track A) Protein size markers 10-180 kDa, track B) Total cell protein of induced culture, track C) Media fraction of induced culture, track D) Soluble fraction and track E) Insoluble fraction. Migration of the protein size markers are indicated on the left hand side of the gel and the position of the NSP5 fusion is indicated by the yellow arrow.

Panel B) Expression of NSP6 with a His fusion tag. Track A) Protein size markers 10-180 kDa, track B) Total cell protein of induced culture, track C) Media fraction of induced culture, track D) Soluble fraction and track E) Insoluble fraction. Migration of the protein size markers are indicated on the left hand side of the gel and the position of the NSP6 fusion is indicated by the yellow arrow.

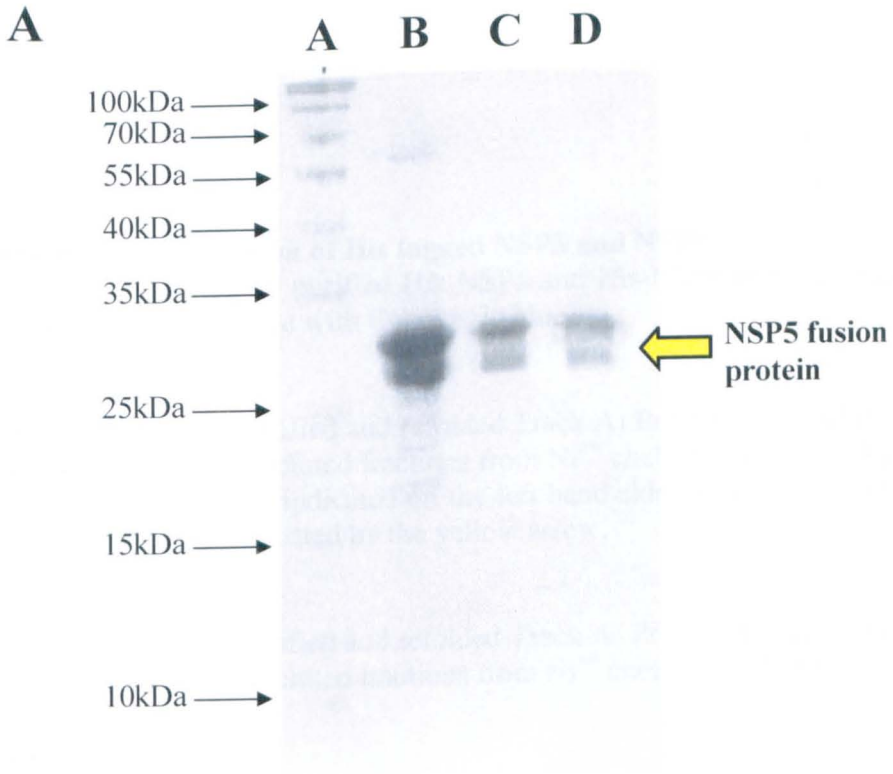
A
A B C D
100kDa
70kDa
55kDa
40kDa
35kDa
25kDa
15kDa
10kDa
NSP5 fusion protein

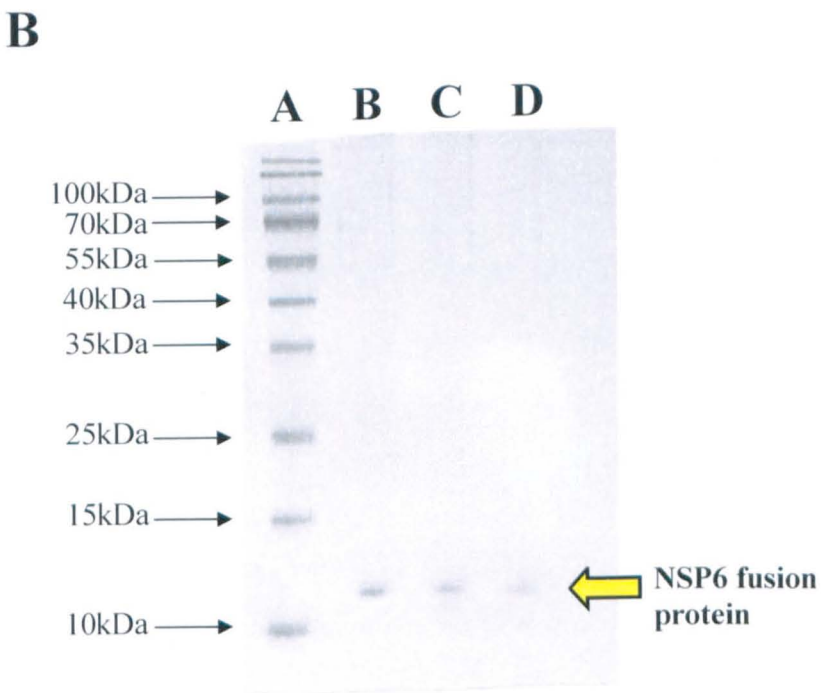
B
A B C D
100kDa
70kDa
55kDa
40kDa
35kDa
25kDa
15kDa
10kDa
NSP6 fusion protein

Figure 3.26 Purification of His tagged NSP5 and NSP6
SDS-PAGE analysis of purified His-NSP5 and His-NSP6 protein eluted from Ni^{++} chelating column stained with Coomassie blue.

Panel A) His-NSP5 purified and refolded Track A) Protein size markers 10-180 kDa, tracks B-D) His-NSP5 eluted fractions from Ni^{++} chelating column. Migration of the protein size markers is indicated on the left hand side of the gel and the position of the NSP5 fusion is indicated by the yellow arrow.

Panel B) His-NSP6 purified and refolded Track A) Protein size markers 10-180 kDa, tracks B-D) His-NSP6 eluted fractions from Ni^{++} chelating column.

3.4. Discussion

Work presented in this chapter has shown the cloning, expression and purification strategies used in order to obtain purified NSP5 and NSP6. In the process of cloning the NSP5 (ORF1) and NSP6 (ORF2) coding sequences into the required vectors several changes from the published UKtc bovine rotavirus strain gene 11 sequence were identified, some of which lead to changes in the amino acid sequences of NAP5 and NSP6. These changes make the gene 11 sequence of the UKtc strain more homologues with other rotavirus gene 11 sequences.

The original strategy was to utilise a GST tag and purification on GSH-agarose. However this was not possible because the GST-NSP6 protein was expressed in the insoluble fraction and the GST-NSP5 protein degraded when cut with Factor Xa to remove the GST tag after purification.

The second expression strategy employed was to use a vector that contained a His tag on the end of a large linker region for purification. Although large amounts of the His tagged proteins were obtained using this approach, removal of the 6xHis tag and the linker region was problematic leading to highly degraded protein. However it did generate purified protein that was used to generate monospecific antisera against the NSP5 and NSP6 protein.

To produce highly pure protein required for functional assays PCR was used to fuse a 6xHis tag directly onto the amino terminus of NSP5 and NSP6. This approach allowed single step purification of NSP5 and NSP6. The purified NSP6 protein was again used to generate monospecific antisera. The purified NSP5 protein was seen to exist in two forms migrating at 26 and 28 kDa in PAGE. Both forms

were confirmed by mass spectrometry to be NSP5 possibly indicating that autophosphorylation was occurring during *E. coli* protein expression.

The work in this chapter has demonstrated the means by which purified protein and monospecific antisera were produced to the two rotavirus proteins NSP5 and NSP6 for use in future experiments.

Results

Chapter 4

Expression and Localisation of

NSP5 and NSP6

4.1 Aims

The aims of the work described in this chapter were to examine the expression and intracellular localisation of the NSP5 and NSP6 proteins encoded by rotavirus gene 11.

4.2 Introduction

NSP5 and NSP6 proteins have both been localised to the viroplasm of infected cells and shown to be expressed throughout the rotavirus infection (Petrie *et al.*, 1884; Mattion *et al.*, 1991). The NSP6 protein was detected as a 12 kDa protein expressed at low levels (Mattion *et al.*, 1991; Torres-vega *et al.*, 2000). The NSP5 protein was found in infected cells as three isoforms differing in their level of phosphorylation. These isoforms are found at 26, 28 and 30-34 kDa when analysed by SDS-PAGE (Welch *et al.*, 1989; Afrikanova *et al.*, 1996; Poncet *et al*,. 1997; Blackhall *et al.*, 1997). NSP2 has been shown to upregulate the phosphorylation of NSP5 from the 26 and 28 kDa isoforms to the hyperphosphorylated 30-34 kDa isoform (Afrikanova *et al.*, 1998). A number of studies have indicated that NSP5 has some level of autophosphorylation activity but was unable to form the hyperphosphorylated isoform by this means (Blackhall *et al.*, 1997; Blackhall *et al.*, 1998).

The formation of viroplasm-like structures in the absence of a rotavirus infection has been observed in cells transfected with plasmids expressing NSP5 and another rotavirus protein NSP2 (Fabbretti *et al.*, 1999). A number of deletion

mutants were used to determine that the N-terminus of NSP5 was essential for binding of NSP2 (Frabbretti *et al.*, 1999).

The exact distribution of NSP6 still remains unclear, Mattion *et al* stated that when their anti-NSP6 sera was used in immunofluorescence experiments the NSP6 was found in discrete foci smaller than that of the NSP5, which they claimed were potentially the viroplasms (Mattion *et al.*, 1991). Nothing more is known about the expression of NSP6, other than it has been immunoprecipitated from cells infected with the YM and SA11 rotavirus strains and that co-imunoprecipitation of NSP5 and NSP6 was achieved by using cells transfected with the open reading frames of the two proteins (Mattion *et al.*, 1991; Torres-Vega *et al.*, 2000).

4.3 Results

4.3.1. Expression of the NSP5 and NSP6 proteins *in vitro*

A coupled *in vitro* transcription/translation system was used to investigate expression levels of the proteins transcribed from the rotavirus UKtc strain gene 11. A gene 11 cDNA was sub-cloned into the expression vector PCIneo positioning it downstream of the T7 promoter (Figure 4.1). This construct was used in the *in vitro* transcription/translations system to express the two viral proteins which were radio-labelled by the addition of ^{35}S Methionine to the reaction mixture. Autoradiography was used to detect the radio-labelled NSP5 and NSP6 proteins. The NSP5 protein appeared as expected, at the 26 – 28 kDa and NSP6 was detected at 12 kDa in much smaller amounts (Figure 4.2).

In order to verify that the protein detected at 12 kDa was indeed NSP6 and not simply a prematurely terminated fragment of NSP5, the ORF2 of gene 11 (i.e. the NSP6 coding region) was cloned separately into the PCIneo vector. Using this construct a large amount of NSP6 protein was produced at 12 kDa, which was not detected when only the PCIneo vector was used in the expression system (Figure 4.2).

4.3.2. Hyperphosphorylation of NSP5 in the coupled *in vitro* transcription/translation system

The protein expressed from the gene11-PCIneo construct in the coupled *in vitro* transcription/translation system was incubated overnight at 20°C. The incubated NSP5 protein was able to form the higher hyperphosphorylated form which could be seen at the 30-34 kDa band of protein (Figure 4.3). However, a control sample left at 4°C overnight did not form the hyperphosphorylated NSP5 isoform. This indicates that hyperphosphorylation of NSP5 can occur in the absence of NSP2 either by the presence of cellular kinases in the reaction mixture or by a low level of NSP5 autophosphorylation over an extended incubation period.

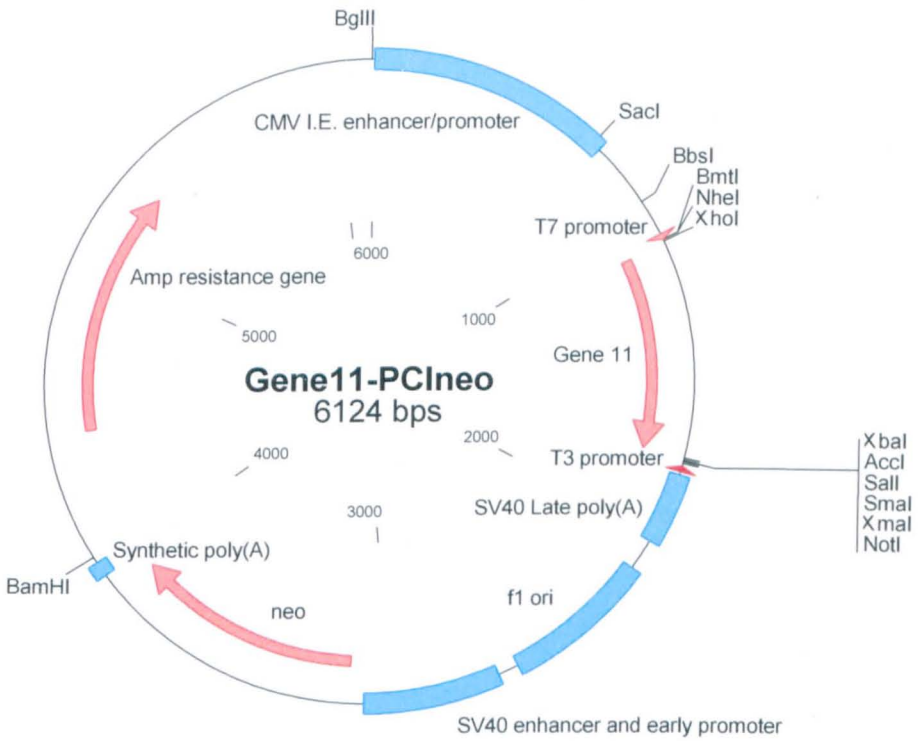

Figure 4.1 Schematic diagram of the structure of gene 11 in the PCIneo expression vector

The rotavirus gene 11 was amplified from the pET42b-gene11 plasmid by PCR using primers that introduced an *Xho*I restriction site at the 5' termini and an *Xba*I restriction site at the 3' termini. The PCR product and the PCIneo vector were both cut with these restriction enzymes and gel purified. The two cDNA's were ligated and transformed into *E. coli* as described in the Materials and Methods.

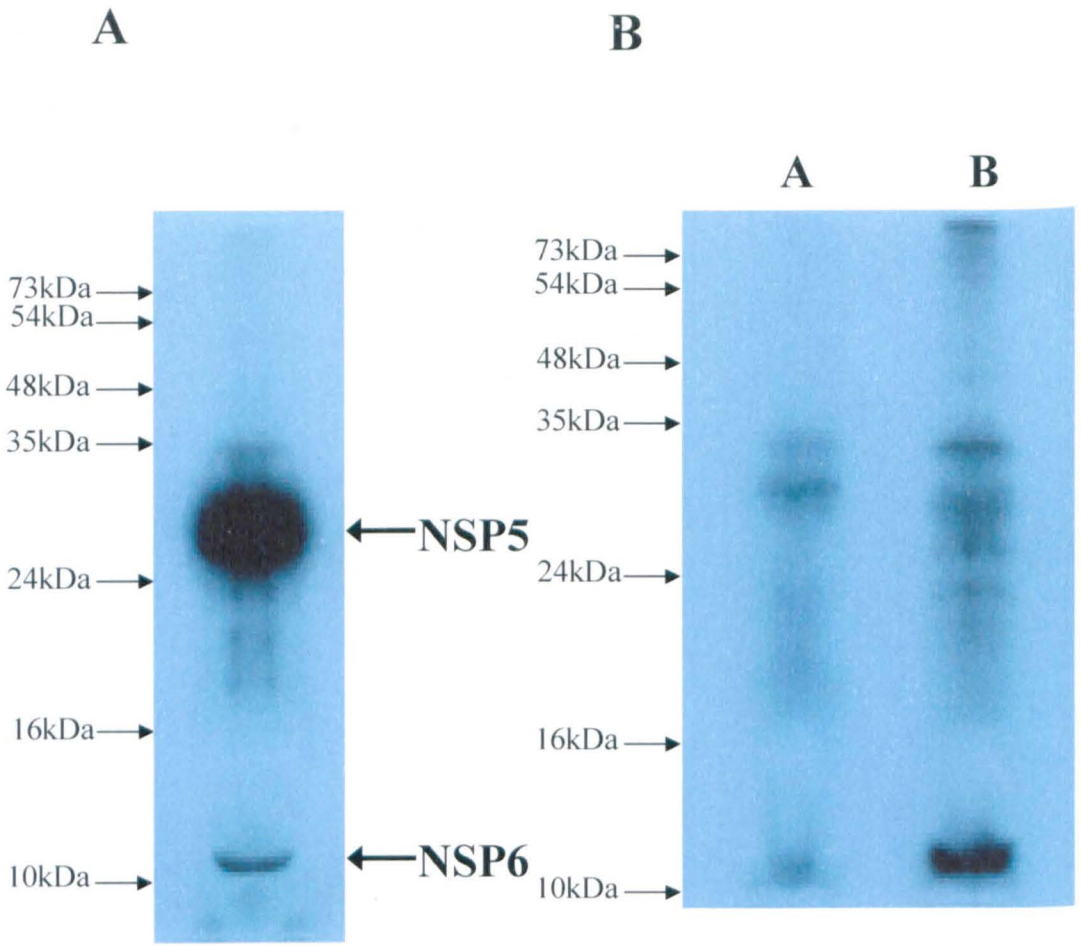
A
B
A
B
73kDa
54kDa
48kDa
35kDa
24kDa
16kDa
10kDa
NSP5
NSP6
73kDa
54kDa
48kDa
35kDa
24kDa
16kDa
10kDa

Figure 4.2 Expression of NSP5 and NSP6 from gene 11 and detection of the NSP6 protein expressed from a coupled *in vitro* transcription/translations system

Panel A) Gene 11 of the UKtc strain of rotavirus was cloned into the PCIneo expression vector (gene11-PCIneo). *In vitro* transcription/translation using this viral cDNA construct was carried out as described in the Materials and Methods. The protein products were analysed by PAGE as described in the Materials and Methods. After drying, the gel was autoradiographed as described in the Materials and Methods. The migration positions of the molecular weight size markers are indicated on the left hand side of the autoradiogram and the positions of NSP5 and NSP6 are indicated by arrows on the right hand side.

Panel B) The NSP6 coding region was cloned into the PCIneo expression vector (NSP6-PCIneo). *In vitro* transcription/translation reaction was carried out as described in the Materials and Methods. The protein products were analysed by PAGE as described in the Materials and Methods. After drying, the gel was autoradiographed as described in the Materials and Methods. Track A) shows protein expression from the PCIneo plasmid and track B) shows protein expression from the Gene11-PCIneo construct. The migration positions of the molecular weight size markers are indicated on the left hand side of the autoradiogram.

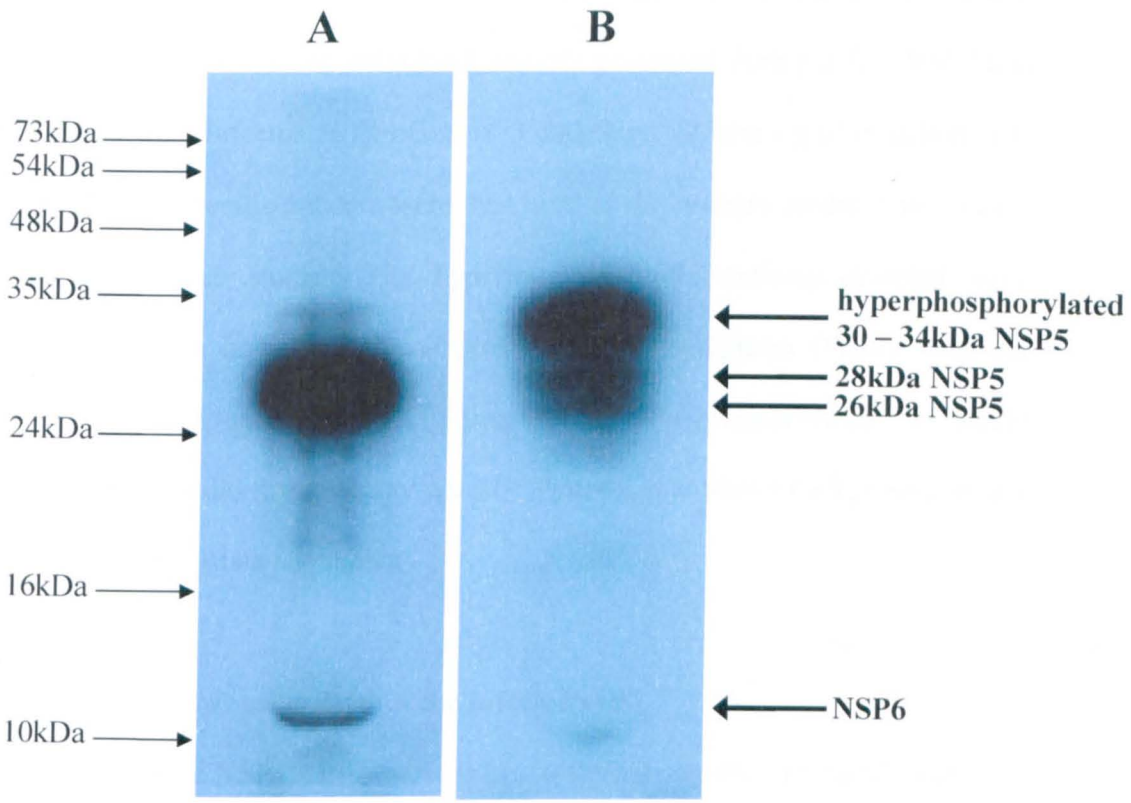

Figure 4.3 Hyperphosphorylation of the NSP5 in the coupled *in vitro* transcription/translations system

Protein expressed from the gene11-PCIneo construct in the coupled *in vitro* transcription/translation system was incubated O/N at either 20°C or 4°C.

In vitro transcription/translation using this viral cDNA construct was carried out as described in the Materials and Methods and the reaction mixture split into two equal halves one of which was incubated O/N at 4°C and the other at 20°C. The protein products were analysed by PAGE as described in the Materials and Methods. After drying the gel was autoradiographed as described in the Materials and Methods. Track A) shows the proteins present after O/N incubation at 4°C and track B) shows the proteins after O/N incubation at 20°C. The migration positions of the molecular weight size markers are indicated on the left hand side of the autoradiogram and the positions of NSP6 and the different phosphorylated isoforms of NSP5 are indicated by arrows on the right hand side.

4.3.3. Detection of NSP5 and NSP6 by immunofluorescence

Immunofluorescence experiments on cells infected with the UKtc rotavirus strain were undertaken using polyclonal antisera generated from purified NSP5 and NSP6. Cells were infected at an m.o.i. of 3 and fixed 12 hours post infection. The polyclonal monospecific antisera were then used as the primary antibody in indirect immunofluorescence studies. The hyperimmune NSP5 antisera detected large punctate occlusion bodies of the viroplasms in the cytoplasm (Figure 4.4). As expected no specific staining for NSP5 was seen with the preimmune sera. However the NSP6 antisera did not give any specific fluorescence above background at any time post infection (data not shown).

4.3.4. Viroplasm formation within the infected cell

The localisation of NSP5 to the viroplasms was first reported in early studies of rotaviruses (Gallegos & Patton, 1989). A time course study was performed to investigate the intracellular distribution of NSP5 and the viroplasms it forms, cells were fixed at time points of 2, 4, 6, 10, 16, and 24 hours post infection and stained with NSP5 antisera (Figure 4.5). The results indicated that there were few viroplasms evident at the earliest time point but this number rose dramatically over the following 2 hours. At 6 hours post infection the number appeared to decrease, possibly as a result of viroplasms coalescing. Consistent with this interpretation was the fact that the size of the viroplasms began increasing at approximately this time. At 16 hours, large occlusion bodies could be seen that were much fewer in number than at earlier time points. The last time point, 24 hours, showed little change from

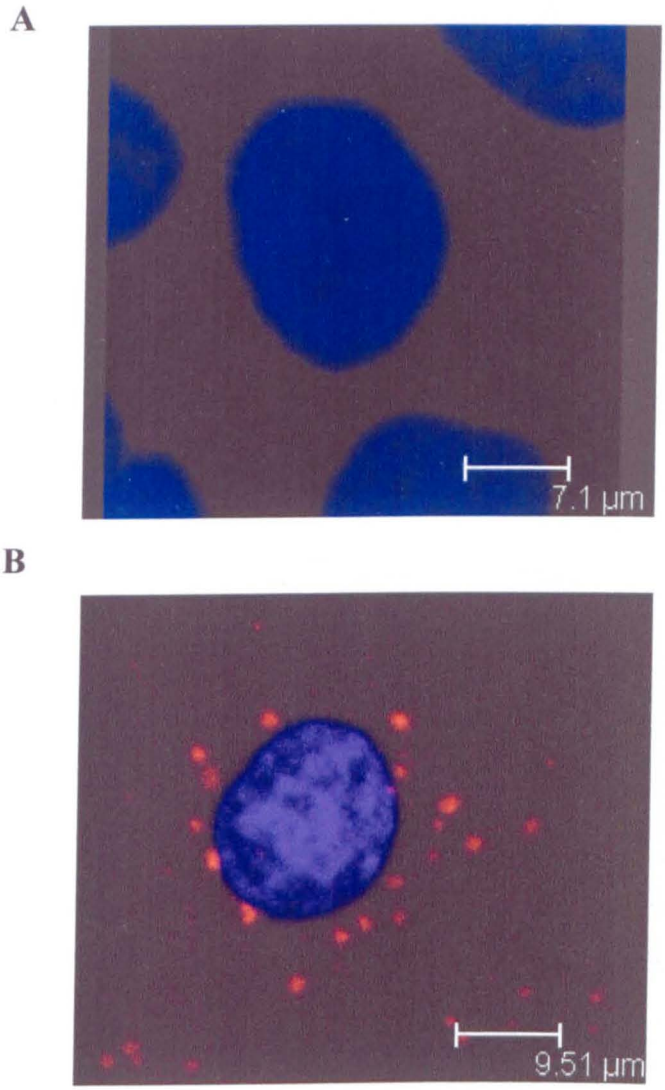

Figure 4.4 Localisation of NSP5 in virus infected cells by indirect immunofluorescence

Confluent monolayers of BSC1 cells were infected with the UKtc strain of rotavirus at an m.o.i. of 3. At 16 hours post infection the cells were fixed using methanol at -20°C. The fixed cells were then stained with either panel A) guinea pig pre-immune sera or panel B) a 1:200 dilution of guinea pig anti NSP5 sera. This was followed by staining with the secondary antibody goat anti guinea pig Alexa fluor 594 (red). Nuclei were stained with DAPI (blue) and fluorescence was detected using confocal microscopy as described in the Materials and Methods. Size of scale bar is indicated on images.

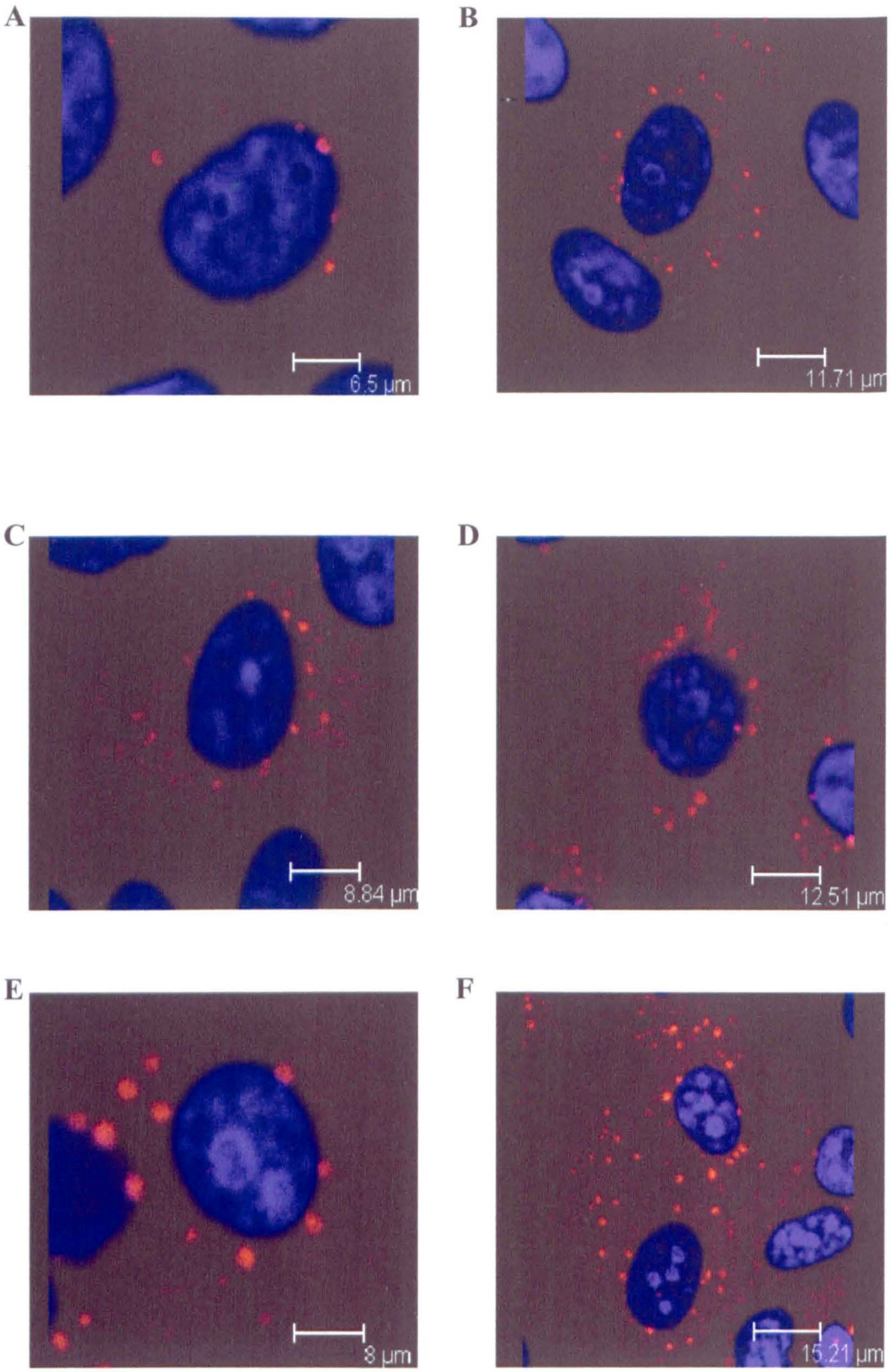
A
6.5 µm
B
11.71 µm
C
8.84 µm
D
12.51 µm
E
8 µm
F
15.21 µm

Figure 4.5 Time course of viroplasm formation in virus infected cells
Confluent monolayers of BSC1 cells were infected with the UKtc strain of rotavirus at an m.o.i. of 3. The cells were then fixed using methanol at -20°C at several time points panel A) 2 hours post infection, panel B) 4 hours post infection, panel C) 6 hours post infection, panel D) 10 hours post infection, panel E) 16 hours post infection and panel F) 24 hours post infection.

The fixed cells were then stained using a 1:200 dilution of guinea pig anti NSP5 sera, followed by staining with the secondary antibody goat anti guinea pig Alexa fluor 594. Nuclei were stained with DAPI and fluorescence was detected using confocal microscopy as described in the Materials and Methods. Size of scale bar is indicated on images.

that evident at 16 hours however there was a small increase in the number of viroplasms, possibly due to secondary rounds of replication from newly synthesised core particles.

4.3.5. Morphology of the NSP5 protein within the viroplasm

In the later time points as the viroplasms began to increase in size, ring structures were observed. However in the lower confocal slices there appeared to be a base to these rings indicating more of a cup shape to the distribution of the NSP5 protein. By viewing individual images of a confocal series which pass through a viroplasm it was possible to view this cup shape of the viroplasm (Figure 4.6). Also the impression gained from studying the viroplasms was that most of the viroplasms appeared to be localised to the lower half of the cells i.e. towards the side attached to the tissue culture flask.

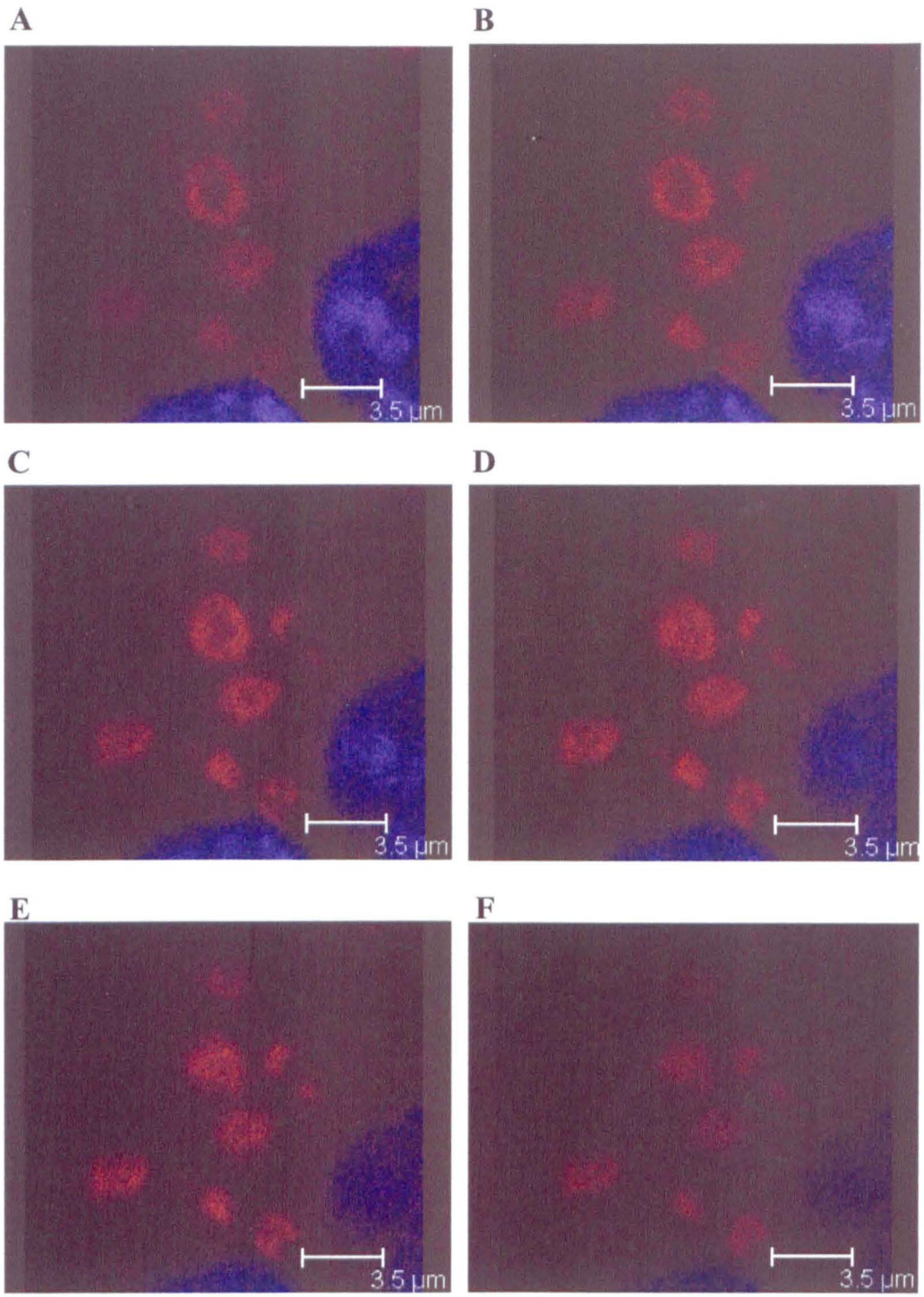
A
B
C
D
E
F
3.5 µm
3.5 µm
3.5 µm
3.5 µm
3.5 µm
3.5 µm

Figure 4.6 Morphology of NSP5 within the viroplasm
Horizontal stack of a confocal series showing NSP5 distribution within viroplasms. Confluent monolayers of BSC1 cells were infected with the UKtc strain of rotavirus at an m.o.i. of 3. The cells were then fixed using methanol at -20°C at 16 hours post infection. The fixed cells were then stained using a 1:200 dilution of guinea pig anti NSP5 sera, followed by staining with the secondary antibody goat anti guinea pig Alexa fluor 594. Nuclei were stained with DAPI and fluorescence was detected using confocal microscopy as described in the Materials and Methods. Size of scale bar is indicated on images.

4.3.6. Detection of the NSP6 protein in virus infected cells

Two polyclonal antisera were generated against the purified NSP6 protein (as stated in the previous chapter), one in a rabbit and the second in a rat. NSP6 expression could not be detected above background using immunofluorescence with either of these sera and Western blot on infected cell lysate did not detect the presence of any NSP6 protein. However the sera could be used to detect purified His-NSP6 protein by Western blot analysis (Figure 4.7).

Immunoprecipitation of radio-labelled protein was the only method by which NSP6 could be detected in virus infected cells. Infected cells were labelled with ^{35}S methionine for 5 hours beginning at 3 hours post infection. These cells were then lysed and immunoprecipitation performed using either the NSP5 or NSP6 sera. The immunoprecipitated proteins were separated on a 14% SDS-PAGE gel and proteins detected by autoradiography. The immunoprecipitation detected both NSP5 and NSP6, but the level of NSP6 detected was significantly lower than that of NSP5 (Figure 4.8). Several large bands appeared to be non-specifically precipitated by both sera. These non-specific bands were also precipitated using monospecific sera to VP7 (Figure 4.9a) and when using only the protein A sepharose beads in a precipitation without any sera (Figure 4.9b). No NSP5 or NSP6 proteins were precipitated from uninfected cells or by using beads alone, demonstrating the specificity of the two sera.

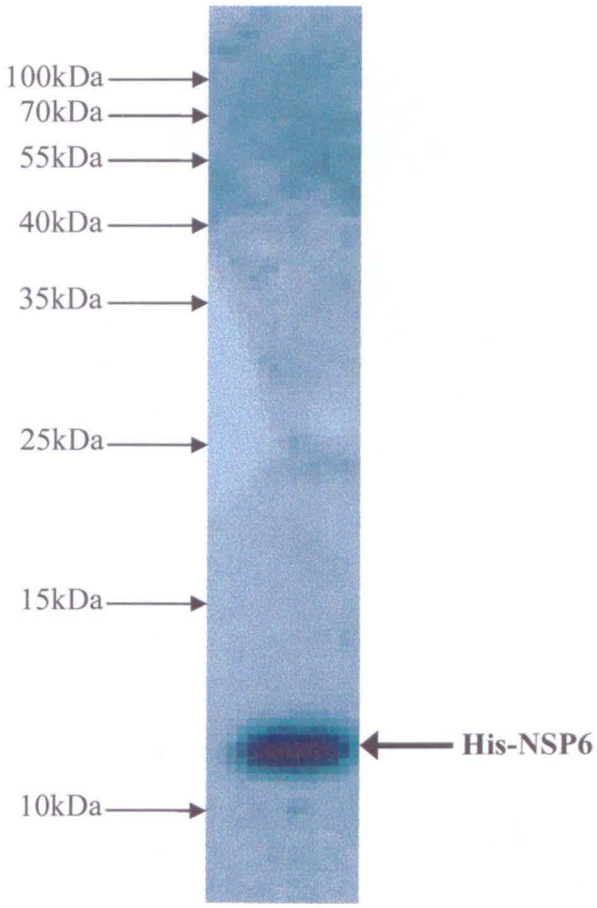

Figure 4.7 Detection of purified NSP6 protein by Western blot
100ng of purified NSP6 protein was run on a 14% SDS-PAGE gel and transferred to a nitrocellulose ECL membrane as described in the Materials and Methods. A Western blot was carried out using the Amersham ECL Western blot kit as described in the Materials and Methods. The Western blot was probed with 1:10,000 dilution of rabbit anti NSP6 sera and with the secondary HRP-conjugated goat anti rabbit at a dilution of 1:20,000. The NSP6 protein was then detected by exposure to X-ray film. The migration positions of the molecular weight size markers are indicated on the left hand side of the Western blot and the positions of the His-NSP6 is indicated by arrows on the right hand side.

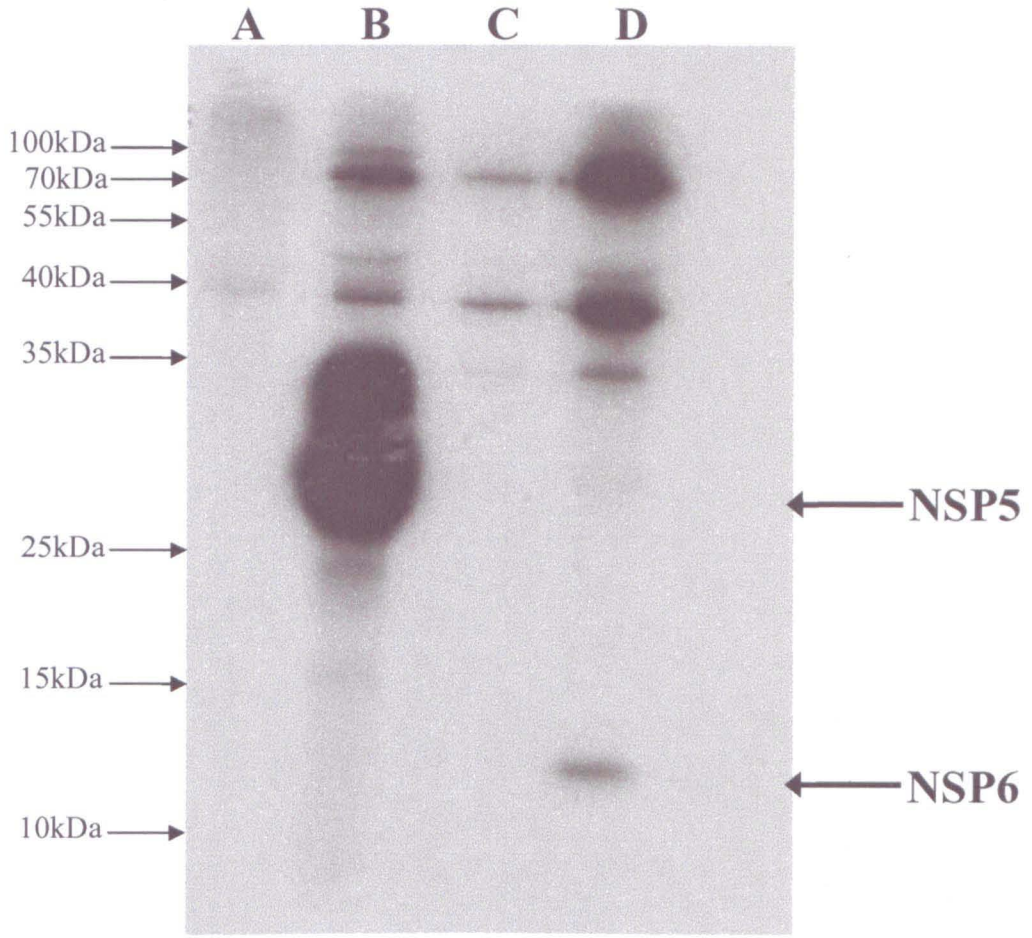

Figure 4.8 Immunoprecipitation of NSP5 and NSP6 from virus infected cells
Confluent monolayers of BSC1 cells were infected with the UKtc strain of rotavirus at an m.o.i. of 3. The cells were overlaid with methionine free DMEM and incubated at 37°C for 3 hours to deplete the methionine pool. The medium was then removed and replaced with methionine free DMEM containing approximately 200µCi of ^{35}S methionine and incubated for a further 5 hours. Cells were harvested in 500µl of RIPA lysis buffer. Immunoprecipitation was then performed using either the guinea pig anti NSP5 polyclonal sera or the rabbit anti NSP6 polyclonal sera as described in the Materials and Methods. The precipitated proteins were fractionated on a 14% SDS-PAGE gel and detected by autoradiography as described in the Materials and Methods. Track A) Immunoprecipitation using NSP5 pre immune sera, track B) Immunoprecipitation using NSP5 hyper immune sera, track C) Immunoprecipitation using NSP6 pre immune sera and track D) Immunoprecipitation using NSP6 hyper immune sera. The migration positions of the molecular weight size markers are indicated on the left hand side of the autoradiogram and the positions of NSP5 and NSP6 are indicated by arrows on the right hand side.

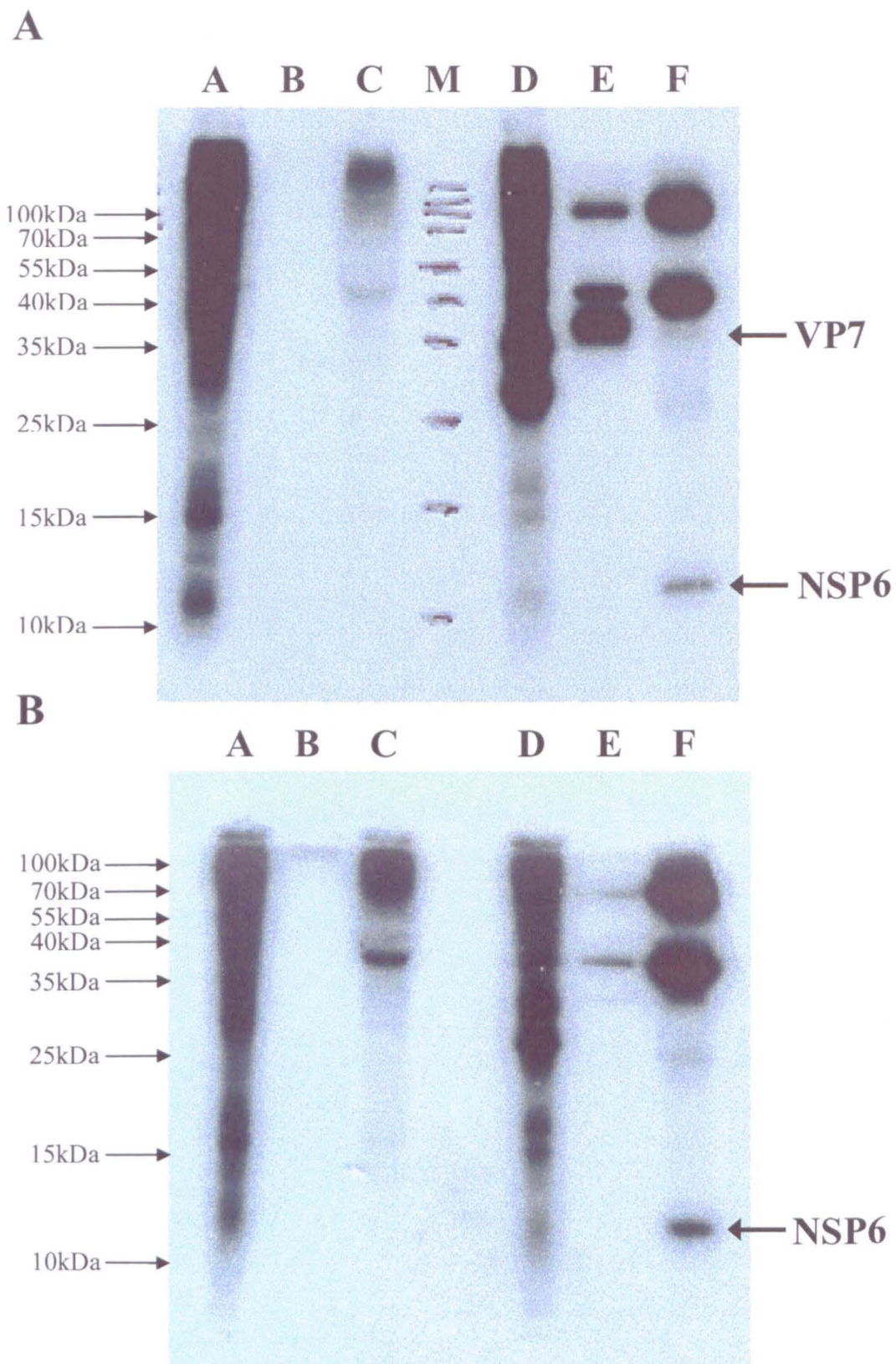
A
A B C M D E F
100kDa
70kDa
55kDa
40kDa
35kDa
25kDa
15kDa
10kDa
VP7
NSP6
B
A B C D E F
100kDa
70kDa
55kDa
40kDa
35kDa
25kDa
15kDa
10kDa
NSP6

Figure 4.9 Autoradiograms showing immunoprecipitation of NSP6 and VP7 showing the presence of non-specific bands and immunoprecipitation of uninfected and infected cells using protein A sepharose beads only or with NSP6 polyclonal antisera

Confluent monolayers of BSC1 cells were infected with the rotavirus UKtc strain at an m.o.i. of 3. The cells were overlaid with methionine minus DMEM and incubated at 37°C for 3 hours to deplete the methionine pool. The medium was then removed and replaced with methionine free DMEM containing approximately 200µCi of ^{35}S methionine and incubated for a further 5 hours. Cells were harvested in 500µl of RIPA lysis buffer as described in the Materials and Methods.

Panel A) Immunoprecipitation was then performed using either rabbit anti VP7 polyclonal antisera or rabbit anti NSP6 polyclonal antisera on uninfected or infected cells as described in the Materials and Methods. Track A) Uninfected cell whole lysate, track B) Immunoprecipitation of uninfected cells using VP7 antisera, track C) Immunoprecipitation of uninfected cells using NSP6 antisera, track M) position of molecular weight markers, track D) Infected cell whole lysate, track E) Immunoprecipitation of infected cells using VP7 antisera and track F) Immunoprecipitation of infected cells using NSP6 antisera. The migration positions of the molecular weight size markers are indicated on the left hand side of the autoradiogram.

Panel B) Immunoprecipitation was then performed using either protein A sepharose beads only or with rabbit anti NSP6 polyclonal antisera on uninfected or infected cells As described in the Materials and Methods. Track A) Uninfected cell whole lysate, track B) Immunoprecipitation of uninfected cells using protein A sepharose beads only, track C) Immunoprecipitation of uninfected cells using NSP6 antisera, track D) Infected cell whole lysate, track E) Immunoprecipitation of infected cells using protein A sepharose beads only and track F) Immunoprecipitation of infected cells using NSP6 antisera. The migration positions of the molecular weight size markers are indicated on the left hand side of the autoradiogram.

4.3.7. Kinetics of NSP6 expression during a rotavirus infection

A confluent monolayer of cells was infected with the UKtc strain of rotavirus at an m.o.i. of 3 to produce one step growth conditions. The cells were then pulse labelled with ^{35}S methionine for 1 hour at 2, 3, 4, 6 and 8 hours post infection. Immunoprecipitation of the resulting pulsed cells lysates was then performed using rabbit anti NSP6 sera to determine the level of NSP6 expression over the course of the virus replication cycle (Figure 4.10). There appeared to be little NSP6 expressed at the 2-3 hour time point but after this there was a steady but low rate of NSP6 expression (Figure 4.10). There appeared to be slightly less NSP6 found in the 8 hour time point but, this may have been due to a reduction in the number of cells as a result of virus induced cell lysis (Figure 4.10).

4.3.8. Stability of the NSP6 protein within the rotavirus infected cell

To test the stability of NSP6 pulse chase analysis was used. Infected cells were pulsed with ^{35}S methionine for 5 hours and then chased with an excess of cold methionine for a further 2 hours before harvesting. The cells were lysed and immunoprecipitations performed using either the anti NSP5 or anti NSP6 sera. The relative abundance of the two proteins in the pulse and chase samples were then compared by SDS-PAGE. There were approximately equivalent amounts of NSP5 in both the pulse and chase lanes showing NSP5 was stable over the chase period. By contrast virtually all of the NSP6 had disappeared from the chase lane (Figure 4.11). This showed that NSP6 is unstable in virus infected cells and is turned over at a much higher rate than any of the other viral proteins.

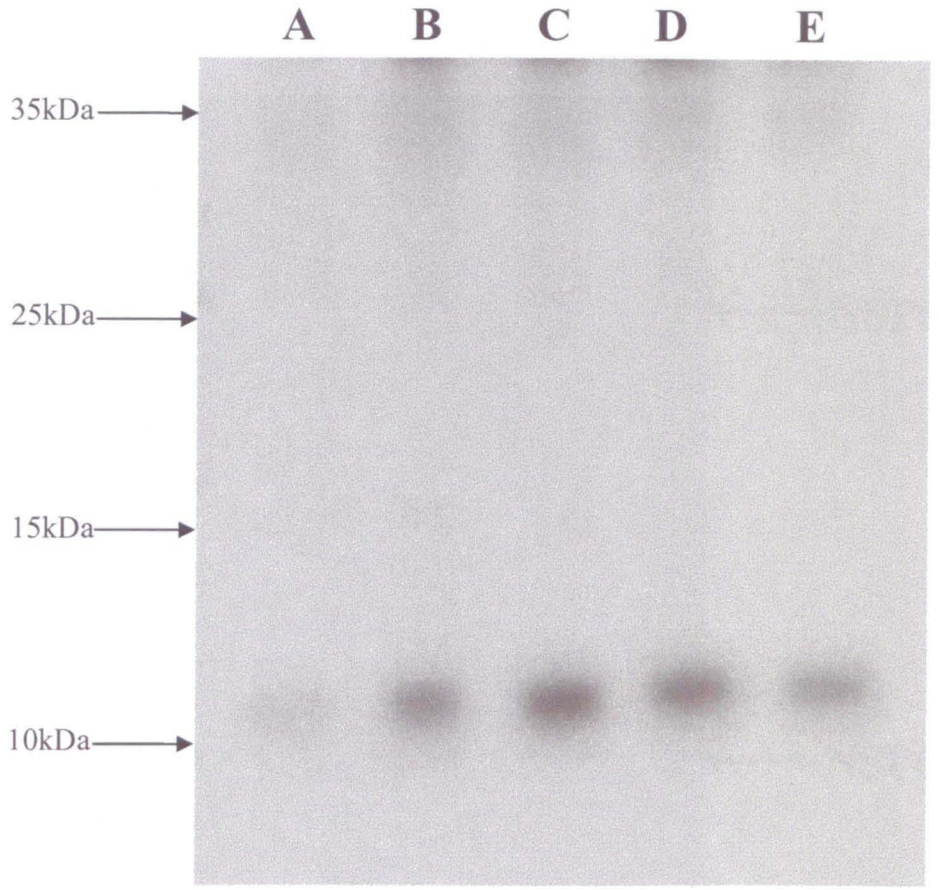

Figure 4.10 Immunoprecipitation of the NSP6 protein over the course of a rotavirus infection

A confluent monolayer of BSC1 cells was infected with rotavirus at an m.o.i. of 3 to produce one step growth conditions. These cells were then pulse labelled with ^{35}S methionine for 1 hour over the course of the infection at Track A) 2, track B) 3, track C) 4, track D) 6 and track E) 8 hours post infection. Immunoprecipitation was then performed with the rabbit anti NSP6 sera as described in the Materials and Methods to determine the level of NSP6 expression over the course of an infection. The migration positions of the molecular weight size markers are indicated on the left hand side of the autoradiogram.

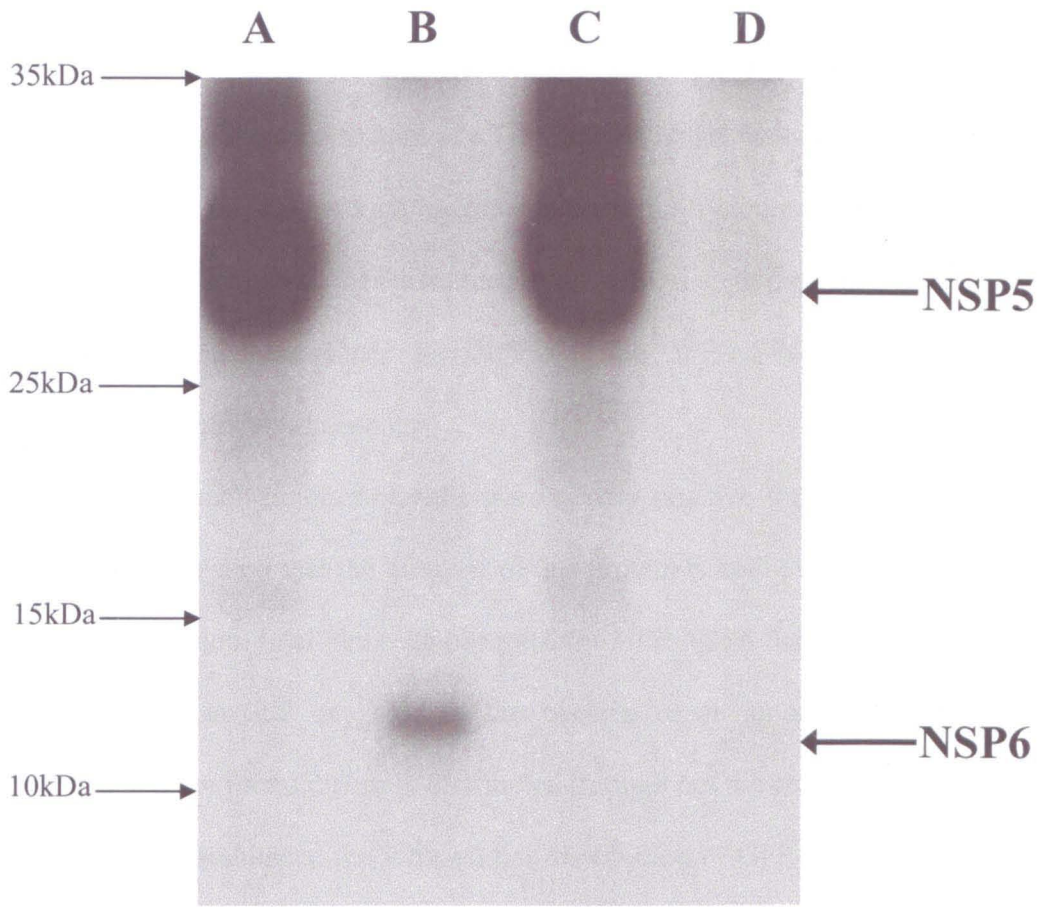

Figure 4.11 Analysis of NSP6 stability in virus infected cells
Confluent monolayers of BSC1 cells were infected with the UKtc strain of rotavirus at an m.o.i. of 3. The cells were overlaid with methionine free DMEM and incubated at 37°C for 3 hours to deplete the methionine pool. The medium was then removed and replaced with methionine free DMEM containing approximately 200µCi of ^{35}S methionine and incubated for a further 5 hours. Half of the cells were harvested in 500µl of RIPA lysis buffer. The remaining cells were overlaid with DMEM containing 50x the normal level of cold methionine and incubated for a further 2 hours before harvesting. Immunoprecipitation was then performed using either the guinea pig anti NSP5 polyclonal sera or the rabbit anti NSP6 polyclonal sera as described in the Materials and Methods. The precipitated proteins were then separated by 14% SDS-PAGE gel showing track A) Immunoprecipitation of NSP5 from infected cells after 5 hour pulse, track B) Immunoprecipitation of NSP6 after 5 hour pulse, track C) Immunoprecipitation of NSP5 after 2 hour chase and track D) Immunoprecipitation of NSP6 after 2 hour chase. The migration positions of the molecular weight size markers are indicated on the left hand side of the autoradiogram and the positions of NSP5 and NSP6 are indicated by arrows on the right hand side.

4.3.9. Localisation of the NSP6 protein within the infected cell

The failure to detect fluorescence in virus infected cells using the NSP6 antisera prompted the construction of a GFP tagged NSP6 fusion. The coding region of the NSP6 protein was inserted in-frame into the multi-cloning site of the phrGFP-N1 vector this vector was then transfected into BSC-1 cells and incubated at 37°C for 48 hours. The intracellular distribution of the GFP-NSP6 fusion protein was studied using confocal microscopy.

Only a small number of cells were clearly positive for fluorescence of the GFP-NSP6 suggesting that the turnover of this protein is high even in the absence of a rotavirus infection. In all the cells observed the GFP-NSP6 fusion protein appeared to be clustered around one side of the nucleus in an amorphous mass in the cytoplasm and not found diffusely distributed through out the cell (Figure 4.12).

Having established the intracellular distribution of GFP-NSP6 in transfected cells, the effect of a rotavirus infection upon this distribution was investigated. Cells were transfected with GFP-NSP6 and 48 hours post transfection infected with the UKtc strain of rotavirus. Sera against NSP5 were used to localise viroplasms within the infected cell (Figure 4.13). A control experiment was set up in which GFP alone was transfected into cells which were subsequently infected with UKtc, the results showed that GFP remained diffuse throughout the cell and did not redistribute to viroplasms (Figure 4.13). Figure 4.14 shows a number of cells infected with rotavirus, one of which that had also been transfected with the GFP-NSP6 expressing plasmid the distribution of the GFP-NSP6 (green) and the NSP5 (red) can be clearly seen. The GFP-NSP6 fusion protein was found to redistribute into small

discrete spherical structures, which co-localised with the NSP5 protein within the viroplasms (Figure 4.14). Figure 4.15 shows that the GFP-NSP6 appeared to be centred in the middle of the viroplasms rather than distributed around the edge like the NSP5 protein. The distribution was reminiscent of that reported recently for the NSP2 protein (Eichwald *et al.*, 2004).

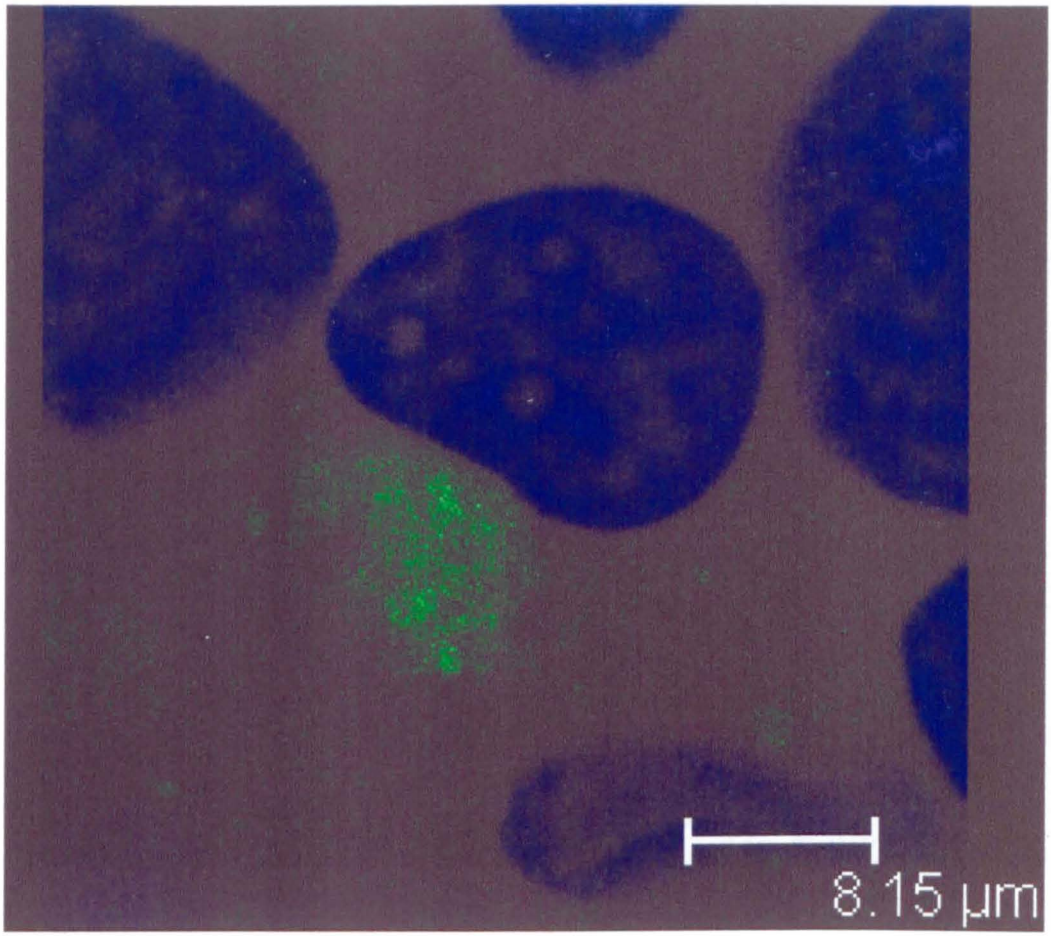

Figure 4.12 Distribution of GFP-NSP6 in transfected cells
Confluent monolayers of BSC1 cells were transfected with the GFP-NSP6 vector using lipofectamine 2000. The cells were incubated for 48 hours at 37°C and fixed using methanol at -20°C. Nuclei were stained with DAPI (blue) and fluorescence of the GFP-NSP6 (green) was detected using confocal microscopy as described in the Materials and Methods. Size of scale bar is indicated on image.

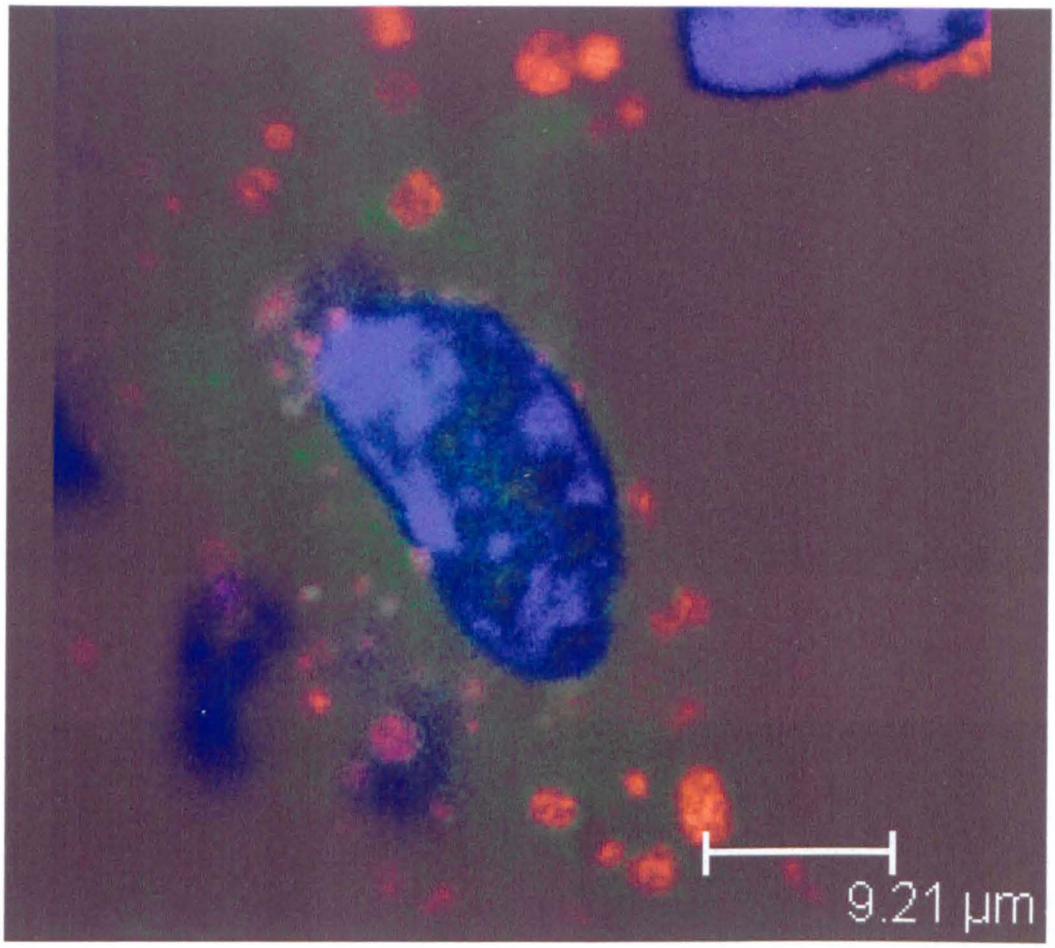

Figure 4.13 Distribution of GFP control in rotavirus infected cells
Confluent monolayers of BSC1 cells were transfected with phrGFP-N1 vector using lipofectamine 2000. The cells were incubated for 48 hours at 37°C and infected with the Uktc strain of rotavirus at an m.o.i. of 3. The cells were incubated at 37°C for a further 8 hours and then fixed using methanol at -20°C. The fixed cells were stained using a 1:200 dilution of guinea pig anti NSP5 sera, followed by staining with the secondary antibody goat anti guinea pig Alexa fluor 594 (red). Nuclei were stained with DAPI (blue) and fluorescence of the GFP (green) was detected using confocal microscopy as described in the Materials and Methods.. Size of scale bar is indicated on image.

A

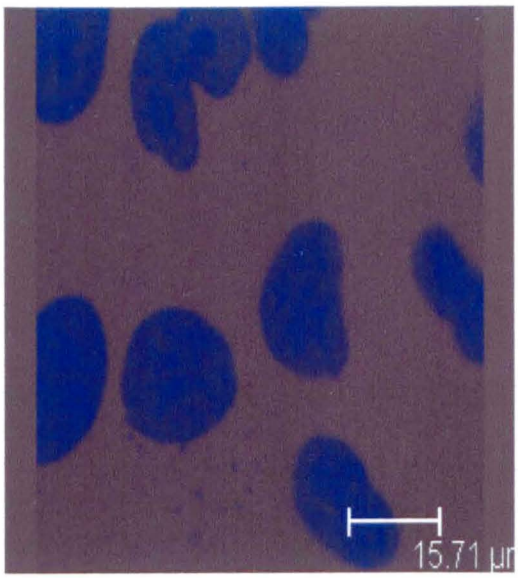

B

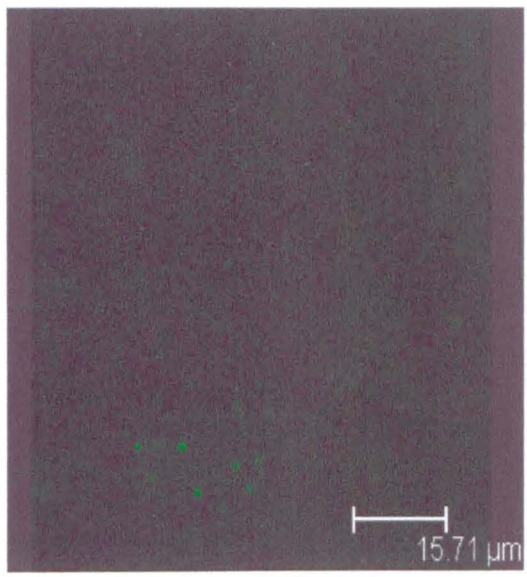

C

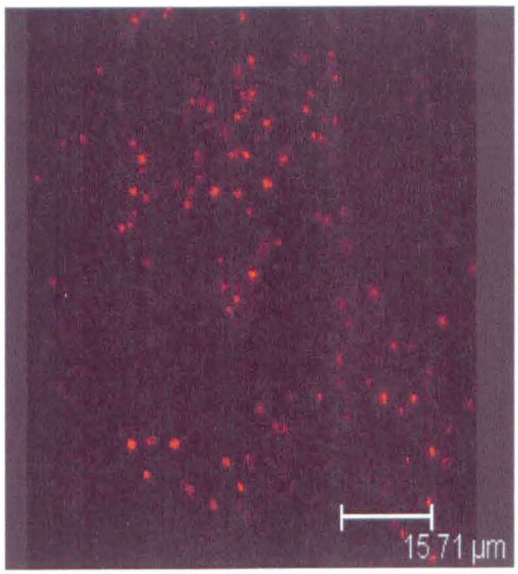

D

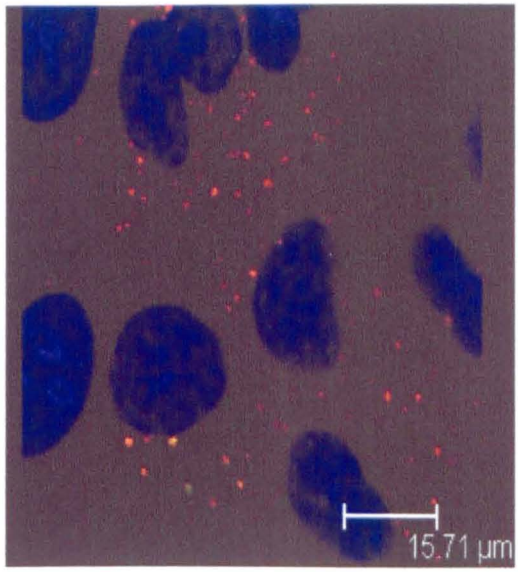

Figure 4.14 Distribution of GFP-NSP6 fusion protein in rotavirus infected cells
Confluent monolayers of BSC1 cells were transfected with the GFP-NSP6 using lipofectamine 2000. The cells were incubated for 48 hours at 37°C and then infected with the Uktc strain of rotavirus at an m.o.i. of 3. The cells were incubated for a further 8 hours at 37°C and then fixed using methanol at -20°C. The fixed cells were stained using a 1:200 dilution of guinea pig anti NSP5 sera, followed by staining with the secondary antibody goat anti guinea pig Alexa fluor 594. Nuclei were stained with DAPI and fluorescence of the GFP-NSP6 was detected using confocal microscopy as described in the Materials and Methods. The four panels above represent the three channels detected using the confocal microscope panel A) nuclei stained with DAPI (blue), panel B) GFP-NSP6 (green), panel C) NSP5 protein stained with Alexa fluor 594 (red) and panel D) merge of all 3 channels. Size of scale bar is indicated on images.

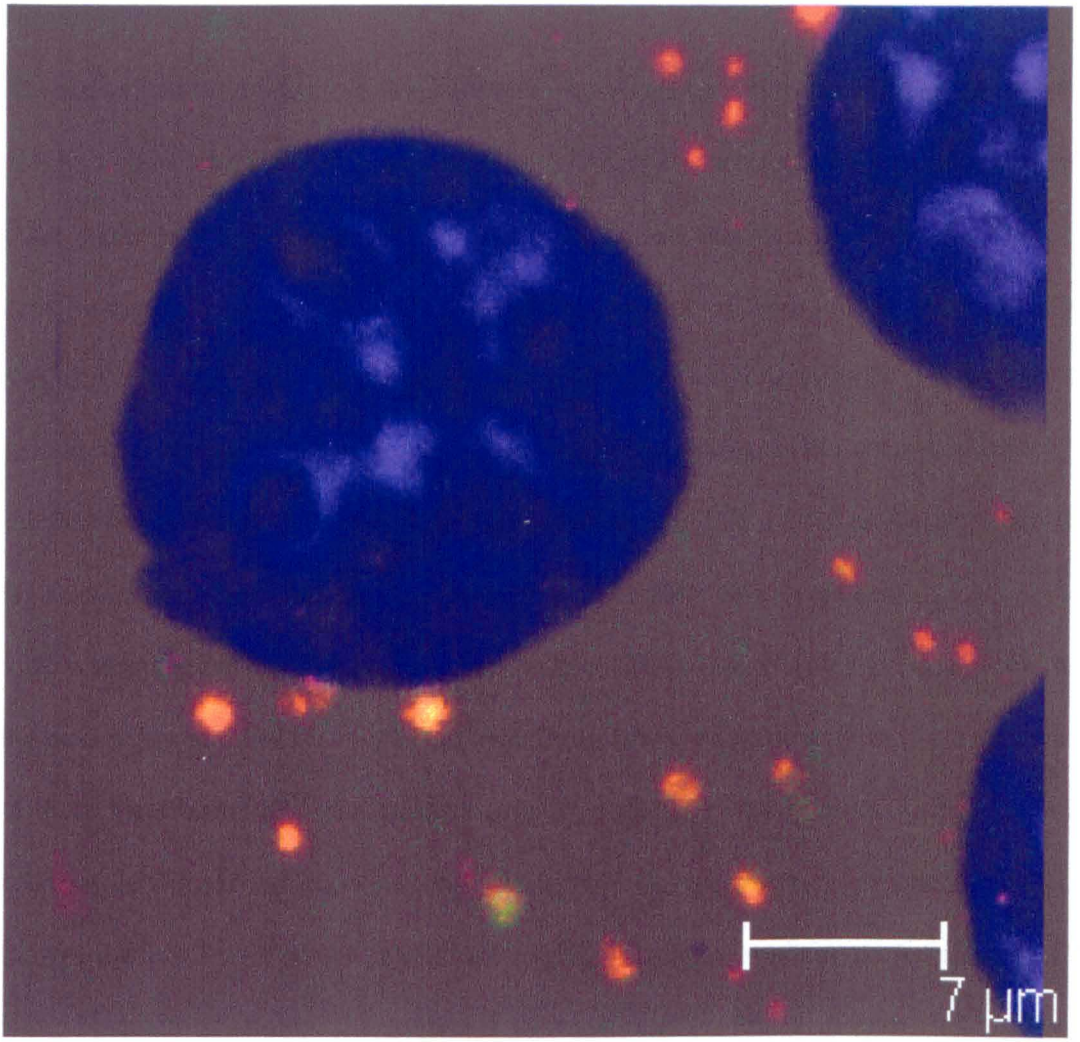

Figure 4.15 Confocal image showing GFP-NSP6 localisation to the centre of the viroplasms

Confocal microscopy image showing localisation of GFP-NSP6 to the viroplasm within cells transfected then infected with rotavirus. Cells were stained using a 1:200 dilution of guinea pig anti NSP5 sera, followed by staining with the secondary antibody goat anti guinea pig Alexa fluor 594 (red). Nuclei were stained with DAPI (blue) and fluorescence of the GFP-NSP6 (green) was detected using confocal microscopy. Size of scale bar is indicated on image.

4.3.10. Viroplasm formation by NSP5 and NSP2 in the absence of other rotavirus proteins

An earlier study carried out by Fabbretti *et al* showed that the NSP2 and NSP5 proteins can form viroplasm-like structures when co-transfected in the absence of other virus proteins (Fabbretti *et al.*, 1999). These experiments were performed using constructs covering the whole coding region of gene 11 or regions still partially encoding the NSP6 protein. More recently an N-terminally tagged NSP5 protein was shown to form these viroplasm-like structures in the absence of NSP2 (Mohan *et al.*, 2004). The NSP5 ORF when expressed with a GFP or HA N-terminal tag formed large punctate structures whereas the NSP5 ORF expressed without such a tag showed a diffuse intracellular distribution (Mohan *et al.*, 2004). To investigate the possibility that the NSP6 protein may be involved in some way in the formation of these viroplasms-like structures, a gene 11 construct was generated which could not encode the second open reading frame. Site directed mutagenesis was used to change the ATG start codon of ORF2 to ACG, thereby preventing the expression of NSP6 without changing the amino acid sequence of NSP5 (Figure 4.16). The experiments using N-terminally tagged NSP5 and untagged NSP5 were replicated with the gene 11 that could not express NSP6. GFP-NSP5 and a GFP-NSP5 ORF2 ATG→ACG (minus-NSP6) fusion constructs were generated and transfected into cells. The GFP-NSP5 formed viroplasm-like structures confirming the results of the previous study by Mohan *et al* (Figure 4.17a) (Mohan *et al.*, 2004). The GFP-NSP5 ORF2 ATG→ACG also formed viroplasm-like structures indicating that NSP6 is unnecessary for viroplasm-like structure formation.

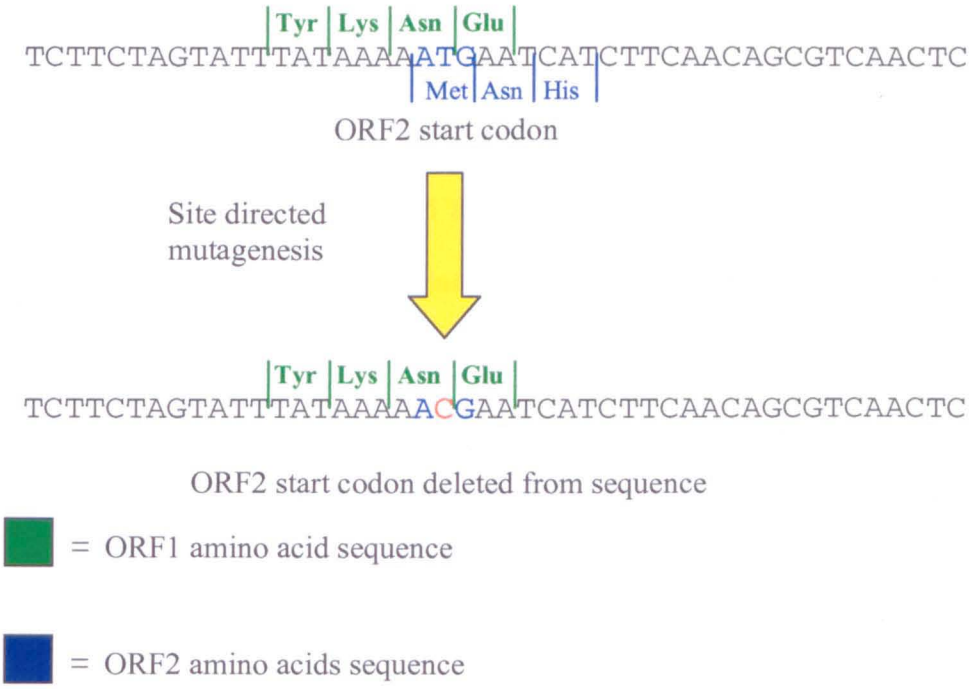

Figure 4.16 Construction of the gene 11 ORF2 ATG→ACG mutant (minus NSP6)

Site directed mutagenesis was used to change an adenine to a cytosine at nucleotide position 81 in the gene 11 sequence. This changes the ATG start codon of NSP6 to a non-functional ACG (ORF2 ATG→ACG). This change maintains the correct amino acid sequence of the NSP5 protein. The amino acid sequence of ORF1 expressing NSP5 can be seen in green and the amino acid sequence of ORF2 expressing NSP6 can be seen in blue. The change from ATG to ACG removes the possibility of NSP6 being expressed with the single base changed being shown in red.
not required for the formation of viroplasm-like structures by the GFP-NSP5 fusion protein (Figure 4.17b).

The same experiment was carried out using untagged full-length gene 11 or gene 11 minus, the start codon for NSP6 in combination with gene 9 (expressing the NSP2 protein of the UKtc rotavirus strain). Gene 9, gene 11 and gene 11 ORF2 ATG→ACG were cloned into the PCIneo mammalian expression vector. Cells transfected with these vectors were stained, using the guinea pig anti NSP5 sera to detect the distribution of the NSP5 and the potential formation of viroplasms. The results showed a diffuse intracellular distribution of NSP5 expressed from gene11-PCIneo and gene11-PCIneo ORF2 ATG→ACG when transfected alone (Figure 4.18a and 4.18b). When gene11-PCIneo was co-transformed with gene9-PCIneo (expressing NSP2) viroplasm-like structures were formed (Figure 4.18c) in agreement with the earlier studies (Fabbretti *et al* 1999). When the gene11-PCIneo ORF2 ATG→ACG was transfected with gene9-PCIneo, the viroplasm-like structures were also formed (Figure 4.18d), taken together these results indicate that NSP6 is not required for NSP5 to distribute to the viroplasm-like structures in transfected cells.

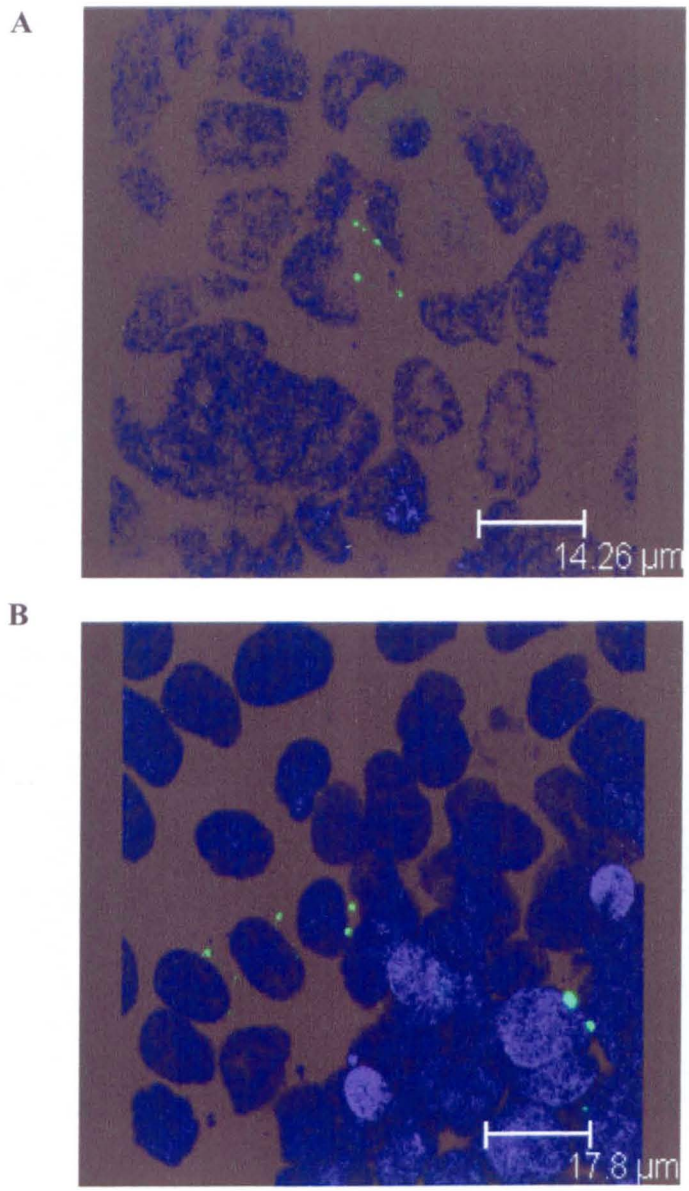

Figure 4.17 GFP-NSP5 viroplasm formation in the absence of other rotavirus proteins

Confluent monolayers of BSC1 cells were transfected with either GFP-NSP5 or GFP-NSP5 ATG→ACG vectors using lipofectamine 2000. The cells were then incubated for 48 hours at 37°C, after this time the cells were fixed with methanol at -20°C and nuclei stained with DAPI (blue). Expression of the GFP was detected using confocal microscopy. Panel A) GFP-NSP5 (green) viroplasm-like structure formation and panel B) GFP-NSP5 ORF2 ATG→ACG (green) viroplasm-like structure formation. Size of scale bar is indicated on images.

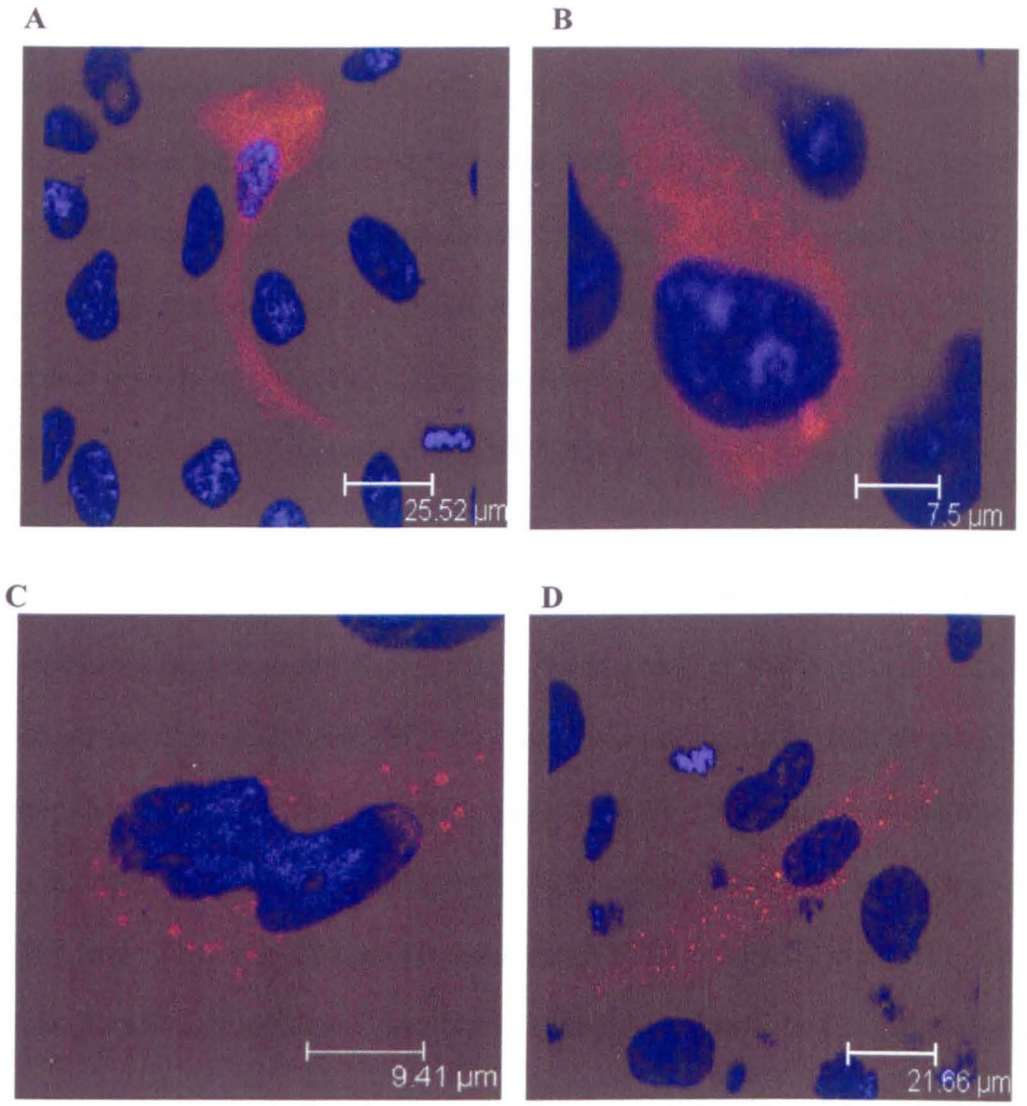

Figure 4.18 Viroplasm formation in the absence of other rotavirus proteins
Confluent monolayers of BSC1 cells were transfected with gene9-PCIneo and either gene11-PCIneo or gene11-PCIneo ORF2 ATG→ACG vectors using lipofectamine 2000. The cells were then incubated for 48 hours at 37°C. After this time the cells were fixed with methanol at -20°C. The fixed cells were then stained using a 1:200 dilution of guinea pig anti NSP5 sera, followed by staining with the secondary antibody goat anti guinea pig Alexa fluor 594. Nuclei were stained with DAPI (blue) and fluorescence was detected using confocal microscopy (Mohan *et al.*, 2004). Panel A) gene11-PCIneo, panel B) gene11-PCIneo ORF2 ATG→ACG, panel C) PCIneo-gene9 and gene11-PCIneo and panel D) gene9-PCIneo and gene11-PCIneo ORF2 ATG→ACG. Size of scale bar is indicated on images.

4.4. Discussion

The work presented in this chapter investigates the kinetics of synthesis and sub-cellular distribution of both NSP5 and NSP6. NSP5 and NSP6 were both expressed from gene 11 in an *in vitro* transcription/translation system. The NSP5 expressed from the *in vitro* transcription/translation system appeared to become hyperphosphorylated when incubated in the rabbit reticulate lysate at 20°C for extended periods of time. This hyperphosphorylation was not seen if the extended incubation was at 4°C, suggesting that NSP5 can be hyperphosphorylated either by cellular kinases or by slow autophosphorylation. NSP2 has been previously shown to enhance hyperphosphorylation (Afrikanova *et al.*, 1998) but this data suggests that hyperphosphorylation is not dependent on the presence of NSP2. Recent work has proposed that the binding of NSP2 may cause a conformational shift in the NSP5 protein that allows it to be phosphorylated at a specific serine residue at position 67. This in turn is proposed to act as the catalyst for subsequent phosphorylation events leading to the formation of hyperphosphorylated NSP5 (Eichwald *et al.*, 2004). The cellular kinases casein kinase I and casein kinase II have both been suggested to be involved in this process (Eichwald *et al.*, 2002; Eichwald *et al.*, 2004). Evidence reported here suggests that cellular kinases may well be able to cause hyperphosphorylation without the presence of NSP2 but at a much slower rate.

Previous work has shown the distribution of NSP5 within the viroplasm to be a ring structure formed around the centre of the viroplasm in which the NSP2 protein can be localised (Eichwald *et al.*, 2004). The viroplasms were also found to decrease

in number but, increase in size over the course of an infection, possibly due to coalescence and fusion of separate viroplasms (Eichwald *et al.*, 2004).

Work presented in this chapter indicates that the number of viroplasms appeared to increase from 2 – 6 hours post infection and then decreases thereafter as their size increases. The increase in the size of the viroplasms along with the decrease in number is consistent with the theory of viroplasm fusion, however no such fusion was directly observed by fluorescence. When viewing a confocal series, the distribution of NSP5 in viroplasms appeared to be cup shaped with the protein forming a ring around the centre of the viroplasm and narrowing into a base at the bottom.

In agreement with previous reports for the YM and SA11 strains of rotavirus, work presented here shows the UKtc strain expresses an identifiable NSP6 protein (Mattion *et al.*, 1991; Torres-Vega *et al.*, 2000). Immunoprecipitation was used to show that in the infected cell NSP6 is expressed at a low level.

Analysis of NSP6 kinetics of synthesis showed that the UKtc rotavirus NSP6 is expressed throughout an infection. The amount expressed at 2 hours post infection was small, however the level of protein increased at 3 hours and was produced at a steady but low rate until 8 hours when its expression reduces slightly. Pulse chase analysis showed that NSP6 had a high rate of turnover, with pulse labelled protein being virtually undetectable at the end of a 2 hour chase period.

NSP6 could not be detected by immunofluorescence using any of the antisera generated to the purified protein. However, GFP-NSP6 fusion protein when expressed in tranfected cells that were subsequently infected with rotavirus,

redistributed from a large amorphous mass within the cytoplasm of transfected cells, to viroplasm structures in the infected cell. The localisation of the GFP-NSP6 fusion protein appeared to be within the centre of the viroplasm, similar to the distribution that has been recently reported for the NSP2 protein (Eichwald *et al.*, 2004). The ability for GFP tagged NSP2 and NSP5 to redistribute to the viroplasm when cells are transfected and then subsequently infected has also been previously demonstrated (Eichwald *et al.*, 2002; Eichwald *et al.*, 2004).

It has been previously shown that NSP2 and NSP5 can form viroplasm-like structures in the absence of a rotavirus (Fabbretti *et al.*, 1999). In these experiments deletion mutants were used to map this interaction however these mutants contained either the whole NSP6 coding region or encoded part of the NSP6 protein. The only deletion mutant still able to form viroplasm-like structure was a deletion mutant lacking the 81 to 130 amino acids from the middle of the NSP5 protein this mutant encodes an NSP6 protein that has a 37 amino acid C-terminal deletion.

A study by Mohan *et al* demonstrated that the NSP5 protein was able to form viroplasm-like structures in the absence of NSP2, provided that the N-terminus was blocked by any non-rotavirus polypeptide and the C-terminus left unmodified (Mohan *et al.*, 2004) and it was postulated that the non-rotavirus polypeptide fusion to NSP5 mimics the binding by NSP2 allowing the formation of viroplasm-like structures. Deletion mutants were again used to map the critical part of NSP5 that contribute to the formation of viroplasm-like structures and again NSP6 or regions of NSP6 were encoded by these mutants. A mutant that lacked the first 65 amino acids still produced viroplasm-like structures but also contained the 59 C-terminal

amino acids of NSP6, which potentially could be initiated from a methionine residue found within the NSP6 sequence.

Work presented here using a mutated gene 11 which cannot express the NSP6 protein demonstrated that NSP6 is not required for the formation of viroplasm-like structures. The effect of silencing NSP6 expression on the formation of viroplasm-like structures was investigated by using mutants unable to code for NSP6 in both studies using transfection of NSP2 and NSP5 coding regions and by using an N-terminally fused GFP-NSP5 protein.

Results

Chapter 5

Investigation into the RNA Binding Ability of NSP6

5.1. Aims

The aim of the work described in this chapter was to determine the RNA binding ability and specificity of the NSP6 protein of the UKtc strain of rotavirus.

5.2. Introduction

The NSP6 protein of rotavirus has previously been localised to viroplasms in the cytoplasm of infected cells (Mattion *et al*, 1991). A number of other viral proteins have also been localised to these cytoplasmic occlusion bodies these are VP1, VP2, VP3, VP6, NSP2 and NSP5. (Petrie *et al.*, 1982; Petrie *et al.*, 1984; Welch *et al.*, 1989; Gonzalez *et al.*, 2000). Viroplasms are the site of synthesis and replication of dsRNA, packaging of viral dsRNA into newly synthesised cores and the stages of viral morphogenesis that produce double-shelled pre-virions (Altenburg *et al.*, 1980; Espaza *et al.*, 1980; Patton & Gallegos, 1990; Wentz *et al.*, 1996; Patton *et al.*, 1997). Within the viroplasms three distinct species of replication intermediate (RI) have been detected, these are termed the pre-core RI, core RI and double-layered RI (Gallegos & Patton, 1989), the pre-core RI is composed of VP1 and VP3 as well as the non-structural proteins NSP1 and NSP3. The core RI contains all of the structural proteins found within the rotavirus single shelled core particle VP1, VP2 and VP3; it also contains the non-structural proteins NSP2 and NSP5. The double-layered RI is identical to the core RI except for the presence of the VP6 protein. All of the viral proteins localised to the viroplasms have been shown to have RNA binding ability, with the exception of the inner shell protein VP6. Some such as VP1, VP3 and NSP2 have only ssRNA binding ability, where as others such as

VP2 and NSP5 have both ssRNA and dsRNA binding ability (Boyle *et al.*, 1986; Kattoura *et al.*, 1992; Patton, 1996; Patton & Chen, 1999; Vende *et al.*, 2002). The defined role of these proteins varies; VP1 is thought to be the viral RNA dependent RNA polymerase. VP2 is an essential part of the replicase complex needed for VP1 function as well as being the major component of the viral core shell, the inner most part of the rotavirus virion. VP3 is the guanylyltransferase capping and methylating protein. There is evidence to suggest that NSP2 and NSP5 are part of the RNA synthesis and packaging machinery of the viroplasm (Bican *et al.*, 1982; Pizarro *et al.*, 1991; Lui *et al.*, 1992; Zeng *et al.*, 1996; Taraporewala & Patton, 2004), and are both essential parts of the viroplasm and needed for replication to occur (Silvestri *et al.*, 2004; Vascotto *et al.*, 2004; Campagna *et al.*, 2005; Lopez *et al.*, 2005). NSP2 has been shown to be a functional octamer and to possess both NTPase and helicase activity, leading to the suggestion that it is the molecular motor that drives the encapsidation of the viral RNA (Taraporewala *et al.*, 1999; Taraporewala & Patton, 2001; Jayaram *et al.*, 2002; Taraporewala *et al.*, 2002). NSP2 also regulates the hyperphosphorylation of NSP5 (Afrikanova *et al.*, 1998).

Despite the data gathered to date it is still the case that the exact role of the non-structural proteins found within the viroplasm remains unclear. The previously described interaction between NSP5 and NSP6, together with the proposed localisation of NSP6 to the viroplasm appears to demonstrate a strong possibility that NSP6 may have a role as an RNA binding protein (Mattion *et al.*, 1991; Gonzalez *et al.*, 1998; Torres-Vega *et al.*, 2000).

5.3. Results

5.3.1. Viral ssRNA binding of the His-NSP6 protein

In order to test the RNA binding capacity of the His-NSP6 protein a filter binding assay, described in the Materials and Methods, was employed. In brief, purified protein was incubated with radio-labelled RNA and passed through a nitrocellulose filter to which only protein adheres. If the protein possesses the ability to bind RNA then radio-labelled RNA will be quantitatively retained on the filter.

NSP5 has been shown to have an equal affinity for ssRNA and dsRNA, consequently the His-NSP5 protein expressed and purified in this study was used in these RNA binding studies as both a comparison to, and positive control for, the NSP6 protein (Vende *et al.*, 2002). BSA was employed as a negative control due to its lack of RNA binding activity.

Firstly the ability of NSP6 to bind viral ssRNA message was investigated. RNA was transcribed *in vitro* from a cDNA clone of rotavirus gene segment 7 (1.059 kb) in the presence of radio-labelled P^{32} UTP and used to assess the affinity of NSP6 for ssRNA. Increasing amounts of BSA, NSP5 or NSP6 (0, 200, 400, 600, 800, 1000ng) were incubated with 500nM of radio-labelled viral RNA and applied to the filter. The amount of radio-labelled RNA retained on the filter was measured by scintillation counting. As expected, the BSA bound little or no RNA compared to background, whereas NSP5 bound increasing amounts of RNA in direct correlation to the amount of protein employed in the assay. NSP6 was also revealed to be a strong RNA binding protein giving a linear increase in ssRNA retained with

increasing protein concentration (Figure 5.1). This assay was repeated using radio-labelled transcripts generated from gene segment 4 (2.362 kb) of the UKtc strain and gave the same result showing that NSP6 has the ability to bind viral ssRNA with high affinity (Figure 5.2). The data shown in figure 5.1 was used to calculate dissociation constants (Kd) of the affinity of NSP5 and NSP6 for ssRNA. The values obtained were of 9.62 $x10^{-10}$ M and 1.28 $x10^{-10}$ M for NSP5 and NSP6 respectively indicating that NSP5 has an approximately 8 fold higher affinity for ssRNA than NSP6.

To gain insight into the nature of the interaction between these two viral proteins and ssRNA, the effect of NaCl concentration on RNA binding was examined. The binding of RNA by NSP6 showed an inverse correlation to NaCl concentration used in the assay (Figure 5.3). This was also true of NSP5, confirming the previously reported results (Vende *et al*, 2002). These data indicate that the basis of the RNA-protein interaction is ionic and that under normal intracellular concentrations of salt (~100mM) both proteins still exhibit strong viral ssRNA binding ability.

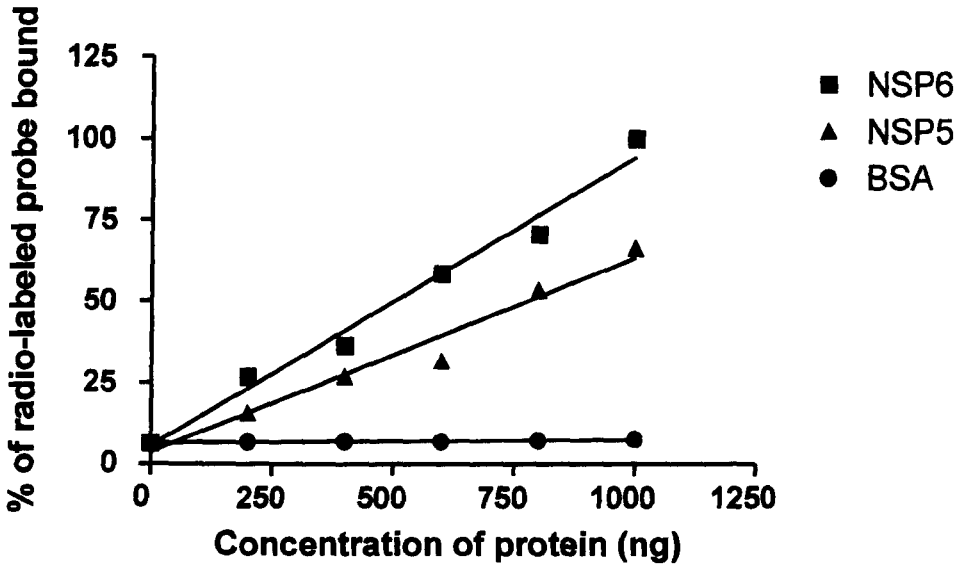

Figure 5.1 Filter binding assay of the relative binding abilities of BSA, NSP5 and NSP6 for radio-labelled rotavirus gene 7 ssRNA
Reaction mixtures containing 500nM of ^{32}P-labelled rotavirus gene segment 7 ssRNA and varying amounts of NSP5, NSP6 or BSA (0, 200, 400, 600, 800 and 1000ng) were incubated at 30°C for 30 minutes. ^{32}P-labelled rotavirus gene segment 7 ssRNA protein complexes were recovered by filtration through nitrocellulose and the amount of RNA bound measured by a scintillation counter. The highest value of counts per minute bound by NSP6 was given a value of 100% and the normalised values plotted as a function of the concentration of the proteins in the reaction mixtures.

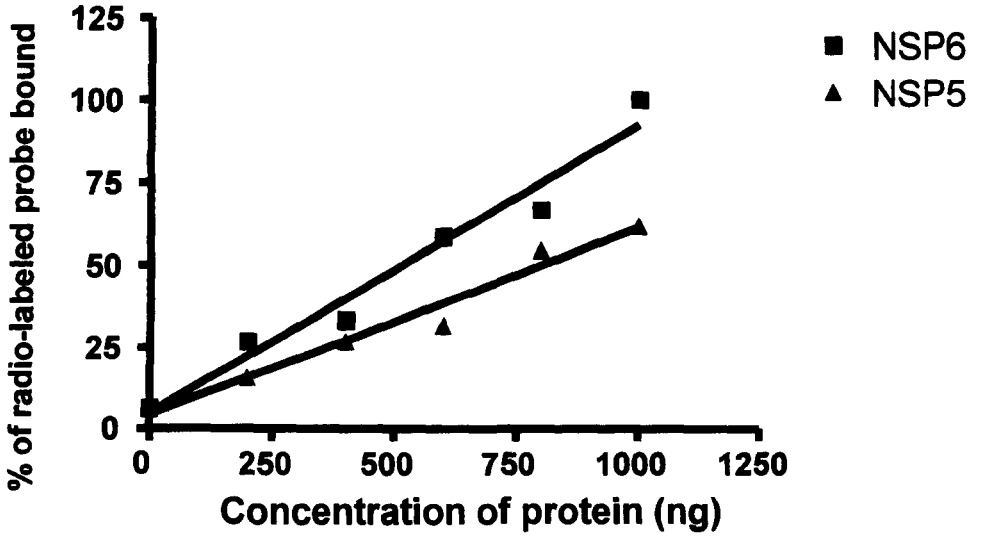

Figure 5.2 Filter binding assay of the relative binding abilities of NSP5 and NSP6 for radio-labelled rotavirus gene 4 ssRNA

Reaction mixtures containing 500nM of ^{32}P-labelled rotavirus gene segment 7 ssRNA and varying amounts of NSP5 or NSP6 (0, 200, 400, 600, 800 and 1000ng) were incubated at 30°C for 30 minutes. ^{32}P-labelled rotavirus gene segment 4 ssRNA protein complexes were recovered by filtration through nitrocellulose and the amount of RNA bound measured by a scintillation counter. The highest value of counts per minute bound by NSP6 was given a value of 100% and the normalised values plotted as a function of the concentration of the proteins in the reaction mixtures.

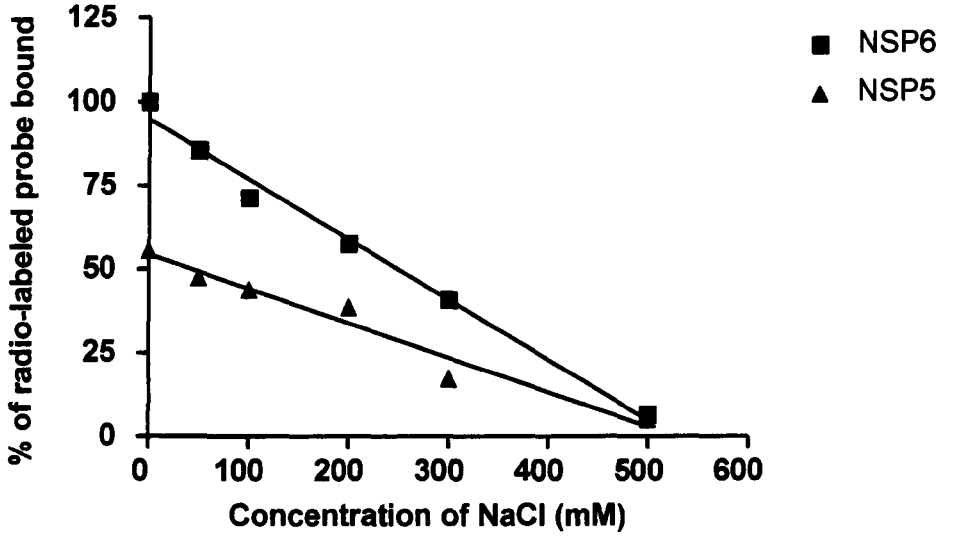

Figure 5.3 Filter binding assay of the effect of NaCl concentration on the relative binding abilities of NSP5 and NSP6 for radio-labelled rotavirus gene 7 ssRNA

Reaction mixtures containing 500nM of ^{32}P-labelled rotavirus gene segment 7 ssRNA and a set concentration of 1000ng of NSP5 or NSP6 were incubated in binding buffer containing increasing of NaCl (0, 50, 100, 200, 300, and 500mM), at 30°C for 30 minutes. ^{32}P-labelled rotavirus gene segment 7 ssRNA protein complexes were recovered by filtration through nitrocellulose and the amount of RNA bound measured by a scintillation counter. The values were normalised using the value of the ^{32}P-labelled-NSP6 in 0mM NaCl as 100%. The normalised values were then plotted as a function of the concentration of NaCl in the reaction mixtures.

In order to verify these findings a gel mobility shift assay was employed to study the ssRNA binding ability of NSP6. These assays depend on the fact that when analysed on agarose or polyacrylamide gels complexes of RNA and proteins have retarded mobility compared to that of free RNA. Assays were performed using radio-labelled ssRNA covering the 5'-terminal 100 nucleotides of the rotavirus gene segment 5 as a probe. The radio-labelled probe and purified NSP6 were mixed, incubated and fractionated on a 1% agarose gel. The results (Figure 5.4) show that as the concentration of NSP6 used in the assay was increased, so were the amounts of RNA retardation evident on the gel, confirming that NSP6 has viral ssRNA binding ability.

Additionally a gel mobility shift assay was used to confirm the previous results demonstrating the effect of NaCl concentration on RNA binding of NSP6. The assay was performed, as before, with the exception that the binding buffers used in this assay varied in the concentration of NaCl. The results (Figure 5.5) showed an inverse correlation between NaCl concentration and the amount of RNA bound to NSP6 and retained on the filter, confirming an ionic interaction.

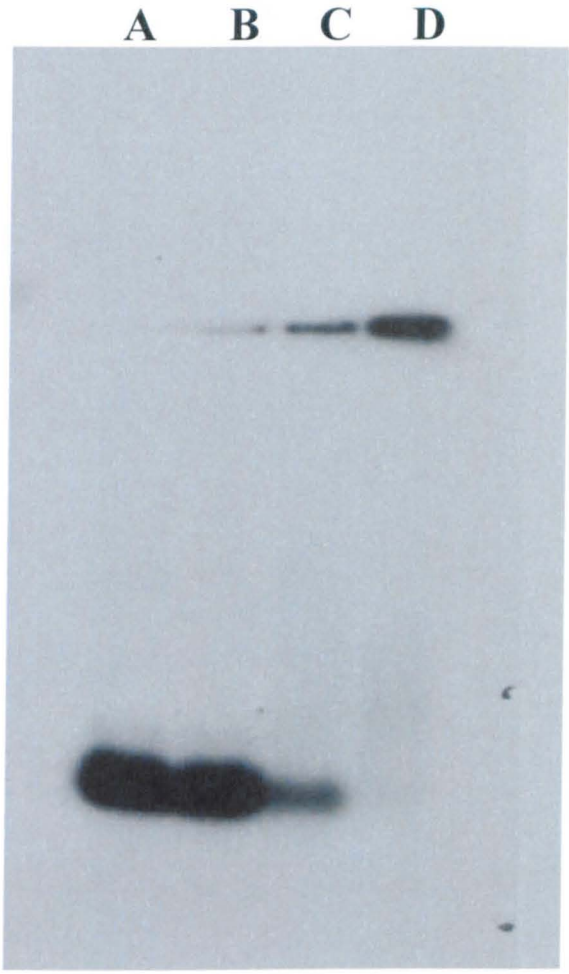

Figure 5.4 Gel mobility shift assay of radio-labelled RNA mobility on an agarose gel with increasing concentrations of NSP6 protein
Radio-labelled ssRNA fragments of the 5' terminal 100 nucleotides of the rotavirus gene segment 4 were used to in this assay. 500nM of radio-labelled probe and increasing amounts of the purified NSP6 (0, 200, 600 and 1000ng) were mixed, incubated for 30°C for 30 minutes and loaded onto a 1% agarose gel. The gel was electrophoresed at 10 milliamps for 1 hour, dried and exposed to X-ray film. Autoradiography was then performed at -70°C O/N and the film developed in an automatic X-ray developer. Track A) Control track with no added NSP6, track B) 200ng of NSP6 added to the assay, track C) 600ng of NSP6 added to the assay, track D) 1µg of NSP6 added to the assay.

Figure 5.5 Gel mobility shift assay showing the effect of increasing NaCl concentration on radio-labelled RNA mobility

500nM of radio-labelled probe and 500ng of the purified NSP6 were mixed and incubated in buffer containing increasing concentrations of NaCl (100, 200, 500, and 1000mM) for 30°C for 30 minutes and loaded onto a 1% agarose gel. The gel was electrophoresed at 10 milliamps for 1 hour, dried and exposed to X-ray film. Autoradiography was then performed at -70°C O/N and the film developed in an automatic X-ray developer. Track A) Assay carried out at 100mM NaCl, track B) Assay carried out at 200mM NaCl, track C) Assay carried out at 300mM NaCl, track D) Assay carried out at 500mM NaCl.

5.3.2. Cellular ssRNA binding of His-NSP6

To investigate the ability of NSP6 to bind to non-viral ssRNA, two cellular genes were transcribed in the presence of ^{32}P UTP and used in filter binding assays. The actin (1.128kb) and luciferase (1.652kb) genes were used in these assays and again both NSP5 and NSP6 showed strong affinity for the ssRNA transcripts derived from both genes (Figures 5.6a and 5.6b). Each of these ssRNA binding assays appeared to have a linear correlation between the amount of protein present in the assay and the amount of radio-labelled RNA retained on the filter. The amount of ssRNA binding appeared to be equivalent to that demonstrated in the filter binding assays using ssRNA of a viral origin.

5.3.3. Specificity of ssRNA binding by His-NSP6

A competition assay was used to determine the specificity of ssRNA binding by His-NSP6. This was performed to establish if the protein had any affinity for viral ssRNA over cellular ssRNA. A standard filter binding assay was carried out using radio-labelled gene segment 7 ssRNA, with the addition of an increasing concentration of cold competitor RNA of, either rotavirus gene segment 7 ssRNA or luciferase ssRNA. Cold competitor ssRNA was added at 0%, 25%, 50%, 100%, 200% and 500% of the quantity of radio-labelled gene segment 7 present. Both of the cold competitor ssRNA's reduced the amount of radio-labelled RNA retained on the filter with equal efficiency indicating that NSP6 has a sequence independent affinity for ssRNA (Figure 5.7).

A

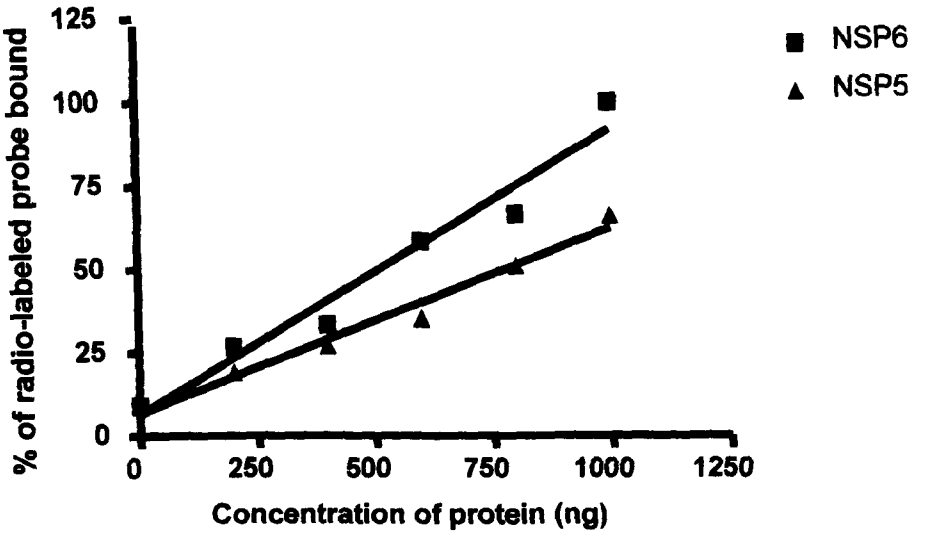
% of radio-labeled probe bound
125
100
75
50
25
0
0
250
500
750
1000
1250
Concentration of protein (ng)
NSP6
NSP5

B

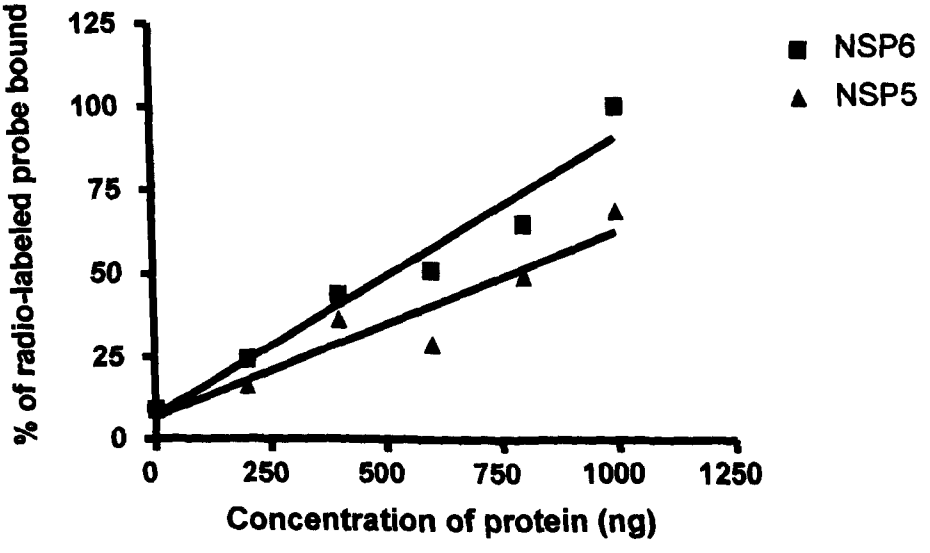
% of radio-labeled probe bound
125
100
75
50
25
0
0
250
500
750
1000
1250
Concentration of protein (ng)
NSP6
NSP5

Figure 5.6 Filter binding assay measuring the relative binding abilities of NSP5 and NSP6 for non-viral ssRNA
Panel A) Reaction mixtures containing 500nM of ^{32}P-labelled Actin ssRNA and varying amounts of NSP5 or NSP6 (0, 200, 400, 600, 800 and 1000ng) were incubated at 30°C for 30 minutes. P^{32}-labelled ssRNA protein complexes were recovered by filtration through nitrocellulose and the amount of RNA bound measured by a scintillation counter.

Panel B) Reaction mixtures containing 500nM of ^{32}P-labelled Luciferase ssRNA and varying amounts of NSP5 or NSP6 (0, 200, 400, 600, 800 and 1000ng) were incubated at 30°C for 30 minutes. P^{32}-labelled ssRNA protein complexes were recovered by filtration through nitrocellulose and the amount of RNA bound measured by a scintillation counter.

The highest value of counts per second bound by NSP6 was given a value of 100% and the normalised values plotted as a function of the concentration of the proteins in the reaction mixtures.

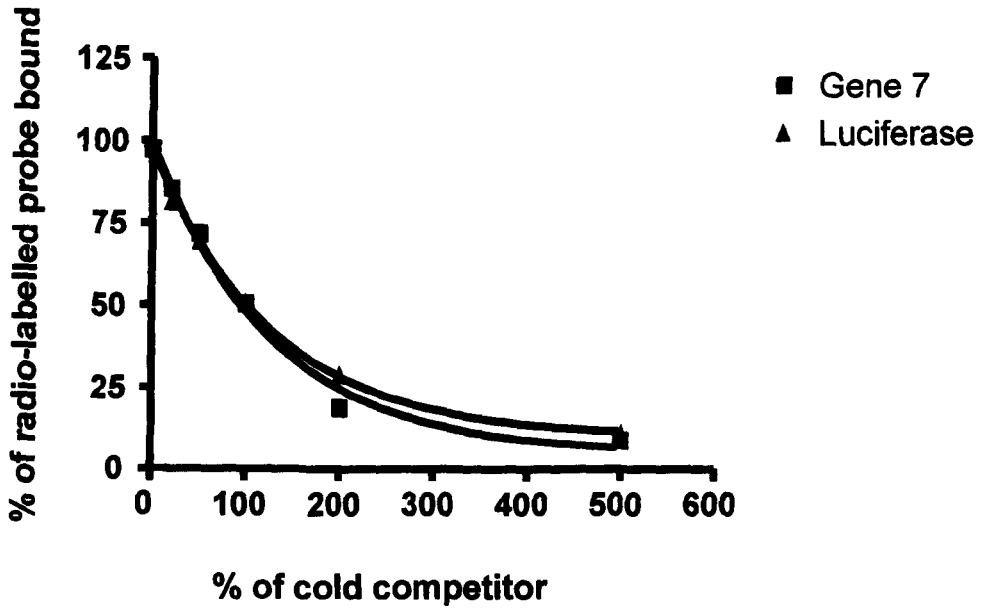

Figure 5.7 Competition filter binding assay of unlabelled rotavirus gene segment 7 ssRNA or Luciferase ssRNA competing with ^{32}P-labelled rotavirus gene segment 7 ssRNA for binding by the NSP6 purified protein

Reaction mixtures containing 500nM of P^{32}-labelled rotavirus gene segment 7 ssRNA and 1000ng of NSP6 were incubated with increasing amounts of unlabelled rotavirus gene segment 7 ssRNA or Luciferase ssRNA (0, 20, 50, 100, 200 and 500% of the amount of radio-labelled gene segment 7 present in the assay). These reaction mixtures were incubated at 30°C for 30 minutes. P^{32}-labelled rotavirus gene segment 7 ssRNA protein complexes were recovered by filtration through nitrocellulose and the amount of RNA bound measured by a scintillation counter. The 0% competitor ssRNA value was designated 100% and normalised values plotted as a function of the percentage of the unlabelled competitor ssRNA in the reaction mixtures.

5.3.4. Affinity of the purified His-NSP6 protein for dsRNA and dsDNA

In order to test the binding capability of His-NSP6 for other nucleic acid molecules a filter binding competition assay was again used. Rotavirus gene segment 7 ssRNA, purified whole virus dsRNA and rotavirus gene segment 7 in the PCIneo vector dsDNA and linearised using the *Xba*I restriction enzyme were used as competitors for the radio-labelled gene segment 7 transcripts. The results (Figure 5.8) showed that the dsRNA and dsDNA interfered with the radio-labelled RNA binding to NSP6 with similar efficiency to that of the ssRNA, indicating that NSP6 appears to have an almost equal affinity for each type of nucleic acid molecule.

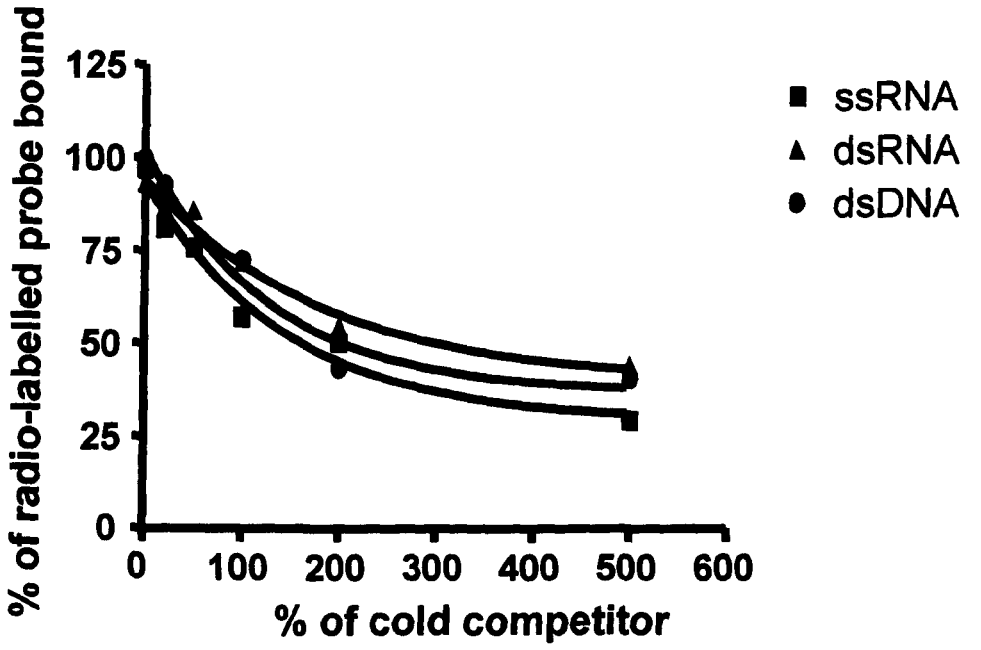

Figure 5.8 Competition filter binding assay of unlabelled ssRNA, dsRNA or dsDNA against ^{32}P-labelled rotavirus gene segment 7 ssRNA for binding by NSP6

Reaction mixtures containing 500nM of P^{32}-labelled rotavirus gene segment 7 ssRNA and 1000ng of NSP6 were incubated with increasing amounts of unlabelled rotavirus gene segment 7 ssRNA, whole virion dsRNA or rotavirus gene segment 7 in the PCIneo vector dsDNA, linearised using the *Xba*I restriction enzyme (0, 20, 50, 100, 200 and 500% of the amount of radio-labelled gene segment 7 present in the assay). These reaction mixtures were incubated at 30°C for 30 minutes. P^{32}-labelled rotavirus gene segment 7 ssRNA protein complexes were recovered by filtration through nitrocellulose and the amount of RNA bound measured by a scintillation counter. The 0% competitor dsDNA value was designated 100% as it had the highest percentage of probe bound and normalised values plotted as a function of the percentage of the unlabelled competitor in the reaction mixtures.

5.4. Discussion

The results presented in this chapter define the RNA binding ability of the His-NSP6 protein. They demonstrate that both His-NSP5 and His-NSP6, the expression and purification of which are described in earlier chapters, are functionally active. In the case of His-NSP5 the results obtained concur with previous findings regarding the RNA binding ability of the protein (Vende *et al.*, 2002).

The RNA binding capacity of NSP6 had not been previously characterised. Work in this chapter demonstrates that NSP6 has affinity for ssRNA in a sequence independent manner and additionally has close to equal affinity for ssRNA, dsRNA and dsDNA. It can be concluded from these data that NSP6 is a sequence independent nucleic acid binding protein. The NSP6 K_{Diss} for ssRNA was found to be eight fold lower than that for NSP5.

The finding that NSP6 localises to the viroplasm occlusion bodies within the infected cell and its interaction with NSP5 were both clear indicators of a possible RNA binding capability for the protein and an indication that NSP6 might be implicated in the complex events of RNA synthesis and replication within the viroplasm (Gonzalez *et al.*, 1998; Mattion *et al.*, 1991; Torres-Vega *et al.*, 2000). The evidence presented here for the RNA binding of both ssRNA and dsRNA by NSP6 strongly support this hypothesis. The RNA binding capability of NSP6 also matches that of NSP5, both proteins are strong binders of ssRNA and dsRNA, unlike the other non-structural protein (NSP2) found within the viroplasm, which only has affinity for ssRNA. The sequence independent nature of the binding demonstrated

by NSP6 has also been observed previously for NSP5 and NSP2 (Kattoura *et al.*, 1992; Vende *et al.*, 2004).

Results

Chapter 6

Investigation into the Mechanism of Expression of NSP6 from the Second ORF of Rotavirus Gene Segment 11

6.1. Aims

The aims of the work presented in this chapter are to investigate the factors involved in the translation of the second open reading frame of rotavirus gene 11, which encode the NSP6 protein.

6.2. Introduction

6.2.1. The effect of Rotaviruses on cellular translation

The rotavirus gene segments are all monocistronic with the exception of gene 11 which has been found to encode for two proteins (Estes & Cohan, 1989; Mattion *et al.*, 1991). The mRNA of members of the Reoviridae family serves two distinct functions within the infected cell; it is used in translation to generate viral proteins and it acts as a template for the synthesis of minus strands in the production of progeny genomic dsRNA (Nonoyama *et al.*, 1974). The viral mRNAs lack a poly(A) tail but do have a 5'-terminal cap structure $m^7GpppG^{(m)}Gpy$ (Imai *et al.*, 1983; McCrae & McCorquodale, 1983). The rotavirus mRNA sequences contain untranslated regions (UTR's) flanking the open reading frames, both of these regions vary widely between individual genes with the exception of short 5' and 3' consensus sequences. These short consensus sequences at the 5' and 3' termini are 5'-GGC-poly(A/U)-3' and 5'-AUGUGACC-3' respectively (Desselberger & McCrae, 1994). The levels of the different mRNA species and their corresponding proteins have been measured and this revealed that there was both transcriptional and translational control of viral gene expression (Johnson & McCrae, 1989).

Rotaviruses block translation of cellular mRNA in mammalian cells leading to preferential translation of viral mRNA. In mammalian cells a range of protein-protein and protein-RNA interactions cause recognition and initiation of translation by the ribosome. The 5' cap structure and 3' poly(A) tail are recognised by translational initiation factor eIF4E and poly(A)-binding protein (PABP) respectively (Sachs *et al.*, 1997; Sachs *et al.*, 2000). This leads to the recruitment of other proteins, eIF4G binds to both eIF4E and PABP leading to mRNA circularisation (Wells *et al.*, 1998). Then eIF3 joins this complex and is followed by the 40S small ribosomal subunit (Pestova & Hellen, 1999; Preiss & Hentze. 1999), which has a Met-tRNA$_i$-eIF2-GTP complex attached to it (Maitra *et al.*, 1982).

After the 40S ribosomal subunit has bound to the 5' cap structure it scans along the mRNA in a 5' to 3' direction until it reaches an AUG initiation codon (Kozak, 1980). In eukaryotic cellular mRNAs this is generally the most 5' proximal AUG, a feature known as the position effect (reviewed in Kozak, 2002). Initiation at this AUG is also regulated by the surrounding sequence or "context" of the AUG. The Kozak consensus sequence GCCRCCaugG, where R is a purine, has been found to be optimal for the recognition by the 40S subunit of an AUG start codon. The most important features of this consensus sequence are the purine at position -3 and the guanidine at position +4 (Kozak, 1989). These two nucleotides positions have been shown to be the key nucleotides in the consensus sequence and deletion or substitution mutation of these has been shown to be detrimental to the initiation of translation at an AUG start codon (Kozak, 1986). Following recognition of the AUG start codon by the 40S subunit hydrolysis of eIF2-GTP to eIF2-GDP occurs, in a

process mediated by eIF5. This hydrolysis allows recruitment of the 60S subunit, leading in turn to the formation of the 80S ribosome complex and the start of the elongation process (Chakrabarti & Maitra, 1991).

Rotaviruses circumvent these normal cellular processes through the action of the non-structural protein NSP3 which is a functional homologue of PABP and has been shown to bind eIF4G with a higher affinity than PABP (Both *et al.*, 1984; Imataka *et al.*, 1998; Piron *et al.*, 1998 and Groft & Burley, 2002). The NSP3 protein specifically binds to the 3' terminus of viral mRNAs through recognition of the consensus sequence UGACC and because it competes effectively with PABP for binding of the translation initiation complex viral mRNA is preferentially translated. This leads to the shut off of host cell protein synthesis and results in the inability of capped and polyadenylated cellular mRNA to be translated (Poncet *et al.*, 1994).

Gene 11 is the only polycistronic rotavirus gene segment, expressing both NSP5 and NSP6 (Mattion *et al.*, 1991). The 92aa NSP6 protein is expressed in a plus one frame with respect to the larger NSP5 and its coding sequence is found entirely within the NSP5 ORF. The mechanism by which the translation from this second ORF occurs has not been previously examined. However, in other studies a variety of mechanisms have been observed for achieving translation from a non 5' proximal AUG. These are reviewed below:

6.2.2. Internal ribosome entry sites (IRES)

This method of translation initiation has been found in several virus families but was first defined in the *Picornaviridae*. The members of this virus family have a

positive sense RNA genome, with a genome linked protein (VPg) found at the 5' end of their mRNA in place of the usual cap structure. They also have long 5' non-coding regions of between 610-1200 nucleotides. These regions are highly structured and have been implicated as the IRES allowing the 40S ribosomal subunit to bind to the mRNA molecule and promote initiation of translation from a non 5' proximal AUG. The region involved in this IRES function has been shown to form stable secondary and tertiary structures which are thought to facilitate the 40S ribosomal subunit binding (Jang *et al.*, 1990; Pelletier & Sonenberg, 1988). Work performed on the Foot and Mouth disease virus (FMDV) IRES has identified five structural domains containing conserved sequence within the IRES element (Martinez-Salas *et al.*, 2002). These domains have been shown to be the binding sites for several key proteins of the initiation complex: eIF4G interacts with domain 4, eIF4B with domain 5, eIF3 with domain 3 and the polypyrimidine tract binding protein (PTB) binds at the 5' and 3' termini of the IRES (Martinez-Salas *et al.*, 2002). These structural features of the FMDV IRES were also observed within the IRES elements of both hepatitis C virus and encephalomyocarditis virus (Luz & Beck, 1991; Kolupaeva *et al.*, 1996; Lopez de Quinto & Martinez-Salas, 2000; Lopez de Quinto *et al.*, 2001).

6.2.3. Leaky scanning

Leaky scanning involves the bypassing of the 5' proximal AUG initiation codon by some fraction of the 40S ribosomal subunits scanning a mRNA. These subunits then continue until encountering another suitable AUG initiation codon,

this occurs as a result of the 5' proximal AUG being in a suboptimal Kozak consensus sequence (Kozak, 1989). As previously stated the Kozak consensus sequence (GCCA/GCCAUGG) is crucial in dictating the efficiency with which an AUG is recognised as an initiation codon (Kozak, 1987). Initiation codons in poor consensus sequences may not signal the initiation of translation to all 40S ribosomal subunits. The 40S ribosomal subunits which fail to initiate translation will continue to scan along the mRNA until the next AUG with a suitable Kozak consensus sequence. The features that define suboptimal Kozak consensus sequence vary, but usually involve the absence of the purine preferentially adenine, at the -3 position and/or the guanine at position +4 (Kozak, 1986). Leaky scanning has been found to be a common mechanism employed by viruses for the translation of two or more proteins from a single piece of mRNA (Bustamante & Hull, 1998; Kozak, 2002; Schneider & Mohr, 2004).

6.2.4. Frameshifting

This mechanism of translation has been found in several retroviruses including, human immunodeficiency virus (HIV) (Jacks *et al.*, 1988). In this case expression of proteins from an overlapping open reading frame is achieved by a ribosome shifting position by one nucleotide to allow translation of the non 5' proximal ORF. This can be a -1 nucleotide frameshift, as occurs in the gag-pol region of HIV or a +1 nucleotide frameshift, as seen in the yeast retrotransposon Ty (Jacks *et al.*, 1988; Belcourt & Farabaugh, 1990). The position at which frameshifting occurs is dictated by a heptanucleotide sequence referred to as a

slippery sequence. The slippery sequence has been defined as XXXYYYZ with X being any nucleotide, Y being either A or U and Z may again be any nucleotide (Dinman *et al.*, 1991; Jacks *et al.*, 1988). The slippery sequence varies between different viruses from AAAAAAC in mouse mammary tumour virus, to AAAUUUA in Rous sarcoma virus and UUUUUUA in HIV (Hatfield *et al*,. 1989). A further feature of these regions is that 5-9 nt downstream of the slippery sequence is a RNA pseudoknot (Jacks *et al.*, 1988; Brierley *et al.*, 1989). The ribosome pauses when it reaches the pseudoknot and the slippery sequence causes the tRNA in the A and P sites of the ribosome to shift frame either -1 or +1 and re-establish binding before continuing translation in the new ORF (Farabaugh, 1996).

6.2.5. Ribosomal shunt

Ribosomal shunting as a mechanism for the expression of an alternate ORF has been described for several viruses, Cauliflower mosaic virus (CaMV) (Futterer *et al.*, 1993) adenoviruses (Yueh & Schneider, 1996), Sendai virus (Curran & Kolakofsky, 1988; Latorre *et al.*, 1998) and most recently in duck hepatitis B virus (DHBV) (Sen *et al.*, 2004). It occurs when the 40S ribosomal subunit binds to the 5' end of mRNA, begins to scan and then, due to the presence of secondary structural elements within the 5' UTR, is "shunted" to a different position downstream, skipping large regions of the mRNA (Futterer *et al.*, 1993). This mechanism is most dramatically shown in Sendai virus, where the start of the P/C mRNA contains initiation sites for several proteins P, C', C, Y1 and Y2, with C' ORF having the first initiation codon (ACG) at position 81. Although it has a non-AUG start codon the C'

ORF is then expressed using the conventional 5' scanning initiation. The P and C proteins (which initiate at positions 104 and 114 respectively) are expressed via leaky scanning and when site directed mutagenesis was used to improve the Kozak consensus sequence around the initiation codon of the C' ORF, expression of the P and C proteins were lost. The expression of the Y1 and Y2 proteins which initiate at positions 183 and 201 respectively, downstream of the P and C start codons were not lost following site directed mutagenesis (Curran & Kolakofsky, 1989). The translation initiation of these proteins was found to be via ribosomal shunting, with the first 50 nucleotides of the P/C gene being required for this to occur and ribosomes shunted from this 5' terminal region directly to the initiation codons of the Y1 and Y2 ORF's (Latorre *et al.*, 1998).

6.3. Results

6.3.1. Mechanism of expression of the second open reading frame of gene 11

The second ORF of the rotavirus gene 11 is in a +1 frameshift relative to that of the first ORF and initiates 56 bases from the ATG start codon of ORF1. As previously indicated a number of possible mechanisms exist for achieving the expression of NSP6 from ORF2.

6.3.2. Experimental approach

Three approaches were used in order to assess each of the possible mechanisms for achieving the expression of NSP6, RNA secondary structure

prediction, a coupled *in vitro* transcription/translation system and a reporter gene expression system.

RNA secondary structure prediction was used to investigate the possible existence of stable secondary structures formed by the RNA molecule. Several different types of these structures have been found to be required for the function of IRES elements, ribosomal shunting and frameshifting.

The coupled *in vitro* transcription/translation system allows rapid analysis of protein expression from the cDNA clone of a gene of interest. Deletion mutants and site directed mutagenesis were used in order to determine the features of gene 11 that influence protein expression in such a system. Additionally this system was utilised to detect the presence of any cap-independent initiation mechanisms (such as an IRES element) within gene 11 by employing constructs of gene 11 containing upstream sequences that block the scanning of ribosomes to the normal initiation codons. The rationale of this approach was that if ribosomal scanning was blocked but NSP5 and/or NSP6 expression could still be detected, then it would be a strong indication of the presence of an IRES element.

The coupled *in vitro* transcription/translation system was also used to detect the possible presence of leaky scanning within the gene 11 sequence. Mutational analysis was employed to examine the effect of removal of the initiation codon of ORF1 on the expression from ORF2. Increased expression levels from ORF2 would suggest a leaky scanning mechanism of expression.

As an alternative approach to investigating the possible presence of a leaky scanning mechanism a reporter gene expression system was employed. Fusions

between cDNA of gene 11 and the CAT reporter gene were constructed replacing the NSP6 coding region with the CAT gene. Site directed mutagenesis was again used to generate a mutant that lacked the ORF1 initiation codon to determine what effect this had on expression of CAT from the second ORF. Mutants were also created in which the ORF1 initiation codon was placed into a better Kozak consensus sequence with the purpose of determining if this had a detrimental effect of ORF2 expression. If expression from the second ORF was found to be dependent on the context surrounding the first ORF initiation codon, then this would point towards a leaky scanning mechanism of expression. By contrast IRES elements and ribosomal shunting are not dependent on the context of the first ORF initiation codon as both bypass upstream initiation codons using RNA secondary structural elements.

6.3.3. RNA secondary structure prediction of gene 11

Several of the possible expression mechanisms for NSP6 require the presence of specific RNA secondary structures. The standard RNA secondary structure prediction algorithm of Zucker was used to investigate the RNA folding pattern of the gene 11 RNA sequence. The resulting prediction (Figure 6.1a and 6.1b) showed that there was some potential for the formation of secondary structures in the 5' portion of gene 11, but these were primarily in the region of the gene following the initiation codon of the second ORF and were low in GC pairing, suggesting that they would not have a high level of stability.

IRES elements are characterised by their ability to form stable secondary structures to allow binding of ribosomes and initiation of translation. There was no evidence of highly stable folded hairpins at the 5' terminus of gene 11 strongly suggesting that no IRES element was present.

Frameshifting requires the presence of a stable pseudoknot downstream of a heptanucleotide sequence with the structure XXXYYYZ at which the frameshift occurs. Examination of the primary sequence of gene 11 showed that the required heptanucleotide sequence was not present in the RNA and secondary structure analysis (Figure 6.1a) does not predict the formation of a pseudoknot after the ORF2 initiation codon.

Ribosomal shunting uses secondary structures to reposition ribosomes from the 5' proximal of a RNA molecule to an internal position before an initiation codon. This has been documented to be associated with several hairpins such as those found in adenovirus RNA (Yueh & Schneider, 1996). Although gene 11 does appear to possess some hairpins in the 5' proximal region (Figure 6.1b) these are small and do not contain a high amount of GC base pairing in contrast to those RNA determined to exhibit ribosomal shunting.

A

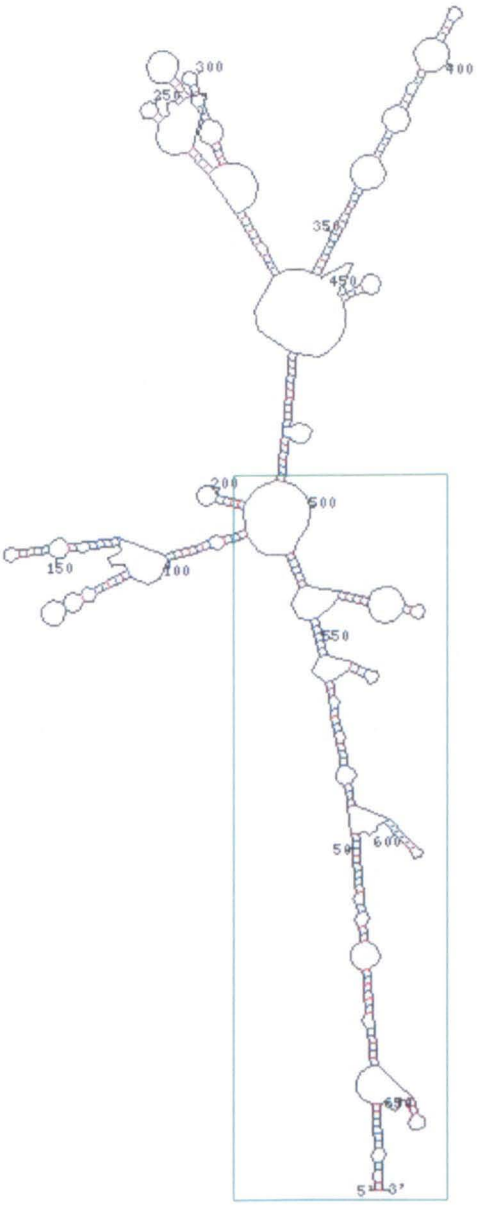

dG = -162.07 [initially -174.2] gene 11

B

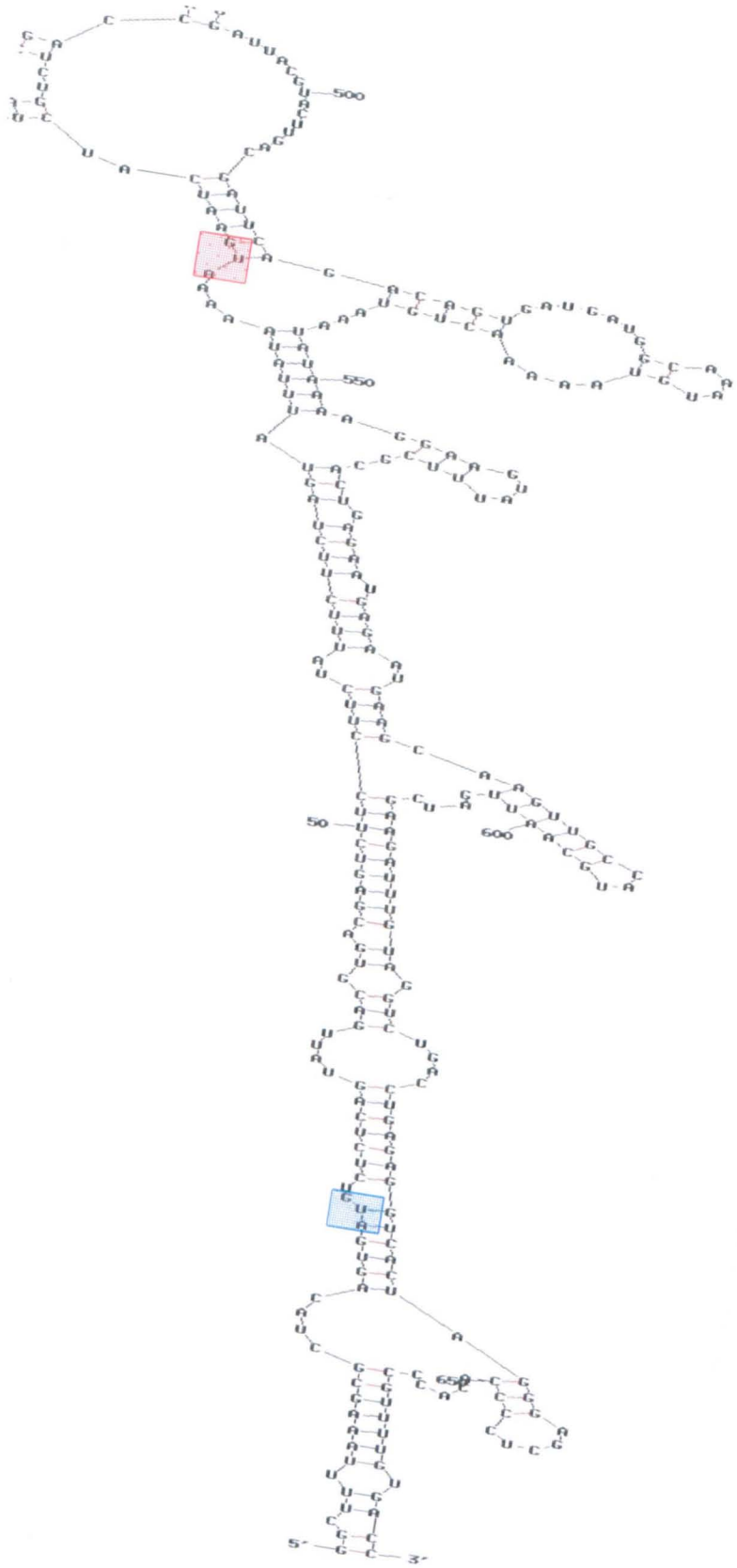

Figure 6.1 Secondary structure prediction of the rotavirus gene 11
Panel A) Secondary structure prediction of rotavirus gene 11 performed using the standard Zuker method. 50 nucleotide blocks are indicated on the plot and at the bottom of the plot there is the value of the structures dG (free energy at 37°C). The area enlarged in panel B is outlined in green.

Panel B) Enlargement from Zuker plot in panel A showing the area containing ORF1 and ORF2 start codons, which are highlighted by the blue and red boxes respectively.

6.3.4. Effect of gene 11 untranslated regions on the expression of NSP5 and NSP6

A cDNA, lacking the 5' and 3' UTR's of gene 11, was generated using PCR and cloned into the PCIneo vector. Expression of NSP5 and NSP6 from this vector was compared to that from PCIneo containing the full length gene 11 sequence using the coupled *in vitro* transcription/translation system (Figure 6.2). There were no apparent differences in the amount of NSP5 and NSP6 expressed from the two clones. This suggests that the 5' and 3' UTR's do not affect the levels of expression of the two proteins when expressed in the coupled *in vitro* system used in this study. Ribosomal shunting and IRES elements are dependent on the formation of secondary structures usually found within the 5' sequence of a gene. The observation that the loss of these regions does not effect expression of NSP5 and NSP6 suggests that the RNA secondary structures required for these mechanisms of expression are not present within gene 11, as predicted by the RNA secondary structure model.

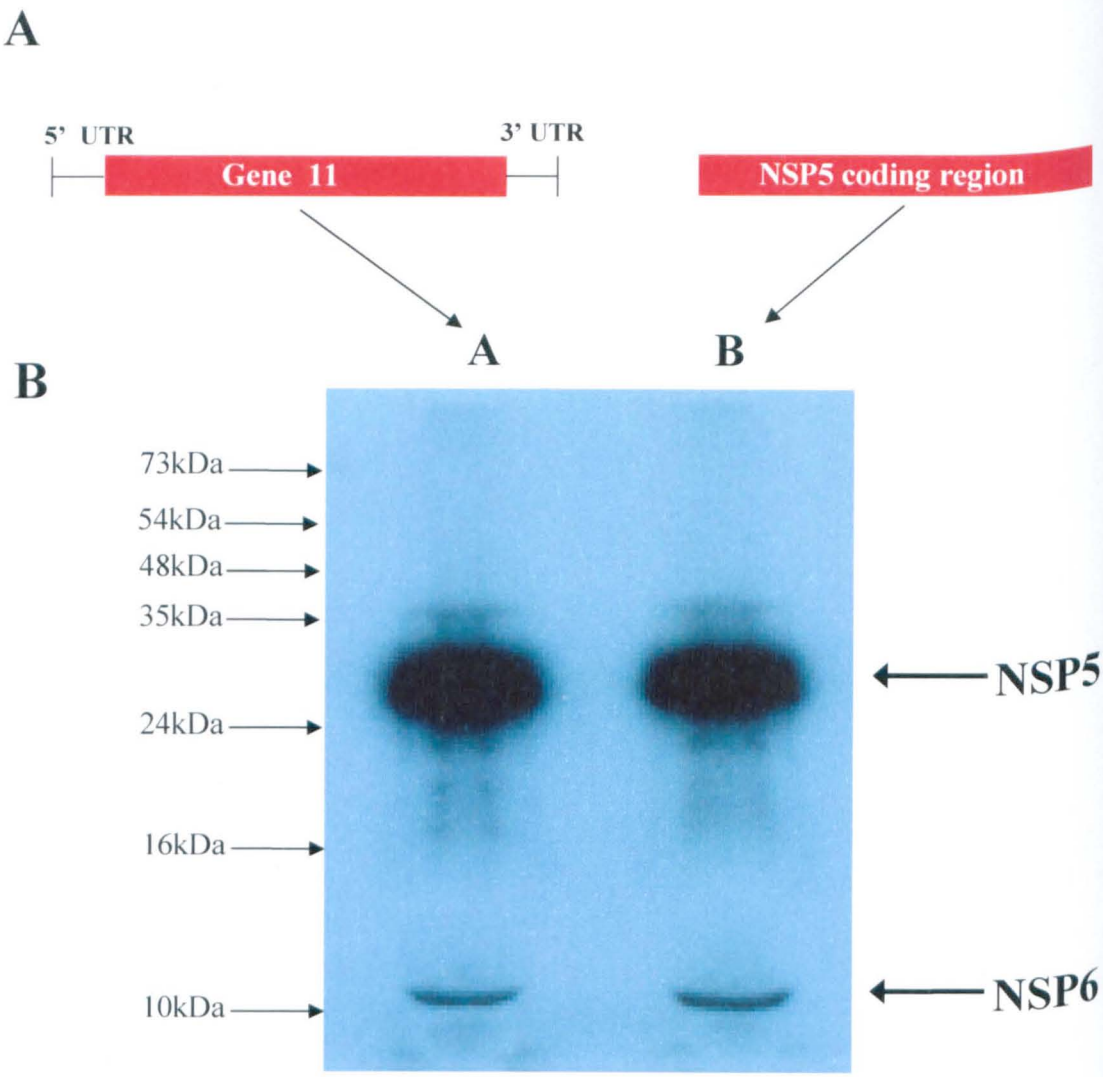
A
5' UTR
3' UTR
Gene 11
NSP5 coding region
A
B
B
73kDa
54kDa
48kDa
35kDa
24kDa
16kDa
10kDa
NSP5
NSP6

Figure 6.2 Effect of the gene 11 untranslated regions on expression of the NSP5 and NSP6 proteins

Panel A) Schematic representation of gene 11 with and without the 5' and 3' untranslated regions (UTR's). The 5' UTR is 21 nucleotides in length and the 3' UTR is 49 nucleotides in length.

Panel B) In order to assess the effect of the 5' and 3' UTR's on the expression of NSP5 and NSP6 the NSP5 coding region was cloned into the PCIneo expression vector and its expression in the coupled *in vitro* transcription/translation system compared to that of the gene11-PCIneo construct. *In vitro* transcription/translation using these cDNA constructs was carried out as described in the Materials and Methods. The protein products were analysed by PAGE as described in the Materials and Methods. After drying the gel was autoradiographed as described in the Materials and Methods. Track A shows protein expression from the gene11-PCIneo construct and track B shows protein expression from the NSP5-PCIneo (without the 5' and 3' termini) construct. The migration positions of the molecular weight size markers are indicated on the left hand side of the autoradiogram and the positions of NSP5 and NSP6 are indicated by arrows on the right hand side.

6.3.5. Investigation into the presence of an IRES element within the gene 11 sequence

IRES elements allow ribosomal binding in a cap-independent manner, to directly investigate whether or not an IRES was present within gene 11, the coding region for the cellular gene actin was inserted at the 5' end of gene 11, preventing any expression of the NSP5 and NSP6 proteins by cap-dependent ribosome scanning. Placing the actin ORF in front of the gene 11 sequence would stop ribosomes reaching ORF1 and ORF2 via scanning as the ribosomes terminate and detach from the RNA after the actin stop codon, thus any expression of NSP5 and NSP6 must be mediated by a cap-independent mechanism. Plasmids carrying the Actin gene (Actin-PCIneo), the actin-gene 11 fusion (Actin-gene11-PCIneo) and an actin-gene 11 fusion in which the ATG start codon of NSP5 had been made non-functional by site directed mutagenesis (Actin-gene11 t23c-PCIneo) (Figure 6.3), were all tested in the coupled *in vitro* transcription/translation system. The results (Figure 6.4) showed that only the actin protein was expressed and neither NSP5 nor NSP6 expression could be detected from any of the three constructs. Taken together these results and the apparent efficient expression from ORF2 from cDNA with a 5' UTR deletion strongly suggest that expression of NSP6 does not involve a cap-independent IRES based mechanism.

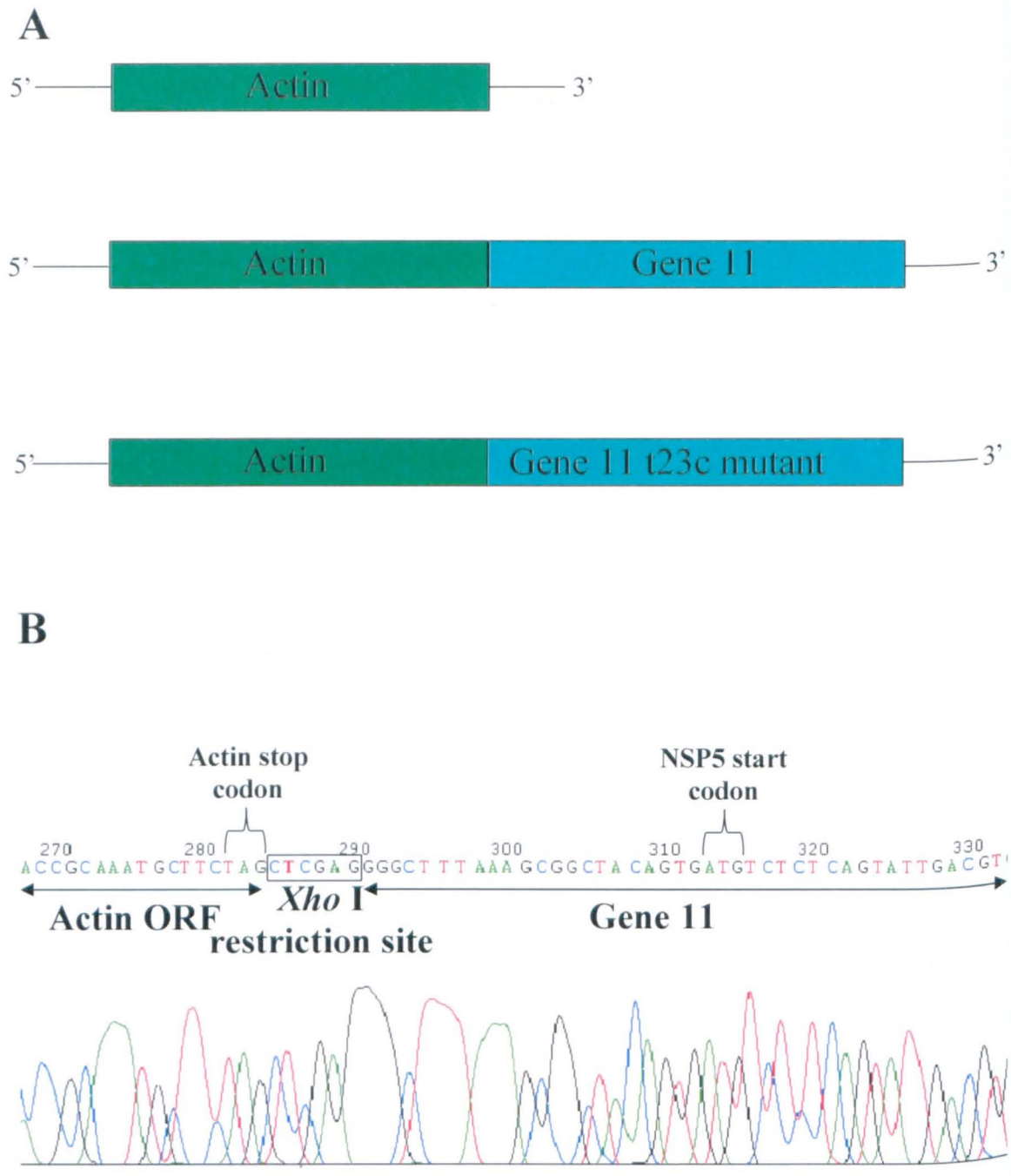
A
5'
Actin
3'
5'
Actin
Gene 11
3'
5'
Actin
Gene 11 t23c mutant
3'
B
Actin stop codon
NSP5 start codon
270
280
290
300
310
320
330
ACCGCAAATGCTTCTAGCTCGAGGGGCTTTAAAGCGGCTACAGTGATGTCTCTCAGTATTGACGT
Actin ORF
Xho I restriction site
Gene 11

Figure 6.3 Construction of actin-gene 11 fusions plasmids to investigate the possible presence of an IRES element is the gene 11 sequence
The coding region of the actin gene was positioned before the gene 11 sequence. The Actin-PCIneo plasmid was provided by Dr A.C. Marriott, University of Warwick. Using PCR the actin gene was amplified with a *Nhe*I restriction enzyme site at the 5' terminus and an *Xho*I restriction enzyme site at the 3' terminus. Using these restriction enzyme sites the actin gene was then cloned into the gene11-PCIneo and Gene11 t23c-PCIneo vectors (which cannot express the NSP5 protein) as described in the Materials ad Methods..

Panel A) Schematic representation of the actin gene, Actin-gene11-PCIneo construct and Actin-gene11 t23c-PCIneo construct (which cannot express the NSP5 protein).

Panel B) DNA sequence chromatogram of Actin-gene11-PCIneo construct showing the junction between the actin ORF and the gene11 sequence separated by the *Xho*I restriction site. The stop codon of the actin ORF and the start codon of the NSP5 ORF are identified at the top of the chromatogram.

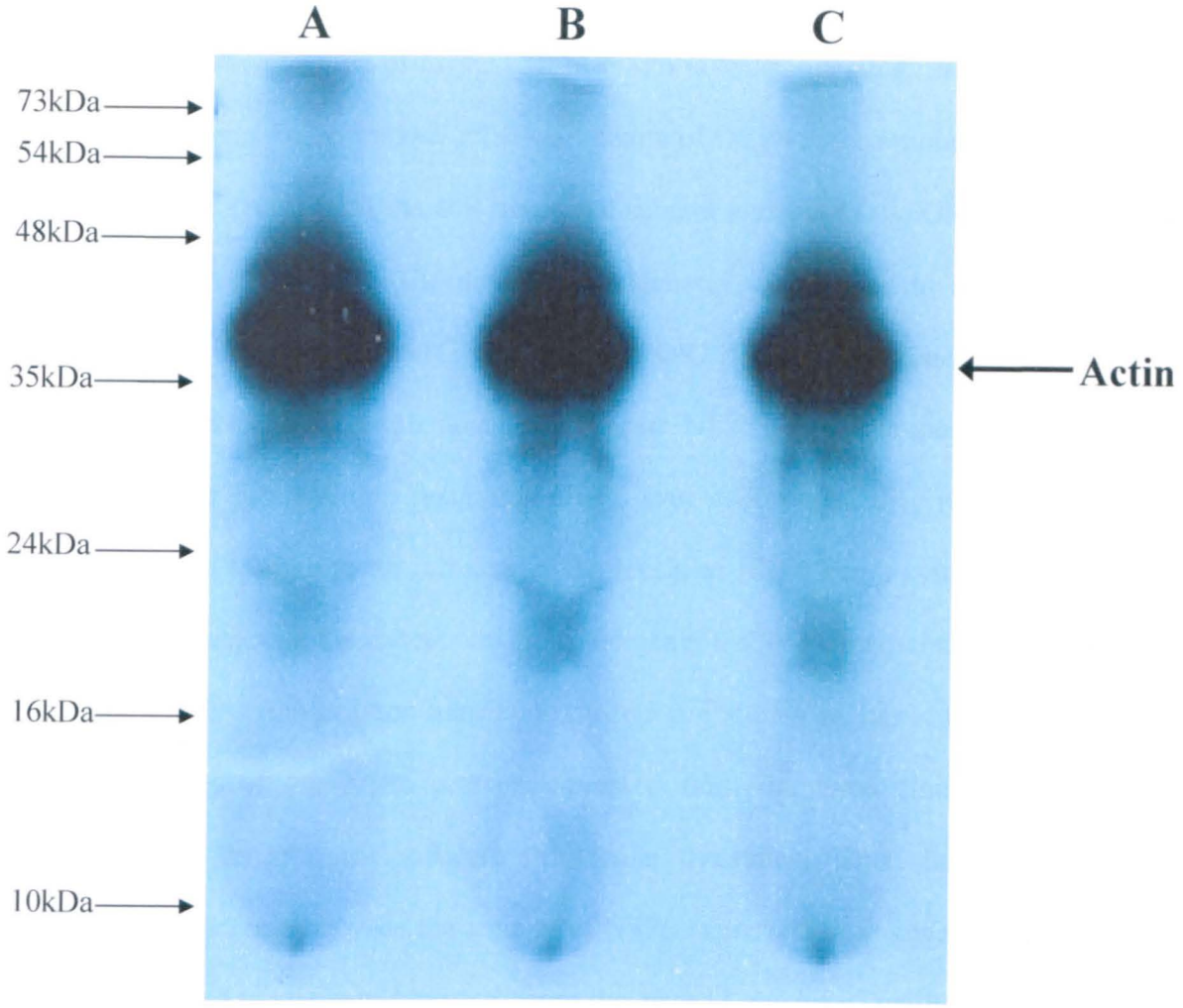

Figure 6.4 Analysis of Actin-Gene 11 fusion constructs to probe for the presence of an IRES element in rotavirus gene 11

Plasmid cDNA constructs of track A) Actin-PCIneo, track B) Actin-gene11-PCIneo and track C) Actin-gene11 t23c-PCIneo were used in the coupled *in vitro* transcription/translation system. The *in vitro* transcription/translation was carried out as described in the Materials and Methods. The protein products were analysed by PAGE as described in the Materials and Methods. After drying the gel was autoradiographed as described in the Materials and Methods. The migration positions of the molecular weight size markers are indicated on the left hand side of the autoradiogram and the position of the expressed actin protein is shown on the right hand side.

6.3.6. Investigation of a possible context-dependent leaky scanning mechanism of NSP6 expression from ORF2

An alternative method of expression of NSP6 is leaky scanning, in which a number of ribosomes fail to initiate at the start codon of ORF1 and continue to scan along the RNA molecule until the 40S ribosomal subunit encounters the ORF2 start codon. To test this possibility site directed mutagenesis was applied to a cDNA clone of gene 11 to replace the ATG start codon of ORF1 with ACG (gene11 t23c-PCIneo). The cDNA is therefore unable to express NSP5 and ribosomes should continue scanning past the non functional ORF1 start codon until they reach the ORF2 start codon leading to an increase in the levels of NSP6 being synthesised. The results of examining the expression from the gene11 t23c-PCIneo construct in the coupled *in vitro* transcription/translation system are shown in figure 6.5. The relative intensities of the NSP6 protein expressed from the three clones were quantified using image quant software (Molecular dynamics). This showed an almost two fold increase between the amount of NSP6 expressed from gene 11 t23c –PCIneo, compared to amounts expressed from the gene 11 and NSP5 coding region constructs (Figure 6.6).

There appeared to be a small amount of protein at the NSP5 molecular weight, this could be due to alternate codon usage for initiation at the mutated ACG ORF1 start codon or may possibly be background from the coupled *in vitro* transcription/translation system (see Chapter 4, Figure 4.2b).

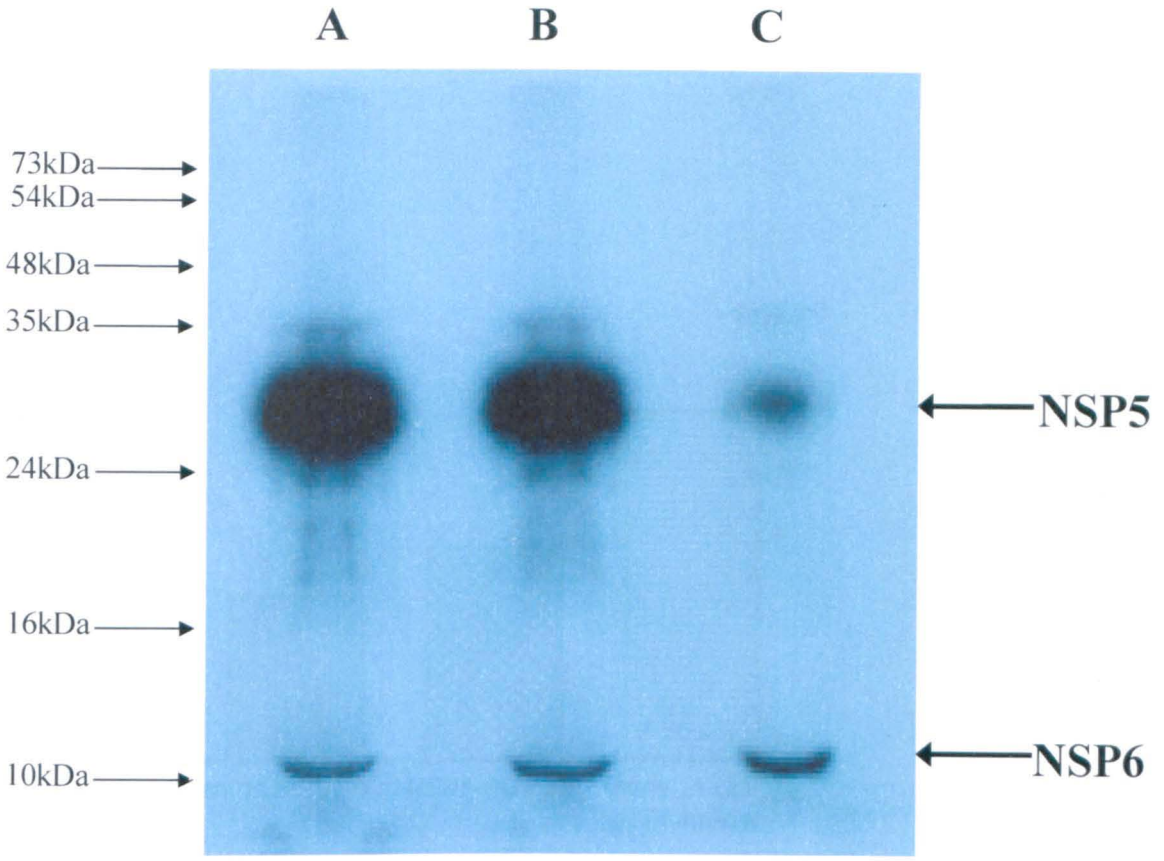

Figure 6.5 Analysis of the effect of removing the NSP5 ATG on ribosome read-through and effect on expression of NSP6 from ORF2 of rotavirus gene 11
In order to assess the possible leaky scanning mechanism of expression from ORF2 of gene 11 constructs were used in the coupled *in vitro* transcription/translation system. The *In vitro* transcription/translation reaction was carried out as described in the Materials and Methods. The protein products were analysed by PAGE as described in the Materials and Methods. After drying the gel was autoradiographed as described in the Materials and Methods. Track A) shows expression from the gene11-PCIneo construct, track B) shows expression from the NSP5-PCIneo construct and track C) shows expression from the gene11-PCIneo t23c construct (which has a non-functional ORF1 start codon). The migration positions of the molecular weight size markers are indicated on the left hand side of the autoradiogram and the positions of NSP5 and NSP6 are indicated by arrows on the right hand side.

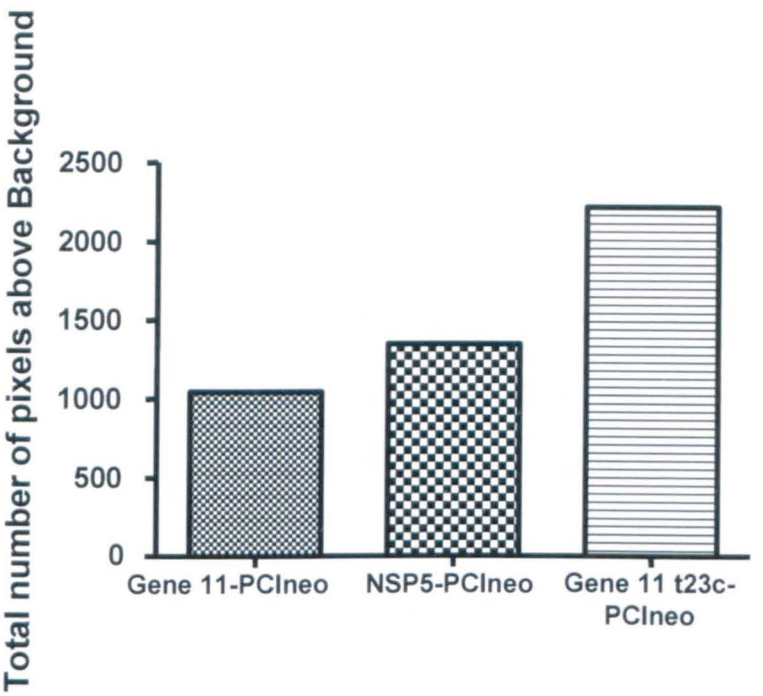

Figure 6.6 Quantification of autoradiograph shown in figure 6.5
The relative intensities of the NSP6 protein in the three tracks from figure 6.5 were quantified using image quant software (Molecular dynamics).

6.3.7. Investigation into leaky scanning expression with the CAT reporter system

To facilitate simpler measurement of the levels of expression from the second ORF of gene 11 a cDNA was constructed in which the NSP6 coding region was replaced with that of the reporter gene CAT, the product of which can be easily assayed. Figure 6.7 shows a strategy employing sequential PCR with 4 overlapping primers which was used to place the 5' 80 nucleotides of the gene 11 sequence (up to the ATG of ORF2) upstream of the 5' of the CAT gene, such that any expression from ORF2 would result in the expression of CAT reporter protein (Figure 6.7). The gene 11-CAT fusion was ligated into the PCIneo expression vector using the *Xho*I and *Xba*I restriction sites to create gene11-CAT-PCIneo.

In order to analyse the effect of the 5' UTR of gene 11 on the expression of the second ORF another, construct was made which lacked the 5' UTR sequence of gene 11 and began with the ATG start codon of ORF1 (ORF1-CAT).

6.3.8. Detection of CAT expression from the gene11-CAT fusion construct

The expression of CAT from the full length gene11-CAT fusion was examined. Cells were transfected with a CAT PCIneo positive control plasmid, a PCIneo negative control plasmid or a gene11-CAT PCIneo plasmid. At 48 hours post transfection cells were lysed and CAT expression levels assayed. The results (Figure 6.8) showed that significant CAT expression from the second open reading frame of the gene11-CAT construct could be detected.

A

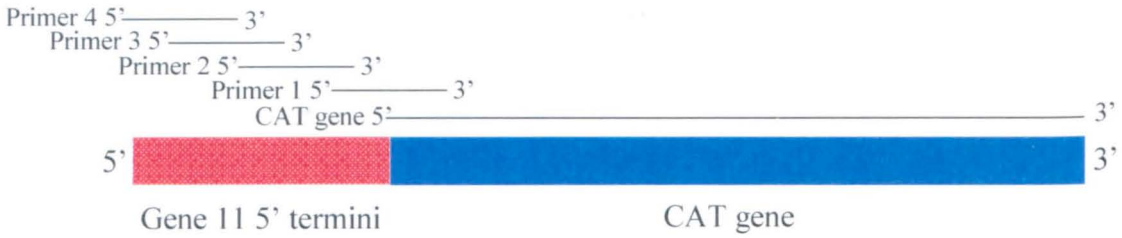
Primer 4 5'
3'
Primer 3 5'
3'
Primer 2 5'
3'
Primer 1 5'
3'
CAT gene 5'
3'
5'
3'
Gene 11 5' termini
CAT gene

B

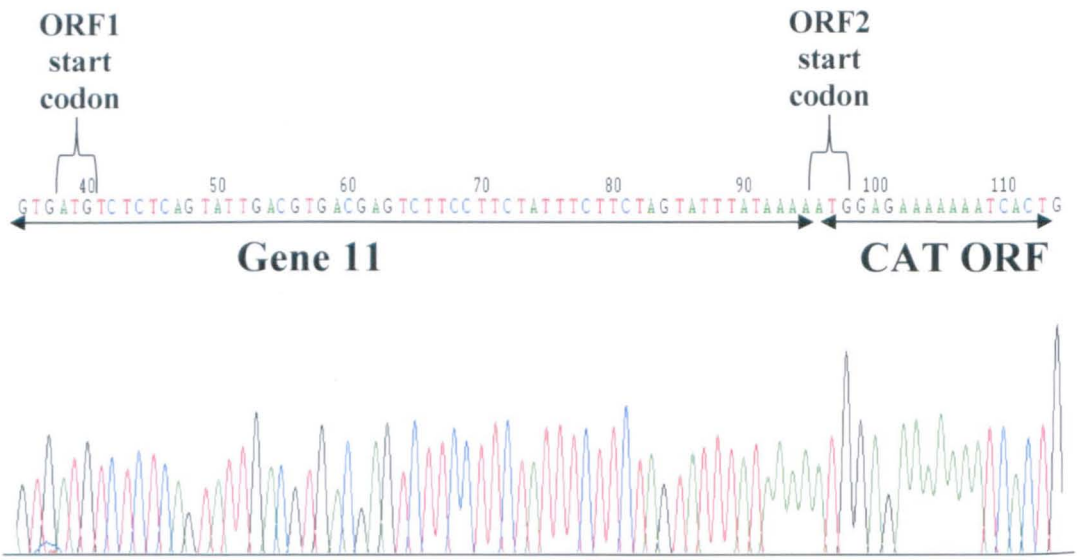
ORF1
start
codon
ORF2
start
codon
40
50
60
70
80
90
100
110
GTGATGTCTCTCAGTATTGACGTGACGAGTCTTCCTTCTATTTCTTCTAGTATTTATAAAAATGGAGAAAAAAATCACTG
Gene 11
CAT ORF

C

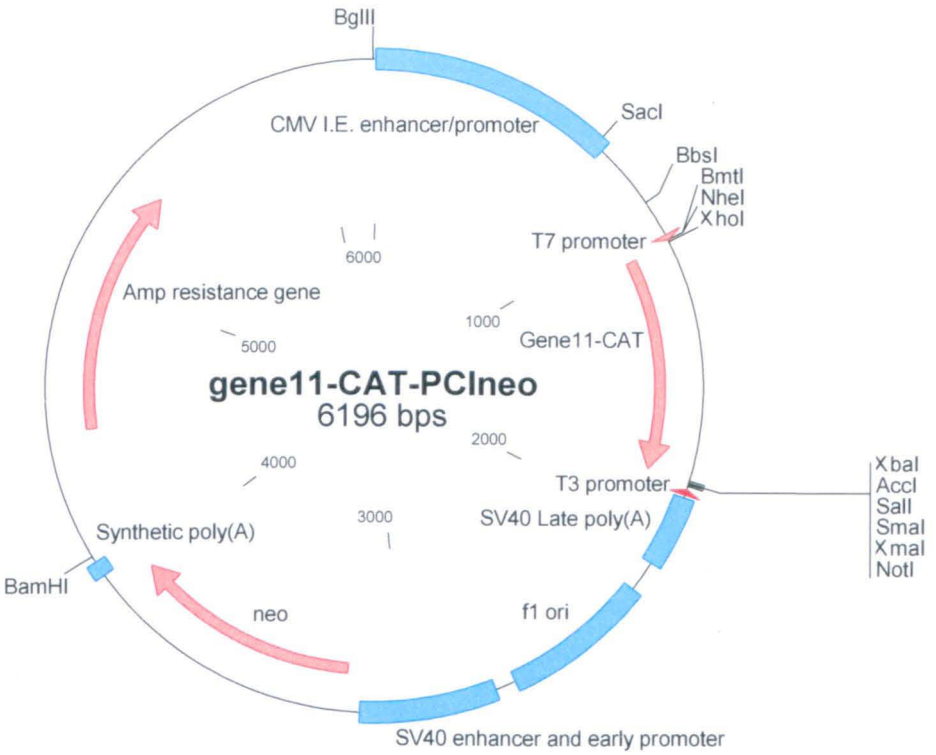

Figure 6.7 Construction of the gene11-CAT-PCIneo construct
Panel A) The 5'-terminal 80 nucleotides of rotavirus gene 11 (seen in red) was placed onto the 5' terminus of the CAT gene by sequential PCR using 4 oligonucleotide primers. The CAT reporter ORF (seen in blue) was positioned such that it now lay after the ORF2 start codon.

Panel B) DNA sequence chromatogram of gene11-CAT-PCIneo construct showing the junction between the 80 5' nucleotides of gene 11 and the CAT ORF. The ORF1 start codon of gene 11 and the ORF2 start codon which indicates the start of the CAT gene are identified at the top of the chromatogram.

Panel C) Sequential PCR was used to place the 5' 80 nucleotides of gene 11 onto the 5' termini of the CAT ORF. PCR product and the PCIneo vector were both cut with *Xho*I and *Xba*I restriction enzymes and gel purified. A ligation was performed and the resulting vector (gene11-CAT-PCIneo) was transformed into *E. coli* as described in the Materials and Methods.

A

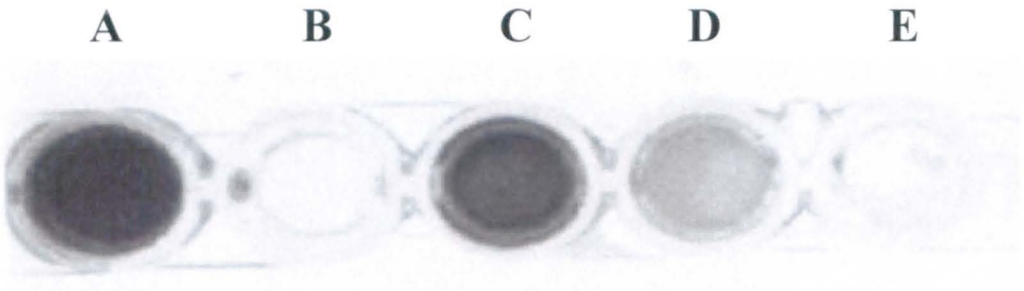
A
B
C
D
E

B

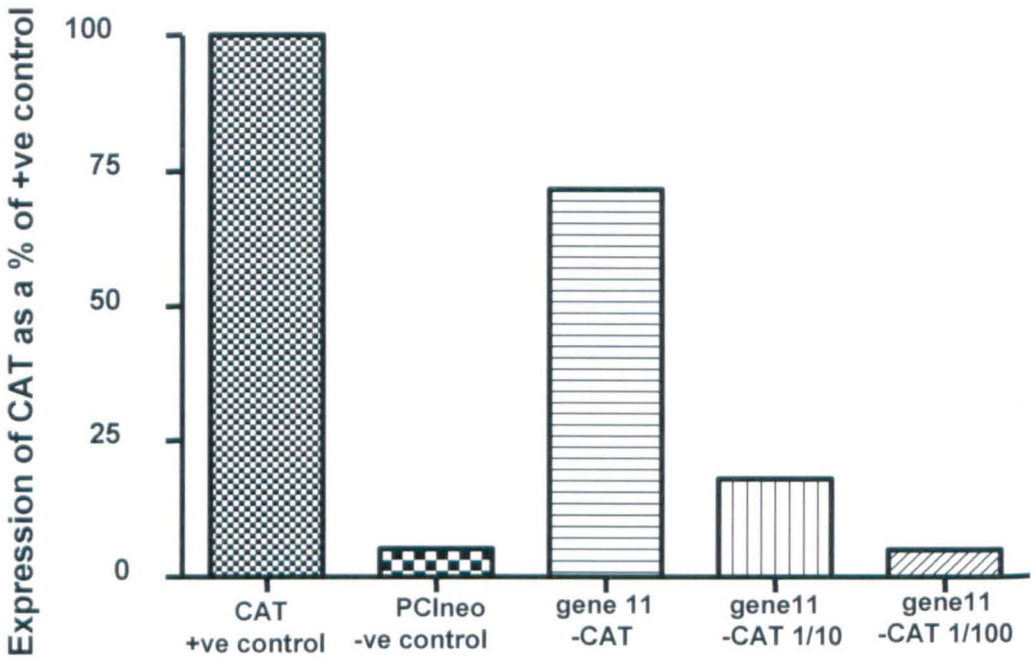
Expression of CAT as a % of +ve control
100
75
50
25
0
CAT
+ve control
PCIneo
-ve control
gene 11
-CAT
gene11
-CAT 1/10
gene11
-CAT 1/100

Figure 6.8 CAT assay for the detection of CAT expressed from the gene-11-CAT-PCIneo construct

Panel A) Confluent monolayers of BSC-1 cells were transfected with appropriate plasmids and after 48 hours incubation at 37°C harvested in lysis buffer. CAT assays were performed on the cell lysates using the CAT detection kit (Roche) as described in the Materials and Methods. A = CAT +ve control, B = PCIneo –ve control, C = gene11-CAT-PCIneo undiluted lysate, D = gene11-CAT-PCIneo 1/10 diluted lysate and E = gene11-CAT-PCIneo 1/100 diluted lysate.

Panel B) Bar graph of the expression of CAT protein from the samples described in panel A. All values are normalised with the CAT +ve control ascribed a value of 100%.

6.3.9. Generation of mutants to test for the presence of leaky scanning expression of ORF2

Having established the validity of using this approach to measure expression levels from ORF2 of gene 11, several mutants of the gene11-CAT fusion plasmid were constructed in order to investigate whether leaky scanning was the mechanism responsible for ORF2 expression. Leaky scanning has been shown to be dependent on the Kozak consensus sequence around the first ORF, the context surrounding the first initiation codon dictates the level of readthrough and any change to this context would have a dramatic effect on the expression of the second ORF. If this mechanism was responsible for expression from ORF2 then improving the Kozak consensus sequence around the first ORF would diminish expression of the second. In addition if the first ORF ATG start codon is made non-functional, expression from the second ORF would be greatly increased due to ribosomes now bypassing the first mutated ATG and initiating at ORF2.

Mutations were made around the ATG start codon of ORF1 to either improve its Kozak consensus sequence or to render the NSP5 start codon non-functional (Figure 6.9). Thus the GAGATGT sequence around the ORF1 start codon was mutated to generate either a partial Kozak consensus sequence in which the thymidine in position +4 was changed to a guanidine creating GAGATGG (gene11-CAT-PCIneo t25g) or a full Kozak consensus sequence ACCATGG in which four nucleotides were mutated (gene11-CAT-PCIneo g19a, a20c, g21c, t25g) (Figure 6.9). To generate a cDNA carrying a non-functional NSP5 start codon the adenine of the ATG was mutated to a guanine (gene11-CAT-PCIneo a22g) (Figure 6.9).

Kozak consensus sequence: **ACCAUGG**

Sequence surrounding the Gene 11 ORF1 start codon:

UACAGUGAUGUCU

gene 11 t25g ORF1 start codon sequence:

UACAGUGAUGGCU

gene 11 g20a/t21c/g22c/t25g ORF1 start codon sequence:

UACAACCAUGGCU

gene 11 a22g ORF1 start codon sequence:

UACAGUGGUGGCU

Figure 6.9 Gene11-CAT mutants
Site directed mutagenesis was used to mutate the AUG start codon of the first ORF to either a nonfunctional GUG or to place it in a better Kozak consensus sequence in the gene11-CAT-PCIneo construct. The AUG ORF start codon is underlined and the changes made by site directed mutagenesis can be seen in red.

6.3.10. Effect of the gene 11 UTR on CAT expression from ORF2

The data collected from the assay (Figure 6.10) for CAT expression from these mutants showed that the cDNA of the gene11-CAT construct which contained the 5'UTR of gene 11, had a small increase in the amount of CAT produced compared to that of the ORF1-CAT construct, which lacked the 5' UTR (Figure 6.10). This is contrary to what had been obsereved in the coupled *in vitro* transcription/translation system, in which no visible difference was discerned between the amount of NSP6 expressed from a construct containing the UTR and a construct without this sequence as detected by autoradiography.

6.3.11. Effect of improving the context of the ORF1 Kozak consensus sequence on CAT expression from ORF2

The t25g mutant, which had a partial Kozak consensus sequence showed a large reduction in CAT expression compared to that of the gene11-CAT construct (Figure 6.10). The mutant in which a full Kozak consensus sequence (ACCAUGG) was generated around ORF1 showed levels of CAT expression that were only slightly above background (Figure 6.10). This strongly indicates that in this case the vast majority of ribosomes were initiating at the first ATG start codon of the cDNA and hence cannot bypass it to initiate translation at the second ATG start codon and allow CAT expression.

6.2.12. Effect of removing the ORF1 initiation codon on the expression of CAT from ORF2

Consistent with the above findings, when the first ATG initiation codon was mutated to a non-functional GTG codon, the expression of CAT increased to a level comparable to that of the CAT positive control (Figure 6.10). This suggests that when the first ATG initiation codon was removed, the ribosomes preferentially scanned to the second ATG start codon and then began translation. These data are all consistent with a cap-dependent leaky scanning mechanism being responsible for the translation of NSP6 from the second ORF in rotavirus gene 11.

A

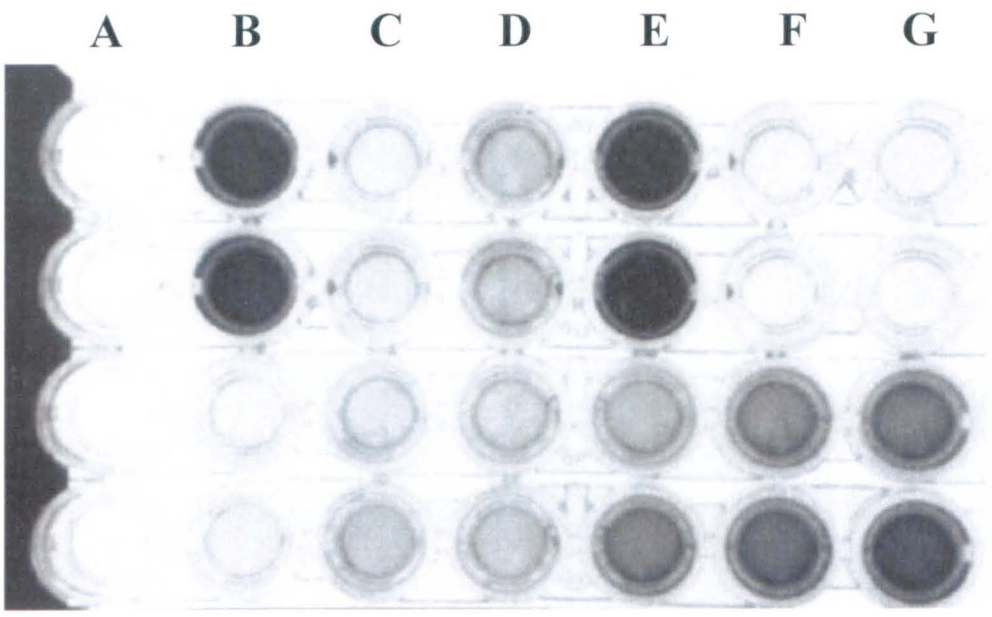
A
B
C
D
E
F
G
1
2
3
4

B

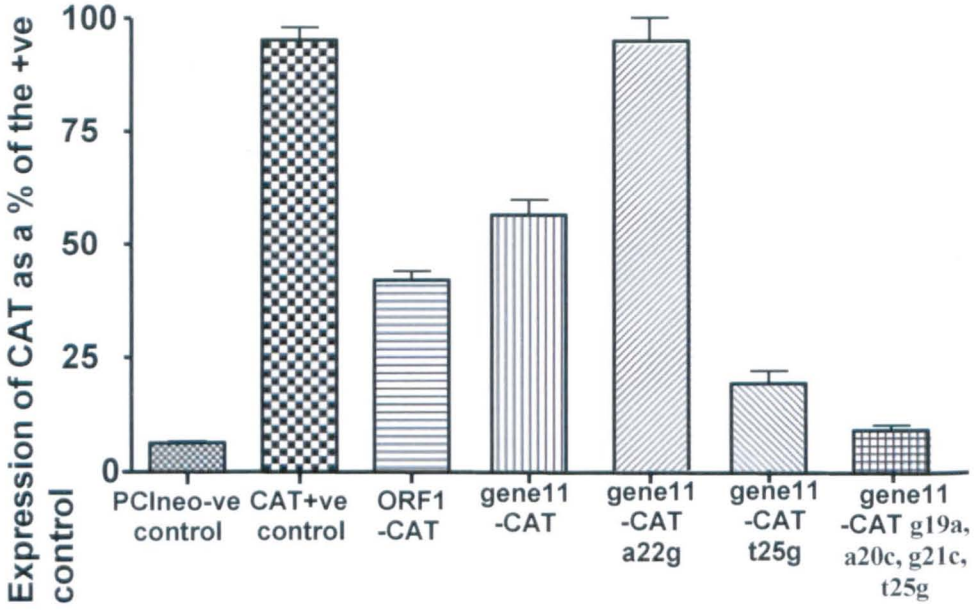
Expression of CAT as a % of the +ve control
100
75
50
25
0
PCIneo-ve control
CAT+ve control
ORF1 -CAT
gene11 -CAT
gene11 -CAT a22g
gene11 -CAT t25g
gene11 -CAT g19a, a20c, g21c, t25g

Figure 6.10 CAT assays to determine the effect of nucleotide changes around the ATG start codon on the expression of CAT from ORF2 of the rotavirus gene 11

Panel A) Confluent monolayers of BSC-1 cells were transfected with the appropriate plasmids and after 48 hours incubation at 37°C harvested in lysis buffer. CAT assays were performed on the cell lysates using the CAT detection kit (Roche) as described in the Materials and Methods. A1 & A2 = PCIneo –ve control, B1 & B2 = CAT +ve control, C1 & C2 = ORF1-CAT, D1 & D2 = gene11-CAT, E1 & E2 = gene11-CAT t23c, F1 & F2 = gene11-CAT t25g, G1 & G2 = gene11-CAT g19a, a20c, g21c, t25g, A3 & A4 = 0pg CAT standard, B3 & B4 = 50pg CAT standard, C3 & C4 = 100pg CAT standard, D3 & D4 = 150pg CAT standard, E3 & E4 = 200pg CAT standard, F3 & F4 = 300pg CAT standard and G3 & G4 = 400pg CAT standard.

Panel B) Bar graph of the expression of CAT protein from the samples described in panel A. All values are normalised with the CAT +ve control ascribed a value of 100%.

6.4. Discussion

Work presented in this chapter had as its aim the investigation of the mechanism of expression of NSP6 from the second ORF of gene 11. A number of possible mechanisms use secondary structures formed by the 5' termini of mRNA to aid initiation of translation. RNA secondary structure prediction showed little secondary structure at the 5' termini of gene 11 mRNA consistent with those known to influence translation in other systems. In addition deletion of the 5' UTR from this mRNA did not appear detrimental to the expression of the NSP5 and NSP6 proteins in a coupled *in vitro* transcription/translation system. The lack of appropriate predicted RNA secondary structure and the deletion of the 5' UTR not affecting efficient protein expression *in vitro* would indicate that translational mechanisms such as IRES elements and ribosomal shunting are not involved.

In order to exclude the possible existence of an IRES element within gene 11, dicistronic gene fusions were constructed in which the actin gene was inserted in front of gene 11. These cDNA constructs only expressed actin and demonstrated that there was no expression of gene 11 proteins downstream of the actin ORF, indicating the absence of any cap-independent expression mechanisms in gene 11.

To assess the possible expression of NSP6 via a leaky scanning mechanism the 5' 80 nucleotides of gene 11 were placed before the CAT reporter gene sequence. This was done in such a way that the CAT gene initiated from the ORF2 position. The expression of CAT from the second ORF of the gene 11 fusion was tested with the ORF1 AUG start codon in a variety of Kozak consensus sequences, this showed that the expression of CAT from the second ORF was diminished when

ORF1 AUG start codon was placed into a better consensus sequence and greatly improved when the ORF1 AUG was removed. This suggests that the expression of ORF2 was dependent on the proportion of ribosomes initiating translation at the ORF1 AUG. This context-dependent manner of ORF2 expression can only be attributed to leaky scanning. A small decrease in efficiency of expression was seen when the 5' gene 11 UTR was removed in this system, which was not seen in a similar experiment using the coupled *in vitro* transcription/translation system.

Other mechanisms such as ribosomal shunting are not affected by the context in which the first AUG initiation codon is found and also predominantly require the presence of secondary structural elements at the 5' terminus, which are not present in the gene 11 RNA. Rotavirus RNA is very A/U rich and secondary structure prediction of gene 11 shows only limited secondary structure at the 5' terminus and little stable G/C bonding. Ribosomal shunting is also not affected by the context around the initiation codon of the first ORF.

Frameshifting is also unlikely as this would produce a fusion of the 5' of NSP5 and then slippage to engage the ORF of NSP6, which has not been detected in NSP6 protein recovered *in vivo*. Furthermore the gene 11 sequence does not contain the required slippery sequence or pseudoknot required for this mechanism of translation to occur.

The work presented in this chapter indicates that the most likely mechanism of expression of rotavirus gene 11 second ORF is leaky scanning. The efficiency of expression from ORF2 appears to be directly related to the context of the Kozak consensus sequence surrounding the initiation codon of ORF1. Thus the expression

of NSP6 appears to be controlled at the translational level by the amount of ribosomal read through at the first ATG start codon. However, it is difficult to determine if the low level of NSP6 expression detected in the cells during virus infection is due to low level leaky scanning or to the high protein turnover noted in other experiment performed as part of this study.

Discussion

Chapter 7

Rotaviruses are the major etiological agent for gastroenteritis in children and young animals (Kapikain *et al.*, 2001). They possess a dsRNA genome composed of 11 segments which encode six structural and six non-structural proteins. The gene segments are monocistronic with the exception of the smallest gene segment 11 which encodes two proteins. The complex interactions involved in virus replication and the role that the non-structural proteins play in these events is not yet fully understood (Estes, 2001). However, those non-structural proteins that have been associated with the formation of the large occlusion bodies termed viroplasms have been shown using siRNA and intracellular antibodies, to be essential for virus replication (Vascotto *et al.*, 2004; Silvestri *et al.*, 2005; Lopez *et al.*, 2005). The viroplasms are the site of synthesis and replication of dsRNA, packaging of viral dsRNA into newly synthesised cores and the steps of viral morphogenesis that result in the formation of double-shelled pre-virions (Altenburg *et al.*, 1980; Espaza *et al.*, 1980; Patton & Gallegos, 1990; Wentz *et al.*, 1996; Patton *et al.*, 1997).

Two proteins NSP5 and NSP6 have been shown to be encoded by gene segment 11 in overlapping reading frames (Dyall-Smith *et al.*, 1981; Mattion *et al.*, 1991). The NSP5 protein has been identified as a major component of viroplasms (Petrie *et al.*, 1984; Fabbretti *et al.*, 1999; Eichwald *et al.*, 2004), whereas only tentative observations have linked NSP6 localisation to be within these structures (Mattion *et al.*, 1991).

An *in vitro* transcription/translation system was used to study the expression of proteins from gene segment 11. NSP5 and NSP6 were both clearly expressed in this system, which was also employed to investigate the phosphorylation of NSP5.

When isolated from infected cells NSP5 exists in three isoforms which vary on their level of phosphorylation and can be identified because of the retardation caused by phosphorylation when the proteins are fractionated by SDS-PAGE. The three isoforms of NSP5 migrate at 26, 28 and 30-34 kDa (Welch *et al.*, 1989; Afrikanova *et al.*, 1996; Poncet *et al*,. 1997; Blackhall *et al.*, 1997). It has been suggested that NSP5 has putative autocatalytic kinase activity potentially leading to autophosporylation of the protein (Welch *et al.*, 1989; Poncet *et al.*, 1997; Torres-Vegas, 2000). In addition the generation of the hyperphosphorylsated form of the protein (30-34 kDa) has been shown to be up-regulated by the presence of NSP2 (Afrikanova *et al.*, 1998). In the results reported here, NSP5 expressed from the coupled *in vitro* transcription/translation system appeared to become hyperphosphorylated when incubated in the rabbit reticulate lysate at 20°C for extended periods of time. This hyperphosphorylation was not seen if the extended incubation was at 4°C. Work presented here suggests that NSP5 can be hyperphosphorylated in the coupled *in vitro* transcription/translation system in the absence of NSP2 either by cellular kinases within in the rabbit reticulate lysate or by slow autophosphorylation. There is recent evidence to suggest that NSP2 may cause a conformational shift in the NSP5 protein that allows it to be phosphorylated at a specific serine residue at position 67 (Eichwald *et al.*, 2004). The phosphorylation at this residue is thought to lead to subsequent phosphorylation events which in turn lead to the generation of the hyperphosphorylated form of the protein (Eichwald *et al.*, 2004). Two cellular kinases casein kinase I and casein kinase II have been suggested to be involved in NSP5 phosphorylation (Eichwald *et al.*, 2002; Eichwald

et al., 2004). Evidence reported here suggests that cellular kinases may well be able to cause hyperphosphorylation without the presence of NSP2 but at a much slower rate.

To further investigate the function of NSP5 and NSP6 cDNA's of both ORF were cloned into the pET expression vector system to facilitate the production and purification of the two proteins. GST tagged fusions were originally used for purification but these proved to be unstable during the purification process and consequently large amounts of protein could not be obtained. Subsequent purification attempts using a modified pET vector constructed in the rotavirus lab (Chung, 2004) again proved unable to provide suitable purified protein. However, purified protein was obtained via construction of cDNA fusion constructs containing a 6xHis tag at the 5' terminus of the NSP5 or NSP6 ORF's. The His tagged ORF constructs were separately cloned into a modified pET42b vector which lacked the GST tagging region usually found in this vector. The His-NSP5 protein was shown by mass spectroscopy to exist in two forms at 26 and 28 kDa this being the correct size to be the two lower phosphorylated forms found within the infected cells. This might be an indication of autophosphorylation occurring during prokaryote protein expression. Purified NSP5 and NSP6 were then used to generate monospecific polyclonal antisera for each protein.

NSP5 has previously been shown to localise to the viroplasms within infected cells (Petrie *et al.*, 1984). It has also been observed that the number and size of these viroplasms changes over the course of an infection with the number of viroplasms decreasing as their size increases (Eichwald *et al.*, 2004).

Work presented here using immunofluorescence to detect the distribution of the NSP5 protein over the course of a rotavirus infection indicated that the number of viroplasms appeared to increase from 2 – 6 hours post infection and then decreases thereafter as their size increased. One suggestion put forward for the decrease in viroplasm number and increase in size is coalescence and fusion of separate viroplasms (Eichwald *et al.*, 2004) however, there was no direct observation of fusion using fluorescence microscopy. There appeared to be an increase in the number of viroplasms at the last time point, this may be an indication of newly formed double layered particles causing secondary rounds of replication leading to the formation of new viroplasms.

The distribution of NSP5 within the viroplasm was seen by Eichwald *et al* (2004) to be a ring shape, surrounding the NSP2 which appeared to form the core of the viroplasm. From observations made while viewing confocal images the distribution of NSP5 within the viroplasm appeared to be cup shaped with the protein forming a ring around the centre of the viroplasm and narrowing into a base at the end of the confocal series. How this distribution may contribute to the function of NSP5 in unknown.

NSP6 was not detectable by immunofluorescence or Western blotting using either rabbit anti-NSP6 or rat anti-NSP6 sera but could be immunoprecipitated from cells infected with the UKtc strain of rotavirus. Immunoprecipitation showed that NSP6 was expressed at a low level throughout the course of an infection. The amount expressed at 2 hours post infection was smaller than that evident at 3 hours and it continued to be produced at a steady but low rate until 8 hours when its

expression reduced slightly. Previous work has shown that NSP6 could be immunoprecipitated at 8 hours post infection (Torres-vega *et al.*, 2000). Pulse chase analysis performed in this study showed for the first time that NSP6 had a high rate of turnover with NSP6 pulse labelled protein virtually undetectable at the end of a 2 hour chase period. This is unusual among the rotavirus proteins which do not show such high turn over (McCrae & Faulkner-Valle, 1981).

To determine the distribution of NSP6 within a rotavirus infected cell a GFP–NSP6 fusion was constructed. When this fusion protein was expressed in tranfected cells it appeared to form a large amorphous mass within the cytoplasm. When cells transfected with the fusion construct were subsequently infected with rotavirus, the expressed fusion protein was redistributed to viroplasm structures in the infected cell. The localisation of the GFP-NSP6 fusion protein appeared to be within the centre of the viroplasm, similar to the distribution reported recently for the NSP2 protein (Eichwald *et al.*, 2004). It was only possible to find a limited number of cells with detectable levels of GFP-NSP6, a possible indicator that NSP6 still has a high rate of turnover when expressed in the absence of other viral proteins.

From work done in previous studies (Mattion *et al.*, 1991) it has become widely accepted that NSP6 localises to the viroplasms however these claims are not fully supported by the evidence presented. In the experiments performed by Mattion *et al* immunofluorescence images were generated using hyperimmune sera from animals inoculated with recombinant baculovirus lysate, containing either the NSP6 ORF or a complete gene 11 sequence. Immunofluorescence using the NSP6 specific sera does show what are termed discrete foci within rotavirus infected cells.

However, the immunofluorescence image that corresponds to NSP5 localising to the same structures was performed using the sera generated against the recombinant baculovirus lysate containing the whole gene 11 and thus contained antibodies to both NSP5 and NSP6, a fact that had been previously demonstrated in the same publication (Mattion *et al.*, 1991). This means that both NSP5 and NSP6 would be stained by the same sera and if the foci that NSP6 was localised to were not the viroplasms then no distinction could be made between the two. The image generated from this sera not only showed discrete foci but also a large amount of diffuse cytoplasmic staining making any detection of separate species of foci based on size or morphology impossible. Therefore the co-localisation of NSP5 and NSP6 to the viroplasm of infected cells by these means should only be tentatively suggested. Work performed during the course of this investigation using the GFP-NSP6 construct has definitively shown by double immunofluorescence confocal microscopy of NSP5 and NSP6 co-localise to viroplasms within infected cells.

With the localisation of NSP6 to the viroplasms confirmed the question of whether the NSP6 protein is essential for viroplasm formation was addressed. It has been previously shown that NSP2 and NSP5 can form viroplasm-like structures in the absence of a rotavirus infection (Fabbretti *et al.*, 1999) and that NSP5 when expressed with fusions of other proteins or peptides at its N terminus can also form viroplasm-like structures in the absence of NSP2 (Mohan *et al.*, 2003). However, these studies used a range of NSP5 deletion mutants in order to assess which regions of NSP5 were crucial to form the viroplasm-like structures. These mutants contained either the whole NSP6 coding region or encoded part of the NSP6 protein. In order

to assess the effect NSP6 has on the formation of viroplasm-like structures a gene 11 cDNA which contains a mutated nonfunctional ORF2 start codon was constructed by site-directed mutagenesis. As the construct had a mutated ORF2 start codon there would be no expression of the NSP6 protein. The construct was then used in transfection experiments along with the NSP2 ORF in order to assess the formation of viroplasm-like structures.

Experiments performed using the gene 11 unable to express NSP6 showed that NSP6 was not required for the formation of viroplasm-like structures. Cells transfected with an NSP2 construct and a gene 11 mutant which could not express NSP6 were still capable of forming viroplasm-like structures. To confirm these findings a N-terminally fused GFP-NSP5 mutant which was unable to express NSP6 was used, as stated above it was found that GFP-NSP5 fusions were able to form viroplasm-like structures in the absence of NSP2 (Mohan *et al.*, 2003). Transfection of the GFP-NSP5 mutant which could not express NSP6 showed formation of viroplasm-like structures. This evidence shows that NSP6 is not required for the formation of viroplasm-like structures by NSP5 and NSP2 or by GFP-NSP5. This suggests that NSP6 does not a play a major structural role in formation of the viroplasms.

The localisation of NSP6 to the viroplasm was a strong indication of it being a potential RNA binding protein. NSP2 and NSP5 have both been shown to have RNA binding ability (Kattoura *et al.*, 1992; Vende *et al.*, 2002), with NSP2 binding ssRNA in a sequence independent manner (Kattoura *et al.*, 1992) and NSP5 binding

both ssRNA and dsRNA with equal affinity in a sequence independent manner (Vende *et al.*, 2002).

Using both filter binding and gel retardation assays the RNA binding ability of NSP6 was characterised. NSP6 was found to bind ssRNA in a sequence independent manner and a close to equal affinity for ssRNA, dsRNA and dsDNA. From this data it can be concluded that NSP6 is a sequence independent nucleic acid binding protein. The K_{Diss} of NSP6 for ssRNA was found to be some eight fold lower than that of NSP5, showing NSP5 has a far greater affinity for RNA than NSP6. The identification of an RNA binding ability for NSP6 suggests a possible role along side NSP2 and NSP5 in the RNA replication and packaging events which occur within the viroplasm however, the exact RNA-protein and protein-protein interactions involved still remain unclear.

The mechanism of expression of ORF2 from rotavirus gene 11 was also investigated. The NSP6 ORF is encoded in a +1 frame shift from that of the NSP5 ORF and is contained entirely within the NSP5 ORF. Several possible mechanisms could be utilised for the expression of NSP6 and these were addressed in this study. Data presented here suggests a leaky scanning mechanism for NSP6 expression. The expression of NSP6 from the second ORF was found to be dependent upon the Kozak consensus sequence surrounding the first ORF (NSP5) start codon suggesting that expression involved a fraction of scanning ribosomes failing to initiate at the ORF1 start codon but continuing to scan to the ORF2 start codon were they initiate protein synthesis.

The significance of the NSP6 protein in virus replication has come under scrutiny as some rotavirus gene 11's that have been sequenced do not appear to encode this protein. Two human virus isolates Mc323 (Kojima *et al.*, 1996) and 512-C (Wu *et al.*, 1998) do not posses the NSP6 start codon. In addition two viruses have been discovered that appear to have truncated NSP6 ORF's, the Alabama strain of lapine virus (Gorziglia *et al.*, 1989) lacks the 5' terminus of the NSP6 ORF but an internal start codon may express a 79aa protein and the porcine OSU strain (Gonzalez & Burrone, 1989) which potentially encodes for a 51aa NSP6 protein due to a premature stop codon found in the NSP6 ORF. This is based entirely on sequence data and as yet no attempts have been made to identify the NSP6 protein expressed by these strains. The lack of sequence conservation and its seemingly low level of expression in virus infected cells, has led to the suggestion that NSP6 may play a non-essential regulatory role within a rotavirus infection (Lopez *et al.*, 2005; Mattion *et al.*, 1991; Torres-Vega *et al.*, 2000). The interaction domain of NSP5 that binds the NSP6 protein is found at its C-terminus a region which is also crucial for NSP5 dimerisation and hyperphosphorylation perhaps suggesting a regulatory role for NSP6 in these events (Torres-Vega, *et al.*, 2000). Recent work using siRNA and intracellular antibodies has demonstrated that NSP5 is essential for viroplasm formation and virus replication. These studies were performed using the Alabama and OSU strains in order to try and circumvent the issue of knockdown in the level of NSP6 contributing to the effect seen by knockdown of NSP5 (Vasscotto *et al.*, 2004; Lopez *et al.*, 2005). Whether there is expression of NSP6 in a truncated form from these strains and if the regions expressed are functionally active for example

still able to bind RNA and what affect this may have on the observations seen in these experiments is a matter that requires further investigation.

The NSP6 protein is the most uncharacterised of all the rotavirus proteins and this study has been aimed at increasing the understanding of this the smallest protein expressed by the virus and investigating its possible role in virus replication. Work presented here suggests that NSP6 may have a more central role in virus replication than previously thought. The high rate of NSP6 turnover may be an indication of a regulatory protein but how this is coupled to a possible role in the complex events within the viroplasm is unknown. Its RNA binding ability indicates a possible place for NSP6 in the events of RNA replication and packaging and there is the possibility that it may act as a mediator between NSP2 and NSP5.

Despite the progress made in this and previous studies a great many questions remain unanswered about NSP5 and NSP6 and there is an extensive amount of future research on this area. The lack of a reverse genetics system to knock out specific genes has hampered research into rotaviruses however there are many other techniques available which offer great insight into protein function. The crystal structure of NSP5 and NSP6 would yield new insights into their functions, much has been learnt from the resolution of the NSP2 proteins crystal structure (Jayaram *et al.*, 2002). One such area where this type of study would be useful would be the elucidation of the residues in NSP5 and NSP6 involved in RNA binding.

An area of further investigation is the high rate of turnover of NSP6, the determination of the mechanism of this degradation may yield some insights into its

function. A first step would be to perform pulse chase analysis using a cDNA of the NSP6 ORF transfected into cells to determine the rate of turnover of NSP6 in the absence of a viral infection. Determining the signal for degradation may also be important as NSP6 may contain a novel degradation signal that has not been seen before.

Another area of investigation might be to determine if there is any interaction between NSP2 and NSP6. Co-immunoprecipitation, yeast or mammalian two hybrid and GST pull down analysis could be used in order to experimentally confirm this interaction. If found to be true this would be an important step in further understanding the relationship between the non-structural proteins found within the viroplasm. To understand the complex interactions found in the viroplasm the interactions between these proteins and their functional abilities as multimers should be investigated and not just their individual attributes. One such area would be studying what effect if any NSP6 may have on NSP5 phosphorylation and how this relates to the ability of NSP2 to enhance NSP5 phosphorylation to form the hyperphosphorylated isoform.

The events that occur within the viroplasm which play a role in virus replication are still not fully understood and many challenges lie ahead. This investigation has shed new light on NSP6 the most uncharacterised of the rotavirus proteins and attempted to investigate how this protein may be involved in the virus replication cycle.

Bibliography

Affranchino, J. L. and Gonzalez, S. A. (1997). Deletion mapping of functional domains in the rotavirus capsid protein VP6. *J Gen Virol* **78 (Pt 8)**, 1949-55.

Afrikanova, I., Fabbretti, E., Miozzo, M. C. and Burrone, O. R. (1998). Rotavirus NSP5 phosphorylation is up-regulated by interaction with NSP2. *J Gen Virol* **79 (Pt 11)**, 2679-86.

Afrikanova, I., Miozzo, M. C., Giambiagi, S. and Burrone, O. (1996). Phosphorylation generates different forms of rotavirus NSP5. *J Gen Virol* **77 (Pt 9)**, 2059-65.

Ahmed, M. U., Kobayashi, N., Wakuda, M., Sanekata, T., Taniguchi, K., Kader, A., Naik, T. N., Ishino, M., Alam, M. M., Kojima, K. et al. (2004). Genetic analysis of group B human rotaviruses detected in Bangladesh in 2000 and 2001. *J Med Virol* **72**, 149-55.

Almeida, J. D., Bradburne, A. F. and Wreghitt, T. G. (1979). The effect of sodium thiocyanate on virus structure. *J Med Virol* **4**, 269-77.

Altenburg, B. C., Graham, D. Y. and Estes, M. K. (1980). Ultrastructural study of rotavirus replication in cultured cells. *J Gen Virol* **46**, 75-85.

Amersham Biosciences. (2003a). The Recombinant Protein Handbook: Protein Amplification and Simple Purification.

Amersham Biosciences. (2003b). Protein Purification Handbook

Arias, C. F., Lopez, S. and Espejo, R. T. (1982). Gene protein products of SA11 simian rotavirus genome. *J Virol* **41**, 42-50.

Au, K. S., Chan, W. K., Burns, J. W. and Estes, M. K. (1989). Receptor activity of rotavirus nonstructural glycoprotein NS28. *J Virol* **63**, 4553-62.

Au, K. S., Mattion, N. M. and Estes, M. K. (1993). A subviral particle binding domain on the rotavirus nonstructural glycoprotein NS28. *Virology* **194**, 665-73.

Ausbel, F. M. (1998). Current Protocols in Molecular Biology: Wiley Interscience. USA.

Ball, J. M., Tian, P., Zeng, C. Q., Morris, A. P. and Estes, M. K. (1996). Age-dependent diarrhea induced by a rotaviral nonstructural glycoprotein. *Science* **272**, 101-4.

Ballard, A., McCrae, M. A. and Desselberger, U. (1992). Nucleotide sequences of normal and rearranged RNA segments 10 of human rotaviruses. *J Gen Virol* **73 (Pt 3)**, 633-8.

Banerjee, A. K. and Shatkin, A. J. (1970). Transcription in vitro by reovirus-associated ribonucleic acid-dependent polymerase. *J Virol* **6**, 1-11.

Barro, M., Mandiola, P., Chen, D., Patton, J. T. and Spencer, E. (2001). Identification of sequences in rotavirus mRNAs important for minus strand synthesis using antisense oligonucleotides. *Virology* **288**, 71-80.

Barro, M. and Patton, J. T. (2005). Rotavirus nonstructural protein 1 subverts innate immune response by inducing degradation of IFN regulatory factor 3. *Proc Natl Acad Sci U S A* **102**, 4114-9.

Bass, D. M., Baylor, M., Chen, C. and Upadhyayula, U. (1995). Dansylcadaverine and cytochalasin D enhance rotavirus infection of murine L cells. *Virology* **212**, 429-37.

Bastardo, J. W. and Holmes, I. H. (1980). Attachment of SA-11 rotavirus to erythrocyte receptors. *Infect Immun* **29**, 1134-40.

Baybutt, H. N. and McCrae, M. A. (1984). The molecular biology of rotaviruses. VII. Detailed structural analysis of gene 10 of bovine rotavirus. *Virus Res* **1**, 533-41.

Belcourt, M. F. and Farabaugh, P. J. (1990). Ribosomal frameshifting in the yeast retrotransposon Ty: tRNAs induce slippage on a 7 nucleotide minimal site. *Cell* **62**, 339-52.

Bern, C. a. G., R. (1994). Impact of diarrheal diseases worldwide. In *Viral Infection of the Gastroentestinal Track.* New York: Marcel Dekker.

Berois, M., Sapin, C., Erk, I., Poncet, D. and Cohen, J. (2003). Rotavirus nonstructural protein NSP5 interacts with major core protein VP2. *J Virol* **77**, 1757-63.

Bican, P., Cohen, J., Charpilienne, A. and Scherrer, R. (1982). Purification and characterization of bovine rotavirus cores. *J Virol* **43**, 1113-7.

Bishop, R. F., Davidson, G. P., Holmes, I. H. and Ruck, B. J. (1973). Virus particles in epithelial cells of duodenal mucosa from children with acute non-bacterial gastroenteritis. *Lancet* **2**, 1281-3.

Blackhall, J., Fuentes, A., Hansen, K. and Magnusson, G. (1997). Serine protein kinase activity associated with rotavirus phosphoprotein NSP5. *J Virol* **71**, 138-44.

Blackhall, J., Munoz, M., Fuentes, A. and Magnusson, G. (1998). Analysis of rotavirus nonstructural protein NSP5 phosphorylation. *J Virol* **72**, 6398-405.

Both, G. W., Bellamy, A. R. and Siegman, L. J. (1984). Nucleotide sequence of the dsRNA genomic segment 7 of Simian 11 rotavirus. *Nucleic Acids Res* **12**, 1621-6.

Both, G. W., Mattick, J. S. and Bellamy, A. R. (1983a). Serotype-specific glycoprotein of simian 11 rotavirus: coding assignment and gene sequence. *Proc Natl Acad Sci U S A* **80**, 3091-5.

Both, G. W., Siegman, L. J., Bellamy, A. R. and Atkinson, P. H. (1983b). Coding assignment and nucleotide sequence of simian rotavirus SA11 gene segment 10: location of glycosylation sites suggests that the signal peptide is not cleaved. *J Virol* **48**, 335-9.

Boyle, J. F. and Holmes, K. V. (1986). RNA-binding proteins of bovine rotavirus. *J Virol* **58**, 561-8.

Bridger, J. C. (1994). Non-group A rotaviruses: Viral infections of the gastrointestinal tract. New York: Marcel Dekker.

Bridger, J. C., Clarke, I. N. and McCrae, M. A. (1982). Characterization of an antigenically distinct porcine rotavirus. *Infect Immun* **35**, 1058-62.

Bridger, J. C., Pedley, S. and McCrae, M. A. (1986). Group C rotaviruses in humans. *J Clin Microbiol* **23**, 760-3.

Brierley, I., Digard, P. and Inglis, S. C. (1989). Characterization of an efficient coronavirus ribosomal frameshifting signal: requirement for an RNA pseudoknot. *Cell* **57**, 537-47.

Brottier, P., Nandi, P., Bremont, M. and Cohen, J. (1992). Bovine rotavirus segment 5 protein expressed in the baculovirus system interacts with zinc and RNA. *J Gen Virol* **73 (Pt 8)**, 1931-8.

Bustamante, P. I. H., R. (1998). Plant virus gene expression strategies. *Electronic Journal of Biotechnology* **1**.

Campagna, M., Eichwald, C., Vascotto, F. and Burrone, O. R. (2005). RNA interference of rotavirus segment 11 mRNA reveals the essential role of NSP5 in the virus replicative cycle. *J Gen Virol* **86**, 1481-7.

Chakrabarti, A. and Maitra, U. (1991). Function of eukaryotic initiation factor 5 in the formation of an 80 S ribosomal polypeptide chain initiation complex. *J Biol Chem* **266**, 14039-45.

Chan, W. K., Au, K. S. and Estes, M. K. (1988). Topography of the simian rotavirus nonstructural glycoprotein (NS28) in the endoplasmic reticulum membrane. *Virology* **164**, 435-42.

Charpilienne, A., Abad, M. J., Michelangeli, F., Alvarado, F., Vasseur, M., Cohen, J. and Ruiz, M. C. (1997). Solubilized and cleaved VP7, the outer glycoprotein of rotavirus, induces permeabilization of cell membrane vesicles. *J Gen Virol* **78 (Pt 6)**, 1367-71.

Chemello, M. E., Aristimuno, O. C., Michelangeli, F. and Ruiz, M. C. (2002). Requirement for vacuolar H+ -ATPase activity and Ca2+ gradient during entry of rotavirus into MA104 cells. *J Virol* **76**, 13083-7.

Chen, C. M., Hung, T., Bridger, J. C. and McCrae, M. A. (1985). Chinese adult rotavirus is a group B rotavirus. *Lancet* **2**, 1123-4.

Chen, D., Barros, M., Spencer, E. and Patton, J. T. (2001). Features of the 3'-consensus sequence of rotavirus mRNAs critical to minus strand synthesis. *Virology* **282**, 221-9.

Chen, D., Gombold, J. L. and Ramig, R. F. (1990). Intracellular RNA synthesis directed by temperature-sensitive mutants of simian rotavirus SA11. *Virology* **178**, 143-51.

Chen, D. and Patton, J. T. (1998). Rotavirus RNA replication requires a single-stranded 3' end for efficient minus-strand synthesis. *J Virol* **72**, 7387-96.

Chen, D., Zeng, C. Q., Wentz, M. J., Gorziglia, M., Estes, M. K. and Ramig, R. F. (1994). Template-dependent, in vitro replication of rotavirus RNA. *J Virol* **68**, 7030-9.

Chizhikov, V. and Patton, J. T. (2000). A four-nucleotide translation enhancer in the 3'-terminal consensus sequence of the nonpolyadenylated mRNAs of rotavirus. *Rna* **6**, 814-25.

Chnaiderman, X, J., Diaz, J., Magnusson, G., Liprandi, F. and Spencer, E. (1998) Charaterization of a rotavirus rearranged gene 11 by gene reassortment. *Arch Virol* **143**, 1711-1722.

Chnaiderman, X, J., Barro, M. and Spencer, E. (2002). NSP5 phosphorylation regulates the fate of viral mRNA in rotavirus infected cells. *Arch Virol* **147**, 1899-911.

Chung, K. T. (2004). Interactions and Functions of rotavirus Non-Structural Proteins NSP1 and NSP3. In *Biological Sciences*: University of Warwick.

Ciarlet, M., Crawford, S. E., Cheng, E., Blutt, S. E., Rice, D. A., Bergelson, J. M. and Estes, M. K. (2002a). VLA-2 (alpha2beta1) integrin promotes rotavirus entry into cells but is not necessary for rotavirus attachment. *J Virol* **76**, 1109-23.

Ciarlet, M. and Estes, M. K. (1999). Human and most animal rotavirus strains do not require the presence of sialic acid on the cell surface for efficient infectivity. *J Gen Virol* **80 (Pt 4)**, 943-8.

Ciarlet, M., Ludert, J. E., Iturriza-Gomara, M., Liprandi, F., Gray, J. J., Desselberger, U. and Estes, M. K. (2002b). Initial interaction of rotavirus strains with N-acetylneuraminic (sialic) acid residues on the cell surface correlates with VP4 genotype, not species of origin. *J Virol* **76**, 4087-95.

Clark, S. M., Roth, J. R., Clark, M. L., Barnett, B. B. and Spendlove, R. S. (1981). Trypsin enhancement of rotavirus infectivity: mechanism of enhancement. *J Virol* **39**, 816-22.

Clarke, I. N. and McCrae, M. A. (1983). The molecular biology of rotaviruses. VI. RNA species-specific terminal conservation in rotaviruses. *J Gen Virol* **64 (Pt 9)**, 1877-84.

Cohen, J. (1977). Ribonucleic acid polymerase activity associated with purified calf rotavirus. *J Gen Virol* **36**, 395-402.

Cohen, J., Charpilienne, A., Chilmonczyk, S. and Estes, M. K. (1989). Nucleotide sequence of bovine rotavirus gene 1 and expression of the gene product in baculovirus. *Virology* **171**, 131-40.

Cohen, J., Laporte, J., Charpilienne, A. and Scherrer, R. (1979). Activation of rotavirus RNA polymerase by calcium chelation. *Arch Virol* **60**, 177-86.

Conner, M. E., Matson, D. O. and Estes, M. K. (1994). Rotavirus vaccines and vaccination potential. *Curr Top Microbiol Immunol* **185**, 285-337.

Control, C. f. D. (1999). Intussusception among recipients of rotavirus vaccine--United States, 1998-1999. *MMWR Morb Mortal Wkly Rep* **48**, 577-581.

Cook, J. P. and McCrae, M. A. (2004). Sequence analysis of the guanylyltransferase (VP3) of group A rotaviruses. *J Gen Virol* **85**, 929-32.

Crawford, S. E., Labbe, M., Cohen, J., Burroughs, M. H., Zhou, Y. J. and Estes, M. K. (1994). Characterization of virus-like particles produced by the expression of rotavirus capsid proteins in insect cells. *J Virol* **68**, 5945-52.

Crowley, D. S., Ryan, M. J. and Wall, P. G. (1997). Gastroenteritis in children under 5 years of age in England and Wales. *Commun Dis Rep CDR Rev* **7**, R82-6.

Cuadras, M. A., Arias, C. F. and Lopez, S. (1997). Rotaviruses induce an early membrane permeabilization of MA104 cells and do not require a low intracellular Ca2+ concentration to initiate their replication cycle. *J Virol* **71**, 9065-74.

Curran, J. and Kolakofsky, D. (1988). Scanning independent ribosomal initiation of the Sendai virus X protein. *Embo J* **7**, 2869-74.

Curran, J. and Kolakofsky, D. (1989). Scanning independent ribosomal initiation of the Sendai virus Y proteins in vitro and in vivo. *Embo J* **8**, 521-6.

Delorme, C., Brussow, H., Sidoti, J., Roche, N., Karlsson, K. A., Neeser, J. R. and Teneberg, S. (2001). Glycosphingolipid binding specificities of rotavirus: identification of a sialic acid-binding epitope. *J Virol* **75**, 2276-87.

Denisova, E., Dowling, W., LaMonica, R., Shaw, R., Scarlata, S., Ruggeri, F. and Mackow, E. R. (1999). Rotavirus capsid protein VP5* permeabilizes membranes. *J Virol* **73**, 3147-53.

Deo, R. C., Groft, C. M., Rajashankar, K. R. and Burley, S. K. (2002). Recognition of the rotavirus mRNA 3' consensus by an asymmetric NSP3 homodimer. *Cell* **108**, 71-81.

Desselberger, U. (1996). Genome rearrangements of rotaviruses. *Adv Virus Res* **46**, 69-95.

Desselberger, U. and McCrae, M. A. (1994). The rotavirus genome. *Curr Top Microbiol Immunol* **185**, 31-66.

Dinman, J. D., Icho, T. and Wickner, R. B. (1991). A -1 ribosomal frameshift in a double-stranded RNA virus of yeast forms a gag-pol fusion protein. *Proc Natl Acad Sci U S A* **88**, 174-8.

Dormitzer, P. R. and Greenberg, H. B. (1992). Calcium chelation induces a conformational change in recombinant herpes simplex virus-1-expressed rotavirus VP7. *Virology* **189**, 828-32.

Dormitzer, P. R., Nason, E. B., Prasad, B. V. and Harrison, S. C. (2004). Structural rearrangements in the membrane penetration protein of a non-enveloped virus. *Nature* **430**, 1053-8.

Dowling, W., Denisova, E., LaMonica, R. and Mackow, E. R. (2000). Selective membrane permeabilization by the rotavirus VP5* protein is abrogated by mutations in an internal hydrophobic domain. *J Virol* **74**, 6368-76.

Dunn, S. J., Cross, T. L. and Greenberg, H. B. (1994). Comparison of the rotavirus nonstructural protein NSP1 (NS53) from different species by sequence analysis and northern blot hybridization. *Virology* **203**, 178-83.

Dyall-Smith, M. L., Azad, A. A. and Holmes, I. H. (1983). Gene mapping of rotavirus double-stranded RNA segments by northern blot hybridization: application to segments 7, 8, and 9. *J Virol* **46**, 317-20.

Dyall-Smith, M. L. and Holmes, I. H. (1981). Gene-coding assignments of rotavirus double-stranded RNA segments 10 and 11. *J Virol* **38**, 1099-103.

Eichwald, C., Jacob, G., Muszynski, B., Allende, J. E. and Burrone, O. R. (2004a). Uncoupling substrate and activation functions of rotavirus NSP5: phosphorylation of Ser-67 by casein kinase 1 is essential for hyperphosphorylation. *Proc Natl Acad Sci U S A* **101**, 16304-9.

Eichwald, C., Rodriguez, J. F. and Burrone, O. R. (2004b). Characterization of rotavirus NSP2/NSP5 interactions and the dynamics of viroplasm formation. *J Gen Virol* **85**, 625-34.

Eichwald, C., Vascotto, F., Fabbretti, E. and Burrone, O. R. (2002). Rotavirus NSP5: mapping phosphorylation sites and kinase activation and viroplasm localization domains. *J Virol* **76**, 3461-70.

Ericson, B. L., Graham, D. Y., Mason, B. B. and Estes, M. K. (1982). Identification, synthesis, and modifications of simian rotavirus SA11 polypeptides in infected cells. *J Virol* **42**, 825-39.

Ericson, B. L., Graham, D. Y., Mason, B. B., Hanssen, H. H. and Estes, M. K. (1983a). Two types of glycoprotein precursors are produced by the simian rotavirus SA11. *Virology* **127**, 320-32.

Ericson, B. L., Petrie, B. L., Graham, D. Y., Mason, B. B. and Estes, M. K. (1983b). Rotaviruses code for two types of glycoprotein precursors. *J Cell Biochem* **22**, 151-60.

Esparza, J., Gorziglia, M., Gil, F. and Romer, H. (1980). Multiplication of human rotavirus in cultured cells: an electron microscopic study. *J Gen Virol* **47**, 461-72.

Estes, M. K. (2001). Rotaviruses and their replication. In *Field virology*, vol. 2 (eds B. N. Fields D. M. Knipe P. M. Howley and D. E. Griffin), pp. 1787-1833. Philadelphia;London: Lippincott Williams & Wilkins.

Estes, M. K. and Cohen, J. (1989). Rotavirus gene structure and function. *Microbiol Rev* **53**, 410-49.

Estes, M. K., Crawford, S. E., Penaranda, M. E., Petrie, B. L., Burns, J. W., Chan, W. K., Ericson, B., Smith, G. E. and Summers, M. D. (1987). Synthesis and immunogenicity of the rotavirus major capsid antigen using a baculovirus expression system. *J Virol* **61**, 1488-94.

Estes, M. K., Graham, D. Y. and Dimitrov, D. H. (1984). The molecular epidemiology of rotavirus gastroenteritis. *Prog Med Virol* **29**, 1-22.

Estes, M. K., Graham, D. Y., Smith, E. M. and Gerba, C. P. (1979). Rotavirus stability and inactivation. *J Gen Virol* **43**, 403-9.

Fabbretti, E., Afrikanova, I., Vascotto, F. and Burrone, O. R. (1999). Two non-structural rotavirus proteins, NSP2 and NSP5, form viroplasm-like structures in vivo. *J Gen Virol* **80 (Pt 2)**, 333-9.

Farabaugh, P. J. (1996). Programmed translational frameshifting. *Microbiol Rev* **60**, 103-34.

Fiore, L., Greenberg, H. B. and Mackow, E. R. (1991). The VP8 fragment of VP4 is the rhesus rotavirus hemagglutinin. *Virology* **181**, 553-63.

Flewett, T. H., Bryden, A. S., Davies, H., Woode, G. N., Bridger, J. C. and Derrick, J. M. (1974). Relation between viruses from acute gastroenteritis of children and newborn calves. *Lancet* **2**, 61-3.

Frangioni, J. V. and Neel, B. G. (1993). Solubilization and purification of enzymatically active glutathione S-transferase (pGEX) fusion proteins. *Anal Biochem* **210**, 179-87.

Fuentes-Panana, E. M., Lopez, S., Gorziglia, M. and Arias, C. F. (1995). Mapping the hemagglutination domain of rotaviruses. *J Virol* **69**, 2629-32.

Fukudome, K., Yoshie, O. and Konno, T. (1989). Comparison of human, simian, and bovine rotaviruses for requirement of sialic acid in hemagglutination and cell adsorption. *Virology* **172**, 196-205.

Fukuhara, N., Nishikawa, K., Gorziglia, M. and Kapikian, A. Z. (1989). Nucleotide sequence of gene segment 1 of a porcine rotavirus strain. *Virology* **173**, 743-9.

Fukuhara, N., Yoshie, O., Kitaoka, S. and Konno, T. (1988). Role of VP3 in human rotavirus internalization after target cell attachment via VP7. *J Virol* **62**, 2209-18.

Fukuhara, N., Yoshie, O., Kitaoka, S., Konno, T. and Ishida, N. (1987). Evidence for endocytosis-independent infection by human rotavirus. *Arch Virol* **97**, 93-9.

Futterer, J., Kiss-Laszlo, Z. and Hohn, T. (1993). Nonlinear ribosome migration on cauliflower mosaic virus 35S RNA. *Cell* **73**, 789-802.

Gajardo, R., Vende, P., Poncet, D. and Cohen, J. (1997). Two proline residues are essential in the calcium-binding activity of rotavirus VP7 outer capsid protein. *J Virol* **71**, 2211-6.

Gallegos, C. O. and Patton, J. T. (1989). Characterization of rotavirus replication intermediates: a model for the assembly of single-shelled particles. *Virology* **172**, 616-27.

Glass, R. I., Bresee, J. S., Parashar, U., Miller, M. and Gentsch, J. R. (1997). Rotavirus vaccines at the threshold. *Nat Med* **3**, 1324-5.

Glass, R. I., Bresee, J. S., Parashar, U., Turcios, R., Fischer, T., Jiang, B., Widdowson, M. A. and Gentsch, J. (2005). Rotavirus vaccines: past, present, and future. *Arch Pediatr* **12**, 844-7.

Glass, R. I., Lang, D. R., Ivanhoff, B. N. and Compans, R. W. (1996). Introduction: Rotavirus - from basic research to a vaccine. *J. Infect. Dis.* **174**, S1-S2.

Gombold, J. L., Estes, M. K. and Ramig, R. F. (1985). Assignment of simian rotavirus SA11 temperature-sensitive mutant groups B and E to genome segments. *Virology* **143**, 309-20.

Gonzalez, R. A., Espinosa, R., Romero, P., Lopez, S. and Arias, C. F. (2000). Relative localization of viroplasmic and endoplasmic reticulum-resident rotavirus proteins in infected cells. *Arch Virol* **145**, 1963-73.

Gonzalez, R. A., Torres-Vega, M. A., Lopez, S. and Arias, C. F. (1998). In vivo interactions among rotavirus nonstructural proteins. *Arch Virol* **143**, 981-96.

Gonzalez, S. A. and Burrone, O. R. (1989). Porcine OSU rotavirus segment II sequence shows common features with the viral gene of human origin. *Nucleic Acids Res* **17**, 6402.

Gonzalez, S. A. and Burrone, O. R. (1991). Rotavirus NS26 is modified by addition of single O-linked residues of N-acetylglucosamine. *Virology* **182**, 8-16.

Gorziglia, M., Larrea, C., Liprandi, F. and Esparza, J. (1985). Biochemical evidence for the oligomeric (possibly trimeric) structure of the major inner capsid polypeptide (45K) of rotaviruses. *J Gen Virol* **66 (Pt 9)**, 1889-900.

Gorziglia, M., Nishikawa, K. and Fukuhara, N. (1989). Evidence of duplication and deletion in super short segment 11 of rabbit rotavirus Alabama strain. *Virology* **170**, 587-90.

Gouet, P., Diprose, J. M., Grimes, J. M., Malby, R., Burroughs, J. N., Zientara, S., Stuart, D. I. and Mertens, P. P. (1999). The highly ordered double-stranded RNA genome of bluetongue virus revealed by crystallography. *Cell* **97**, 481-90.

Graff, J. W., Mitzel, D. N., Weisend, C. M., Flenniken, M. L. and Hardy, M. E. (2002). Interferon regulatory factor 3 is a cellular partner of rotavirus NSP1. *J Virol* **76**, 9545-50.

Graham, K. L., Halasz, P., Tan, Y., Hewish, M. J., Takada, Y., Mackow, E. R., Robinson, M. K. and Coulson, B. S. (2003). Integrin-using rotaviruses bind alpha2beta1 integrin alpha2 I domain via VP4 DGE sequence and recognize alphaXbeta2 and alphaVbeta3 by using VP7 during cell entry. *J Virol* **77**, 9969-78.

Green, K. Y., Midthun, K., Gorziglia, M., Hoshino, Y., Kapikian, A. Z., Chanock, R. M. and Flores, J. (1987). Comparison of the amino acid sequences of the major neutralization protein of four human rotavirus serotypes. *Virology* **161**, 153-9.

Greenberg, H., McAuliffe, V., Valdesuso, J., Wyatt, R., Flores, J., Kalica, A., Hoshino, Y. and Singh, N. (1983). Serological analysis of the subgroup protein of rotavirus, using monoclonal antibodies. *Infect Immun* **39**, 91-9.

Grimes, J. M., Burroughs, J. N., Gouet, P., Diprose, J. M., Malby, R., Zientara, S., Mertens, P. P. and Stuart, D. I. (1998). The atomic structure of the bluetongue virus core. *Nature* **395**, 470-8.

Groft, C. M. and Burley, S. K. (2002). Recognition of eIF4G by rotavirus NSP3 reveals a basis for mRNA circularization. *Mol Cell* **9**, 1273-83.

Guerrero, C. A., Zarate, S., Corkidi, G., Lopez, S. and Arias, C. F. (2000). Biochemical characterization of rotavirus receptors in MA104 cells. *J Virol* **74**, 9362-71.

Guo, C. T., Nakagomi, O., Mochizuki, M., Ishida, H., Kiso, M., Ohta, Y., Suzuki, T., Miyamoto, D., Hidari, K. I. and Suzuki, Y. (1999). Ganglioside GM(1a) on the cell surface is involved in the infection by human rotavirus KUN and MO strains. *J Biochem (Tokyo)* **126**, 683-8.

Gutierrez, M. F., Riano, M., Matiz, A., Corredor, C., Humphrey, C., Wang, Y., Glass, R.I. and Jiang, B. (2003). Group C rotavirus as a major cause of diarrhea amoung children in Colombia. In *8th International Symposium on dsRNA Viruses.* Lucca, Italy.

Guzman, E. and McCrae, M. A. (2005). Molecular characterization of the rotavirus NSP4 enterotoxin homologue from group B rotavirus. *Virus Res* **110**, 151-60.

Hatfield, D., Feng, Y. X., Lee, B. J., Rein, A., Levin, J. G. and Oroszlan, S. (1989). Chromatographic analysis of the aminoacyl-tRNAs which are required for translation of codons at and around the ribosomal frameshift sites of HIV, HTLV-1, and BLV. *Virology* **173**, 736-42.

Hill, C. L., Booth, T. F., Prasad, B. V., Grimes, J. M., Mertens, P. P., Sutton, G. C. and Stuart, D. I. (1999). The structure of a cypovirus and the functional organization of dsRNA viruses. *Nat Struct Biol* **6**, 565-8.

Holmes, I. H. (1996). Development of rotavirus molecular epidemiology: electropherotyping. *Arch Virol Suppl* **12**, 87-91.

Hoshino, Y., Gorziglia, M., Valdesuso, J., Askaa, J., Glass, R. I. and Kapikian, A. Z. (1987). An equine rotavirus (FI-14 strain) which bears both subgroup I and subgroup II specificities on its VP6. *Virology* **157**, 488-96.

Hoshino, Y. and Kapikian, A. Z. (1996). Classification of rotavirus VP4 and VP7 serotypes. *Arch Virol Suppl* **12**, 99-111.

Hua, J., Chen, X. and Patton, J. T. (1994). Deletion mapping of the rotavirus metalloprotein NS53 (NSP1): the conserved cysteine-rich region is essential for virus-specific RNA binding. *J Virol* **68**, 3990-4000.

Hua, J. and Patton, J. T. (1994). The carboxyl-half of the rotavirus nonstructural protein NS53 (NSP1) is not required for virus replication. *Virology* **198**, 567-76.

Huilan, S., Zhen, L. G., Mathan, M. M., Mathew, M. M., Olarte, J., Espejo, R., Khin Maung, U., Ghafoor, M. A., Khan, M. A., Sami, Z. et al. (1991). Etiology of acute diarrhoea among children in developing countries: a multicentre study in five countries. *Bull World Health Organ* **69**, 549-55.

Hung, T., Chen, G. M., Wang, C. G., Chou, Z. Y., Chao, T. X., Ye, W. W., Yao, H. L. and Meng, K. H. (1983). Rotavirus-like agent in adult non-bacterial diarrhoea in China. *Lancet* **2**, 1078-9.

Hung, T., Chen, G. M., Wang, C. G., Fan, R. L., Yong, R. J., Chang, J. Q., Dan, R. and Ng, M. H. (1987). Seroepidemiology and molecular epidemiology of the Chinese rotavirus. *Ciba Found Symp* **128**, 49-62.

Imai, M., Akatani, K., Ikegami, N. and Furuichi, Y. (1983). Capped and conserved terminal structures in human rotavirus genome double-stranded RNA segments. *J Virol* **47**, 125-36.

Imataka, H., Gradi, A. and Sonenberg, N. (1998). A newly identified N-terminal amino acid sequence of human eIF4G binds poly(A)-binding protein and functions in poly(A)-dependent translation. *Embo J* **17**, 7480-9.

Invitrogen. (2004). TA cloning® kit user manual. Version V.

Isa, P., Realpe, M., Romero, P., Lopez, S. and Arias, C. F. (2004). Rotavirus RRV associates with lipid membrane microdomains during cell entry. *Virology* **322**, 370-81.

Jacks, T., Power, M. D., Masiarz, F. R., Luciw, P. A., Barr, P. J. and Varmus, H. E. (1988). Characterization of ribosomal frameshifting in HIV-1 gag-pol expression. *Nature* **331**, 280-3.

Jang, S. K., Pestova, T. V., Hellen, C. U., Witherell, G. W. and Wimmer, E. (1990). Cap-independent translation of picornavirus RNAs: structure and function of the internal ribosomal entry site. *Enzyme* **44**, 292-309.

Jayaram, H., Estes, M. K. and Prasad, B. V. (2004). Emerging themes in rotavirus cell entry, genome organization, transcription and replication. *Virus Res* **101**, 67-81.

Jayaram, H., Taraporewala, Z., Patton, J. T. and Prasad, B. V. (2002). Rotavirus protein involved in genome replication and packaging exhibits a HIT-like fold. *Nature* **417**, 311-5.

Johnson, M. A. and McCrae, M. A. (1989). Molecular biology of rotaviruses. VIII. Quantitative analysis of regulation of gene expression during virus replication. *J Virol* **63**, 2048-55.

Jourdan, N., Brunet, J. P., Sapin, C., Blais, A., Cotte-Laffitte, J., Forestier, F., Quero, A. M., Trugnan, G. and Servin, A. L. (1998). Rotavirus infection reduces sucrase-isomaltase expression in human intestinal epithelial cells by perturbing protein targeting and organization of microvillar cytoskeleton. *J Virol* **72**, 7228-36.

Jourdan, N., Maurice, M., Delautier, D., Quero, A. M., Servin, A. L. and Trugnan, G. (1997). Rotavirus is released from the apical surface of cultured human intestinal cells through nonconventional vesicular transport that bypasses the Golgi apparatus. *J Virol* **71**, 8268-78.

Kabcenell, A. K. and Atkinson, P. H. (1985). Processing of the rough endoplasmic reticulum membrane glycoproteins of rotavirus SA11. *J Cell Biol* **101**, 1270-80.

Kabcenell, A. K., Poruchynsky, M. S., Bellamy, A. R., Greenberg, H. B. and Atkinson, P. H. (1988). Two forms of VP7 are involved in assembly of SA11 rotavirus in endoplasmic reticulum. *J Virol* **62**, 2929-41.

Kalica, A. R., Flores, J. and Greenberg, H. B. (1983). Identification of the rotaviral gene that codes for hemagglutination and protease-enhanced plaque formation. *Virology* **125**, 194-205.

Kaljot, K. T., Shaw, R. D., Rubin, D. H. and Greenberg, H. B. (1988). Infectious rotavirus enters cells by direct cell membrane penetration, not by endocytosis. *J Virol* **62**, 1136-44.

Kapikian, A. Z. (1994). Jennerian and modified jennerian approach to vaccination against rotavirus diarrea in infants and young children: Viral infections of the gastrointestinal tract. New York: Marcel Dekker.

Kapikian, A. Z., Y. Hoshino, and R. M. Chanock. (2001). Rotaviruses. In *Field virology*, vol. 2 (eds B. N. Fields D. M. Knipe P. M. Howley and D. E. Griffin), pp. 1787-1833. Philadelphia;London: Lippincott Williams & Wilkins.

Kattoura, M. D., Chen, X. and Patton, J. T. (1994). The rotavirus RNA-binding protein NS35 (NSP2) forms 10S multimers and interacts with the viral RNA polymerase. *Virology* **202**, 803-13.

Kattoura, M. D., Clapp, L. L. and Patton, J. T. (1992). The rotavirus nonstructural protein, NS35, possesses RNA-binding activity in vitro and in vivo. *Virology* **191**, 698-708.

Kearney, K., Chen, D., Taraporewala, Z. F., Vende, P., Hoshino, Y., Tortorici, M. A., Barro, M. and Patton, J. T. (2004). Cell-line-induced mutation of the rotavirus genome alters expression of an IRF3-interacting protein. *Embo J* **23**, 4072-81.

Keljo, D. J., Kuhn, M. and Smith, A. (1988). Acidification of endosomes is not important for the entry of rotavirus into the cell. *J Pediatr Gastroenterol Nutr* **7**, 257-63.

Kingston, B. and Brent, R. (2002) Chapter 16 Protein Expression. *Current Protocols in Molecular Biology*. John Wiley and Sons, New York.

Kojima, K., Taniguchi, K. and Kobayashi, N. (1996a). Species-specific and interspecies relatedness of NSP1 sequences in human, porcine, bovine, feline, and equine rotavirus strains. *Arch Virol* **141**, 1-12.

Kojima, K., Taniguchi, K., Urasawa, T. and Urasawa, S. (1996b). Sequence analysis of normal and rearranged NSP5 genes from human rotavirus strains isolated in nature: implications for the occurrence of the rearrangement at the step of plus strand synthesis. *Virology* **224**, 446-52.

Kolupaeva, V. G., Hellen, C. U. and Shatsky, I. N. (1996). Structural analysis of the interaction of the pyrimidine tract-binding protein with the internal ribosomal entry site of encephalomyocarditis virus and foot-and-mouth disease virus RNAs. *Rna* **2**, 1199-212.

Kouvelos, K., Petric, M. and Middleton, P. J. (1984a). Comparison of bovine, simian and human rotavirus structural glycoproteins. *J Gen Virol* **65 (Pt 7)**, 1211-4.

Kouvelos, K., Petric, M. and Middleton, P. J. (1984b). Oligosaccharide composition of calf rotavirus. *J Gen Virol* **65 (Pt 7)**, 1159-64.

Kozak, M. (1980). Evaluation of the "scanning model" for initiation of protein synthesis in eucaryotes. *Cell* **22**, 7-8.

Kozak, M. (1986). Point mutations define a sequence flanking the AUG initiator codon that modulates translation by eukaryotic ribosomes. *Cell* **44**, 283-92.

Kozak, M. (1987). An analysis of 5'-noncoding sequences from 699 vertebrate messenger RNAs. *Nucleic Acids Res* **15**, 8125-48.

Kozak, M. (1989). The scanning model for translation: an update. *J Cell Biol* **108**, 229-41.

Kozak, M. (2002). Pushing the limits of the scanning mechanism for initiation of translation. *Gene* **299**, 1-34.

Krishnan, T., Sen, A., Choudhury, J. S., Das, S., Naik, T. N. and Bhattacharya, S. K. (1999). Emergence of adult diarrhoea rotavirus in Calcutta, India. *Lancet* **353**, 380-1.

Kumar, A., Charpilienne, A. and Cohen, J. (1989). Nucleotide sequence of the gene encoding for the RNA binding protein (VP2) of RF bovine rotavirus. *Nucleic Acids Res* **17**, 2126.

Labbe, M., Baudoux, P., Charpilienne, A., Poncet, D. and Cohen, J. (1994). Identification of the nucleic acid binding domain of the rotavirus VP2 protein. *J Gen Virol* **75 (Pt 12)**, 3423-30.

Laemmli, U. K. (1970). Cleavage of structural proteins during the assembly of the head of bacteriophage T4. *Nature* **227**, 680-5.

LaMonica, R., Kocer, S. S., Nazarova, J., Dowling, W., Geimonen, E., Shaw, R. D. and Mackow, E. R. (2001). VP4 differentially regulates TRAF2 signaling, disengaging JNK activation while directing NF-kappa B to effect rotavirus-specific cellular responses. *J Biol Chem* **276**, 19889-96.

Latorre, P., Kolakofsky, D. and Curran, J. (1998). Sendai virus Y proteins are initiated by a ribosomal shunt. *Mol Cell Biol* **18**, 5021-31.

Lawton, J. A., Estes, M. K. and Prasad, B. V. (1997). Three-dimensional visualization of mRNA release from actively transcribing rotavirus particles. *Nat Struct Biol* **4**, 118-21.

Liu, M., Mattion, N. M. and Estes, M. K. (1992). Rotavirus VP3 expressed in insect cells possesses guanylyltransferase activity. *Virology* **188**, 77-84.

Londrigan, S. L., Graham, K. L., Takada, Y., Halasz, P. and Coulson, B. S. (2003). Monkey rotavirus binding to alpha2beta1 integrin requires the alpha2 I domain and is facilitated by the homologous beta1 subunit. *J Virol* **77**, 9486-501.

Lopez de Quinto, S., Lafuente, E. and Martinez-Salas, E. (2001). IRES interaction with translation initiation factors: functional characterization of novel RNA contacts with eIF3, eIF4B, and eIF4GII. *Rna* **7**, 1213-26.

Lopez de Quinto, S. and Martinez-Salas, E. (2000). Interaction of the eIF4G initiation factor with the aphthovirus IRES is essential for internal translation initiation in vivo. *Rna* **6**, 1380-92.

Lopez, S. and Arias, C. F. (2004). Multistep entry of rotavirus into cells: a Versaillesque dance. *Trends Microbiol* **12**, 271-8.

Lopez, S., Espinosa, R., Greenberg, H. B. and Arias, C. F. (1994). Mapping the subgroup epitopes of rotavirus protein VP6. *Virology* **204**, 153-62.

Lopez, S., Lopez, I., Romero, P., Mendez, E., Soberon, X. and Arias, C. F. (1991). Rotavirus YM gene 4: analysis of its deduced amino acid sequence and prediction of the secondary structure of the VP4 protein. *J Virol* **65**, 3738-45.

Lopez, T., Camacho, M., Zayas, M., Najera, R., Sanchez, R., Arias, C. F. and Lopez, S. (2005a). Silencing the morphogenesis of rotavirus. *J Virol* **79**, 184-92.

Lopez, T., Rojas, M., Ayala-Breton, C., Lopez, S. and Arias, C. F. (2005b). Reduced expression of the rotavirus NSP5 gene has a pleiotropic effect on virus replication. *J Gen Virol* **86**, 1609-17.

Lowry, O. H., Rosebrough, N. J., Farr, A. L. and Randall, R. J. (1951). Protein measurement with the Folin phenol reagent. *J Biol Chem* **193**, 265-75.

Ludert, J. E., Michelangeli, F., Gil, F., Liprandi, F. and Esparza, J. (1987). Penetration and uncoating of rotaviruses in cultured cells. *Intervirology* **27**, 95-101.

Lundgren, O., Peregrin, A. T., Persson, K., Kordasti, S., Uhnoo, I. and Svensson, L. (2000). Role of the enteric nervous system in the fluid and electrolyte secretion of rotavirus diarrhea. *Science* **287**, 491-5.

Luongo, C. L., Reinisch, K. M., Harrison, S. C. and Nibert, M. L. (2000). Identification of the guanylyltransferase region and active site in reovirus mRNA capping protein lambda2. *J Biol Chem* **275**, 2804-10.

Luz, N. and Beck, E. (1991). Interaction of a cellular 57-kilodalton protein with the internal translation initiation site of foot-and-mouth disease virus. *J Virol* **65**, 6486-94.

Maass, D. R. and Atkinson, P. H. (1990). Rotavirus proteins VP7, NS28, and VP4 form oligomeric structures. *J Virol* **64**, 2632-41.

Mackow, E. M. (2002). Human group B and C rotaviruses. In: M.J. Blaser, Editor, *Infections of the Gastrointestinal Tract* (second ed.): Lippincott Williams and Wilkins, Philadelphia.

Maitra, U., Stringer, E. A. and Chaudhuri, A. (1982). Initiation factors in protein biosynthesis. *Annu Rev Biochem* **51**, 869-900.

Mansell, E. A., Ramig, R. F. and Patton, J. T. (1994). Temperature-sensitive lesions in the capsid proteins of the rotavirus mutants tsF and tsG that affect virion assembly. *Virology* **204**, 69-81.

Martinez-Salas, E., Lopez de Quinto, S., Ramos, R. and Fernandez-Miragall, O. (2002). IRES elements: features of the RNA structure contributing to their activity. *Biochimie* **84**, 755-63.

Mattsui, S. M., Mackow, E. R., Matsuno, S., Paul, P. S. and Greenburg, H. B. (1990) Sequence analysis of gene 11 equivalents from "short" and "super-short" strains of rotavirus. *J. Virol* **64**, 120-124.

Mattion, N. M., Cohen, J., Aponte, C. and Estes, M. K. (1992). Characterization of an oligomerization domain and RNA-binding properties on rotavirus nonstructural protein NS34. *Virology* **190**, 68-83.

Mattion, N. M., Cohen, J., Estes, M. (1994). The rotavirus proteins: Viral infections of the gastrointestinal tract. New York: Marcel Dekker.

Mattion, N. M., Mitchell, D. B., Both, G. W. and Estes, M. K. (1991). Expression of rotavirus proteins encoded by alternative open reading frames of genome segment 11. *Virology* **181**, 295-304.

Mayo, M. A. (2005). Changes to virus taxonomy 2004. *Archives to virology* **150**, 180-198.

McCormack, S. J., Thomis, D. C. and Samuel, C. E. (1992). Mechanism of interferon action: identification of a RNA binding domain within the N-terminal region of the human RNA-dependent P1/eIF-2 alpha protein kinase. *Virology* **188**, 47-56.

McCrae, M. A. and Faulkner-Valle, G. P. (1981). Molecular biology of rotaviruses. I. Characterization of basic growth parameters and pattern of macromolecular synthesis. *J Virol* **39**, 490-6.

McCrae, M. A. and McCorquodale, J. G. (1982). The molecular biology of rotaviruses. II. Identification of the protein-coding assignments of calf rotavirus genome RNA species. *Virology* **117**, 435-43.

McCrae, M. A. and McCorquodale, J. G. (1983). Molecular biology of rotaviruses. V. Terminal structure of viral RNA species. *Virology* **126**, 204-12.

McNulty, M. S., Curran, W. L. and McFerran, J. B. (1976). The morphogenesis of a cytopathic bovine rotavirus in Madin-Darby bovine kidney cells. *J Gen Virol* **33**, 503-8.

Mendez, E., Lopez, S., Cuadras, M. A., Romero, P. and Arias, C. F. (1999). Entry of rotaviruses is a multistep process. *Virology* **263**, 450-9.

Mertens, P. (2004). The dsRNA viruses. *Virus Res* **101**, 3-13.

Michelangeli, F., Ruiz, M. C., del Castillo, J. R., Ludert, J. E. and Liprandi, F. (1991). Effect of rotavirus infection on intracellular calcium homeostasis in cultured cells. *Virology* **181**, 520-7.

Mitchell, D. B. and Both, G. W. (1990). Completion of the genomic sequence of the simian rotavirus SA11: nucleotide sequences of segments 1, 2, and 3. *Virology* **177**, 324-31.

Mitzel, D. N., Weisend, C. M., White, M. W. and Hardy, M. E. (2003). Translational regulation of rotavirus gene expression. *J Gen Virol* **84**, 383-91.

Mohan, K. V., Muller, J., Som, I. and Atreya, C. D. (2003). The N- and C-terminal regions of rotavirus NSP5 are the critical determinants for the formation of viroplasm-like structures independent of NSP2. *J Virol* **77**, 12184-92.

Moon, H. (1994). Pathophysiology of viral diarrhea: Viral infections of the gastrointestinal tract. New York: Marcel Dekker.

Mossel, E. C. and Ramig, R. F. (2003). A lymphatic mechanism of rotavirus extraintestinal spread in the neonatal mouse. *J Virol* **77**, 12352-6.

Musalem, C. and Espejo, R. T. (1985). Release of progeny virus from cells infected with simian rotavirus SA11. *J Gen Virol* **66 (Pt 12)**, 2715-24.

Nabi, I. R. and Le, P. U. (2003). Caveolae/raft-dependent endocytosis. *J Cell Biol* **161**, 673-7.

Narang, H. K. and Codd, A. A. (1983). Action of commonly used disinfectants against enteroviruses. *J Hosp Infect* **4**, 209-12.

Nibert, M. N. and Schiff, L. A. (2001). Reoviruses and their replication. In *Field virology*, vol. 2 (eds B. N. Fields D. M. Knipe P. M. Howley and D. E. Griffin), pp. 1679-1728. Philadelphia;London: Lippincott Williams & Wilkins.

Nonoyama, M., Millward, S. and Graham, A. F. (1974). Control of transcription of the reovirus genome. *Nucleic Acids Res* **1**, 373-85.

Novagen. (2003). pET System Manual. 10th Edition.

Novagen. (2004). Factor Xa kits. User Protocol TB205. Rev.B 1004

Offit, P. A. (1994). Virus-specific cellular immune response to intestinal infection: Viral infections of the gastrointestinal tract. New York: Marcel Dekker.

Offit, P. A. and Blavat, G. (1986). Identification of the two rotavirus genes determining neutralization specificities. *J Virol* **57**, 376-8.

Okada, J., Kobayashi, N., Taniguchi, K. and Urasawa, S. (1999). Analysis on reassortment of rotavirus NSP1 genes lacking coding region for cysteine-rich zinc finger motif. *Arch Virol* **144**, 345-53.

Padilla-Noriega, L., Paniagua, O. and Guzman-Leon, S. (2002). Rotavirus protein NSP3 shuts off host cell protein synthesis. *Virology* **298**, 1-7.

Parashar, U. D., Bresee, J. S., Gentsch, J. R. and Glass, R. I. (1998). Rotavirus. *Emerg Infect Dis* **4**, 561-70.

Parashar, U. D., Hummelman, E. G., Bresee, J. S., Miller, M. A. and Glass, R. I. (2003). Global illness and deaths caused by rotavirus disease in children. *Emerg Infect Dis* **9**, 565-72.

Parez, N., Garbarg-Chenon, A., Fourgeux, C., Le Deist, F., Servant-Delmas, A., Charpilienne, A., Cohen, J. and Schwartz-Cornil, I. (2004). The VP6 protein of rotavirus interacts with a large fraction of human naive B cells via surface immunoglobulins. *J Virol* **78**, 12489-96.

Patton, J. T. (1990). Evidence for equimolar synthesis of double-strand RNA and minus-strand RNA in rotavirus-infected cells. *Virus Res* **17**, 199-208.

Patton, J. T. (1995). Structure and function of the rotavirus RNA-binding proteins. *J Gen Virol* **76 (Pt 11)**, 2633-44.

Patton, J. T. (1996). Rotavirus VP1 alone specifically binds to the 3' end of viral mRNA, but the interaction is not sufficient to initiate minus-strand synthesis. *J Virol* **70**, 7940-7.

Patton, J. T. and Chen, D. (1999). RNA-binding and capping activities of proteins in rotavirus open cores. *J Virol* **73**, 1382-91.

Patton, J. T. and Gallegos, C. O. (1990). Rotavirus RNA replication: single-stranded RNA extends from the replicase particle. *J Gen Virol* **71 (Pt 5)**, 1087-94.

Patton, J. T., Jones, M. T., Kalbach, A. N., He, Y. W. and Xiaobo, J. (1997). Rotavirus RNA polymerase requires the core shell protein to synthesize the double-stranded RNA genome. *J Virol* **71**, 9618-26.

Patton, J. T., Salter-Cid, L., Kalbach, A., Mansell, E. A. and Kattoura, M. (1993). Nucleotide and amino acid sequence analysis of the rotavirus nonstructural RNA-binding protein NS35. *Virology* **192**, 438-46.

Patton, J. T. and Spencer, E. (2000). Genome replication and packaging of segmented double-stranded RNA viruses. *Virology* **277**, 217-25.

Patton, J. T., Wentz, M., Xiaobo, J. and Ramig, R. F. (1996). cis-Acting signals that promote genome replication in rotavirus mRNA. *J Virol* **70**, 3961-71.

Pedley, S., Bridger, J. C., Brown, J. F. and McCrae, M. A. (1983). Molecular characterization of rotaviruses with distinct group antigens. *J Gen Virol* **64 (Pt 10)**, 2093-101.

Pedley, S., Hundley, F., Chrystie, I., McCrae, M. A. and Desselberger, U. (1984). The genomes of rotaviruses isolated from chronically infected immunodeficient children. *J Gen Virol* **65 (Pt 7)**, 1141-50.

Pelletier, J. and Sonenberg, N. (1988). Internal initiation of translation of eukaryotic mRNA directed by a sequence derived from poliovirus RNA. *Nature* **334**, 320-5.

Perez, J. F., Ruiz, M. C., Chemello, M. E. and Michelangeli, F. (1999). Characterization of a membrane calcium pathway induced by rotavirus infection in cultured cells. *J Virol* **73**, 2481-90.

Peric, M., Mayus, K., Vonderfecht, S. and Eiden, J.J. (1991). Comparison f group B rotavirus genes 9 and 11. J Gen Virol **72**, 2801-4.

Pesavento, J. B., Crawford, S. E., Roberts, E., Estes, M. K. and Prasad, B. V. (2005). pH-induced conformational change of the rotavirus VP4 spike: implications for cell entry and antibody neutralization. *J Virol* **79**, 8572-80.

Pestova, T. V. and Hellen, C. U. (1999). Ribosome recruitment and scanning: what's new? *Trends Biochem Sci* **24**, 85-7.

Petrie, B. L., Graham, D. Y. and Estes, M. K. (1981). Identification of rotavirus particle types. *Intervirology* **16**, 20-8.

Petrie, B. L., Graham, D. Y., Hanssen, H. and Estes, M. K. (1982). Localization of rotavirus antigens in infected cells by ultrastructural immunocytochemistry. *J Gen Virol* **63**, 457-67.

Petrie, B. L., Greenberg, H. B., Graham, D. Y. and Estes, M. K. (1984). Ultrastructural localization of rotavirus antigens using colloidal gold. *Virus Res* **1**, 133-52.

Piron, M., Delaunay, T., Grosclaude, J. and Poncet, D. (1999). Identification of the RNA-binding, dimerization, and eIF4GI-binding domains of rotavirus nonstructural protein NSP3. *J Virol* **73**, 5411-21.

Piron, M., Vende, P., Cohen, J. and Poncet, D. (1998). Rotavirus RNA-binding protein NSP3 interacts with eIF4GI and evicts the poly(A) binding protein from eIF4F. *Embo J* **17**, 5811-21.

Pizarro, J. L., Sandino, A. M., Pizarro, J. M., Fernandez, J. and Spencer, E. (1991). Characterization of rotavirus guanylyltransferase activity associated with polypeptide VP3. *J Gen Virol* **72 (Pt 2)**, 325-32.

Poncet, D., Aponte, C. and Cohen, J. (1993). Rotavirus protein NSP3 (NS34) is bound to the 3' end consensus sequence of viral mRNAs in infected cells. *J Virol* **67**, 3159-65.

Poncet, D., Laurent, S. and Cohen, J. (1994). Four nucleotides are the minimal requirement for RNA recognition by rotavirus non-structural protein NSP3. *Embo J* **13**, 4165-73.

Poncet, D., Lindenbaum, P., L'Haridon, R. and Cohen, J. (1997). In vivo and in vitro phosphorylation of rotavirus NSP5 correlates with its localization in viroplasms. *J Virol* **71**, 34-41.

Poruchynsky, M. S. and Atkinson, P. H. (1988). Primary sequence domains required for the retention of rotavirus VP7 in the endoplasmic reticulum. *J Cell Biol* **107**, 1697-706.

Poruchynsky, M. S. and Atkinson, P. H. (1991). Rotavirus protein rearrangements in purified membrane-enveloped intermediate particles. *J Virol* **65**, 4720-7.

Poruchynsky, M. S., Maass, D. R. and Atkinson, P. H. (1991). Calcium depletion blocks the maturation of rotavirus by altering the oligomerization of virus-encoded proteins in the ER. *J Cell Biol* **114**, 651-6.

Poruchynsky, M. S., Tyndall, C., Both, G. W., Sato, F., Bellamy, A. R. and Atkinson, P. H. (1985). Deletions into an NH2-terminal hydrophobic domain result in secretion of rotavirus VP7, a resident endoplasmic reticulum membrane glycoprotein. *J Cell Biol* **101**, 2199-209.

Prasad, B. V., Burns, J. W., Marietta, E., Estes, M. K. and Chiu, W. (1990). Localization of VP4 neutralization sites in rotavirus by three-dimensional cryo-electron microscopy. *Nature* **343**, 476-9.

Prasad, B. V., Rothnagel, R., Zeng, C. Q., Jakana, J., Lawton, J. A., Chiu, W. and Estes, M. K. (1996). Visualization of ordered genomic RNA and localization of transcriptional complexes in rotavirus. *Nature* **382**, 471-3.

Prasad, B. V., Wang, G. J., Clerx, J. P. and Chiu, W. (1988). Three-dimensional structure of rotavirus. *J Mol Biol* **199**, 269-75.

Prasad, B. V. C., W. (1994). Rotaviruses: Structure of rotaviruses. Berlin; London: Springer.

Preiss, T. and Hentze, M. W. (1999). From factors to mechanisms: translation and translational control in eukaryotes. *Curr Opin Genet Dev* **9**, 515-21.

Quan, C. M. and Doane, F. W. (1983). Ultrastructural evidence for the cellular uptake of rotavirus by endocytosis. *Intervirology* **20**, 223-31.

Ramadevi, N., Burroughs, N. J., Mertens, P. P., Jones, I. M. and Roy, P. (1998). Capping and methylation of mRNA by purified recombinant VP4 protein of bluetongue virus. *Proc Natl Acad Sci U S A* **95**, 13537-42.

Ramig, R. F. and Petrie, B. L. (1984). Characterization of temperature-sensitive mutants of simian rotavirus SA11: protein synthesis and morphogenesis. *J Virol* **49**, 665-73.

Reinisch, K. M., Nibert, M. L. and Harrison, S. C. (2000). Structure of the reovirus core at 3.6 A resolution. *Nature* **404**, 960-7.

Richardson, S. C., Mercer, L. E., Sonza, S. and Holmes, I. H. (1986). Intracellular localization of rotaviral proteins. *Arch Virol* **88**, 251-64.

Rolsma, M. D., Kuhlenschmidt, T. B., Gelberg, H. B. and Kuhlenschmidt, M. S. (1998). Structure and function of a ganglioside receptor for porcine rotavirus. *J Virol* **72**, 9079-91.

Ruggeri, F. M. and Greenberg, H. B. (1991). Antibodies to the trypsin cleavage peptide VP8 neutralize rotavirus by inhibiting binding of virions to target cells in culture. *J Virol* **65**, 2211-9.

Ruiz, M. C., Charpilienne, A., Liprandi, F., Gajardo, R., Michelangeli, F. and Cohen, J. (1996). The concentration of Ca2+ that solubilizes outer capsid proteins from rotavirus particles is dependent on the strain. *J Virol* **70**, 4877-83.

Ruiz, M. C., Cohen, J. and Michelangeli, F. (2000). Role of Ca2+in the replication and pathogenesis of rotavirus and other viral infections. *Cell Calcium* **28**, 137-49.

Ruiz, M. C., Diaz, Y., Pena, F., Aristimuno, O. C., Chemello, M. E. and Michelangeli, F. (2005). Ca2+ permeability of the plasma membrane induced by rotavirus infection in cultured cells is inhibited by tunicamycin and brefeldin A. *Virology* **333**, 54-65.

Sabara, M., Ready, K. F., Frenchick, P. J. and Babiuk, L. A. (1987). Biochemical evidence for the oligomeric arrangement of bovine rotavirus nucleocapsid protein and its possible significance in the immunogenicity of this protein. *J Gen Virol* **68 (Pt 1)**, 123-33.

Sachs, A. B., Sarnow, P. and Hentze, M. W. (1997). Starting at the beginning, middle, and end: translation initiation in eukaryotes. *Cell* **89**, 831-8.

Sachs, A. B. and Varani, G. (2000). Eukaryotic translation initiation: there are (at least) two sides to every story. *Nat Struct Biol* **7**, 356-61.

Saif, L. J., Bohl, E. H., Theil, K. W., Cross, R. F. and House, J. A. (1980). Rotavirus-like, calicivirus-like, and 23-nm virus-like particles associated with diarrhea in young pigs. *J Clin Microbiol* **12**, 105-11.

Saif, L. J. and Jiang, B. (1994). Nongroup A rotaviruses of humans and animals. *Curr Top Microbiol Immunol* **185**, 339-71.

Sambrook, J., Fritsch, E. F. and Maniatis, T. (1989). Molecular cloning: a laboratory manual. Cold Spring Harbor, N.Y.: Cold Spring Harbor Laboratory.

Sanchez-San Martin, C., Lopez, T., Arias, C. F. and Lopez, S. (2004). Characterization of rotavirus cell entry. *J Virol* **78**, 2310-8.

Sandino, A. M., Fernandez, J., Pizarro, J., Vasquez, M. and Spencer, E. (1994). Structure of rotavirus particle: interaction of the inner capsid protein VP6 with the core polypeptide VP3. *Biol Res* **27**, 39-48.

Sanger, F., Nicklen, S. and Coulson, A. R. (1977). DNA sequencing with chain-terminating inhibitors. *Proc Natl Acad Sci U S A* **74**, 5463-7.

Santos, N. and Hoshino, Y. (2005). Global distribution of rotavirus serotypes/genotypes and its implication for the development and implementation of an effective rotavirus vaccine. *Rev Med Virol* **15**, 29-56.

Sato, T., Suzuki, H., Kitaoka, S., Konno, T. and Ishida, N. (1986). Patterns of polypeptide synthesis in human rotavirus infected cells. *Arch Virol* **90**, 29-40.

Schneider, R. J. and Mohr, I. (2003). Translation initiation and viral tricks. *Trends Biochem Sci* **28**, 130-6.

Schuck, P., Taraporewala, Z., McPhie, P. and Patton, J. T. (2001). Rotavirus nonstructural protein NSP2 self-assembles into octamers that undergo ligand-induced conformational changes. *J Biol Chem* **276**, 9679-87.

Sen, N., Cao, F. and Tavis, J. E. (2004). Translation of duck hepatitis B virus reverse transcriptase by ribosomal shunting. *J Virol* **78**, 11751-7.

Shahrabadi, M. S., Babiuk, L. A. and Lee, P. W. (1987). Further analysis of the role of calcium in rotavirus morphogenesis. *Virology* **158**, 103-11.

Shahrabadi, M. S. and Lee, P. W. (1986). Bovine rotavirus maturation is a calcium-dependent process. *Virology* **152**, 298-307.

Shaw, A. L., Rothnagel, R., Chen, D., Ramig, R. F., Chiu, W. and Prasad, B. V. (1993). Three-dimensional visualization of the rotavirus hemagglutinin structure. *Cell* **74**, 693-701.

Shaw, R. D., Hempson, S. J. and Mackow, E. R. (1995). Rotavirus diarrhea is caused by nonreplicating viral particles. *J Virol* **69**, 5946-50.

Shen, S., Burke, B. and Desselberger, U. (1994). Rearrangement of the VP6 gene of a group A rotavirus in combination with a point mutation affecting trimer stability. *J Virol* **68**, 1682-8.

Silvestri, L. S., Taraporewala, Z. F. and Patton, J. T. (2004). Rotavirus replication: plus-sense templates for double-stranded RNA synthesis are made in viroplasms. *J Virol* **78**, 7763-74.

Smith, D. B. and Johnson, K. S. (1988). Single-step purification of polypeptides expressed in Escherichia coli as fusions with glutathione S-transferase. *Gene* **67**, 31-40.

Smith, R. E., Kister, S. E. and Carozzi, N. B. (1989). Cloning and expression of the major inner capsid protein of SA-11 simian rotavirus in Escherichia coli. *Gene* **79**, 239-48.

Spencer, E. and Arias, M. L. (1981). In vitro transcription catalyzed by heat-treated human rotavirus. *J Virol* **40**, 1-10.

Stacy-Phipps, S. and Patton, J. T. (1987). Synthesis of plus- and minus-strand RNA in rotavirus-infected cells. *J Virol* **61**, 3479-84.

Stirzaker, S. C., Whitfeld, P. L., Christie, D. L., Bellamy, A. R. and Both, G. W. (1987). Processing of rotavirus glycoprotein VP7: implications for the retention of the protein in the endoplasmic reticulum. *J Cell Biol* **105**, 2897-903.

Su, C. Q., Wu, Y. L., Shen, H. K., Wang, D. B., Chen, Y. H., Wu, D. M., He, L. N. and Yang, Z. L. (1986). An outbreak of epidemic diarrhoea in adults caused by a new rotavirus in Anhui Province of China in the summer of 1983. *J Med Virol* **19**, 167-73.

Suzuki, H., Sato, T., Konno, T., Kitaoka, S., Ebina, T. and Ishida, N. (1984). Effect of tunicamycin on human rotavirus morphogenesis and infectivity. Brief report. *Arch Virol* **81**, 363-9.

Svensson, L., Grahnquist, L., Pettersson, C. A., Grandien, M., Stintzing, G. and Greenberg, H. B. (1988). Detection of human rotaviruses which do not react with subgroup I- and II-specific monoclonal antibodies. *J Clin Microbiol* **26**, 1238-40.

Tam, J. S., Szymanski, M. T., Middleton, P. J. and Petric, M. (1976). Studies on the particles of infantile gastroenteritis virus (orbivirus group). *Intervirology* **7**, 181-91.

Taniguchi, K., Kojima, K. and Urasawa, S. (1996). Nondefective rotavirus mutants with an NSP1 gene which has a deletion of 500 nucleotides, including a cysteine-rich zinc finger motif-encoding region (nucleotides 156 to 248), or which has a nonsense codon at nucleotides 153-155. *J Virol* **70**, 4125-30.

Taraporewala, Z., Chen, D. and Patton, J. T. (1999). Multimers formed by the rotavirus nonstructural protein NSP2 bind to RNA and have nucleoside triphosphatase activity. *J Virol* **73**, 9934-43.

Taraporewala, Z. F. and Patton, J. T. (2001). Identification and characterization of the helix-destabilizing activity of rotavirus nonstructural protein NSP2. *J Virol* **75**, 4519-27.

Taraporewala, Z. F. and Patton, J. T. (2004). Nonstructural proteins involved in genome packaging and replication of rotaviruses and other members of the Reoviridae. *Virus Res* **101**, 57-66.

Taraporewala, Z. F., Schuck, P., Ramig, R. F., Silvestri, L. and Patton, J. T. (2002). Analysis of a temperature-sensitive mutant rotavirus indicates that NSP2 octamers are the functional form of the protein. *J Virol* **76**, 7082-93.

Taylor, J. A., Meyer, J. C., Legge, M. A., O'Brien, J. A., Street, J. E., Lord, V. J., Bergmann, C. C. and Bellamy, A. R. (1992). Transient expression and mutational analysis of the rotavirus intracellular receptor: the C-terminal methionine residue is essential for ligand binding. *J Virol* **66**, 3566-72.

Taylor, J. A., O'Brien, J. A., Lord, V. J., Meyer, J. C. and Bellamy, A. R. (1993). The RER-localised rotavirus intracellular receptor: a truncated purified soluble form is multivalent and binds virus particles. *Virology* **194**, 807-14.

Taylor, J. A., O'Brien, J. A. and Yeager, M. (1996). The cytoplasmic tail of NSP4, the endoplasmic reticulum-localised non-structural glycoprotein of rotavirus, contains distinct virus binding and coiled coil domains. *Embo J* **15**, 4469-76.

Tian, P., Ball, J. M., Zeng, C. Q. and Estes, M. K. (1996a). The rotavirus nonstructural glycoprotein NSP4 possesses membrane destabilization activity. *J Virol* **70**, 6973-81.

Tian, P., Ball, J. M., Zeng, C. Q. and Estes, M. K. (1996b). Rotavirus protein expression is important for virus assembly and pathogenesis. *Arch Virol Suppl* **12**, 69-77.

Tian, P., Hu, Y., Schilling, W. P., Lindsay, D. A., Eiden, J. and Estes, M. K. (1994). The nonstructural glycoprotein of rotavirus affects intracellular calcium levels. *J Virol* **68**, 251-7.

Tian, Y., Tarlow, O., Ballard, A., Desselberger, U. and McCrae, M. A. (1993). Genomic concatemerization/deletion in rotaviruses: a new mechanism for generating rapid genetic change of potential epidemiological importance. *J Virol* **67**, 6625-32.

Torres-Vega, M. A., Gonzalez, R. A., Duarte, M., Poncet, D., Lopez, S. and Arias, C. F. (2000). The C-terminal domain of rotavirus NSP5 is essential for its multimerization, hyperphosphorylation and interaction with NSP6. *J Gen Virol* **81**, 821-30.

Tosser, G., Labbe, M., Bremont, M. and Cohen, J. (1992). Expression of the major capsid protein VP6 of group C rotavirus and synthesis of chimeric single-shelled particles by using recombinant baculoviruses. *J Virol* **66**, 5825-31.

Tucker, A. W., Haddix, A. C., Bresee, J. S., Holman, R. C., Parashar, U. D. and Glass, R. I. (1998). Cost-effectiveness analysis of a rotavirus immunization program for the United States. *Jama* **279**, 1371-6.

Valenzuela, S., Pizarro, J., Sandino, A. M., Vasquez, M., Fernandez, J., Hernandez, O., Patton, J. and Spencer, E. (1991). Photoaffinity labeling of rotavirus VP1 with 8-azido-ATP: identification of the viral RNA polymerase. *J Virol* **65**, 3964-7.

Vascotto, F., Campagna, M., Visintin, M., Cattaneo, A. and Burrone, O. R. (2004). Effects of intrabodies specific for rotavirus NSP5 during the virus replicative cycle. *J Gen Virol* **85**, 3285-90.

Vende, P., Piron, M., Castagne, N. and Poncet, D. (2000). Efficient translation of rotavirus mRNA requires simultaneous interaction of NSP3 with the eukaryotic translation initiation factor eIF4G and the mRNA 3' end. *J Virol* **74**, 7064-71.

Vende, P., Taraporewala, Z. F. and Patton, J. T. (2002). RNA-binding activity of the rotavirus phosphoprotein NSP5 includes affinity for double-stranded RNA. *J Virol* **76**, 5291-9.

Vitour, D., Lindenbaum, P., Vende, P., Becker, M. M. and Poncet, D. (2004). RoXaN, a novel cellular protein containing TPR, LD, and zinc finger motifs, forms a ternary complex with eukaryotic initiation factor 4G and rotavirus NSP3. *J Virol* **78**, 3851-62.

Ward, C. W., Azad, A. A. and Dyall-Smith, M. L. (1985). Structural homologies between RNA gene segments 10 and 11 from UK bovine, simian SA11, and human Wa rotaviruses. *Virology* **144**, 328-36.

Ward, L. A., Rosen, B. I., Yuan, L. and Saif, L. J. (1996). Pathogenesis of an attenuated and a virulent strain of group A human rotavirus in neonatal gnotobiotic pigs. *J Gen Virol* 77 **(Pt 7)**, 1431-41.

Welch, S. K., Crawford, S. E. and Estes, M. K. (1989). Rotavirus SA11 genome segment 11 protein is a nonstructural phosphoprotein. *J Virol* **63**, 3974-82.

Wells, S. E., Hillner, P. E., Vale, R. D. and Sachs, A. B. (1998). Circularization of mRNA by eukaryotic translation initiation factors. *Mol Cell* **2**, 135-40.

Wentz, M. J., Patton, J. T. and Ramig, R. F. (1996a). The 3'-terminal consensus sequence of rotavirus mRNA is the minimal promoter of negative-strand RNA synthesis. *J Virol* **70**, 7833-41.

Wentz, M. J., Zeng, C. Q., Patton, J. T., Estes, M. K. and Ramig, R. F. (1996b). Identification of the minimal replicase and the minimal promoter of (-)-strand synthesis, functional in rotavirus RNA replication in vitro. *Arch Virol Suppl* **12**, 59-67.

Whitfeld, P. L., Tyndall, C., Stirzaker, S. C., Bellamy, A. R. and Both, G. W. (1987). Location of sequences within rotavirus SA11 glycoprotein VP7 which direct it to the endoplasmic reticulum. *Mol Cell Biol* **7**, 2491-7.

Wu, H., Taniguchi, K., Urasawa, T. and Urasawa, S. (1998). Serological and genomic characterization of human rotaviruses detected in China. *J Med Virol* **55**, 168-76.

Xu, L., Tian, Y., Tarlow, O., Harbour, D. and McCrae, M. A. (1994). Molecular biology of rotaviruses. IX. Conservation and divergence in genome segment 5. *J Gen Virol* **75 (Pt 12)**, 3413-21.

Yazaki, K., Mizuno, A., Sano, T., Fujii, H. and Miura, K. (1986). A new method for extracting circular and supercoiled genome segments from cytoplasmic polyhedrosis virus. *J Virol Methods* **14**, 275-83.

Yeager, M., Berriman, J. A., Baker, T. S. and Bellamy, A. R. (1994). Three-dimensional structure of the rotavirus haemagglutinin VP4 by cryo-electron microscopy and difference map analysis. *Embo J* **13**, 1011-8.

Yolken, R., Arango-Jaramillo, S., Eiden, J. and Vonderfecht, S. (1988). Lack of genomic reassortment following infection of infant rats with group A and group B rotaviruses. *J Infect Dis* **158**, 1120-3.

Yolken, R. H., Willoughby, R., Wee, S. B., Miskuff, R. and Vonderfecht, S. (1987). Sialic acid glycoproteins inhibit in vitro and in vivo replication of rotaviruses. *J Clin Invest* **79**, 148-54.

Yueh, A. and Schneider, R. J. (1996). Selective translation initiation by ribosome jumping in adenovirus-infected and heat-shocked cells. *Genes Dev* **10**, 1557-67.

Zarate, S., Espinosa, R., Romero, P., Guerrero, C. A., Arias, C. F. and Lopez, S. (2000a). Integrin alpha2beta1 mediates the cell attachment of the rotavirus neuraminidase-resistant variant nar3. *Virology* **278**, 50-4.

Zarate, S., Espinosa, R., Romero, P., Mendez, E., Arias, C. F. and Lopez, S. (2000b). The VP5 domain of VP4 can mediate attachment of rotaviruses to cells. *J Virol* **74**, 593-9.

Zeng, C. Q., Estes, M. K., Charpilienne, A. and Cohen, J. (1998). The N terminus of rotavirus VP2 is necessary for encapsidation of VP1 and VP3. *J Virol* **72**, 201-8.

Zeng, C. Q., Wentz, M. J., Cohen, J., Estes, M. K. and Ramig, R. F. (1996). Characterization and replicase activity of double-layered and single-layered rotavirus-like particles expressed from baculovirus recombinants. *J Virol* **70**, 2736-42.

Appendix

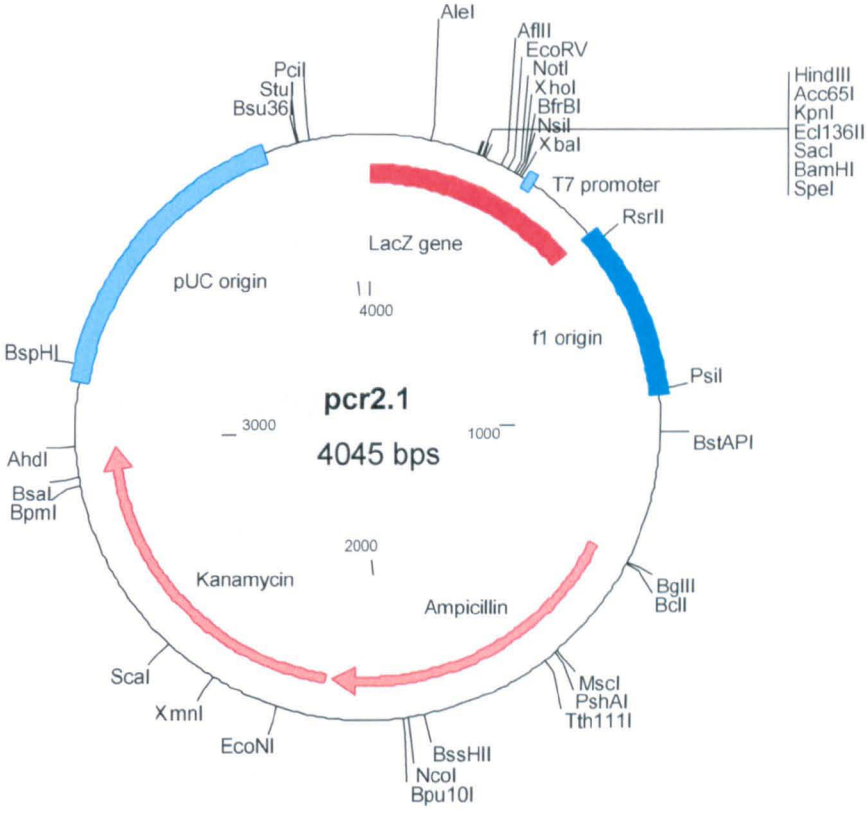

Appendix 1.1 pCR2.1 cloning vector

The TA Cloning® vector, pCR2.1 (Invitrogen) is provided linearised single base tyrosine over hangs for rapid ligation to PCR products generated using *Taq* polymerase with. It contains the lacZ-alpha complementation fragment for blue-white colour screening, ampicillin and kanamycin resistance genes for selection.

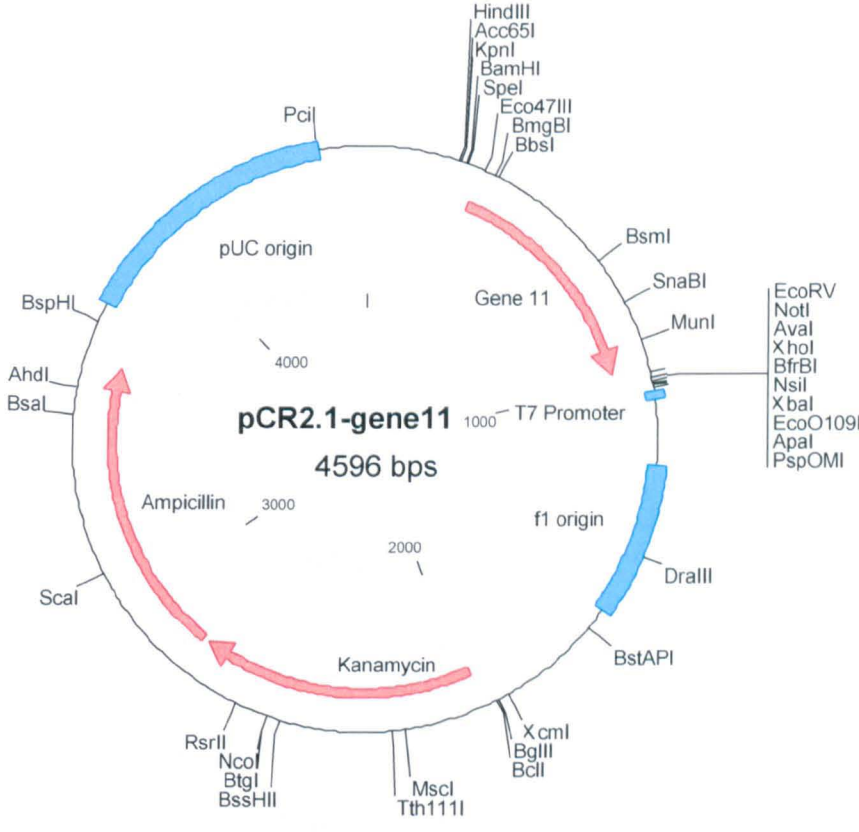

Appendix 1.2 Gene11 cloned into the pCR2.1 expression vector
Gene segment 11 was cloned directly into the pCR2.1 vector by TA cloning to generate pCR2.1-gene11.

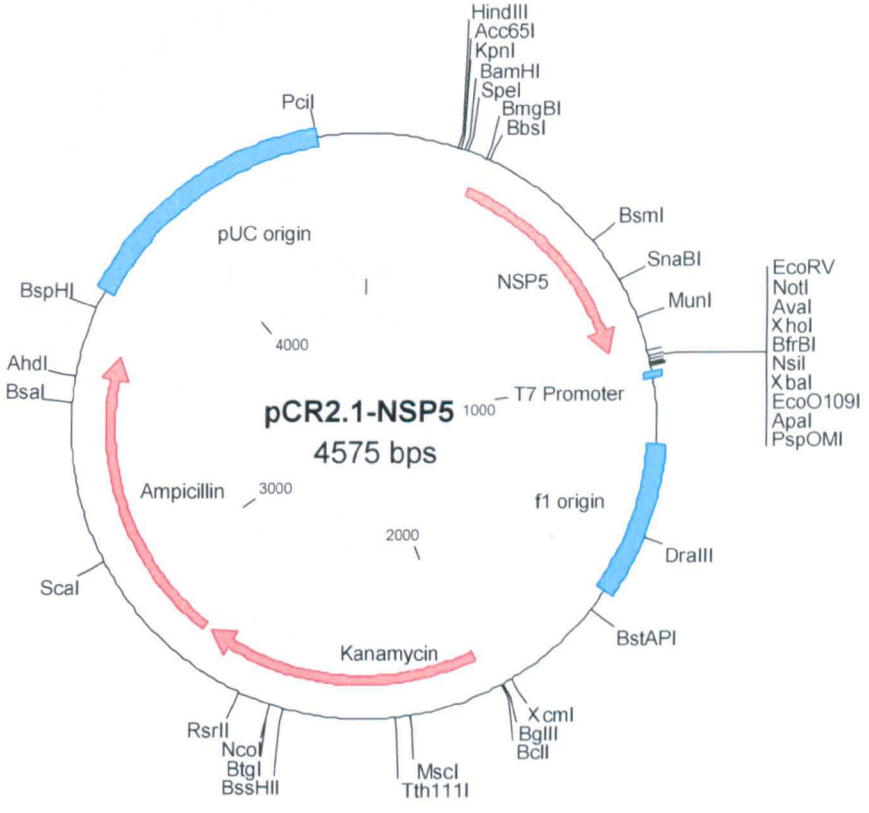

Appendix 1.3 NSP5 cloned into the pCR2.1 expression vector
NSP5 ORF was cloned directly into the pCR2.1 vector by TA cloning to generate pCR2.1-NSP5.

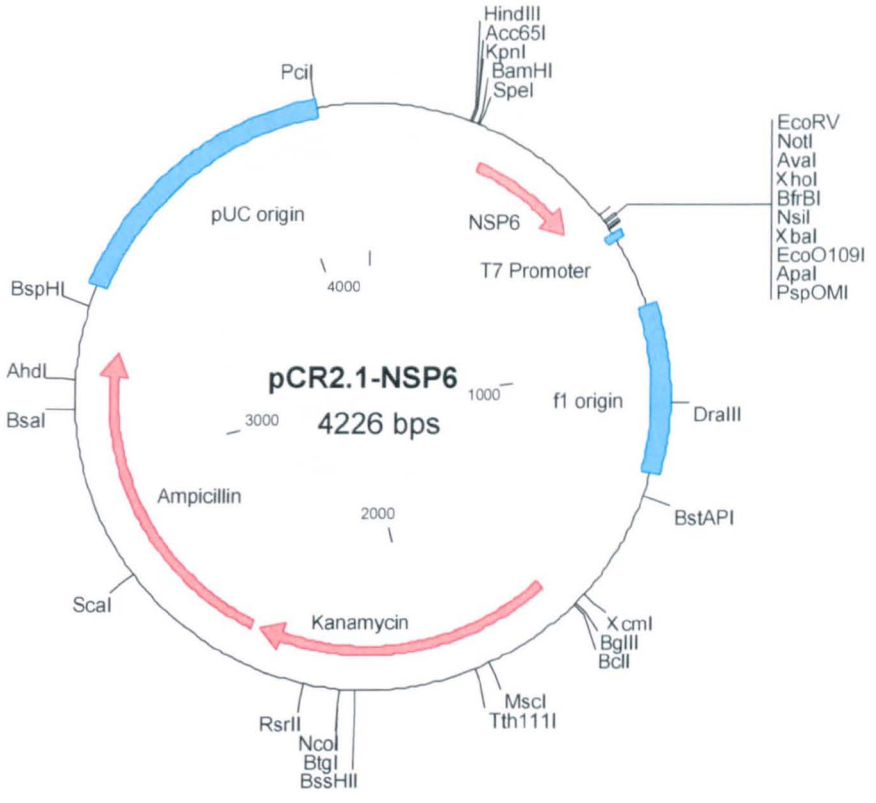

Appendix 1.4 NSP6 cloned into the pCR2.1 expression vector
NSP6 ORF was cloned directly into the pCR2.1 vector by TA cloning to generate pCR2.1-NSP6.

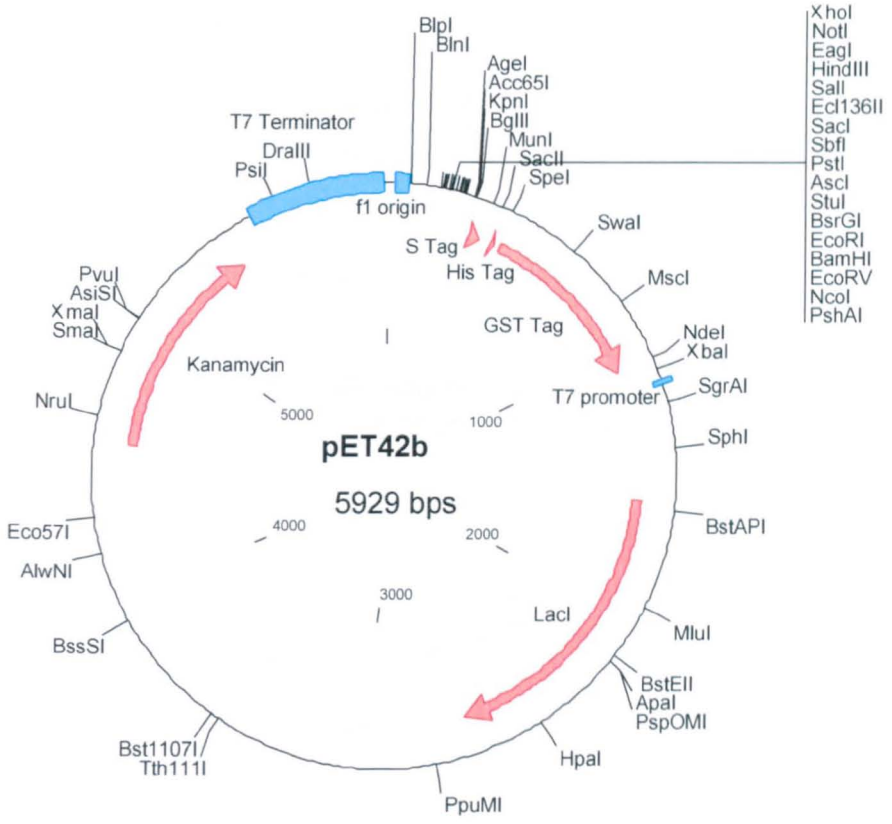

Appendix 1.5 Expression vector pET42b

The pET42b expression vector generates high level expression of fusion proteins with a GST, 6 histidine and S tags. The vector contains a T7 promoter region, multicloning site, Kanamycin resistance gene and factor Xa protease cleavage site for removal of the tag after protein purification.

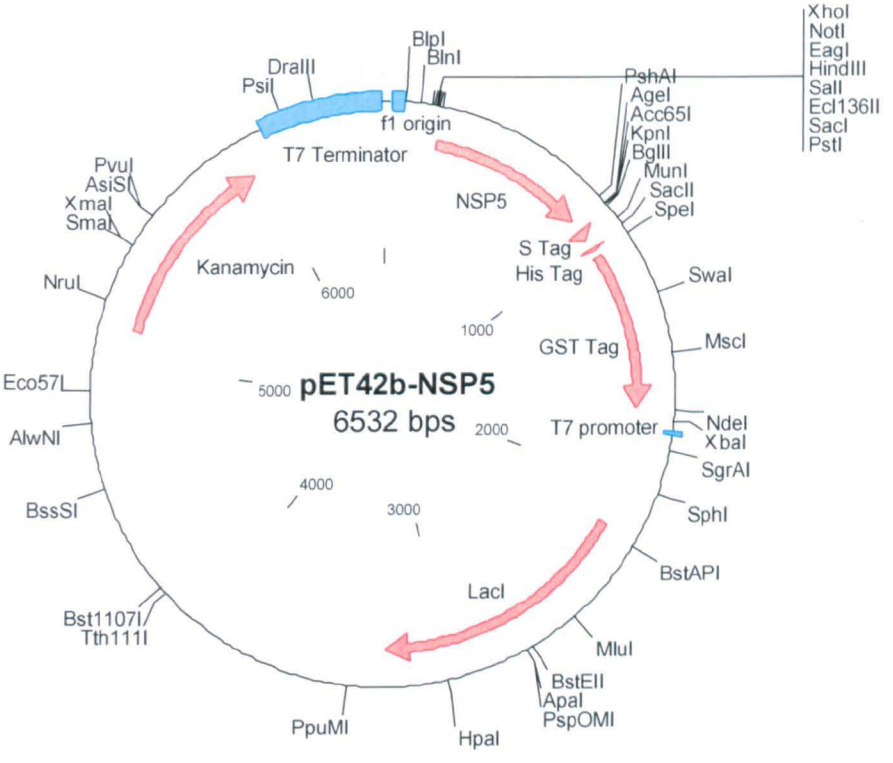

Appendix 1.6 NSP5 ORF cloned into the pET42b expression vector
The NSP5 ORF was cloned into *PshA*I and *Pst*I restriction enzyme sites of the multicloning site of pET42b to generate pET42b-NSP5.

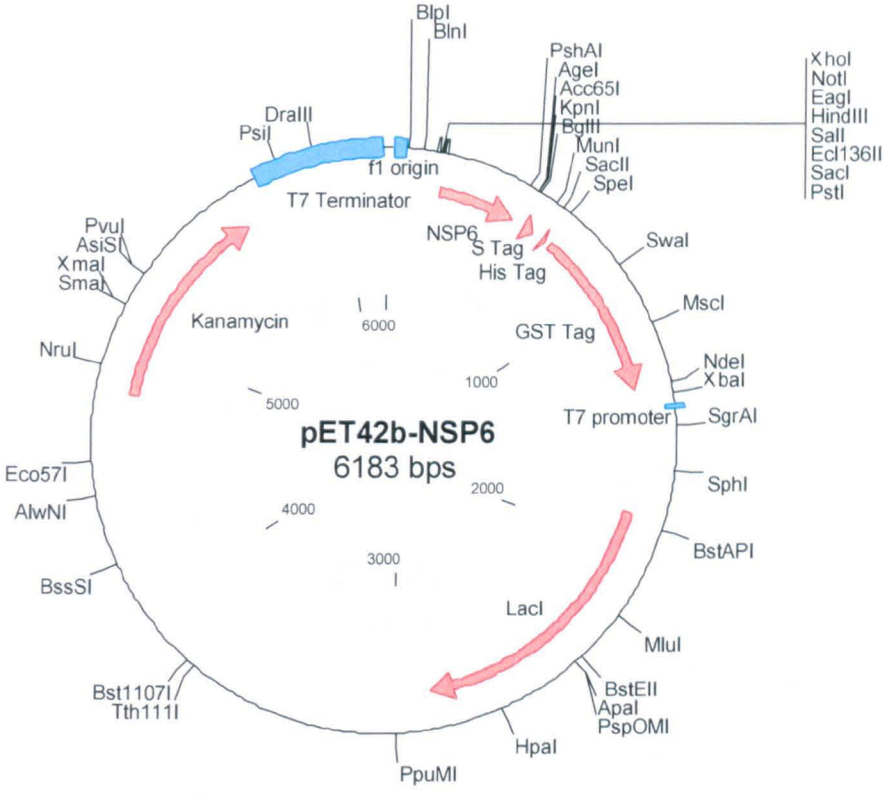

Appendix 1.7 NSP6 ORF cloned into the pET42b expression vector
The NSP6 ORF was cloned into *PshA*I and *Pst*I restriction enzyme sites of the multicloning site of pET42b to generate pET42b-NSP6.

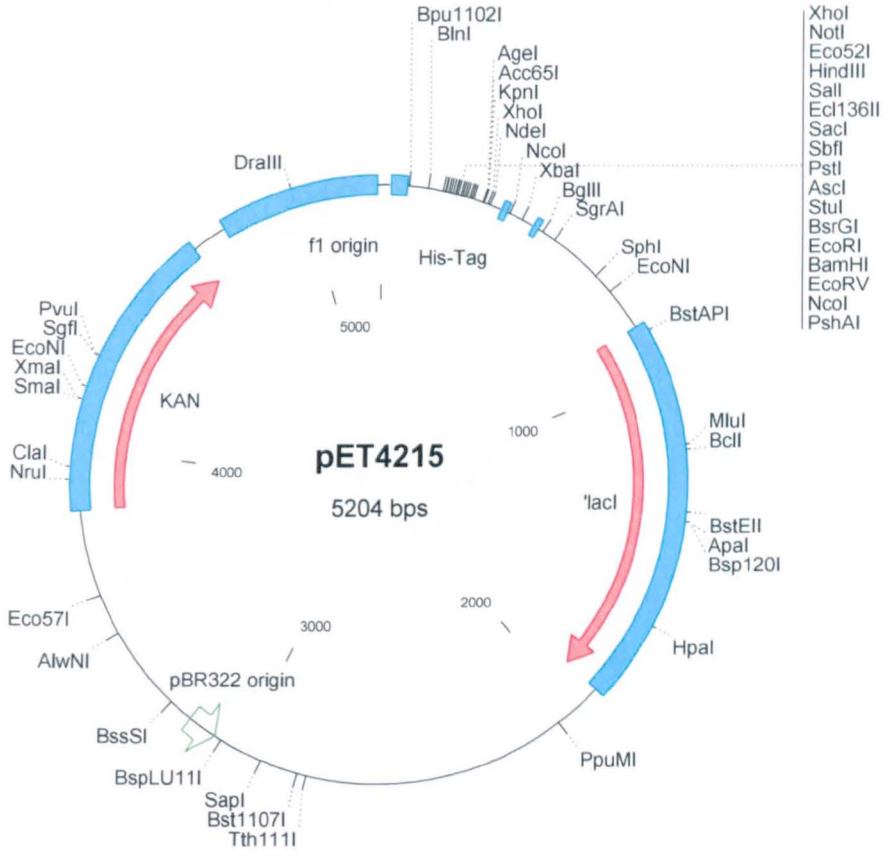

Appendix 1.8 Expression vector pET4215

The pET4215 expression vector generates high level expression of fusion proteins with a 6 histidine tag. The vector contains a T7 promoter region, multicloning site, Kanamycin resistance gene and factor Xa protease cleavage site for removal of the tag after protein purification.

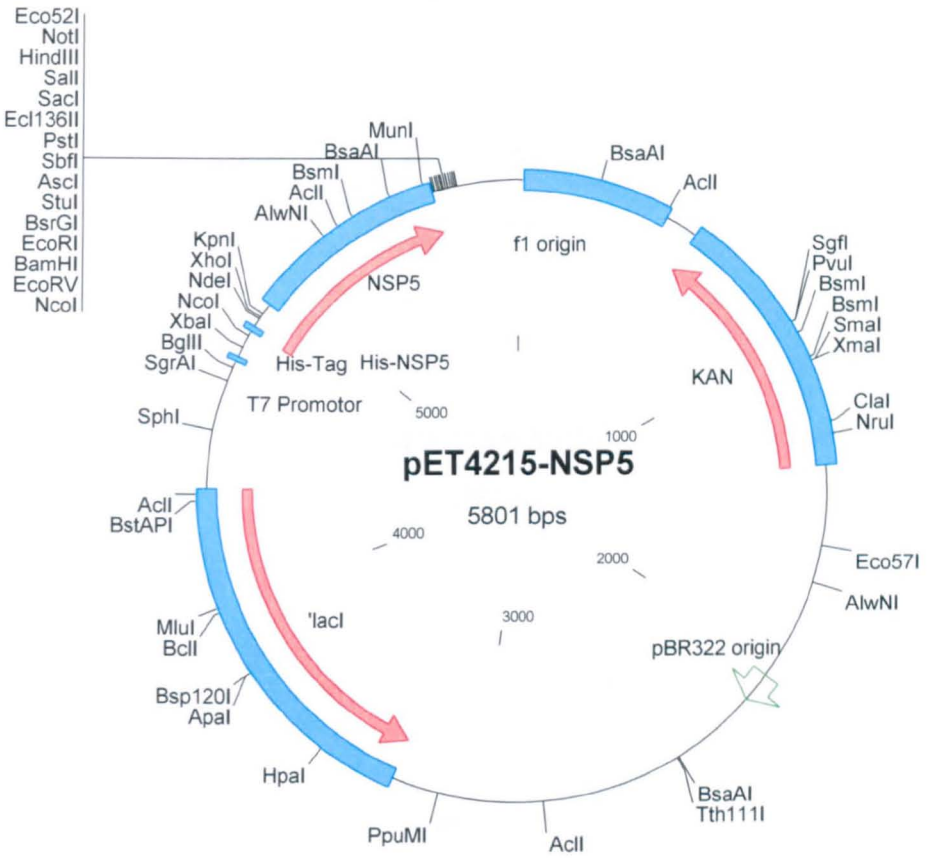

Appendix 1.9 NSP5 ORF cloned into the pET4215 expression vector
The NSP5 ORF was cloned into *Psh A*I and *Pst* I restriction enzyme sites of the multicloning site of pET4215 to generate pET4215-NSP5.

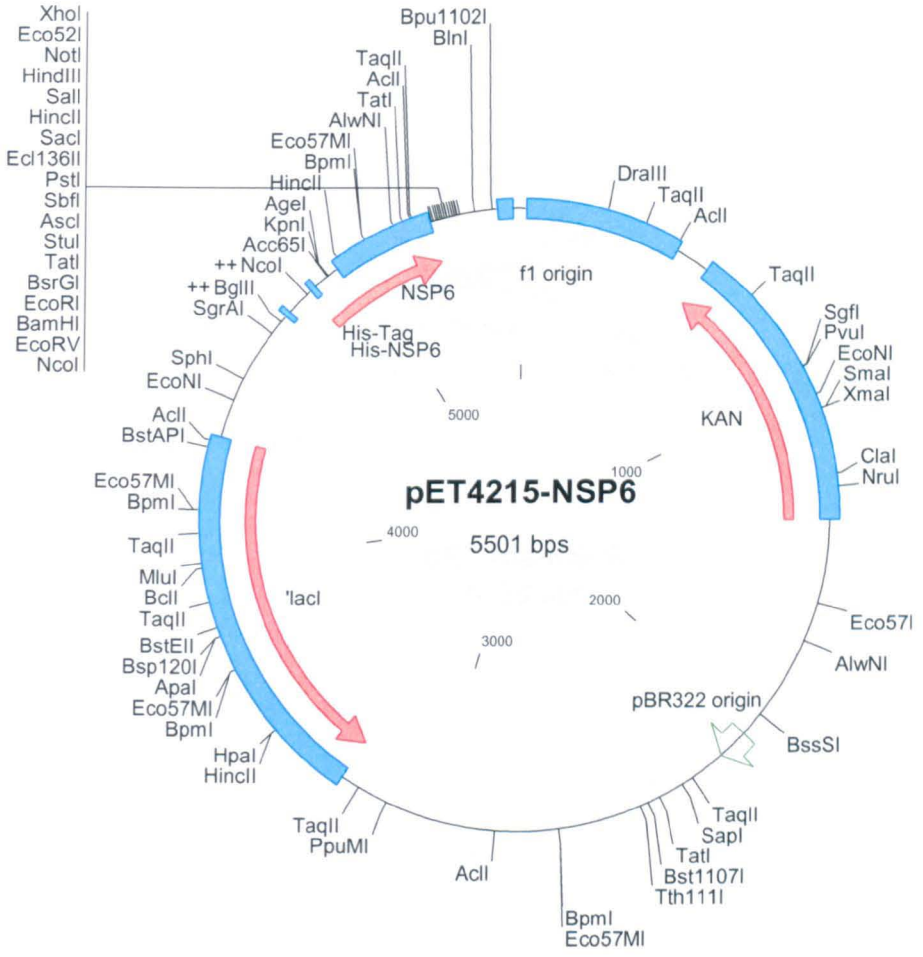

Appendix 1.10 NSP5 ORF cloned into the pET4215 expression vector
The NSP6 ORF was cloned into *Psh A*I and *Pst* I restriction enzyme sites of the multicloning site of pET4215 to generate pET4215-NSP6.

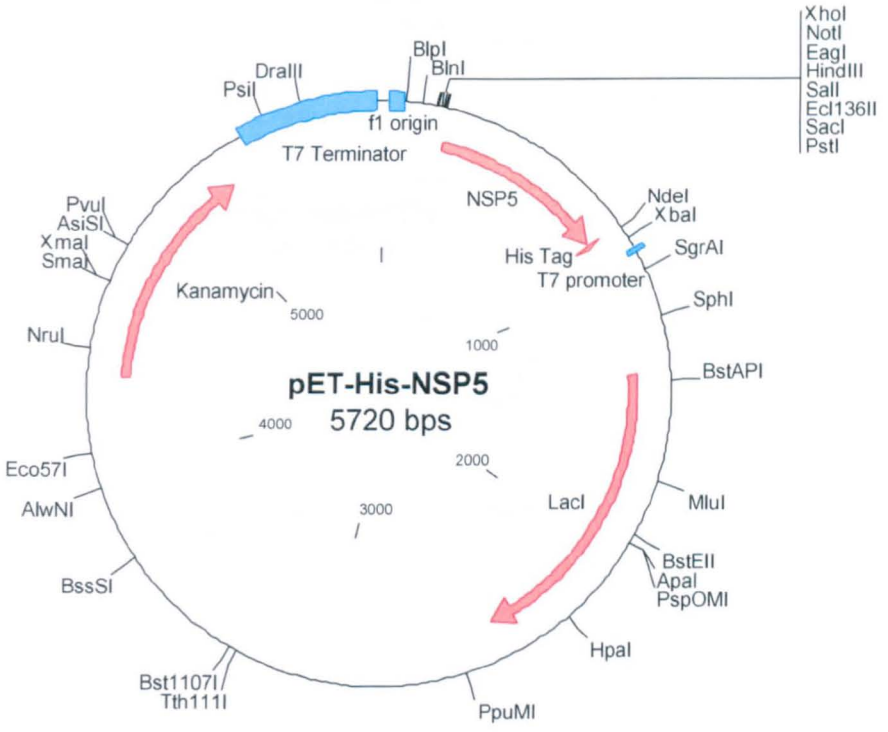

Appendix 1.11 NSP5 ORF cloned into the pET42b expression vector which has had the GST tag region removed.

PCR was used to place the unique restriction sites *Nde* I and *Pst* I at the 5' and 3'respetively and a 6 His tag onto the 5' of the NSP5 ORF this, was subsequently cut with *Nde* I and *Pst* I cloned into pET42b vector that had been also cleaved with *Nde* I and *Pst* I restriction enzymes and then the two cDNA's were ligated to generate pET-His-NSP5.

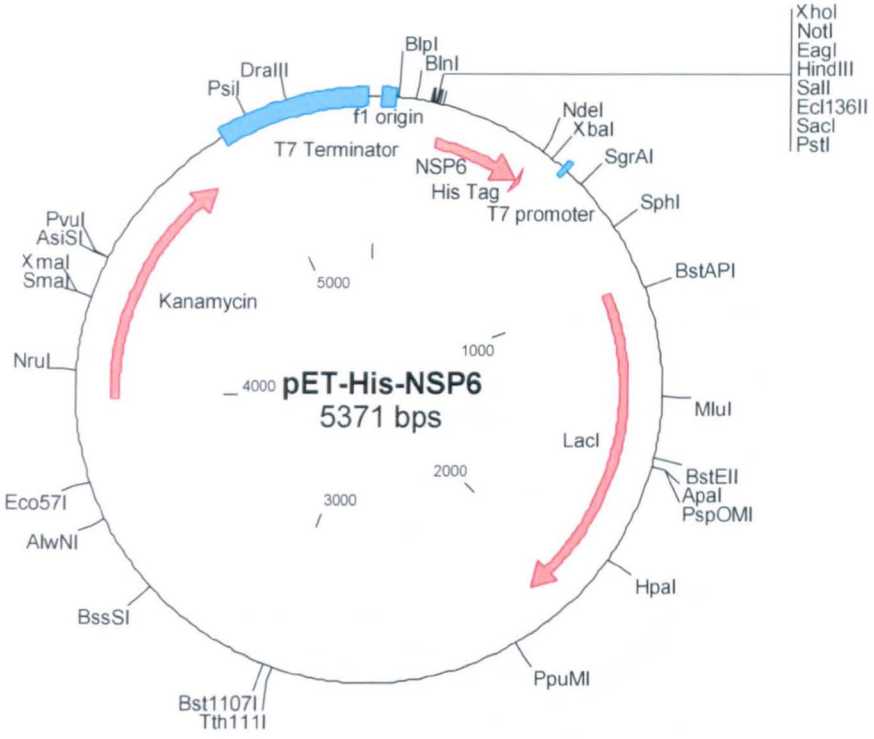

Appendix 1.12 NSP6 ORF cloned into the pET42b expression vector which has had the GST tag region removed.

PCR was used to place the unique restriction sites *Nde* I and *Pst* I at the 5' and 3'respetively and a 6 His tag onto the 5' of the NSP6 ORF this, was subsequently cut with *Nde* I and *Pst* I cloned into pET42b vector that had been also cleaved with *Nde* I and *Pst* I restriction enzymes and then the two cDNA's were ligated to generate pET-His-NSP6.

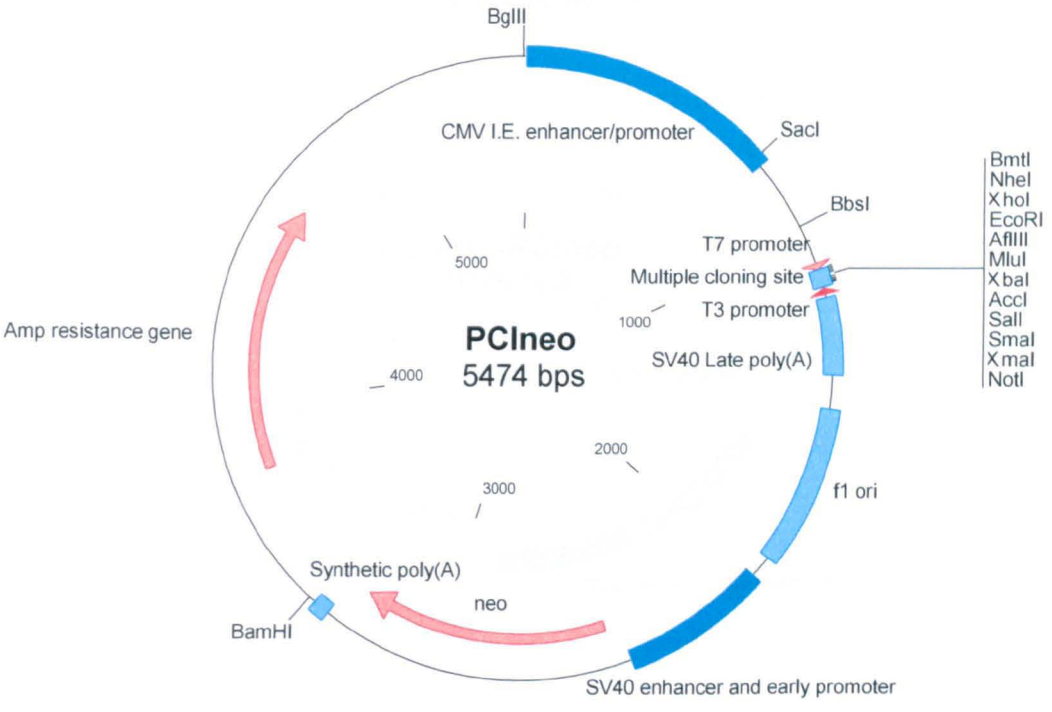

Appendix 2.1 PCIneo expression vector

The PCIneo expression vector contains both the human cytomegalovirus (CMV) immediate early, T7 and T3 promoter regions. The CMV promoter enables expression of cloned inserts in mammalian cells, the T7 and T3 promoter can be used for expression of cloned inserts in *in vitro* expression systems or recombinant cells expressing the T7 or T3 polymerases. The plasmid carries an ampicillin antibiotic resistance gene for selection of transformed bacteria carrying the plasmid during cloning and a neomycin phosphotransferase gene which is a selectable marker in mammalian cells. Also present is the origin of replication of the filamentous phage f1, a multicloning site and following this a SV40 late poly A signal sequence allowing poly adenylation of cloned inserts.

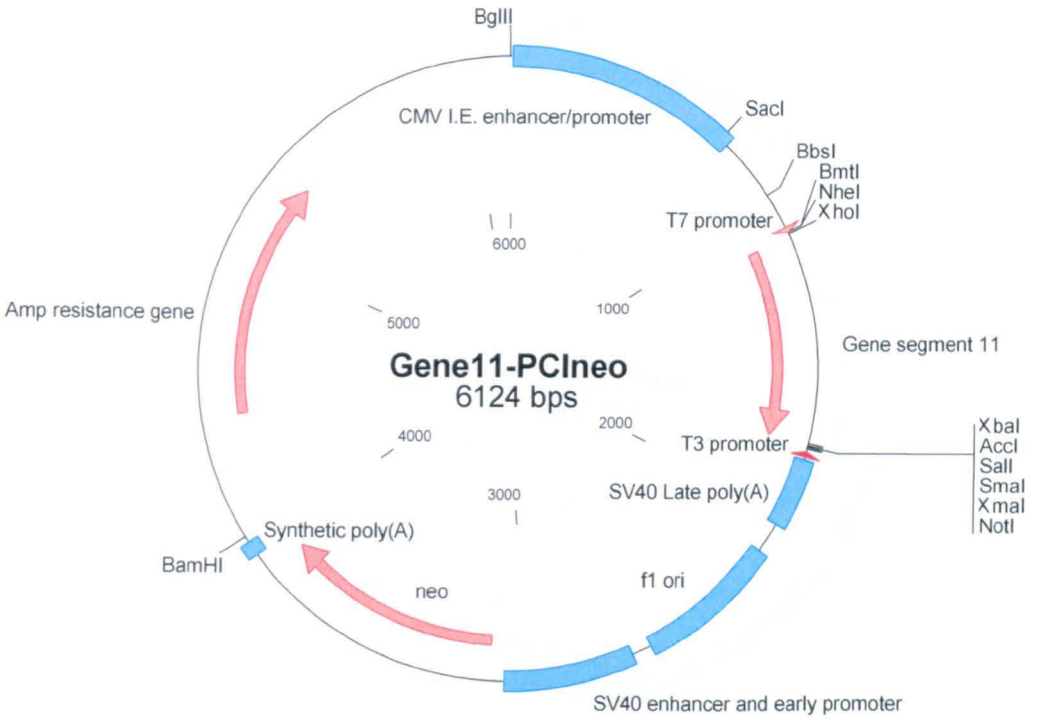

Appendix 2.2 Rotavirus gene segment 11 cloned into the PCIneo expression vector

Rotavirus gene segment 11 was cloned into *Xho* I and *Xba* I restriction enzyme sites of the multicloning site of PCIneo to generate gene11-PCIneo.

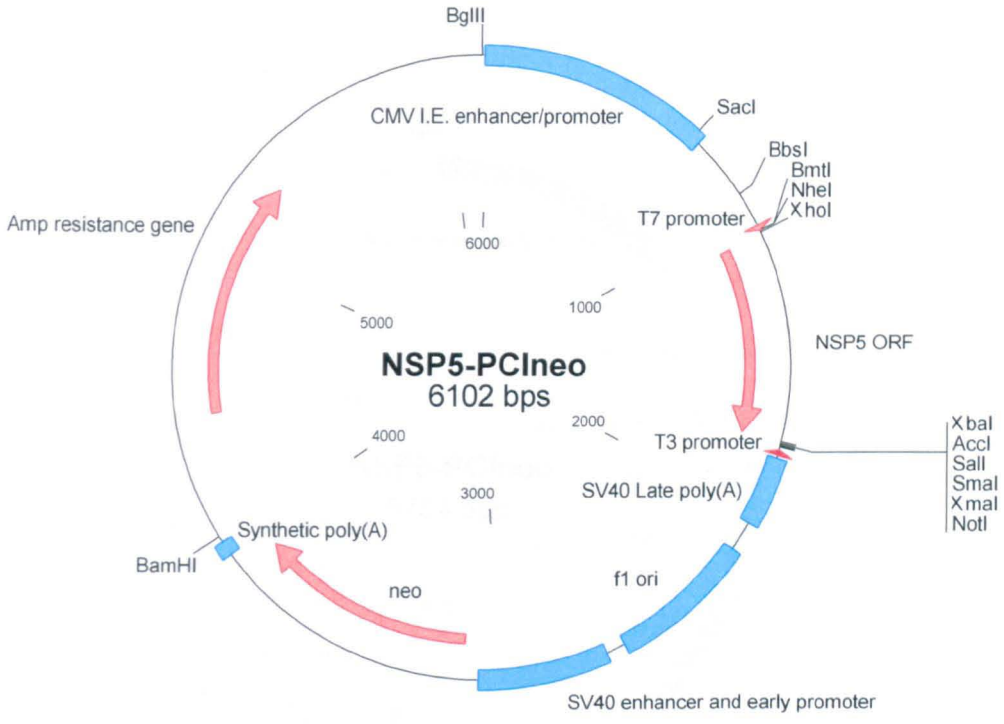

Appendix 2.3 NSP5 ORF cloned into the PCIneo expression vector

The NSP5 ORF was cloned into *Xho* I and *Xba* I restriction enzyme sites of the multicloning site of PCIneo to generate NSP5-PCIneo.

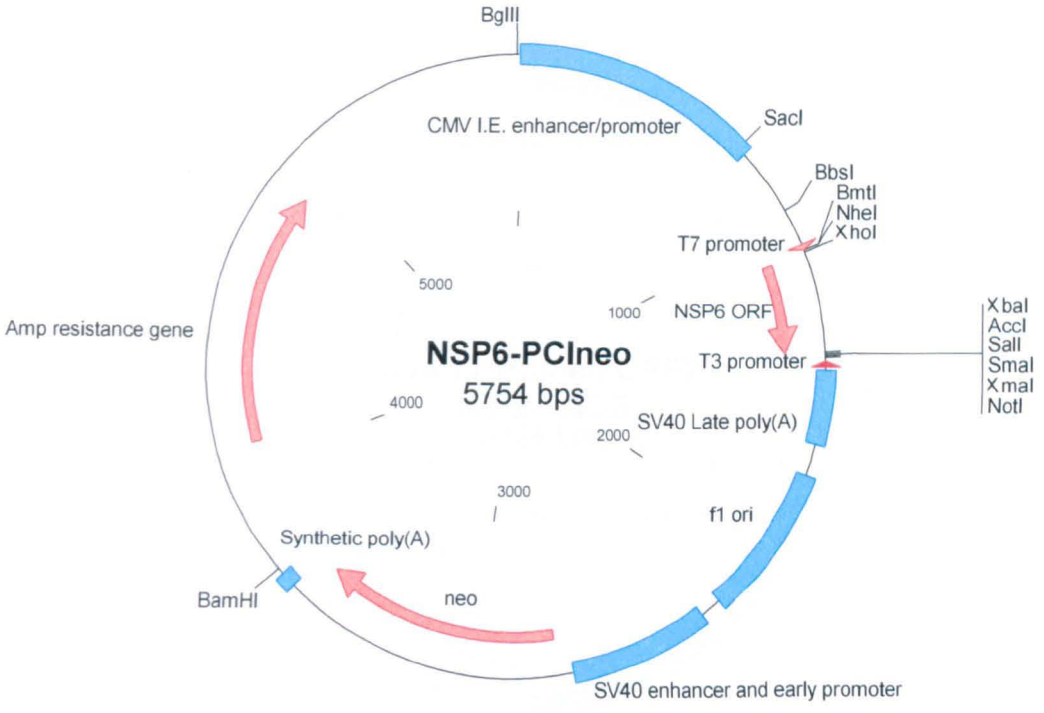

Appendix 2.4 NSP6 ORF cloned into the PCIneo expression vector

The NSP6 ORF was cloned into *Xho* I and *Xba* I restriction enzyme sites of the multicloning site of PCIneo to generate NSP6-PCIneo.

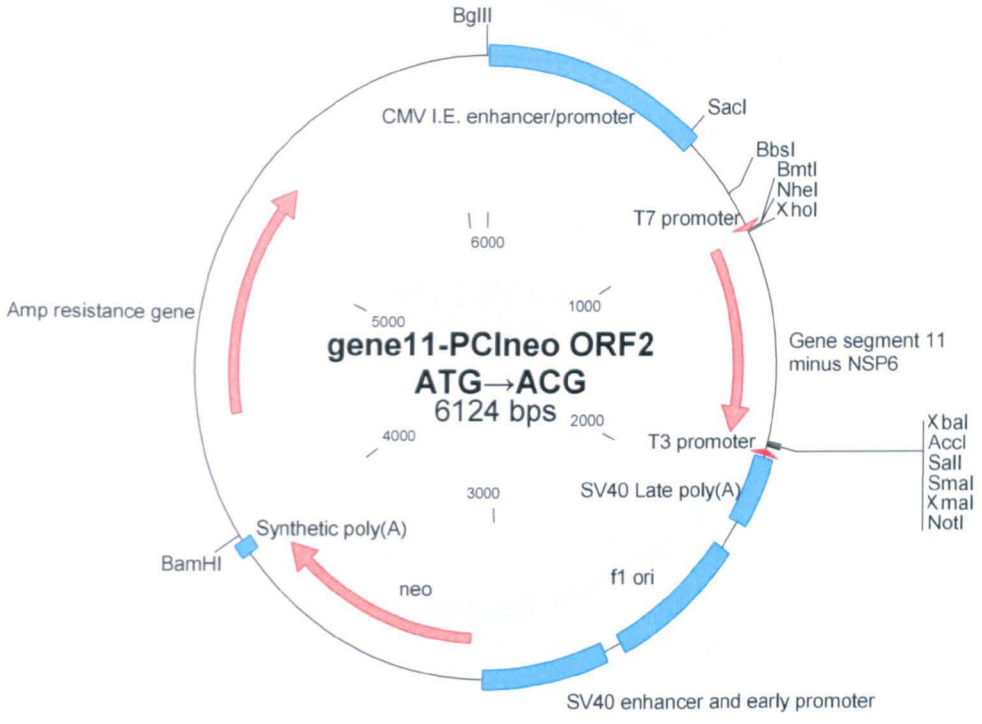

Appendix 2.5 Site directed mutagenesis was used to generate PCIneo-gene11 ORF2 ATG→ACG

Site directed mutagenesis was used to create a mutant gene 11 sequence that could no longer express the NSP6 protein generating gene11 t23c-PCIneo.

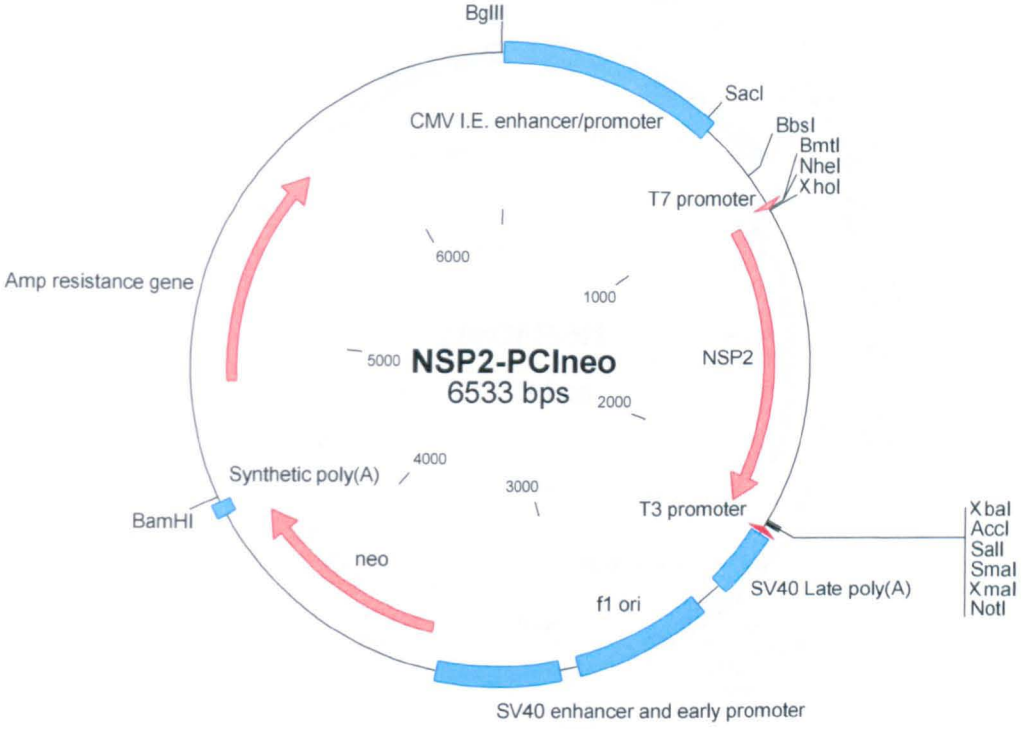

Appendix 2.6 Rotavirus gene segment 7 cloned into the PCIneo expression vector

Rotavirus gene segment 7 was cloned into *Xho* I and *Xba* I restriction enzyme sites of the multicloning site of PCIneo to generate NSP2-PCIneo.

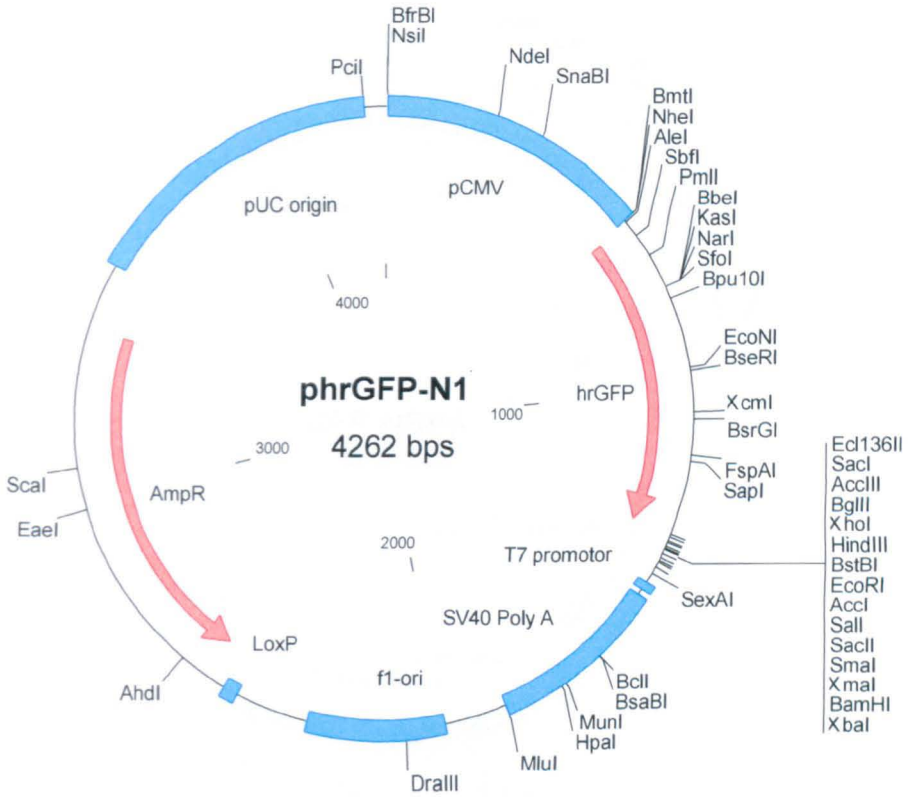

Appendix 2.7 phrGFP-N1 vector

phrGFP-N1 (Stratagene) has the hrGFP gene under the control of the CMV promoter and a multicloning site downstream of the hrGFP gene which is followed by a SV40 polyadenylation signal. When ORF's are subcloned into this vector in frame hrGFP fusion proteins are expressed. The vector also contains an ampicillin antibiotic resistance gene and a LoxP sequence.

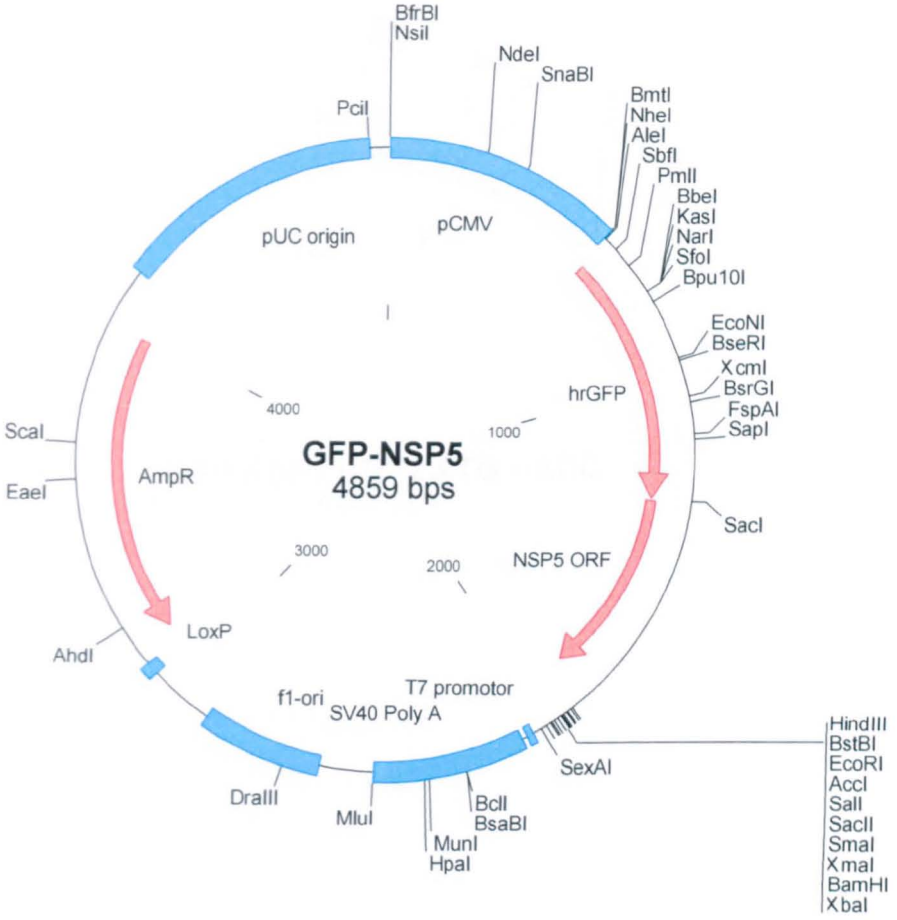

Appendix 2.8 NSP5 ORF cloned into the phrGFP-N1 expression vector

The NSP5 ORF was cloned into *Sac* I and *Hind* III restriction enzyme sites of the multicloning site of PCIneo to generate GFP-NSP5.

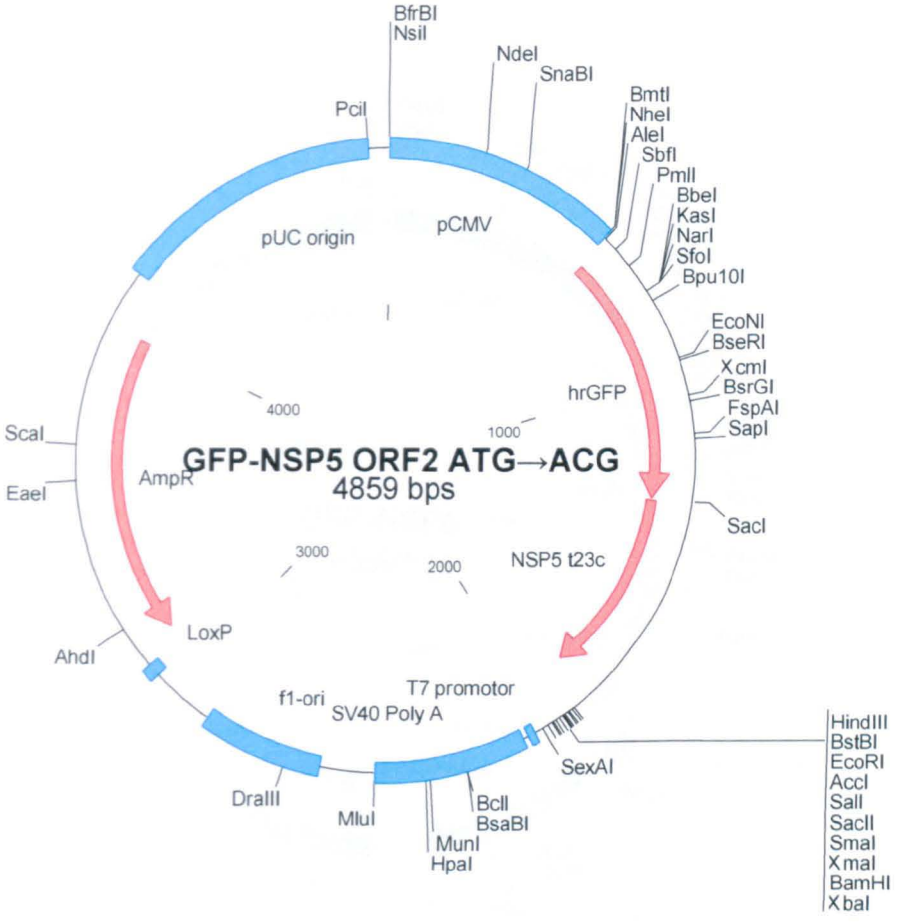

Appendix 2.9 Site directed mutagenesis was used to generate GFP-NSP5 ORF2 ATG→ACG

Site directed mutagenesis was used to create a mutant gene 11 sequence that could no longer express the NSP6 protein generating GFP-NSP5 t23c.

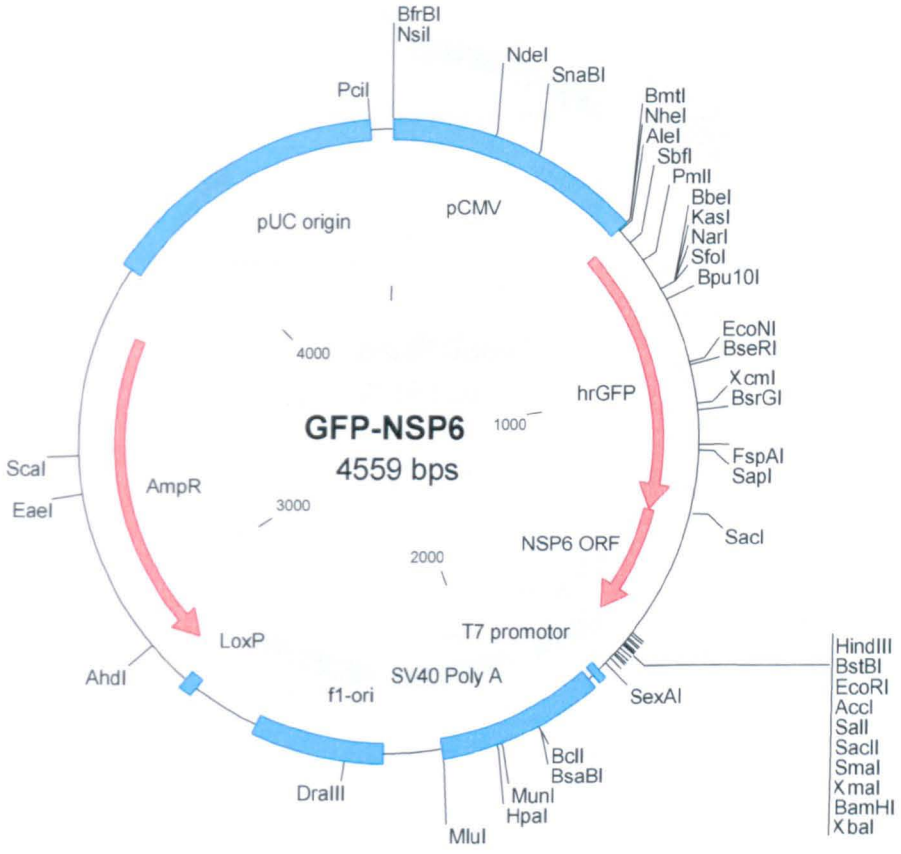

Appendix 2.10 NSP5 ORF cloned into the PCIneo expression vector

The NSP6 ORF was cloned into *Sac* I and *Hind* III restriction enzyme sites of the multicloning site of PCIneo to generate GFP-NSP6.

Appendix 3 – Results Chapter 6

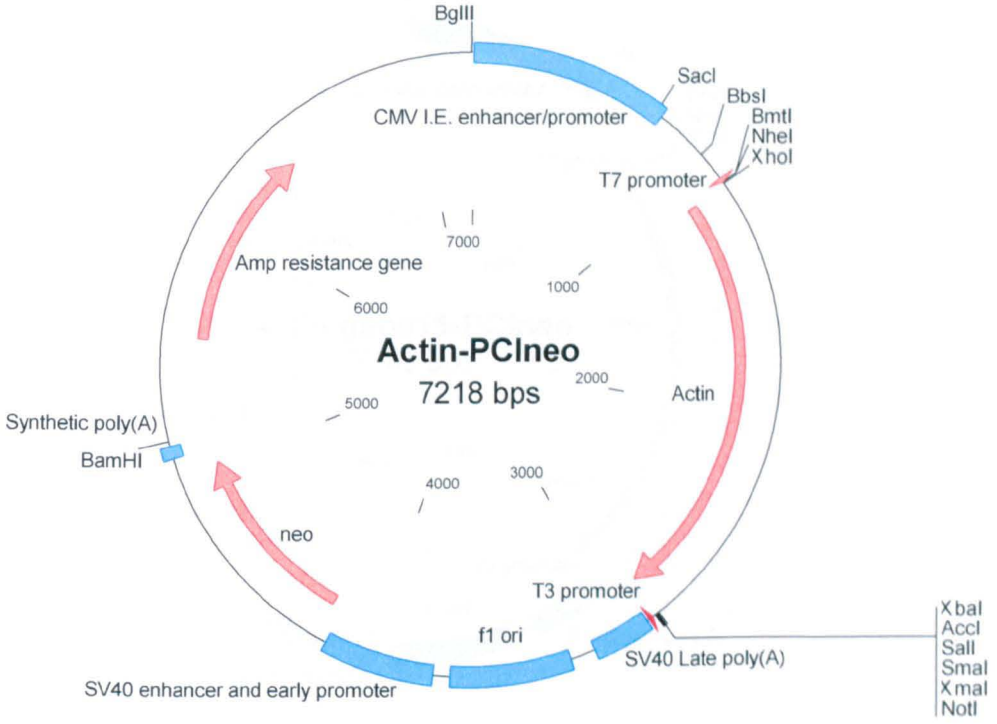

Appendix 3.1 The Actin gene was cloned into the PCIneo expression vector

The Actin gene was cloned into *Nhe* I and *Xho* I restriction enzyme sites of the multicloning site of PCIneo to generate Actin-PCIneo.

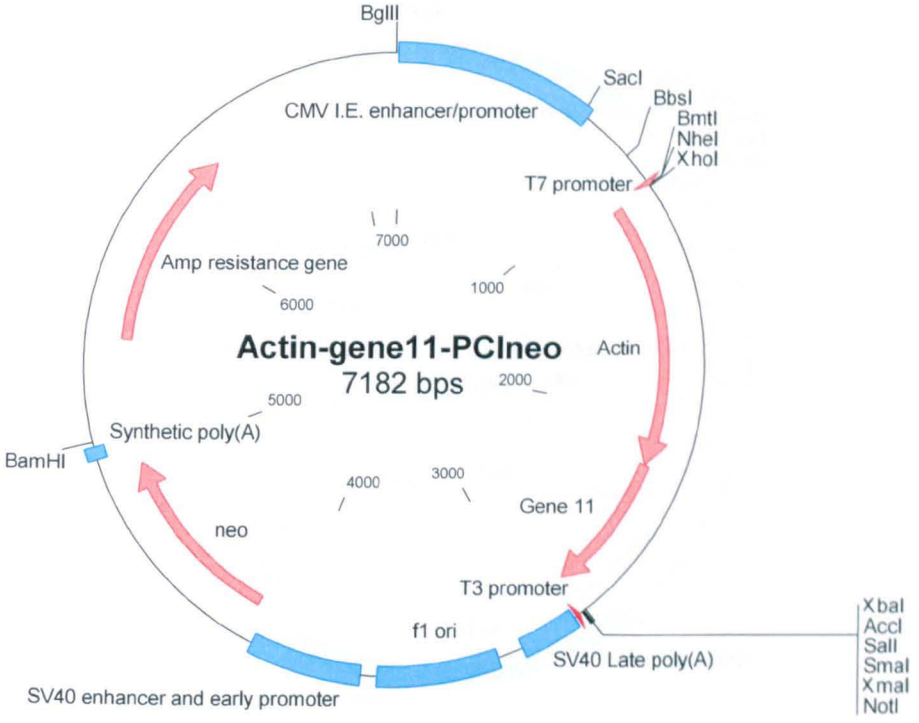

Appendix 3.2 The Actin gene was cloned into the PCIneo-gene11 expression vector

The Actin gene was cloned into *Nhe* I and *Xho* I restriction enzyme sites of the multicloning site of gene11-PCIneo to generate Actin-gene11-PCIneo.

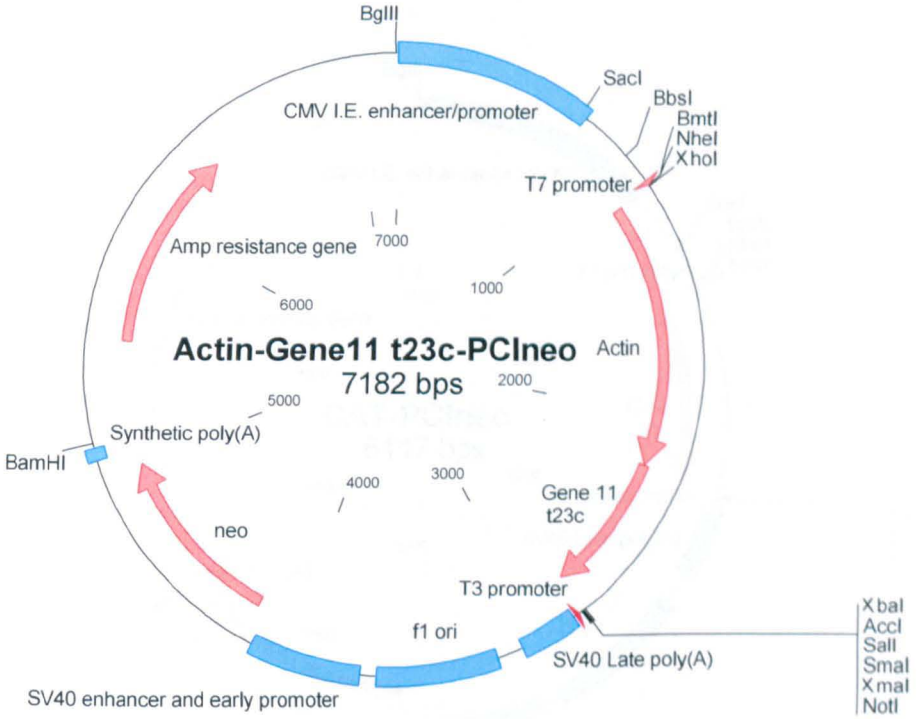

Appendix 3.3 Site directed mutagenesis was used to generate PCIneo-Actin-gene11 t23c

Site directed mutagenesis was used to create a mutation at the start codon of the first ORF of gene 11 making it non-functional to generate Actin-gene11 t23c PCIneo.

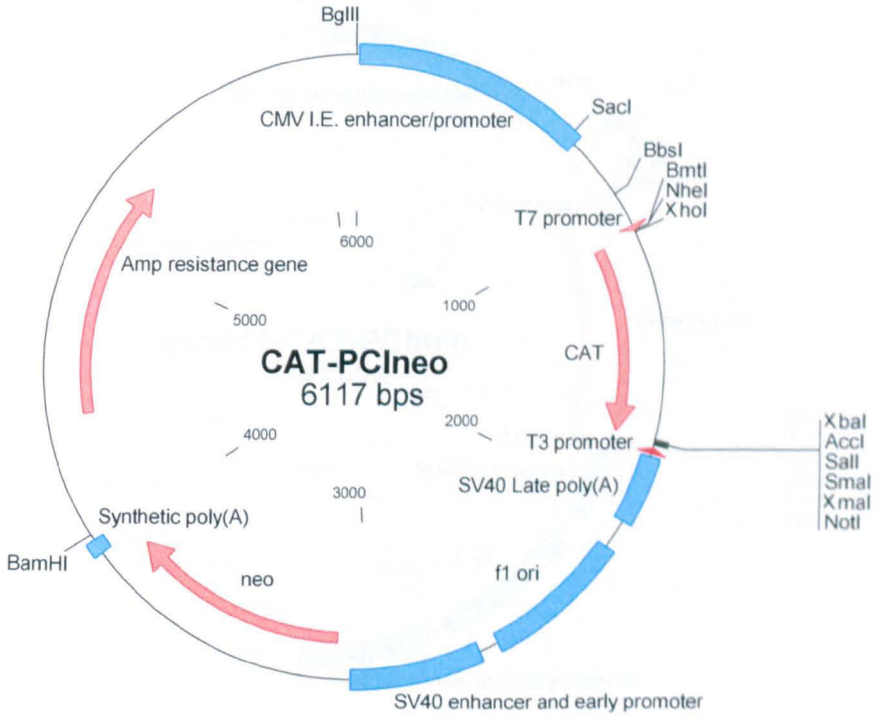

Appendix 3.4 CAT reporter gene cloned into the PCIneo expression vector

The CAT reporter gene cloned sites of the multicloning site of PCIneo to generate CAT-PCIneo was provided by Dr A.C. Marriott, University of Warwick.

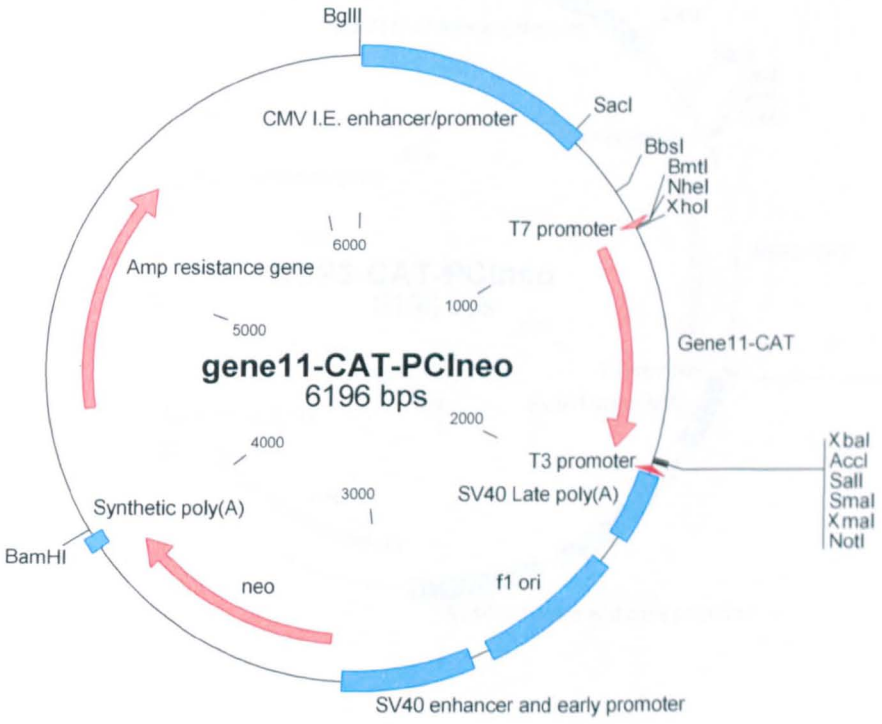

Appendix 3.5 Gene11-CAT fusion cloned into the PCIneo expression vector

Sequential PCR was used to generate a construct of the first 80 nucleotides of gene11 fused to the 5' of the CAT gene ORF, this construct was cloned into *Xho* I and *Xba* I restriction enzyme sites of the multicloning site of PCIneo to generate gene11-CAT-PCIneo.

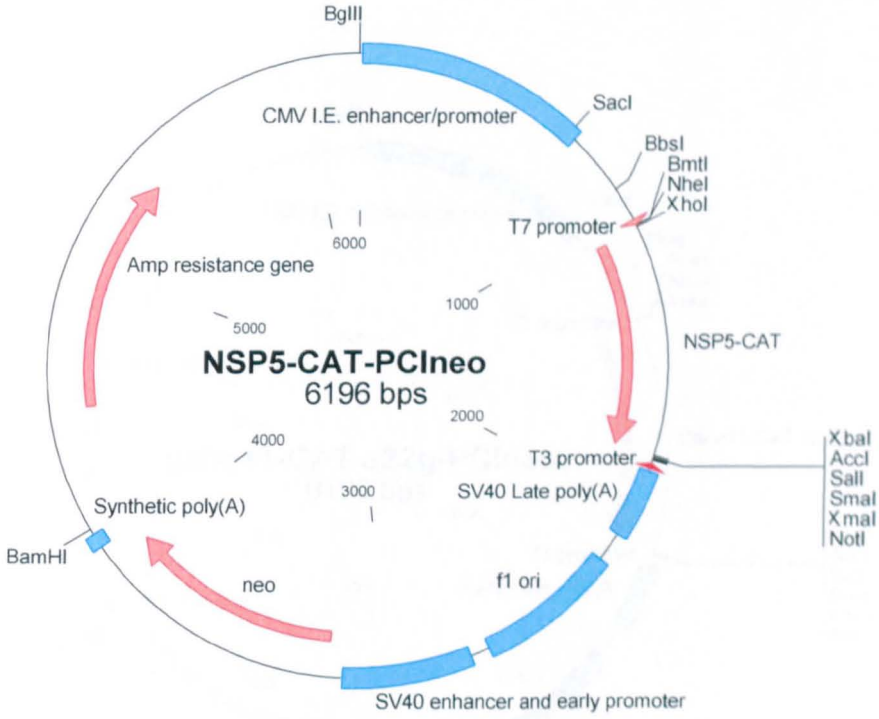

Appendix 3.6 NSP5-CAT fusion cloned into the PCIneo expression vector

Sequential PCR was used to generate a construct of the first 58 nucleotides of the NSP5 ORF fused to the 5' of the CAT gene ORF, this construct was cloned into *Xho* I and *Xba* I restriction enzyme sites of the multicloning site of PCIneo to generate NSP5-CAT-PCIneo.

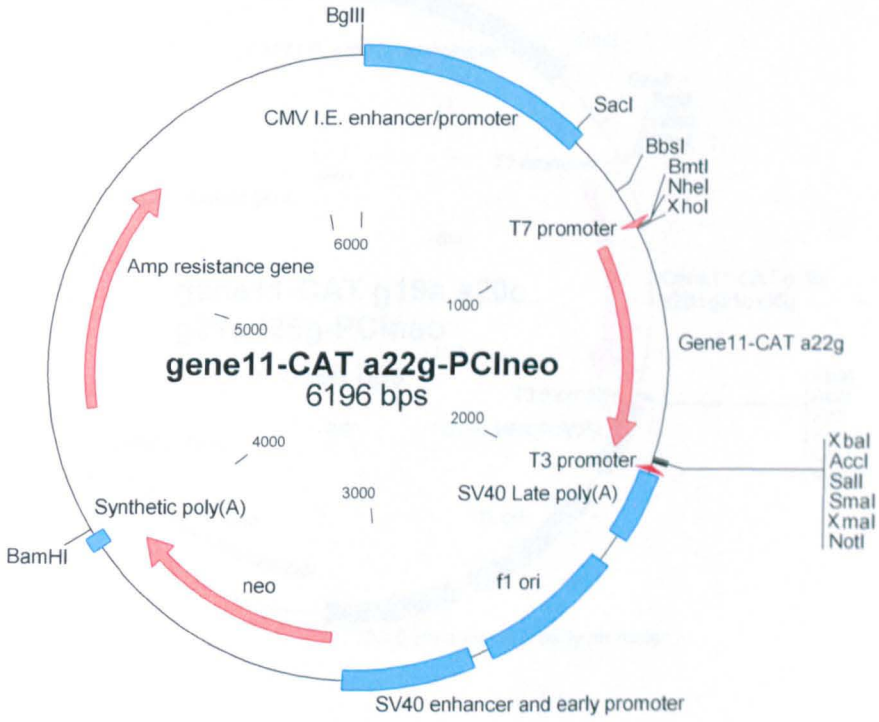

Appendix 3.7 Site directed mutagenesis was used to generate PCI-gene11-CAT a22g

Site directed mutagenesis was used to create a mutation at the start codon of the first ORF making it non-functional to generate gene11-CAT a22g-PCIneo.

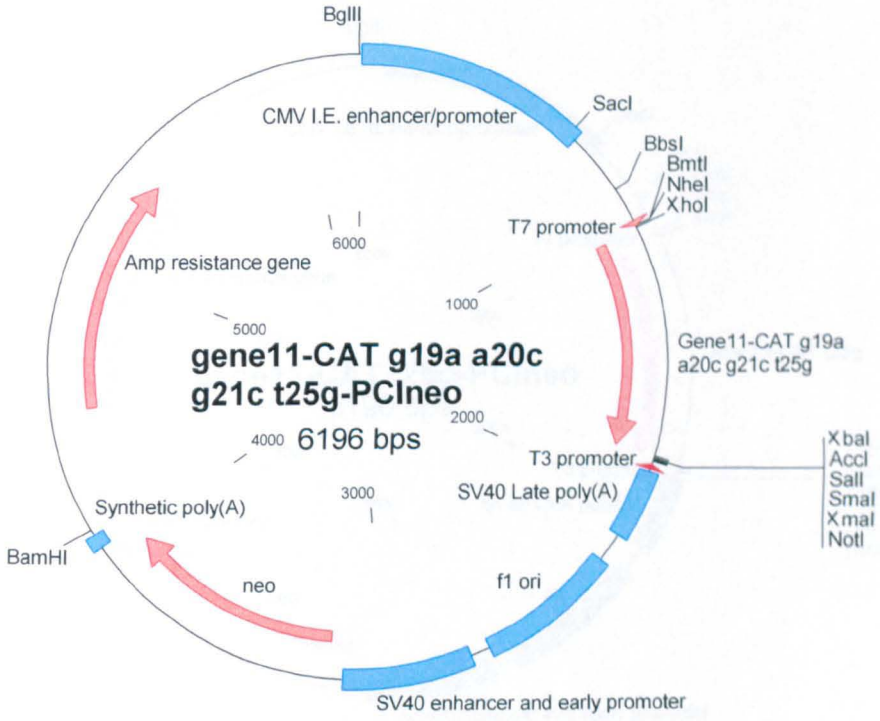

Appendix 3.8 Site directed mutagenesis was used to generate PCI-gene11-CAT g19a a20c g21c t25g

Site directed mutagenesis was used to create a mutant with an improved Kozak consensus sequence surrounding the start codon of the first ORF to generate gene11-CAT g19a a20c g21c t25g-PCIneo.

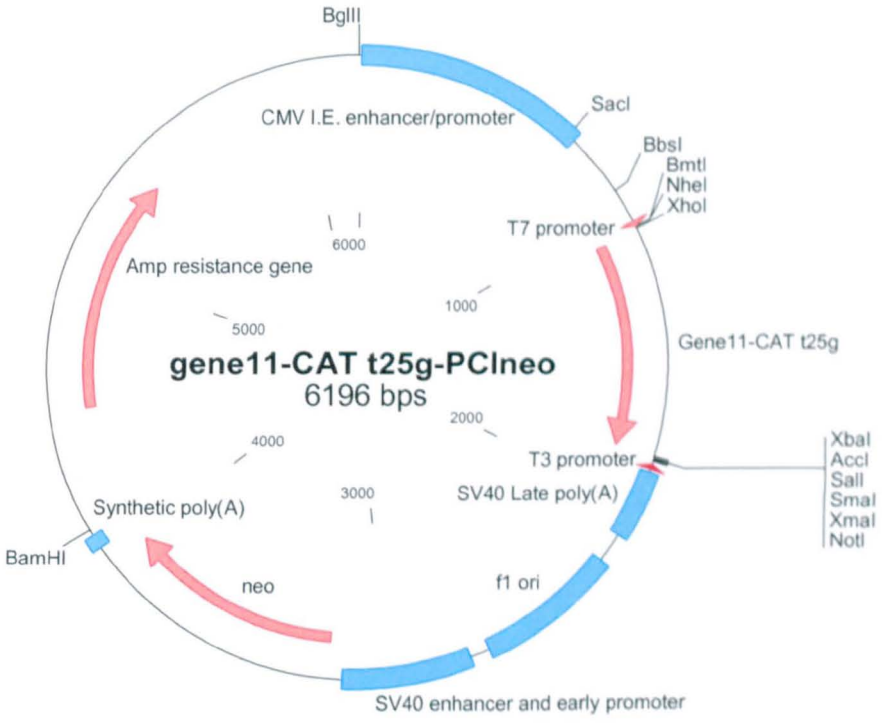

Appendix 3.9 Site directed mutagenesis was used to generate PCIneo-gene11-CAT t25g

Site directed mutagenesis was used to create a mutant with an improved Kozak consensus sequence at the +4 position of the start codon of the first ORF to generate gene11-CAT t25g-PCIneo.